AD_____

Award Number: DAMD17-94-J-4081

TITLE: Cyclin E, a Potential Prognostic Marker in Breast Cancer

PRINCIPAL INVESTIGATOR: Khandan Keyomarsi, Ph.D.

CONTRACTING ORGANIZATION: Health Research, Inc.
                          Rensselaer, New York 12144-3456

REPORT DATE: April 2000

TYPE OF REPORT: Final

PREPARED FOR: U.S. Army Medical Research and Materiel Command
               Fort Detrick, Maryland 21702-5012

DISTRIBUTION STATEMENT: Approved for Public Release;
                        Distribution Unlimited

The views, opinions and/or findings contained in this report are
those of the author(s) and should not be construed as an official
Department of the Army position, policy or decision unless so
designated by other documentation.

20010216 120

REPORT DOCUMENTATION PAGE

Form Approved
OMB No. 074-0188

Public reporting burden for this collection of information is estimated to average 1 hour per response, including the time for reviewing instructions, searching existing data sources, gathering and maintaining the data needed, and completing and reviewing this collection of information. Send comments regarding this burden estimate or any other aspect of this collection of information, including suggestions for reducing this burden to Washington Headquarters Services, Directorate for Information Operations and Reports, 1215 Jefferson Davis Highway, Suite 1204, Arlington, VA 22202-4302, and to the Office of Management and Budget, Paperwork Reduction Project (0704-0188), Washington, DC 20503

1. AGENCY USE ONLY (Leave blank)	2. REPORT DATE April 2000	3. REPORT TYPE AND DATES COVERED Final (1 Oct 94 – 30 Mar 00)

4. TITLE AND SUBTITLE
Cyclin E, a Potential Prognostic Marker in Breast Cancer

5. FUNDING NUMBERS
DAMD17-94-J-4081

6. AUTHOR(S)
Khandan Keyomarsi, Ph.D.

7. PERFORMING ORGANIZATION NAME(S) AND ADDRESS(ES)
Health Research, Inc.

Rensselaer, New York 12144-3456

E-MAIL:
keyomars@wadsworth.org

8. PERFORMING ORGANIZATION REPORT NUMBER

9. SPONSORING / MONITORING AGENCY NAME(S) AND ADDRESS(ES)

U.S. Army Medical Research and Materiel Command
Fort Detrick, Maryland 21702-5012

10. SPONSORING / MONITORING AGENCY REPORT NUMBER

11. SUPPLEMENTARY NOTES
This report contains colored photographs in the Appendices

12a. DISTRIBUTION / AVAILABILITY STATEMENT
Approved for public release; distribution unlimited

12b. DISTRIBUTION CODE

13. ABSTRACT (Maximum 200 Words)

Cyclin E, a G1 cyclin essential for S phase entry with a profound role in oncogenesis, is overexpressed and present in lower molecular weight (LMW) isoforms in breast cancer cells and tumor tissues. Alteration and overexpression of cyclin E are linked to poor patient outcome. We have established the use of cyclin E as a prognostic marker for breast cancer. Tumor specimens from 400 breast cancer patients were examined; changes of cyclin E expression were compared with seven other established tumor markers to patient outcome. Altered expression of cyclin E was observed in 91% of all breast cancers with poor prognosis where patients either died of breast cancer or were still with cancer at the last contact date. Similarly in 93% of all breast cancer patients where cyclin E was either not altered, or its alteration was minimal, patients had a favorable prognosis. We have also deciphered the mechanism of deregulation of cyclin E in breast cancer cells giving rise to the LMW forms of cyclin E. Our studies show that the LMW forms of cyclin E detected at a much higher level in tumor cells, arise from post-translational action of a protease. We have been able to generate and knockout the tumor specific LMW pattern of cyclin E by transient transfection of FLAG-tagged cyclin E constructs harboring these mutations in a breast cancer cell line. We have identified a novel elastase-type consensus sequence in the amino-terminus of cyclin E responsible for generating these tumor specific LMW isoforms. Lastly, studies using the drug Lovastatin demonstrated that this highly prescribed drug used to lower cholesterol levels is also capable of inducing all four cyclin dependent kinase inhibitors (CKIs) in a cell specific manner via cell cycle independent mechanism, through the inhibition of the proteasome. We have also devised a novel treatment strategy that protects normal cells against the toxic effects of chemotherapeutic agents, by reversibly arresting the normal cells in the G1 phase of the cell cycle.

14. SUBJECT TERMS
Cell Cycle, GI Cyclins, Prognostic Marker, Oncogenes (Breast Cancer), Mutations, Signal Transduction, Humans, Anatomical Samples, Breast Cancer

15. NUMBER OF PAGES
217

16. PRICE CODE

17. SECURITY CLASSIFICATION OF REPORT Unclassified	18. SECURITY CLASSIFICATION OF THIS PAGE Unclassified	19. SECURITY CLASSIFICATION OF ABSTRACT Unclassified	20. LIMITATION OF ABSTRACT Unlimited

NSN 7540-01-280-5500

Standard Form 298 (Rev. 2-89)
Prescribed by ANSI Std. Z39-18
298-102

FOREWORD

Opinions, interpretations, conclusions and recommendations are those of the author and are not necessarily endorsed by the U.S. Army.

___ Where copyrighted material is quoted, permission has been obtained to use such material.

___ Where material from documents designated for limited distribution is quoted, permission has been obtained to use the material.

___ Citations of commercial organizations and trade names in this report do not constitute an official Department of Army endorsement or approval of the products or services of these organizations.

N/A In conducting research using animals, the investigator(s) adhered to the "Guide for the Care and Use of Laboratory Animals," prepared by the Committee on Care and use of Laboratory Animals of the Institute of Laboratory Resources, national Research Council (NIH Publication No. 86-23, Revised 1985).

X For the protection of human subjects, the investigator(s) adhered to policies of applicable Federal Law 45 CFR 46.

X In conducting research utilizing recombinant DNA technology, the investigator(s) adhered to current guidelines promulgated by the National Institutes of Health.

X In the conduct of research utilizing recombinant DNA, the investigator(s) adhered to the NIH Guidelines for Research Involving Recombinant DNA Molecules.

N/A In the conduct of research involving hazardous organisms, the investigator(s) adhered to the CDC-NIH Guide for Biosafety in Microbiological and Biomedical Laboratories.

K. Keysmaur ___ 5/1/00
PI - Signature   Date

Table of Contents

5. Introduction

The overall purpose of this 5 year study is to use the altered expression of cyclin E as a diagnostic/prognostic marker and to investigate the mechanisms and repercussions of this alteration in breast cancer.

6. Body

Breast cancer is the most common malignancy and the second leading cause of cancer related deaths among women in the United States. One in eight American women can expect to be afflicted with some form of breast cancer in their lifetime of whom approximately 30% will die from this disease [1]. The prevalence of breast cancer has been increasing since the 1960s. Improvements in screening, detection and treatment, however, have kept mortality rates relatively constant. A comprehensive understanding of the regulation of growth and differentiation of normal breast tissue and the identification of cellular pathways containing new, potential therapeutic and prognostic targets are required to foster more effective clinical strategies.

Cell Cycle: In the past decade new findings in the fields of cell biology and molecular genetics of cancer have revealed a deregulation in the cell cycle as a critical event for the onset of tumorigenesis. Progression through the cell cycle, the sequence of events between two cell divisions, is governed by the actions of positive and negative regulators in the eukaryotic cell. The mammalian cell cycle is positively regulated by complexes of stable kinases termed cyclin dependent kinases (CDKs) and unstable regulatory subunits called cyclins which associate to form hetrodimeric complexes [2-5]. Mitogenic stimuli results in the phosphorylation and thereby activation of cyclin-CDK complexes by CDK activating kinase, CAK [6-8]. The activated cyclin/CDK complexes in turn phosphorylate substrates such as the retinoblastoma protein (pRb)

throughout the cell cycle [2,9,10]. Phosphorylation of pRb which is necessary for the progression through G1 is regulated primarily by cyclin D/CDK4 /CDK6 complexes while the cyclin E/CDK2 complex regulates the passage of cells from late G1 to S phase and further contribute to pRb hyper-phosphorylation [2,3,11]. The hypo-phosphorylated pRb serves as a tumor suppressor by interacting with and inhibiting cellular proteins such as E2F-DP heterodimeric transcription factors which activate many genes required for DNA replication pivotal for G1/S transition [11-14]. The complete hyper-phosphorylation of pRb by cyclin E/CDK2 complexes and consequent activation of E2F-DP transcription complex are thought to play a major role in overcoming of the restriction point [15,16].

Progression through the cell cycle is also negatively regulated by CDK inhibitors, CKIs [17-19]. There are 2 families of structurally distinct CKIs, (I) the CIP/KIP family which inhibits a broad range of CDKs by selectively binding and inhibiting the fully associated cyclin/CDK complexes and (ii) the INK family which binds specifically to CDK4 and/or CDK6 and inhibits complex formation with cyclin D [2,17,19,20]. The CIP/KIP family contains the universal cyclin-CDK inhibitors, p21 and p27 [17,19,21]. Although the CDK inhibitor p21 is a p53-regulated gene [22,23], both p21 and p27 are also regulated through p53 independent pathways [24-29]. Overexpression of p21 and/or p27 lead to cellular arrest at the G1-S boundary by inhibiting the cyclin/cdk complexes active in the G1 phase of the cell cycle.

To date, there are 10 different classes of cyclins (A-J, & L), 9 classes of CDKS (CDK1-9), and 2 classes of CKIs (CIP/KIP and INK) described, some with multiple members [2,19,30]. In normal cells the cyclins, CDKs, and CKIs work in concert to ensure a regulated transition of one phase of the cell cycle to the next. The level and pattern of expression of these regulators during the normal cell cycle are critical for the regulated progression through the cell cycle. In tumor cells this exquisite balance between the positive and negative regulators is not maintained, thus contributing to the transformed phenotype.

Alterations of cyclins D1 and E in cancer: The connection between cyclins CKIs and cancer has been substantiated with the D type cyclins [31-33]. Cyclin D1 was identified simultaneously by several laboratories using independent systems: It was identified in mouse macrophages due to its induction by colony stimulating factor 1 during G1 [34]. It was also identified in complementation studies using yeast strains deficient in G1 cyclins [35,36]; as the product of the bcl-1 oncogene [37], and as the PRAD1 proto-oncogene in some parathyroid tumors where its locus is overexpressed as a result of a chromosomal rearrangement that translocates it to the enhancer of the parathyroid hormone gene [38,39]. In centrocytic B cell lymphomas cyclin D1 (PRAD1/BCL1) is targeted by chromosomal translocations at the BCL1 breakpoint, t(11;14)(q13;q32) [40,41]. Furthermore, the cyclin D1 locus undergoes gene amplification in mouse skin carcinogenesis, as well as in breast, ovarian, esophageal, colorectal and squamous cell carcinomas [42-48]. Several groups have examined the ability of cyclin D1 to transform cells directly in culture with mixed results [46,49-56]. However, the overexpression of cyclin D1 was observed in mammary cells of transgenic mice and results in abnormal proliferation of these cells and the development of mammary adenocarcinomas [57], strengthening the hypothesis that the inappropriate expression of a G1 type cyclin may lead to loss of growth control.

Cyclin E, another G1 cyclin which forms complexes with CDK2 and is essential for S phase entry [55,58], also has a profound role in oncogenesis [59,60]. In dividing cells, the expression of cyclin E increases to a maximum at the G1/S transition, with a peak expression level near the restriction point [35,61]. When coupled to CDK2, the active kinase follows cyclin D/CDK4 in progressively phosphorylating the pRb releasing it from E2F-1. As E2F-1 is released it activates a number of S-phase genes including cyclin E and E2F-1 [62,63]. This state of readiness to enter S-phase requires cyclin E or cells will arrest at this point in the cell cycle [64,65]. For example, functional knockout of cyclin E by injection of anti-cyclin E antibodies into fibroblast cells causes cell arrest in the G1 phase [65]. Conversely, the overexpression of cyclin E protein causes

acceleration through G1 along with a decreased cell size [65,66]. In addition to its requirement for DNA synthesis, cyclin E also plays a key role in senescence [67], development [68,69], and modulation of downstream signals involving pRb [12] and E2F [62,63]. Due to the crucial role that normal expression and activity of cyclin E plays in cell proliferation, any defects in its expression could have a critical effect in oncogenesis.

We and others have reinforced the linkage between oncogenesis and cyclin E by correlating the altered expression of cyclin E to the loss of growth control in breast cancer [44,70,71]. Furthermore several tumor cohort studies (reviewed in [72]) have documented a strong correlation between cyclin E overexpression and poor patient disease-free or overall survival [59,73] and lack of estrogen receptor expression [74-76]. In addition, patients with high cyclin E levels in their tumors had a significantly increased risk of death and/or relapse from breast cancer even if they were node negative [73,75]. In our own studies ([77] and see preliminary results) where we examined tumor specimens from 403 breast cancer patients, we observe that cyclin E protein is the most consistent marker for determining the prognosis of early-stage node negative breast carcinoma. We found that expression of cyclin E is elevated in a subset of tumors from patients diagnosed with Stage 1 breast cancer, who later died of the disease (se preliminary results). Additionally, examination of the oncogenic potential of cyclin E in transgenic mice under the control of the bovine ß-lactoglobulin promoter revealed that lactating mammary glands of the transgenic mice contained hyperplasia and over 10% also developed mammary carcinomas [78]. Lastly, constitutive overexpression of cyclin E (but not cyclin D1 or A) in both immortalized rat embryo fibroblasts and human breast epithelial cells results in chromosome instability [79]. Collectively these data provide strong support for the role of cyclin E overexpression in breast cancer tumorigenesis.

During the first four years of this application we have used cyclin E antibody as a prognostic marker for breast cancer by analyzing breast tumor tissue specimens for the alterations in cyclin

E protein. During the first two years we collected 550 tumor tissue samples from breast cancer patients diagnosed with different stages of breast cancer ranging from pre-malignant to highly invasive. We extracted RNA, DNA and protein from most of these samples. Due to limited sample size received for each patient (i.e 0.1-0.2 g of tissue), protein was initially extracted from all samples and if there was tumor sample left over, DNA and RNA were also extracted. The protein extracts from all 500 samples were then subjected to Western blot analysis and the expression of cyclin E was compared and correlated with other known prognostic markers examined in the same samples. The prognostic markers include, cyclin D1, erbB-2, as well as PCNA to determine the proliferative activity of these samples. We also obtained information on the estrogen and progesterone receptor status of each sample as well as ploidy and proliferation rate as measured by Ki-67. In the second year of this study we analyzed the results obtained in the first year by quantitating the levels of cyclin E in each tumor specimen with that of cyclin D1, erbB2 and PCNA. These analysis were done by performing densitometric scanning on each lane of each gel with each antibody for each patient sample using at least two autoradiographs with different exposures. Such laborious analysis were necessary to accurately determine the level of cyclin E protein in every patient and correlate the alteration of cyclin E protein from each patient to the stage of their disease. During the third year of this application we contacted the 20 hospitals where these samples were obtained, and have been successful in collecting the following information on 400 of these patients: final diagnosis, TNM staging, treatment given, and final outcome (i.e quality of survival). Having all this information we have performed correlative analysis on these samples and evaluate the role of cyclin E as a prognosticator for breast cancer. During the third year of this application we have also developed a new antibody to cyclin E which can be used for detection of the alteration of cyclin E in immunohistochemical analysis using tissue slides obtained from frozen tissue samples.

During the fourth year of this application we added several other cell cycle markers to our panel of tumor markers. These include cyclin D3, p21, p27, p16 and pRb. The reason for the inclusion

of these markers was that several of these markers are thought to functionally interact with or act on cyclin E and hence their over or altered expression in conjunction with cyclin E could have profound effects of prognosis. During the fourth year of the study we have also initiated the statistical analysis of correlating cyclin E overexpression to outcome and determine whether indeed it is an independent tumor marker for poor prognosis.

During the fifth and final year of this application we obtained the final outcome of each of the 403 patients as of the last contact date. This was done to ensure that we have a minimum of 5-year follow up period for all the patients in this study including those who were diagnosed in 1995. Having all the clinical information, including outcome, we are currently in the midst of statistical analysis of the role of cyclin E in breast cancer prognosis. Specifically we will perform statistical analysis on; (1) the associations between cyclin E expression and categorical variables by the X^2 test or Fisher's exact test as appropriate, (2) the associations between cyclin E expression, age, clinical stage, and outcome by student's t test, (3) the survival curves will be estimated using the Kaplan-Meier method and the differences in survival distributions will be evaluated by the generalized Wilcoxon test, and lastly (4) Cox's proportional hazard modeling of factors potentially related to survival will be performed to identify which factors might have a significant influence on survival. The significance level chosen will be $p < 0.05$, and all tests will be two sides. We have provided our preliminary analysis of the expression pattern of cyclin E in breast cancer patients to emphasize the importance of cyclin E in the clinical setting and how our studies and others suggest that not only cyclin E is a powerful prognosticator for breast cancer, but that it may also play a role in the tumorigenesis process.

Below we provide the summary of our published work on the deregulation of cyclin E and detailed descriptions of our most current data on the identification of these LMW forms of cyclin E so prevalently detected in breast cancer cell lines and tumor tissues.

Overexpression of cyclin E LMW forms in breast cancer cell lines. To show the overexpression of cyclin E and the appearance of its LMW isoforms in tumor cells we examined cyclin E expression in a panel of normal mammary epithelial cell strains, immortalized breast cell lines and several breast cancer cell lines. The results show that only in tumor cell lines are these LMW forms of cyclin E overexpressed (Fig 1). The three normal cell strains (70N, 81N and 76N) were established from reduction mammoplasties obtained from three different individuals. Furthermore, at the end of their lifespan, these normal mammary epithelial cells stop proliferating and become senescent [80,81]. The two immortalized cell lines examined were MCF-10A and 76NE6 cell lines. MCF-10A is a near diploid immortalized cell line which is a subline of a breast epithelial cell strain, MCF-10, derived from human fibrocystic mammary tissue which was immortalized after extended cultivation in medium containing low concentrations of calcium [82]. 76NE6 is an immortalized cell line derived from normal mammary epithelial cell strain 76N by infection with human papilloma virus (HPV) 16E6 [83,84]. The E6/p53 interaction promotes degradation/inactivation of p53 resulting in the loss of the normal p53 phenotype [85-87]. Table 1 summarizes the mammary epithelial cell types, estrogen receptor (ER), p53, pRb (retinoblastoma) status of these normal and the 9 established tumor (i.e. 4 ER positive and 5 ER negative) cell lines used. The results from the Western blot revealed that cyclin E protein not only is overexpressed in all the tumor cell lines examined, but is also present in lower molecular weight isoforms. Normal cell strains and immortalized cell lines express predominately the 50 kDa form of cyclin E with very low levels of the LMW isoforms (Fig 1).

Aim 1- Use of cyclin E as a prognostic marker for breast cancer

Overexpression of LMW of cyclin E is linked to poor prognosis in breast cancer. Previously we examined the relevance of cyclin derangement to *in vivo* conditions, by measuring the expression of cyclin E protein in tumor samples versus normal adjacent tissue obtained from patients with various malignancies ([59],see Appendix Ref 1). These analyses revealed that

breast cancers and other solid tumors, as well as malignant lymphocytes from patients with lymphatic leukemia, show severe quantitative and qualitative alteration in cyclin E protein expression independent of the S-phase fraction of the samples [59]. We have recently expanded our analysis of cyclin E as a prognostic marker for breast cancer by examining 403 breast cancer tumors from patients diagnosed with different stages of breast cancer ranging from pre-malignant to highly invasive. The protein extracts from all 403 samples were then subjected to Western blot analysis and the expression of cyclin E was compared and correlated with other known prognostic markers including, cyclin D1, erbB-2, as well as PCNA to determine the proliferative activity of these samples. We also acquired data on the estrogen and progesterone receptor status of each sample as well as ploidy and proliferation rate as measured by Ki-67. Lastly, we obtained follow up information on all patients including: final diagnosis, TNM staging, treatment given, and final outcome (i.e. quality of survival). With this information we have performed correlative analysis on these samples and evaluated the role of cyclin E as a prognosticator for breast cancer. Our final statistical analysis will be completed as soon as the 5-year survival data of all patients (including those diagnosed in 1995) are obtained. Below we show our preliminary data on the role of cyclin E as a prognosticator as compared to cyclin D1 in these 403 samples. The initial demographic data from the patient populations is presented in table 2 and shows the age distribution, ER status and TNM staging of the 403 patients. A representative Western blot analysis of the patients is shown in figure 2A where expression of cyclin E, cyclin D1, and PCNA were examined in 12 patients diagnosed with different stages of breast cancer. The first two lanes of the gel are used as controls and the samples are from normal and tumor-derived breast epithelial cells. Every single gel used for Western blot analysis contained the same normal versus tumor control lanes to ensure proper experimental conditions and similar exposures for each Western blot was used for comparative analysis between the blots. It is evident that as the stage of the cancer increases so does the alteration in cyclin E expression. In tumor tissues from stage I disease, overall cyclin E expression was low and the appearance of the LMW isoforms of cyclin E was minimal. In

tumor samples from stage II patients, the expression of cyclin E and the appearance of the lower molecular weight isoforms of cyclin E were detectable and showed a visible increase in intensity compared to stage I tumors. In stage III tumor tissues, cyclin E expression was much more abundant and the levels of the lower molecular weight isoforms also increased substantially. Lastly, in the metastatic stage IV disease we observe severe overexpression of cyclin E and a significant overexpression of the lower molecular weight isoforms of cyclin E.

Clearly, the expression of cyclin E increases quantitatively and qualitatively with the stage of the disease. We also examined the expression of cyclin D1 and PCNA in the same tissue samples by stripping and reprobing the blots with the aforementioned antibodies. As evident the expression of cyclin D1, was not correlated with the stage of the disease. In fact tumor tissues from Stage I patients who had low cyclin E levels but high proliferation index as indicated by PCNA expression also had high cyclin D1 levels. Hence, cyclin D1 expression although increased according to the proliferation index of the tumors, did not increase with the stage of the disease. The expression of PCNA, proliferating cell nuclear antigen which is often used to measure the proliferation index of a cell or tissue, revealed that although overall the rate of proliferation of tissues with high stage tumors were maximal, low stage tumors can also be highly proliferative. Hence, of the markers examined cyclin E was the most consistent indicator for the stage of the disease independent of the proliferation rate of the tissue being examined. Follow up studies showed that patients whose tumors were analyzed in lanes 7-12 had poor prognosis (i.e. lack of disease free survival).

We next correlated the overexpression of cyclin E and cyclin D1 to patient outcome for all the 403 patients similar to the manner shown in figure 2 and the summary of the results are presented in Table 3. Of the 403 cases, 281 patients had low cyclin E expression and 122 of the patients had high cyclin E expression. Of the patients with low cyclin E expression 93% had good prognosis where the patient has no evidence of disease and is alive and well. Of the 122

cases with high cyclin E expression 91% had poor prognosis where the patient either expired of cancer or the cancer is back in the form of metastasis. Hence, cyclin E overexpression is clearly a good prognosticator for predicting outcome of the patients. On the other hand cyclin D1 was not a good prognosticator of patient outcome because even though cyclin D1 was high in 202/403 patients its overexpression did not correlate with patient outcome as 57% of those cases with high cyclin D1 had good outcome while 43% had poor outcome.

While these results were very exciting and indicated a prognostic role for cyclin E it was crucial to determine if cyclin E is an independent predictor of poor outcome or just another marker for predicting stage of the disease. For that purpose we correlated the overexpression of cyclin E to the stage of the disease and examined patient outcome for each stage (Table 4). These analysis show that cyclin E is a stage independent prognosticator, since cyclin E overexpression leading to patient mortality was observed in every stage of the disease. Of the 122 cases overexpressing cyclin E, 12 cases were diagnosed with stage I and all 12 patients expired of cancer. There were 40 patients diagnosed with stage II disease overexpressing cyclin E and 38 of those patients died of the disease and so on for the other stages (see Table 4).

To further emphasize that cyclin E is indeed a stage independent prognosticator for breast cancer we show a Western blot analysis of cyclin E from tumor of Stage 1 and II breast cancer patients with good and poor prognosis. These results clearly shows that while those patients diagnosed with stage 1 or 2 of the disease which showed no evidence of disease in their follow up did not overexpress cyclin E (i.e patients 1-3), those patients with poor prognosis showed sever overexpression of cyclin E and appearance of the LMW forms. Furthermore, some of the tumors with low cyclin E levels had high levels of cell proliferation (PCNA) expression), and vis a vis. These analysis suggest that this subset of breast tumors with elevated expression of cyclin E, and low levels of cell proliferation (i.e. deregulation of cyclin E expression relative to cell cycle) are also associated with poor prognosis. Our results from these 403 patients suggest that

overexpression of cyclin E is an independent marker from the stage of the disease since patients diagnosed with all 4 stages of the disease whose tumor overexpressed cyclin E had a high chance of poor outcome. Overexpression of cyclin E could also be used as a signal for more aggressive therapy. This conclusion is based on the observation that the only group of patients overexpressing cyclin E who survived were those who were diagnosed with stage III or IV (Table 4) and because of the high stage of their disease received more aggressive therapy (data not shown).

Therefore we speculate that because of the aggressive treatment, these cohort of patients overexpressing cyclin E survived the disease. This prediction is further substantiated with the observation that most of the patients in stage I and II of the disease overexpressing cyclin E who had otherwise favorable predictors did not survive the disease due to more conservative therapy (data not shown). For example the steroid status of most of these stage I and stage I were positive, the patients were lymph node negative, ploidy was near diploid and proliferation was low, yet cyclin E levels were high. Most of these patients were treated with surgery alone or surgery combined with hormonal therapy which was not affective. We suggest that if the expression of cyclin E could have also been used as a predictor, the patient may have been treated more aggressively and the outcome could have been altered. From these results we suggest that cyclin E is a novel prognosticator for breast cancer and could be used in better management of the disease in terms of treatment.

Aim 2: Utilization of cyclin E deletional mutations to detect early metastatic breast cancer.

Early on in the study, during the first year, we determined that the cyclin E forms we had referred to as deletional mutations turned out not to be deletional mutations, but rather splicing variants of cyclin E that are present in both normal and tumor cell lines and tissue samples.

However, these truncated forms of cyclin E will help us decipher the mechanisms of alteration of cyclin E in breast cancer. Even though this aim was elucidated right away, we chose to examine how these alternative splice variants would give rise to the lower molecular weight isoforms we observe in tumor but not normal cells. As a result we expanded this aim to read **"Identification of the lower molecular weight isoforms of cyclin E in tumor cells".** Below is a description of our progress on this aim which is now completed.

Deregulation of cyclin E in breast cancer: The mechanism of cyclin E alteration is in part a result of its deregulation in breast cancer. We have characterized the alteration of cyclin E in breast cancer and have found while cyclin E is cell cycle regulated in normal cells, it is present constitutively and in an active CDK2 complex in synchronized populations of breast cancer cells ([60]-see Appendix Ref 2). We show that cyclin E is present in altered forms in synchronized populations of tumor cells throughout the cell cycle and the kinase activity associated with it, or with CDK2, is also constitutively active. This observation has been corroborated by others in different breast cancer cell lines [88,89]. One consequence of constitutive activation of cyclin E throughout the tumor cell cycle is the possible phosphorylation of substrates at altered points in the cell cycle resulting in loss of checkpoint control during the progression of G1 to S in tumor cells. We provided evidence for such redundant behavior of cyclin E/CDK2 in tumor cells by the ability of this complex to phosphorylate pRb under conditions where cyclin D/CDK complexes have been rendered inactive by overexpression of p16 ([76] see Appendix Ref 3). We show that in some breast tumor cells and tissues, the expression of p16 and pRb are not mutually exclusive as has been shown to be the case in other systems [90-94]. Overexpression of p16 in cells results in sequestering of CDK4 and CDK6, rendering cyclin D1/CDK complexes inactive. However, pRb appears to be phosphorylated throughout the cell cycle following an initial lag. This time course of *in vivo* pRb phosphorylation is similar to that of *in vitro* GST-Rb phosphorylation achieved by cyclin E immunoprecipitates prepared from these synchronized cells (Appendix- Ref 3). The link between cyclin E alteration and pRb inactivation has also been

corroborated by two independent studies [95,96]. Collectively, these studies provide evidence for the deregulation of cyclin E in breast cancer.

Tumor cells process ectopic cyclin E into LMW forms while normal cells do not-To investigate the proteolytic processing of cyclin E in normal and tumor cells creating the LMW isoforms, a series of 5 cyclin E constructs were engineered with the epitope FLAG sequence at the carboxy-terminus are schematically presented in figure 4A. These constructs include cyclin E-L-FLAG (the splice variant with 15 amino acid insertion at the 5' end [65]), E-Flag (the wild-type cyclin E) and three N-terminal truncated cyclin E constructs designated Trunk 1 to 3-FLAG constructs (Fig 4A). These five cyclin E constructs were created to serve two purposes. First, the E-L- and E-FLAG constructs will be used to determine whether a full length cyclin E can give rise to the LMW forms in tumor or normal cells. Additionally these 2 constructs show that the E-L form is the predominant cyclin expressed in both normal and tumor cells (see Fig 5). Secondly, the smaller trunks will be used to bracket the LMW forms expressed in tumor cells. Our previous studies suggest that the endogenous LMW isoforms of cyclin E found in tumor cells are a result of N-terminal deletions of the protein ([60], and data not shown). By comparing the mobility of the cyclin E trunk forms with the cyclin E lower molecular weight forms on a Western blot, the sizes of the isoforms can be more accurately determined.

The expression of the truncated cyclin E cDNAs were first examined by *in vitro* transcription/translation to analyze the sizes of their respective protein products. FLAG tagged cyclin E-L, E, and Trunks 1-3 as well as the pCDNA3.1 vector with no insert, were synthesized by *in vitro* transcription/translation, and then subjected to Western blot analysis with both cyclin E (Fig 4B) and FLAG (Fig 4C) antibodies. In both Western blots, lane 1 represents 50 μg of MDA-MB-157 total cell extract, used for a positive control for the cyclin E antibody (4B) detecting endogenous cyclin E. Lane 1 also serves as a negative control for the FLAG antibody (Fig 4C). Lane 2 is the negative control for the vector pCDNA3.1 with no insert in the

transcription/translation reaction, and shows no cyclin E protein as detected by the cyclin E or FLAG antibodies. Lanes 3-7 are the *in vitro* translated products of the 5 different cyclin E-FLAG constructs. The size difference for each trunk can clearly be seen as each lane shows a smaller size cyclin E band (Fig 4B,C). The predicted sizes of the cyclin E-FLAG trunk forms as determined by sequence information of the proteins produced by the constructs are between 48.0 kDa for E-L-FLAG and 34.8 kDa for Trunk 3-FLAG. The FLAG tag adds an additional 1K to the size of the cyclin E protein (Fig 4A). The actual sizes of the *in vitro* transcribed trunks determined by gel migration are quite different however and range from 52.0 kDa for E-L-FLAG to 34.0 kDa for Trunk 3-FLAG (listed in Table 6). The differences in cyclin E molecular weight determined by Western blotting of the *in vitro* translated constructs versus those predicted from the amino acid sequence, suggest that cyclin E protein migrates anomalously on an SDS-PAGE. In addition, smaller forms of cyclin E are detected on the Western blots, probably the result of alternate translation start sites present within the cyclin E cDNA. For example, cyclin E-L-FLAG also produced a 46.0 kDa band that co-migrates with cyclin E-FLAG, at 46.3 kDa. In addition cyclin E-L, E-, and Trunk-1-FLAG constructs all synthesized a protein migrating at ~41 kDa; this is most likely a translation start site at base pairs 136-138 which is close to Trunk 2-FLAG migrating at 41.2 kDa. Trunk 3-FLAG produces an additional band at 30.6 kDa, which may be from a translation start site at base pairs 358-361 within the middle of the cyclin E gene. The cyclin E constructs used here span the entire range of cyclin E lower molecular weight forms from about 50 kDa to 34 kDa detected in MDA-MB-157 (Fig 1 lane 10) and tumor tissue samples (Figs 2 and 3).

Differential processing of cyclin E in normal versus tumor cells. The *in vitro* translation of the cyclin E constructs generated only the full length and the alternative-start-site protein products (Fig 4B,C). However, the pattern of cyclin E expression in breast cancer cells and tissues is indicative of a more complex processing of cyclin E (Figs 1-3). To compare normal and tumor processing we transfected two different sets of normal and tumor cells with the cyclin E-FLAG constructs and examined the expression and associated kinase activity of the protein

products from these constructs (Fig 5). The cell lines used for these study are the tumor cell lines MDA-MB-157 and MDA-MB-436 and normal cell lines MCF-10A (immortalized) and 76N (mortal) cell strain. All cells were transfected with either the vector backbone, cyclin E-L- or cyclin E-FLAG constructs. We monitored transfection efficiencies by co-transfection with the green fluorescent protein (GFP) expressing vector, (pEGFPC-1) and percent efficiency was determined by measuring GFP expression by flow cytometry (see methods). Table 5 lists the transfection efficiencies of the 4 cell lines used in this study. Following transfection with the indicated vectors and determination of transfection efficiency, cell extracts were prepared and subjected to Western blot analysis with FLAG antibody (Fig 5A, B). The results revealed that in both MDA-MB-157 and MDA-MB-436 tumor cells, the cyclin E-L- and cyclin E-FLAG were processed into several LMW isoforms as well as the full length form, generating a pattern of cyclin E-FLAG expression similar to endogenously expressed cyclin E (Fig 5A, lanes 3 &4). This result suggests that a single full length cyclin E has the ability to give rise to LMW forms in tumor cells. Moreover, these forms most likely arise from a post translational processing event, since the cyclin E cDNA used was isolated from a mature mRNA, already spliced [35,65]. The range of the LMW forms produced from the full length cyclin E-L- and cyclin E-FLAG is from 51 kDa to 34 kDa, which is the same range as endogenous lower molecular weight forms detected in non transfected cells.

The pattern of expression of cyclin E-L- and cyclin E-FLAG in normal cells is quite different than that observed in tumor cells (Fig 5A,B). Transfection of either cyclin E-L- or cyclin E-FLAG into either MCF-10A or 76N cells results mainly in the expression of the full length protein products (Fig 5A, B, lanes 7 and 8). There was a slight expression of LMW forms in normal cells following transfection with cyclin E-FLAG, however the levels of these proteins were much lower than the LMW forms expressed by tumor cells. The inability of normal cells to express high levels of LMW forms of cyclin E-L- or E-FLAG proteins from the full length shows that the LMW processing is much less active in normal cells than tumor cells. The similar Western blot pattern

of expression between endogenous and transfected cyclin E in normal cells again shows that the transfected cyclin E-FLAG constructs are being expressed similarly to the endogenous cyclin E, suggesting that the machinery to process cyclin E may be present in both normal and tumor cells, however this machinery is more active in tumor cells.. We found that the cyclin E-L- and E-FLAG expressed transiently can activate CDK2 and the kinase activation is greater in tumor cells (Fig 5 C, D). Cyclin E associated kinase activity was measured by the phosphorylation of histone H1 in immunoprecipitates prepared from transfected normal and tumor cells using an antibody to FLAG. This analysis revealed the cyclin E-FLAG associated kinase activity was 10-fold higher in tumor than normal cells. This was surprising, since equal amounts of cyclin E-L- or E-FLAG constructs were transfected into the cell lines as determined by efficiency studies (table 5). The increased kinase activity in tumor cells suggests that the LMW isoforms of cyclin E-FLAG products can activate the kinase and that there is more CDK2 present in tumor cells. We also measured the CDK2 associated kinase activity in both normal and tumor cells and found that tumor cells harbor a higher level of CDK2 activity than normal cells (Fig 5 C, D). Transfection of cyclin E-L and E-FLAG in normal and tumor cells increases cyclin E-FLAG associated kinase activity in tumor cells due to the increased processing of these constructs and more CDK2 in tumor cells. Other studies (see Appendix-Ref 4) suggest that the processing of cyclin E in tumor cells is independent of time, transfection efficiency, cell lines used or method of transfection.

Differential processing of all cyclin E-FLAG constructs in normal versus tumor cells. Since tumor cells are able to process the full length cyclin E into lower molecular weight forms, the next step was to determine more precisely which region of cyclin E protein is subject to the processing. Transfection of all 5 cyclin E-FLAG vectors (see Fig 4A) into normal and tumor cells, will bracket the endogenous LMW forms of cyclin E found in tumor cells, and define their approximate mass. MDA-MB-157 and MCF-10A cells were transfected with each of the 5 cyclin E-FLAG constructs (schematically presented in Fig 4A) and the vector backbone, harvested 24

hours post transfection, and subjected to Western blot analysis with FLAG and cyclin E antibodies (Fig 4).

Transfection of each of the cyclin E-FLAG constructs into tumor cells resulted in their processing into lower molecular weight forms which fell within the range of 52K to 36K (Table 6). The largest protein produced from each construct migrated with a similar mobility with that observed by *in vitro* translation (Table 6). However MDA-MB-157 cells were able to further generate lower molecular weight forms from all the constructs. For example, cyclin E-L-FLAG expressed *in vitro* generated 1 major protein migrating at 52.0 kDa, and two minor bands at 46.0 kDa, and 41.8 kDa, detected by a FLAG antibody (See Fig 4B,C and Table 6). However, the same construct transfected in tumor cells generated 6 major proteins migrating between 37 and 52 kDa (Fig 6A, Table 6). This result indicates that alternate translational start sites active in the *in vitro* translation system, do not account for all the lower molecular weight forms of cyclin E produced by tumor cells. Additionally, each of the constructs transfected in the tumor cells is also processed into the next series of lower molecular weight forms, and that the lower molecular weight isoforms common between all constructs co-migrate (Fig 6A, lanes 2-6, Table 6). Since the FLAG tag is on the carboxy-end of each construct, this data provides additional evidence that the processing of cyclin E occurs from the amino terminal end of the cyclin E protein, and that the carboxy-terminus remains intact.

Transfection of MCF-10A cells with each of the cyclin E-FLAG constructs results in mainly the expression of the full length form of each construct with minimal processing (Fig 6B). This is consistent with the results obtained in the transfection of cyclin E-L and E-FLAG constructs into MCF-10A and 76N (Fig 5). The protein products of each MCF-10A transfected cyclin E-FLAG construct migrated with the same mobility as the *in vitro* synthesized form, as well as the longest form of each construct following transfection in MDA-MB-157 cells (Table 6). Based on these comparisons, the sizes of all the cyclin E processed proteins detected in MDA-MB-157 cells

were estimated within 6 amino acids and listed in Table 6. Lastly, expression of total cyclin E (i.e. endogenous + transfected) as detected by cyclin E antibody highlights the levels of overexpression of transfected cyclin E-FLAG in both cell lines (Fig 6A, B). These results show that even though the cyclin E-FLAG constructs were overexpressed in both normal and tumor cells to the same extent, only tumor cells can process cyclin E into LMW isoforms, while normal cells have a reduced capacity for further processing. Identification of the LMW forms of cyclin E in breast cancer cells.

Role of the splice variants-We have used several approaches to identify the cyclin E forms found in tumor cells. Initially we used two different approaches to rule in/rule out whether the shortened mRNA splice variants of cyclin E described to date (see introduction). In the first approach we characterized the cyclin E mRNAs present in normal and tumor cells by Ribonuclease Protection Assay (RPA), which is much more (~100 fold) sensitive assay compared to Northern Blot analysis with levels of detection in the femtogram quantities. We used the RPA to quantitate the cyclin E mRNAs found in normal and tumor cells and also to determine whether there are splice variant differences in these cells which could account for the LMW cyclin E protein forms found in tumor cells. Figure 7A schematically depicts the target RNA (i.e. cyclin E) and the RNA probes complimentary to the cyclin E gene sequence used. We used a single probe (i.e probe 3B) to quantitate cyclin E mRNA in a total of 7 cell lines including 2 derived from normal tissue and 5 derived from tumor tissue. The results of the quantitation show that there are 2-3 copies of cyclin E mRNA per cell in unsynchronized normal breast epithelial cells (76N) and a normal breast cell line (MCF 10A) (Fig 7B). Breast tumor cell lines exhibited a range of cyclin E mRNA expression from as low as 1 copy per cell (MCF 7 and ZR75T) to four copies per cell (MDA-MB-231) to 8 copies per cell (MDA-MB-436) to 40 copies per cell in MDA-MB-157. Human ß-actin was quantitated by RPA in each preparation of total RNA as a control. For comparison, ß-actin was present consistently at about 3000 copies per cell regardless of cell type. The differences in cyclin E mRNA levels between normal and tumor observed, were not enough to account for the LMW forms found in tumor cells. Furthermore, the single probe used

did not detect any splice variant alterations between normal and tumor cells, as only one species of cyclin E was detected in all cells examined (data not shown). For that purpose we used a larger RPA probe (i.e probe 7B) specific for bases 25-523 spanning a portion of the cyclin box, where some of the splice variants of cyclin E have been known to occur, including cyclin ES. Using this probe two distinct protected fragments were detected, one representing the full length mRNA and a second at least 60 bases shorter (Fig 7C). This shorter cyclin E mRNA could represent cyclin ES or another variant with a deletion in the cyclin box region. However no differences in the appearance of this smaller protected fragment was observed between normal and tumor cells examined, suggesting the presence of this splice variant of cyclin E cannot account for the LMW forms of the protein found predominately in tumor cells.

Complementing the RPA analysis of cyclin E mRNA found in normal and tumor cells, we devised a method to enumerate the relative abundance of the known forms of cyclin E mRNA and search for new splice variants (Fig 8). For these studies poly A+ RNA from 76N normal cell strain and MDA MB 157 tumor cell line were prepared and used to create RT-PCR libraries in *E. coli*. Approximately thirty individual cyclin E cDNA containing clones from each cell line were picked from the libraries and plasmids isolated. The plasmids were used as templates in a PCR reaction using the oligonucleotides from the RT-PCR step. The PCR products were digested with a single restriction enzyme, Sau3AI, separated by electrophoresis on a 5% acrylamide gel and stained with ethidium bromide. This strategy can distinguish the various known cyclin E splice variants in each cell line (Fig 8). A clone of each known and new splice variant of cyclin E was also completely sequenced to confirm our restriction mapping strategy. Figure 8 shows the results of the restriction mapping of representative clones found in both normal and tumor cells, depicting a different banding pattern for each clone representing a different variant. The results from the library analysis reveals that the EL form of cyclin E is the dominant species found in normal and tumor cells and that there are no detectable splice variants in the cell lines not already described. Furthermore, we found that the frequency of the known splice variants relative to the EL form

does not differ significantly between normal and tumor cell lines. This analysis allows us to conclude that the major species of cyclin E mRNA is that of the full length (EL) form and not the cyclin E "wild-type" form, as no clones representing the cyclin E 45kDa was detected in either cell lines (see below). For every 30 molecules of cyclin E mRNA 15 are of the EL species while the rest are equally divided among the Δ9, Δ148, ET, ES and assorted combinations of these species. We conclude that any novel cyclin E splice variants undetected by RNase protection and RT-PCR library screening would be too rare to make a significant impact on cyclin E protein expression. Additionally due to the relatively equal abundance of the 5 splice variants of cyclin E in normal and tumor cells, the alternative splicing of cyclin E cannot account for the LMW forms of the protein observed predominately in tumor cells.

Mass Spectrometry Confirms the Predominant Cyclin E is the EL Form: Our RT-PCR restriction mapping strategy (Fig 8) identified E-L as the high molecular weight cyclin E form found in both normal and tumor cells. Cyclin EL is the 15 amino acid elongated variant of cyclin E identified in 1995 [65], while the cyclin E wild type is the 45 kDa protein identified in yeast complementation studies first identifying cyclin E [35,97]. To directly establish the identity of the high molecular weight cyclin E protein found in both normal and tumor cells we purified cyclin E from 2×10^{10} MDA-MB-157 cells (500 mg total cellular extract) with a cyclin E monoclonal antibody (clone HE-111) affinity column. The purified cyclin E was eluted from the column and resolved by SDS PAGE. After silver staining the gel, the band corresponding to the high molecular weight (i.e. 50 kDa) cyclin E was excised, reduced, alkylated and digested with trypsin according to established procedures [98]. The tryptic peptides were extracted from the gel slice and analyzed by matrix-assisted laser desorption/ionization time-of-flight mass spectrometry (MALDI-TOF MS) (Fig 9). Mass spectrometric analysis of the tryptic peptides yielded 10 highly representative peptide sequences detected from both the N- and C-terminal domains of cyclin E. The mass-spectrum of the purified cyclin E tryptic digests as analyzed by MALDI-TOF is depicted in Fig 9A. The alignments of the 9 peptides to cyclin E are shown by solid bars underneath the schematic

representation of cyclin EL (Fig 9B). The shaded region defines the unique cyclin EL sequences not found in the 45 kDa cyclin E. Three of these tryptic peptides contained sequences from N-terminus of the EL form of cyclin E, not present in the 45 kDa form of cyclin E wild-type (5,7,9,10). All 4 peptides contain a methionyl from position 16 (M16) of the intact EL form of cyclin E which could only derive from the EL cyclin E and not the 45 kDa cyclin E. Mass spectrometric peptide sequencing of the 4 peptides containing EL specific sequences was also performed by MALDI combined with postsource decay (PSD) fragment ion mass analysis as described [99]. This sequence analysis confirms that the 50 kDa high molecular weight cyclin E found in both normal and tumor cells is the EL form of cyclin E. The locations of the 10 peptides are listed in Fig 9C.

Identification of cyclin E binding proteins: The cyclin E purification described above not only enabled us to unequivocally identify the 50 kDa cyclin E as the cyclin EL form, but also enabled us to identify cyclin E binding proteins. The HE-111 cyclin E clone used to make the affinity column for the purification of cyclin E has the added advantage of binding to all the LMW forms of cyclin E (Fig 10). Furthermore by using this approach, we were able to identify a number of proteins specifically co-precipitating (i.e. co eluting) with cyclin E. The co-eluting molecules included proteins previously identified to interact with cyclin E containing complexes, such as CDK2, p21 and p27. We identified these proteins both by excising the bands from the silver stained gel (Fig 10A) containing the eluted, purified cyclin E forms and subjecting them to mass spectrometric analysis as described above, and by Western blot analysis (Fig 10B). The tryptic peptides corresponding to individual bands which were analyzed by MALDI-TOF mass spectroscopy reveal that in addition to the expected cyclin E, there are a number of other bands of known and unknown proteins which could be binding to cyclin E. This method has clearly identified several bands, each containing only one protein, such as CDK2 which is a known cyclin E binding or interacting proteins. However, this procedure also identified potential novel cyclin E binding/interacting proteins such as CDK5, HSP27, HSP70, helicase, toposiomerase 1,

BRCA1 associated RING domain protein, U5 snRNP 100 kDa protein, pre-mRNA splicing factor, and CENP-E proteins. The silver stained bands corresponding to some of these proteins are shown in Figure 10A, lane 13 The association of some of the known cyclin E interacting was confirmed by Western blotting. For these analysis we used fractions from different steps of cyclin E purification including starting material, flow through, washed, and eluted fractions. The Western blot analysis of these fractions with antibodies against cyclin E revealed that this purification scheme can also elute all the LMW forms of cyclin E found in tumor cells which we are identifying as cyclin EL-1 to EL-6 (see below for further discussion on this point). Western blot analysis with other known cyclin E binding proteins reveals that cyclin E complexes purified from MDA-MB-157 also contain CDK2, p21, and p27. We are currently obtaining antibodies for some of the other proteins we have found to associate with cyclin E from our mass spectrometric analysis, to use in Western blot analysis. Our future plans are to further characterize these cyclin E binding proteins in normal and tumor cells and identify which cyclin EL LMW form can specifically bind to or interact with which one of these cyclin E associated proteins. Since our purification scheme results in the elution of all the LMW forms of cyclin E and the immune complexes formed with each, we now have the tools to specifically determine the functional significance of each of these LMW forms by determining some of the components of the complexes each one is forming.

Block Deletions and Amino-acyl Substitutions Define the Precise Proteolytic Domain in Cyclin E: To identify the precise locations of where cyclin E is proteolytically processed to generate the LMW forms detected in tumor cells, we transiently transfected mutated and selectively deleted forms of epitope tagged cyclin EL into tumor cells and analyzed their expression by Western blot analysis. These deletional analysis will also determine whether the 45 kDa wild-type form is represented in these LMW forms of cyclin E. Since, the EL mRNA appears to code for the predominant 50kDa form detected by Western blot (Figs 7-10), the EL form of cyclin E was used as the backbone for all subsequent expression vectors. Initially, a

cyclin EL-epitope tagged cDNA was generated by PCR to contain a sequence coding for the 8 amino acid FLAG epitope at the carboxy terminus (see Fig 4A). In figure 4 we showed that transient transfection of cyclin EL-FLAG into MDA-MB-157 resulted in its processing into several LMW isoforms as well as the full-length form (Fig 5). Our results from figures 4-6 also suggest that processing of FLAG tagged cyclin E occurs in a fashion identical to the endogenous cyclin E, producing forms 1 kDa larger (i.e. the mass of FLAG) in the same pattern. A total of 6 cyclin E forms were detected by Western blot which we have termed cyclin EL-1 (longest) to cyclin EL-6 (shortest) (Fig 10B). Since further splicing of the mRNA transcribed from the transfected plasmid is not expected, the altered forms of cyclin E detected by Western blot would have to be generated by post-translational processing. The experiments in figures 4-6 also helped identify the region of cyclin E where proteolytic processing occurs to a 30 amino acid region from residue 64 to 93. To define the exact amino acyl residues involved in the processing a series of block deletions, conservative and non-conservative substitutions were made in amino acyl residues 69-93 (Fig 11). Initially, five successive six amino-acid block deletions of cyclin EL were constructed using oligonucleotides containing the deletions to PCR amplify a domain which was then cloned, sequenced and substituted into the EL-1-FLAG (i.e. full length) expression vector using restriction endonuclease sites. The cyclin E expressed from transiently transfected plasmids was evaluated for proteolytic processing by Western blot with FLAG as before (Fig 11).

These results show that two, six amino-acid block deletions, A (residues 64-69) and B (residues 70-75), were able to prevent the proteolytic processing of cyclin E into bands EL-5 and -6 when transfected into the cell line MDA-MB-157 (Fig 11B). None of the other bands appear to be affected except for the reduction in mass due to the 6-amino acyl deletion A smaller (three amino acyl) block deletion A', reduced but did not eliminate processing (Fig 11B, lane A'). Any other large block deletion further toward the C-terminus had no effect on processing, C, D and E (Fig 11B, lanes C-E). We suspected that the A deletion contained the protease recognition motif and

this domain was targeted for site specific amino acyl substitution. The B deletion may not contain any protease recognition sequence but the deletion brings P76 adjacent to A69 disrupting the ability of the protease to cleave at this site. To test these possibilities, we constructed a series of conserved and unconserved amino-acyl substitutions from amino acid 68-75 (Fig 11C). These substitutions confirm that small hydrophobic amino-acids at positions 68 and 71-75 are not necessary to generate cyclin EL-5 and –6, as seen by the presence of these two LMW forms following individual substitutions of any of these amino acids with alanine or aspartate (Fig 11 C, lanes 2-4 and data not shown). However, the amino acids at position 69 and 70 are required for the generation of both cyclin EL-5 and –6 forms. When the alanine at position 69 (A69) is substitute with aspartate (A69D) or aspartate at position 70 (D70) is substituted by proline (D70P), cyclin E is not cleaved into bands EL-5 and –6 (Fig 11C). Additionally, when alanine is substituted at D70 (D70A) cyclin E is cleaved into the EL-5 and -6 bands, but at much higher levels (Fig 11C, lane 6). Since the bands corresponding to EL-5 and –6 accumulate during the transient transfection, it suggests that the D70A may be a superior substrate for the cyclin E protease than the wild type (compare D70A to EL in panel C). There is precedent for this finding as proline substitution classically converts a substrate into an inhibitor when placed into P1' position of the scissile bond of the proteolytic cleavage site [100].

Cyclin EL-2 and EL-3 do not code for the 45 kDa wild-type form of cyclin E. We suspected that bands EL-2 and -3 represented protein translated from the M16 start site originally thought to be the primary form of cyclin E (i.e. the 45 kDa wild-type form) [35,97]. However, we were surprised when an M16A substitution did not affect the expression of bands EL-2 and -3 (Fig 12). For these analyses we compared the *in vitro* translated products of the mutated constructs of cyclin EL-1, -2, and -4, with the tumor cell transfected proteolytically processed protein products to assess the role of the tumor cell machinery to generate the LMW forms of cyclin E (Fig 12). When the protein from EL-1-FLAG transfected MDA-MB-157 is run side by side with the *in vitro* translated cyclin E products from the same vector, the bands EL-2

and -3 clearly migrate faster than the *in vitro* translation products from the M16 translation start site. This difference in migration between M16 *in vitro* translated band and EL-2 and -3 in the tumor cells, was a hint that M16 may not be required to generate EL-2- the LMW band we suspected to be the 45 kDa cyclin E wild-type [35,97]. We then substituted the methionine on the amino acid 16 and 46 to aspartate to knock out any alternative translation from these sites. The M16A and M46A substitutions clearly eliminate translation starts from these sites when translated *in vitro* (Fig 12, compare lanes 1 to 3 and 5). However only the M46A substitution eliminates EL-4 from transfected MDA-MB-157 cells, while M16A substitution had no effect on the generation of EL-2 (Fig 12). Even though EL-2 and -3 migrate very close to the cyclin E translated from M16, these bands must be created by proteolysis not by alternate translation at M16. The *in vitro* mutagenesis of cyclin E shown here and mass spectrometry and RT-PCR data shown in figures 2 and 3 collectively provide evidence that the high molecular weight form of cyclin E found in tumor cells is the cyclin E-L [65] and that the EL-2 and EL-3 do not code for the 45 kDa cyclin E wild-type form initially cloned as this G1 cyclin [35,97]. Furthermore, EL-4 is the result of alternative translation at M46, since it can be eliminated by mutation of the methionyl at residue 46 into alanine (Fig 12). The cyclin E formed by the translation start at M46 can be detected in both normal and tumor cells (see Fig 1). The proteolytically processed bands however are only seen tumor cells.

Identification of elastase class of enzymes as the protease generating the LMW forms of cyclin E. The results of Fig 11 suggest a novel type of proteolysis cleaving cyclin E in to EL-5 and EL-6. We believe the same type of proteolysis cleaves cyclin E into EL-1 and EL-2. The tumor specific pattern of cyclin E generating EL-1, 2, 5, and 6 is not the result of overexpression or constitutive expression of 50 kDa cyclin E since normal cells transfected with cyclin E under a strong constitutive promoter process cyclin E normally (see Fig 5). The proteolysis we describe also differs from the proteasome proteolysis of cyclin E described by two laboratories nearly simultaneously [101,102]. Although the destruction of cyclin E may be mediated through the

ubiquitination-proteasome pathway in tumor cells, the generation of the LMW forms observed under steady state conditions in tumor cells and tissues may not be generated by the proteasome pathway. The manner by which the proteasome proteolytic machinery degrades proteins, is either all or none. Once a protein has been tagged for proteasome degradation, it is completely degraded. Since the LMW forms of cyclin E are present constitutively in the tumor cells [60], they do not represent the intermediate proteolytic products of degradative machinery. These LMW forms of cyclin E are more likely due to the action of a non-proteasome protease. The processing of cyclin E into its LMW forms, is also different than how other cyclins are proteolyzed in the cell. For example, cyclin D1 is degraded by a calpain protease [103].Cyclin A is cleaved *in vitro* by a p27 dependent protease which removes the destruction box and allows evasion from proteasomal degradation [104].

The proteolysis we describe for cyclin E at A69-D70 does not appear to occur to other cyclins. This site is similar to elastase sensitive sequences containing essential small hydrophobic residues. When A69 is replaced with an aspartyl residue (amino-acyl substitution), the proteolysis is nearly completely blocked. The D70P substitution completely blocks degradation presumably due to the unique imino-peptide bond afforded by the proline residue within the scissile bond. The effect of proline at position 70 is not surprising since this is commonly used in the design of peptide inhibitors of proteases [105]. The involvement of an aspartyl residue in the cleavage site raises the possibility that a caspase protease might be involved, yet the typical DEVD motif is not present. In addition, the cyclin E protease appears to cleave on the N-terminal side of D70, contrary to a caspase cleavage on the C-terminal side of aspartyl residues. For example, a caspase activity which cleaves cyclin A during apoptosis in Xenopus embryos cleaves downstream of a critical aspartyl residue [106]. In the case of cyclin E, the D70A mutation does not block proteolysis of cyclin E and in fact may encourage it (Fig 11). We refer to the cyclin E protease domain stretching from A66-P71 as AVCADP. These are a short hydrophobic stretch of amino acids followed by aspartate-proline. This sequence has the top

PEST score of any PEST domain in cyclin E [107] and is embedded in a random coil (GOR4 predicted) secondary structure (termed loop 2) bearing a striking similarity to the scissile domains of the serine proteinase inhibitors PS and SSI, which could make the AVCADP sequence accessible to the protease. A second cleavage point nearer to the N-terminus in the domain from K32-K48, is currently being characterized and we predict it to be involved in generating the cyclin E bands EL-2 and -3. This site has the sequence VFLQDP, similar to AVCADP and appears to be in a similar random coil structure (GOR4) and is termed loop 1.

The criteria described above for the candidate protease cleaving cyclin E into the EL2, -3, -5 &-6 LMW forms, suggests that this protease may be of the elastase class. To directly address this hypothesis we determined whether purified elastase is capable of cleaving *in vitro* translated cyclin E into its LMW isoforms observed in tumor tissues. As shown in figures 11 & 12 the *in vitro* translated cyclin E-L protein products are the EL-1 and 2 other protein products which initiated alternative translation sites M16 and M46. M46 is responsible for the generation of EL-4. However EL-2, -3, -5, & -6 are not translated *in vitro* from a full-length EL construct. If elastase is the enzyme generating the EL-2, -3, -4, and -5 isoforms of cyclin E, then treatment of the *in vitro* translated cyclin E-L should give rise to these isoforms. We incubated the cyclin EL construct as well as the block deletions and single amino acid mutated constructs of cyclin EL we used in transfection studies presented in figures 11 & 12 in *in vitro* enzyme assays with commercially available porcine pancreatic elastase. These analysis clearly show that the proteolysis of cyclin E in cells is very similar to proteolysis of cyclin E *in vitro* using commercial elastase. *In vitro* translated (reticulocyte lysate) wild type cyclin E and similar proteins translated from constructs containing mutations previously used for transfection, all digest in vitro with a porcine pancreatic elastase, generating a Western blot pattern similar to the *in vivo* (i.e transfected) pattern (Fig 13). Incubation of 10^{-4} units of the purified elastase enzyme with in vitro translated cyclin EL products resulted in generation of and EL-6 (compare lanes 1-no elastase, and lane 2 with elastase). Block deletions A and B knocked out the EL-6 production, while block

deletions A', B, C, and D were incapable of knocking out the EL-6- similar to tumor cell transfection of FLAG tagged cyclin EL constructs. One difference between the elastase/cyclin EL *in vitro* proteolysis versus tumor cell transfection of the same constructs is the appearance of EL5 and EL6 in tumor cells and only EL-6 in *in vitro* elastase enzyme assays. As suggested earlier we believe the generation of the EL5/6 doublet is the result of post-translational modification of EL6-most probably by phosphorylation which cannot be generated *in vitro*.Incubation of the point mutations of cyclin EL constructs by elastase also generated or knocked out the LMW forms of cyclin E as seen with the tumor cell transfection of the same constructs (Fig 13).

For example, incubation of the *in vitro* translated mutant constructs V67D and C68D generated EL6 and EL3, while mutant constructs A69D and D70P knocked out EL-6 but not EL-3. Incubation of the D70-A *in vitro* translated cyclin EL with the elastase resulted in higher amount of EL-6, similar to what observed in tumor cell transfection. One curiosity that the point mutation constructs, and not the block deletion constructs, show is the generation of the EL3 by elastase with the point mutation constructs. The generation of EL-3 in incubation mixtures containing V67D, C68D, and A 69D by elastase may be due to the fact that these point mutations of cyclin EL, render the protein a better substrate for elastase to generate the EL3 band. For the *in vitro* studies described here we used purified porcine elastase enzyme. Even though human and porcine enzyme share close to 98% sequence homology, it is possible that the human elastase may have preferential specificity for both the cyclin E sequences generating the EL2/3 and EL5/6. Alternatively, two different elastases could be generating each of the EL2/3 and EL5/6 LMW isoforms of cyclin E. These hypotheses will be rigorously examined in the specific aims 1 and 3 of our study, once we have identified the exact sequences in cyclin E giving rise to EL2/3 doublet. The results presented in Fig 13 however suggest that elastase could be the serine protease which cleaves cyclin E into its LMW forms. The specificity, regulation and inhibition of this serine protease *in vitro* and in normal and tumor cells will be analyzed by our future studies.

Aims 3 & 4: Role of p21/p27 in G1/S checkpoint control in normal and tumor cells. The 3rd and 4th aims of the study deal with the interplay of the negative cell cycle regulators, p21 and p27, on the overexpression of cyclin E which leads to G1/S checkpoint deregulation in tumor cells. We have made significant strides on these two aims which have resulted in 6 manuscripts, four published and two submitted. Since I have enclosed copies of these manuscripts in the Appendix I will only summarize the results of these three studies in the following paragraphs. As apparent by our findings summarized below, we have completed these two aims.

In the first study entitled "Lovastatin Mediated G1 Arrest in Normal and Tumor Breast Cells is Through Inhibition of CDK2 Activity and Redistribution of p21 and p27, Independent of p53" w e have investigated the nature of the CKIs (p21 and p27) alterations resulting in G1 arrest in both normal and tumor breast cell lines by lovastatin (Appendix- Ref 5). We show that even though lovastatin treatment causes G1 arrest in a wide variety of normal and tumor breast cells irrespective of their p53 or pRb status, the p21 and p27 protein levels are not increased in all cell lines treated suggesting that the increase in p21 and p27 protein expression per se is not necessary for lovastatin mediated G1 arrest. However, the binding of p21 and p27 to CDK2 increases significantly following treatment of cells with lovastatin leading to inhibition of CDK2 activity and a subsequent arrest of cells in G1. The increased CKI binding to CDK2 is achieved by the redistribution of both p21 and p27 from CDK4 to CDK2 complexes subsequent to decreases in CDK4 and cyclin D3 expression following lovastatin treatment. Lastly, we show that lovastatin treatment of 76N-E6 breast cell line with an altered p53 pathway also results in G1 arrest and similar redistribution of CKIs from CDK4 to CDK2 as observed in other breast cell lines examined. These observations suggest that lovastatin induced G1 arrest of breast cell lines is through a p53 independent pathway and is mediated by decreased CDK2 activity through redistribution of CKIs from CDK4 to CDK2.

In the second study entitled "The bi-phasic induction of p21 and p27 in breast cancer cells by modulators of cAMP is post-transcriptionally regulated and independent of the PKA pathway" we show that lovastatin's mechanism of p21 and p27 induction is independent of the PKA pathway (Appendix-Ref 6). Cyclic AMP (cAMP) elevation affects growth arrest and differentiation in a wide variety of breast cell lines, however the mechanisms associated with this process are poorly understood. Previous studies linked cAMP mediated growth arrest in breast tumor cells to increased levels of cyclin kinase inhibitor (CKI), p21. In this study we examined the role of cAMP dependent protein kinase (PKA) on p21 and p27 induction in the breast cancer cell line, MDA-MB-157. The induction of the CKIs by modulators of cAMP such as cholera toxin (CT) + 1-isobutyl-3-methylxanthine (IBMX), and lovastatin, fluctuate with bi-phasic kinetics (though the kinetics of CKI induction with CT + IBMX treatment are different from that of lovastatin) and are depicted by the periodic accumulation of lower molecular weight forms of p21 and p27 which also correlate with fluctuations in CDK2 activity. Using three different approaches we show the cAMP mediated induction of CKIs is independent of PKA activity. In the first approach we treated MDA-MB-157 cells with a variety of cAMP modulators such as CT, IBMX, and Forskolin in the presence or absence of H-89, a potent PKA inhibitor. This analysis revealed that the cAMP activators were capable of inducing p21 even though PKA activity was completely eliminated. In the second approach PKA dominant negative stable clones of MDA-MB-157 treated with CT + IBMX or Forskolin also resulted in p21 induction, in the absence of any PKA activity. Lastly, treatment of MDA-MB-157 cells with lovastatin, another known cAMP modulator which also causes growth arrest, resulted in the induction of p21 and p27 without any increase in PKA activity. Collectively, the above results suggest that the induction of p21 by cAMP is through a novel pathway, independent of PKA activity.

In the third study entitled "Lovastatin induction of CKIs (p21 and p27) and mevalonate reversal of lactacystin are both through modulation of the proteasome, independent of HMG-CoA reductase" we show that the mechanism of lovastatin mediated stabilization of p21 and p27 may be due to a previously unknown function of the pro-drug, ß-lactone ring form of lovastatin to inhibit the

proteasome degradation of these CKIs (Appendix, Ref 7). We show that lovastatin pro-drug (20% of the lovastatin mixture) inhibits the 20S proteasome but does not inhibit HMG-CoA reductase. In addition, many of the properties of proteasome inhibition by the pro-drug are the same as the specific proteasome inhibitor lactacystin. Lastly, mevalonate (used to rescue cells from lovastatin arrest) unexpectedly reverses the lactacystin inhibition of the proteasome. Mevalonate increases the activity of the proteasome, which could result in degradation of the CKIs causing the release of lovastatin- and lactacystin-arrested cells.

In the fourth study entitled "UCN-01 Mediated G1 Arrest in Normal But Not Tumor Breast Cells is pRb Dependent and p53 Independent", we pharmacologically assessed how alteration of G1/S checkpoint could lead to response to inducers of G1 arrest in tumor cells (Apendix-Ref 8). In this study we investigated the growth inhibitory affects of UCN-01 in several normal and tumor-derived human breast epithelial cells. We found that while normal mammary epithelial cells were very sensitive to UCN-01 with an IC_{50} of 10 nM, tumor cells displayed little to no inhibition of growth with any measurable IC_{50} at low UCN-01 concentrations (i.e. 0-80nM). The UCN-01 treated normal cells arrested in G1 phase and displayed decreased expression of most key cell cycle regulators examined, resulting in inhibition of CDK2 activity due to increased binding of p27 to CDK2. Tumor cells on the other hand displayed no change in any cell cycle distribution or expression of cell cycle regulators. Examination of E6 and E7 derived strains of normal cells revealed that pRb and not p53 function is essential for UCN-01 mediated G1 arrest. Lastly, treatment of normal and tumor cells with high doses of UCN-01 (i.e. 300 nM) revealed a necessary role for a functional G1 checkpoint in mediating growth arrest. Normal cells, which have a functional G1 checkpoint, always arrest in G1 even at very high concentrations of UCN-01. Tumor cells on the other hand have a defective G1 checkpoint and only arrest in S phase with high concentrations of UCN-01. The effect of UCN-01 on the cell cycle is thus quite different from staurosporine, a structural analogue of UCN-01, which arrests normal cells in both G1 and G2, while tumor cells arrest only in the G2 phase of the cell cycle. Our results show the different

sensitivity to UCN-01 of normal compared to tumor cells is dependent on a functional pRb and a regulated G1 checkpoint.

In the fifth study entitled "Activation of the estrogen signaling pathway by p21$^{WAF1/CIP1}$ in ER negative breast cancer cells" we show that overexpression of p21 in otherwise ER and p21 negative breast cells, activates the estrogen signaling pathway (Appendix-Ref 9). *Background:* The steroid hormone, estrogen, regulates the proliferation of normal mammary gland as well as most estrogen receptor (ER)-positive mammary carcinomas. Several cell cycle regulatory proteins have been implicated for the growth stimulatory action of estradiol as well as the growth inhibitory activity of anti-estrogens. We propose the novel hypothesis that p21, a cyclin dependent kinase inhibitor which acts as the brake of the cell cycle, plays a significant role in regulating the estrogen receptor (ER) signaling pathway. *Methods*: The effects of p21 on the ER pathway was investigated by overexpression of p21 using a tetracycline inducible system in a breast cancer cell line negative for ER and p21. Activity of the estrogen-signaling pathway was monitored by examining the activity of the ER-promoter-Luciferase and Estrogen-Response-Element (ERE)-Luciferase in transient transfection assays. Additionally the growth modulating affects of estradiol and anti-estrogens were assessed on the p21-overexpressing clones. *Results*: A strong positive correlation was found ($p<0.001$) between the expression of p21 and estrogen receptor in breast cancer cell lines and tumor tissues from 60 breast cancer patients. Overexpression of p21 in a p21 and ER negative cell line leads to induction of ER- and ERE-Luciferase activities in an estrogen responsive manner. The transcriptional activation of both ER- and ERE- was induced significantly by the addition ß-estradiol to the culture medium of the p21 clones. Lastly, the expression of p21 leads to the sensitization of these p21 stable clones to the growth inhibitory effects of a potent anti-estrogen (i.e. ICI 182780) and the growth stimulatory effects of ß-estradiol. *Conclusion:* Taken together, these results suggest that p21 has a novel role in activation of the estrogen-signaling pathway.

In the sixth study entitled "Selective killing of breast cancer cells by reversible, G1 arrest of normal cells" we show that normal proliferating cells can be protected against the toxic effects of chemotherapy by treatment with very low concentrations of Staurosporine (Appendix-Ref 10). *Background:* Two major limiting factors in human cancer chemotherapy are toxicity to the normal tissues and drug resistance in the tumor tissues. We show that taking advantage of cell cycle checkpoint differences between normal and cancer cells can circumvent these limitations and protect the normal proliferating cells from the toxic effects of chemotherapeutic agents. *Methods:* Normal mammary epithelial cells were initially treated with Staurosporine (ST) at cytostatic (i.e. non-lethal) concentrations, which preferentially arrest normal cells in G0/G1 phase of the cell cycle without affecting the proliferation of tumor cells. Following the selective arrest of normal cells in G0/G1, both normal and tumor cells were treated with Doxorubicin or Camptothecin, two cytotoxic (i.e. lethal) chemotherapeutic agents. *Results:* Only tumor cells were selectively killed by chemotherapeutic agents while normal cells were unaffected and resumed proliferation following removal of drug. Additionally, normal circulating lymphocytes induced to proliferate *in vitro* were also protected against the toxic affects of chemotherapeutic agents by ST-mediated G0/G1 arrest. The reversible arrest of normal cells in G0/G1 by ST increased the maximum tolerated doses of Doxorubicin in excess of 100-fold over the concentrations that completely eradicated all tumor cells in culture. ST-mediated G0/G1 arrest is pRb-dependent and p53-independent. It is also accompanied by a rapid and significant decrease in CDK4 protein levels, followed by accumulation of hypo-phosphorylated pRb, increased binding of CKIs (p21, p27) to CDK2, and inhibition of CDK2 activity in normal cells. *Conclusions:* By targeting cancer cells that have defective checkpoints governed by the pRb pathway, while inducing G0/G1 arrest in normal cells, we have designed a strategy to selectively kill breast cancer cells while protecting normal cells.

Figures and Tables:

Cell Lines	Cell Types	ER	P53	Tumorig.	pRB*
1 - 70N	N-mortal	-	+	-	+
2 - 81N	N-mortal	-	+	-	+
3 - 76N	N-mortal	-	+	-	+
4 – MCF-10-A	Immortalized	-	+	-	+
5 – 76NE6	Immortalized	-	-	-	+
6 – MCF-7	A (pe)	+	+	+	+
7 - T47D	DC (pe)	+	-	+	+
8 -BT20	C	+	+	+	+
9 - ZR75T	IDC	+	+	+	+
10 - MDA-MB-157	C (pe)	-	-	+	-
11 - MDA-MB-231	A (pe)	-	-	+	+
12 - MDA-MB-436	A	-	-	+	-
13 - HBL-100	T (bm)SV40	-	-	-	-
14 - HS-578T	DC	-	-	+	-

Table 1: Characterization of normal, immortalized and tumor-derived breast epithelial cells N, normal breast cells from reduction mammoplasty; A, adenocarcinoma; pe, pleural effusion; C, carcinoma; DC, ductal carcinoma; T(bm), tumor breast milk); IDC, infiltrating DC. + Indicates wild type, - mutant or not expressed. * pRb status where + indicates wild type and present in hypo- and hyper-phosphorylated forms and - indicates mutated or virally bound or inactive.
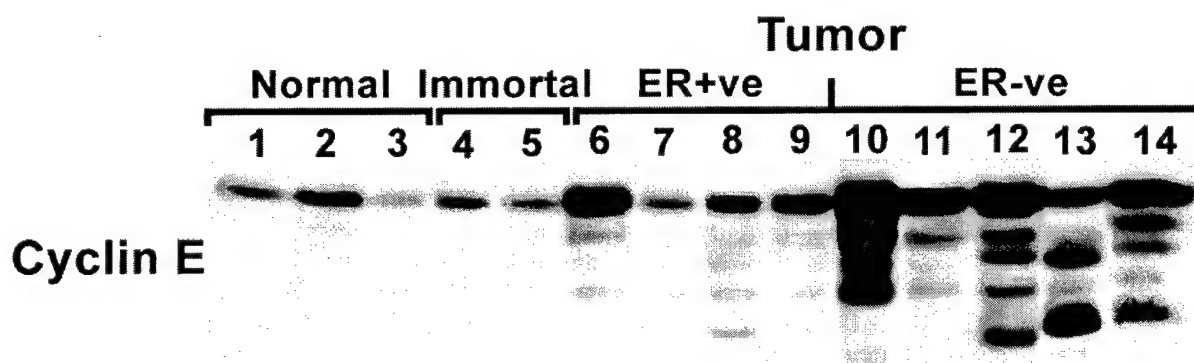
Figure 1. Overexpression of cyclin E LMW forms in breast cancer cell lines. Western blot analysis of cyclin E in normal, immortalized and tumor cell lines. The list of normal cell strains (lanes 1-3), immortalized cell lines (4-5) and tumor cell lines (lanes 7-15) is presented in Table 1 (using identical numbers). 50µg of total cell extract were run on SDS polyacrylamide gels. Proteins were transferred to Immobilon P and blots were incubated with anti-cyclin E and –actin antisera and immuno-reactive proteins detected with the ECL reagent (Amersham).

Total Number of Cases Examined:			403	
Year of Diagnosis:	1990-1995			
Average Follow-up	48 months			
			ER	
			+ve	-ve
Age:	< 50	103 (25%)	57 (55%)	46 (45%)
	≥ 50	300 (75%)	201 (67%)	99 (33%)
Stage Groupings (i.e. TNM)				
		I		125 (31%)
		II		186 (46%)
		III		57 (14%)
		IV		35 (8.7%)

Table 2: Population demographics of patient population used for the cyclin E study.
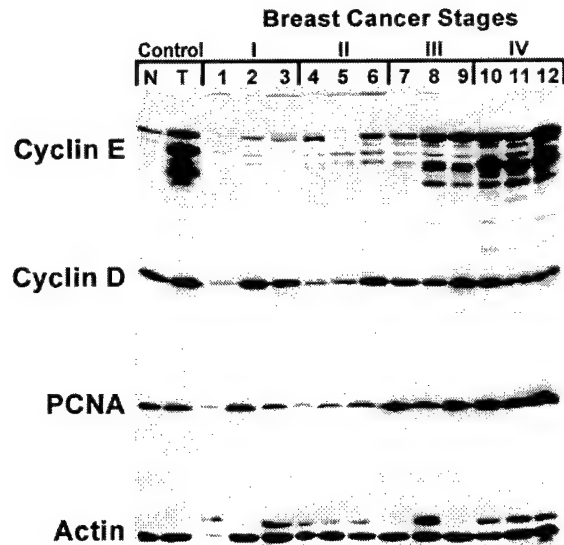
Figure 2: Cyclin E, a potential prognostic marker for breast cancer.

Whole cell lysates were extracted from 12 breast cancer tissues obtained from patients diagnosed with infiltrating ductal carcinoma. The Clinical staging, (i.e. TNM) is indicated. Protein extracts were analyzed on Western blots (50 μg of protein extract/lane) and hybridized with the indicated antibodies. The control lanes correspond to cultured normal and tumor cell lines, where N=76N normal cell strain and T=MDA-MB-157 tumor cell line.

Outcome	Low Cyc. E	High Cyc. E	Total Cases
Alive (NED)	262 (93%)	11 (9%)	273
Dead or with cancer	19 (7%)	111 (91%)	130
Total cases	281	122	403

	Low Cyc. D1	High Cyc. D1	Total Cases
Alive (NED)	146 (73%)	115 (57%)	261
Dead or with cancer	55 (27%)	87 (43%)	142
Total cases	201	202	403

Table 3: Cyclin E, a better prognostic marker for breast cancer than cyclin D1. Levels of cyclins E and D1 were examined by Western blot analysis on 403 breast cancer cases. High and low cyclin E and D1 levels were scored according to densitometric scanning and correlated to patient prognosis. Good prognosis is when the patient is alive, with no evidence of disease (NED) while poor prognosis is when the patient has either expired of the cancer or the cancer has metastasized or relapsed.

Stage	Expired/ With Cancer	Alive (NED)	Total
I	12	0	12
II	38	2	40
III	33	5	38
IV	28	4	32
Total	111	11	122
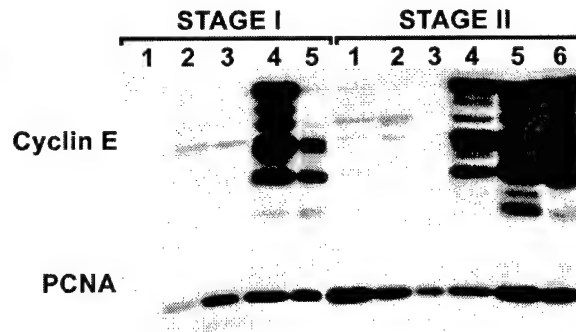
Table 4 and Figure 3: Cyclin E is a stage independent prognosticator for breast cancer. Table 4: The numbers pertain only to those tumors with high cyclin E levels (i.e 122 out of the 403 analyzed by Western blot analysis) and are presented according to the stage of the disease and correlated to patient outcome. Stage of the disease is based on the clinical TNM staging. Good prognosis is when is alive and disease free (i.e NED-no evidence of disease), while poor prognosis is when the patient has either expired of the cancer or the cancer has metastasized or relapsed. **Figure 3:** Whole cell lysates were extracted from 11 breast cancer tissues obtained from patients diagnosed with Stage I (5 patients) and Stage II (6 patients). Protein extracts were analyzed on Western blots (50 μg of protein extract/lane) and hybridized with the indicated antibodies. Patients 1-3 form each stage had a good prognosis (i.e. Alive and NED) while patients 4-5 (Stage I) and 4-6 (Stage II) had poor prognosis and all 5 expired of the disease.
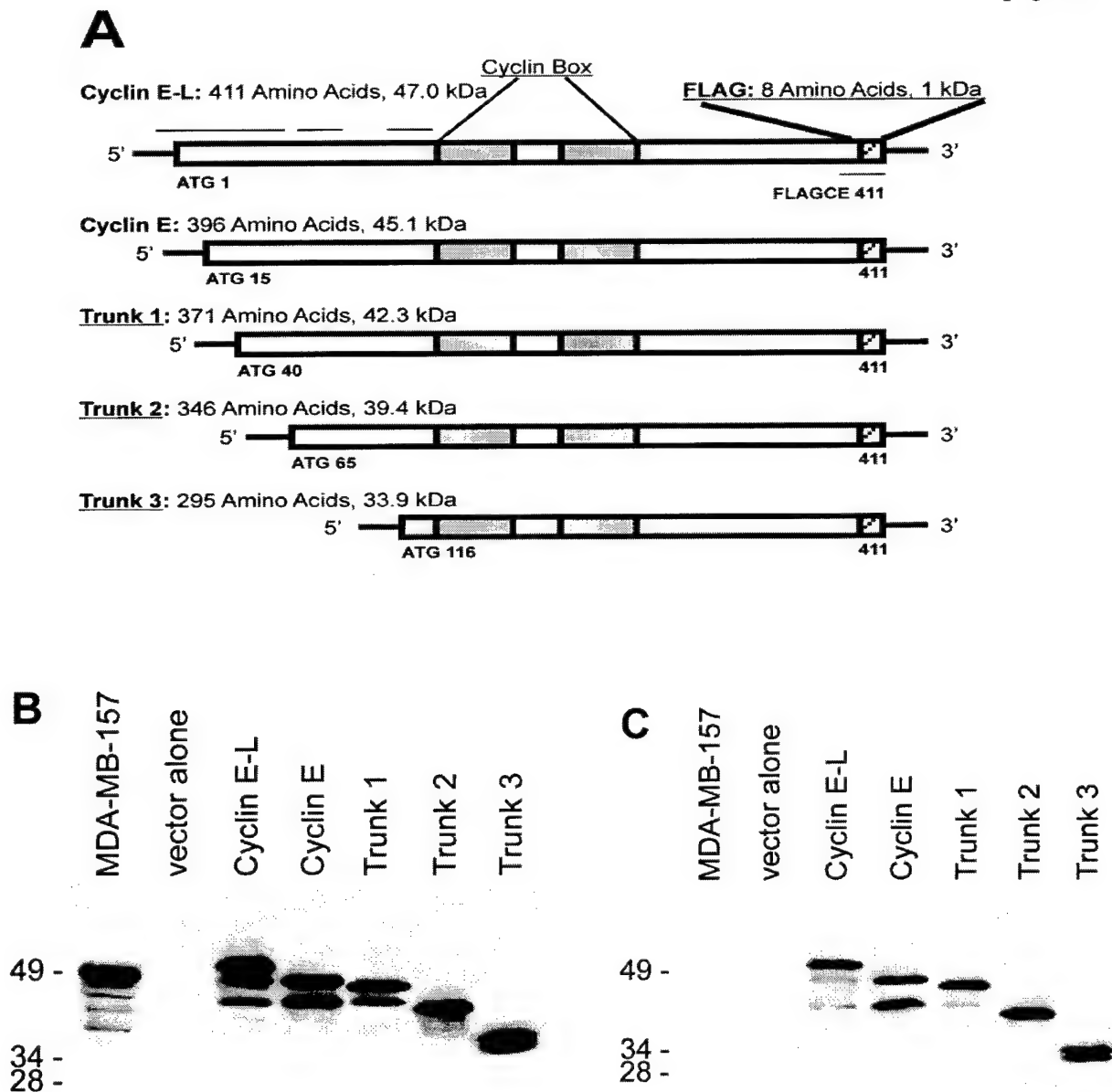
Figure 4: Generation of cyclin E-FLAG constructs, *A Schematic representation of FLAG-tagged cyclin E constructs.* All cyclin E vectors were engineered with a 3' FLAG sequence (FLAGCE) and shown as a right to left arrow, and the 5 different 5' PCR primers used are shown as 5 sequential left to right arrows, representing the 5 different constructs. The FLAG tag region is shown as a hatched box and the cyclin box (CDK binding) region is shown as shaded boxes. The predicted molecular weight of each construct is listed, minus the 1 kDa from the FLAG-tag. *B,C, In vitro translation products of the cyclin E-FLAG constructs.* Cyclin E-FLAG constructs were subjected to *in vitro* translation using the rabbit reticulocyte lysate TNT expression system with a T7 promoter. A one micro-liter aliquot of the translation product was then subjected to Western blot analysis with either *(B)* anti-cyclin E or *(C)* anti-FLAG antibody. For both Western blots lane 1 is 50 µg of MDA-MB-157 cell extract. The vector alone lane is the pCDNA3.1 vector with no insert incubated with the TNT reaction.
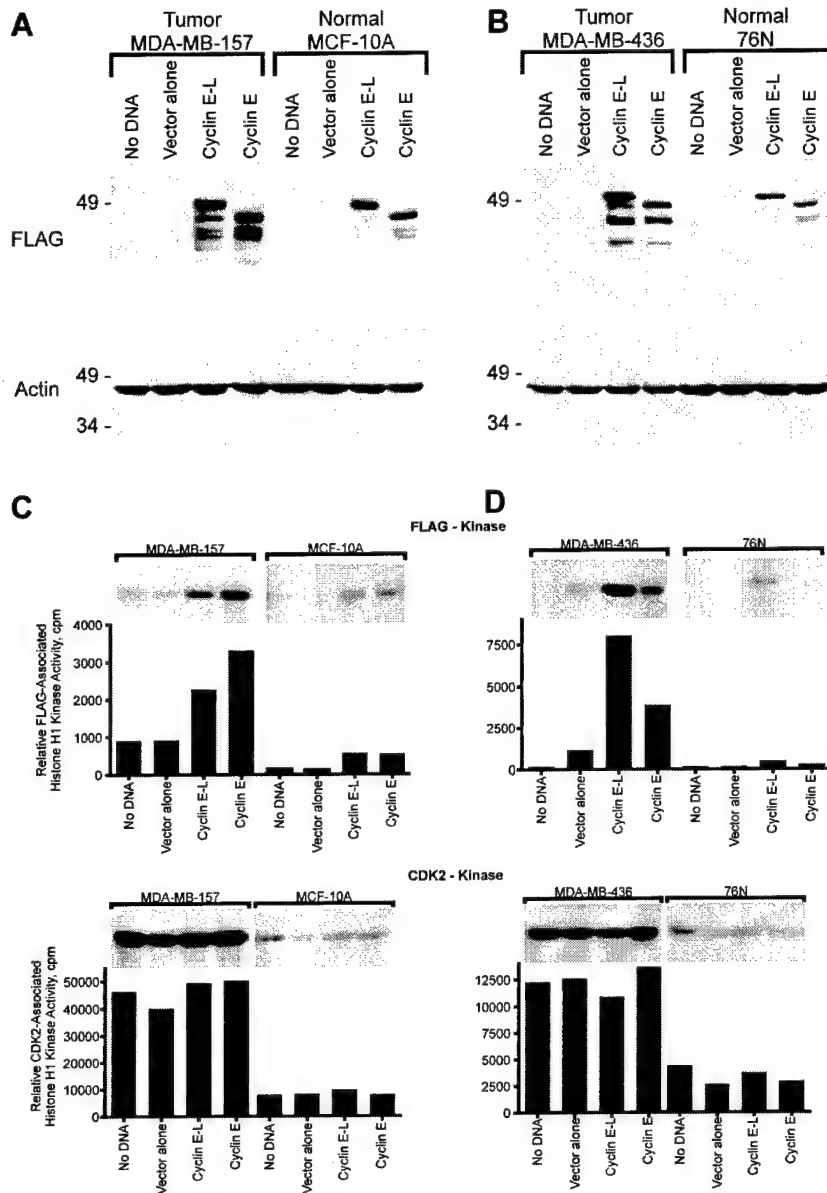
Figure 5: Cyclin E-FLAG is processed into its LMW forms in tumor and not in normal breast cells. Cyclin E-L- and cyclin E-FLAG constructs were transfected into **(A, C)** MDA-MB-157 and MCF-10A or **(B, D)** MDA-MB-436 and 76N cells, harvested 24 hours post transfection and subjected to **(A, B)** Western blot analysis with anti-FLAG and anti-actin antibodies or **(C, D)** Histone H1 kinase analysis. For Western blot analysis 50 µg of protein extract from each condition was analyzed with the indicated antibodies. For kinase activity, equal amounts of protein (100 µg) from cell lysates were prepared from each condition and immunoprecipitated with anti-FLAG or anti-CDK2 antibodies (polyclonal) coupled to protein A beads using histone H1 as substrate. For each condition we show the resulting autoradiogram of the histone H1 SDS-PAGE and its by Cerenkov counting.

CELL LINES	% GFP EXPRESSION
MDA-MB-157	55% (n=10)
MCF-10A	68.4 % (n=10)
MDA-MB-436	14% (n=5)
76N	13% (n=5)

Table 5: Flow cytometric analysis of Green Fluorescent Protein (GFP) expression of transfected cells. Cell lines were co-transfected with cyclin E-FLAG vectors and the pEGFPC-1 vector harboring the cDNA to GFP. Total DNA transfected is 40µg and the ratio of cyclin E-FLAG to GFP vector is 4:1. All cells were transfected by electroporation. Percent GFP expression is measured as a percentage of cells above background fluorescence of cyclin E-FLAG alone and referred to as percent transfection efficiency throughout the text.
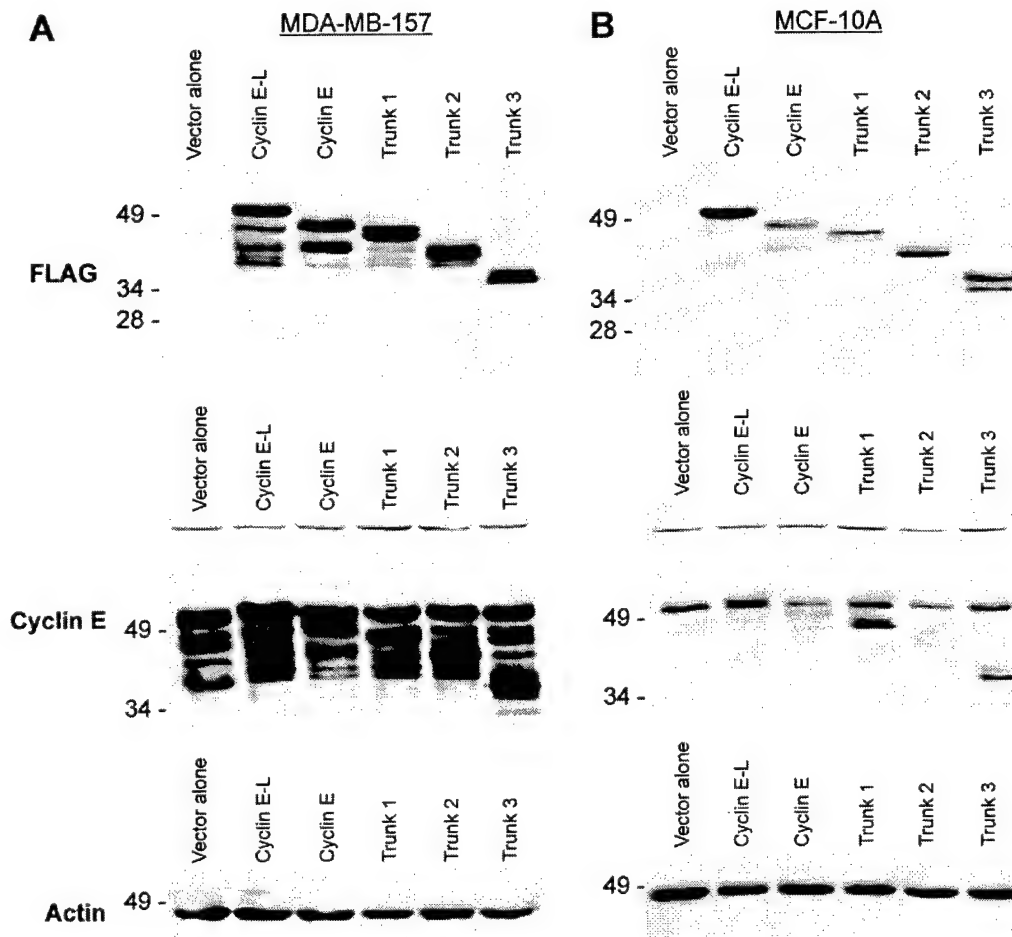
Figure 6: Processing of all the cyclin E- FLAG constructs in tumor but not normal cells. The five different cyclin E-FLAG constructs (see figure 1) or vector alone were transfected into (A) MDA-MB-157 tumor or (B) MCF-10 A normal cell lines, harvested 24 hours post transfection, and subjected to Western blot analysis with the indicated antibodies, actin used for equal loading. The same blots were sequentially hybridized with different antibodies (Fig 2 legends). Vector alone lane is the pCDNA3.1 backbone.

Constructs	Predicted Mass (kDa)	*In vitro* Mass (kDa)	MDA-MB-157 Mass (kDa)	MCF-10A Mass (kDa)
Cyclin E-L-FLAG	48.0	52.0 46.0 41.8	51.9 49.7 45.8 42.6 39.3 37.3	52.0
Cyclin E-FLAG	46.1	46.3 41.5	45.8 42.6 41.2 38.7	46.0
Trunk 1-FLAG	43.3	45.5 41.1	45.5 43.7 41.2 38.7	45.5 43.7
Trunk 2-FLAG	40.4	41.2	42.0 40.3 38.7	41.9
Trunk 3-FLAG	34.8	34.0 36.0	34.5 36.0	34.5 36.0

Table 6: Predicted versus actual mass of cyclin E-Flag constructs translated *in vitro* or transfected into MDA-MB-157 or MCF-10 A cells. The mass determination of *in vitro* translated and transfected protein products of the constructs were analyzed from Western blot analysis performed with anti-FLAG antibody as presented in Figures 1-4. The gels were then scanned and the Kodak Digital Science 1D software (Eastman Kodak Company, New Haven, CT) were used to estimate the actual mass of each protein product detected on Western blot relative to Molecular weight standards run on each gel.

A

C

B

Cell Lines	Cyclin E Copies per cell	Actin Copies per cell
76N	3.1 ± 0.4	3400 ± 10
MCF-10A	2.2 ± 1.1	4200 ± 300
MDA-MB-157	43.5 ± 2.1	2400 ± 10
MDA-MB-231	3.6 ± 1.3	4100 ± 300
MDA-MB-436	8.3 ± 1.4	6300 ± 60
ZR75T	0.9 ± 0.5	3100 ± 200
MCF-7	1.0 ± 0.6	2200 ± 200
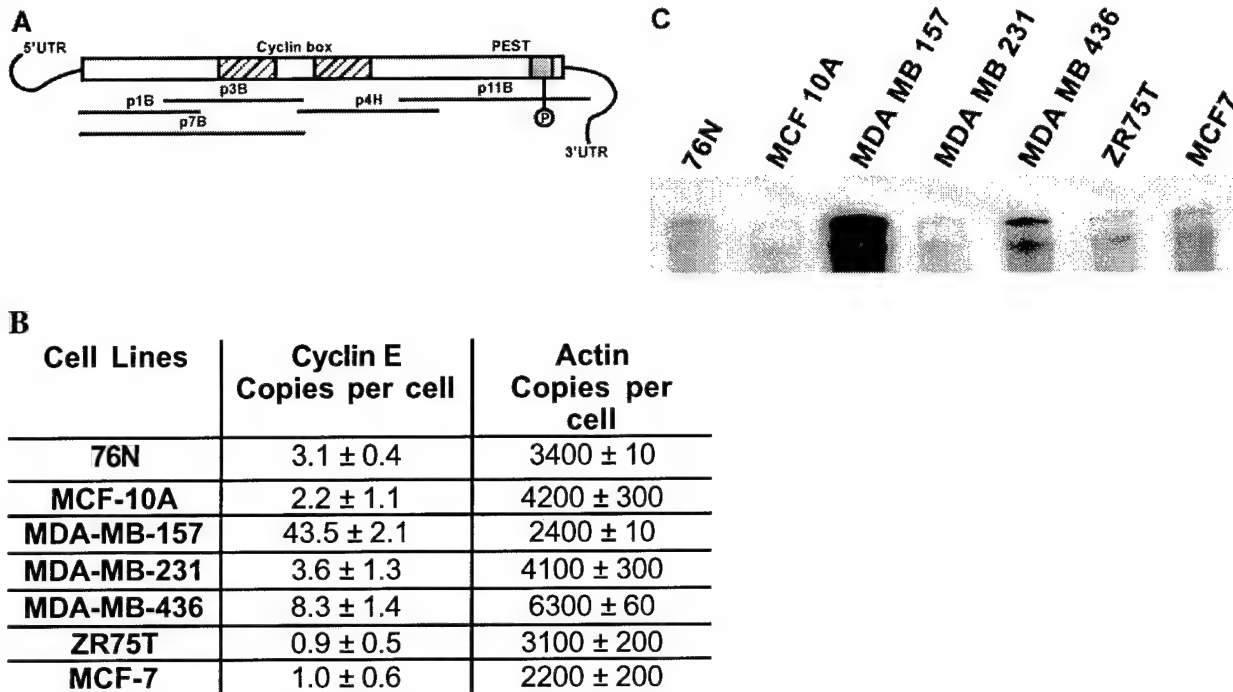
Figure 7: Expression of cyclin E mRNA in breast cancer cell lines. A. Schematic representation of the riboprobes within the cyclin E cDNA used to quantitate cyclin E mRNAs by RPA in normal and tumor cells. **B.** RPA with antisense probe 3B in the normal and tumor cells. The ^{32}P labeled antisense RNA probe protects this region from RNAse digestion, leaving a double stranded fragment which is quantitated by Cerenkov counts. Using the RPA, the cyclin E and actin mRNAs were quantitated in a number of cell lines. **C:** RPA with probe 7B using the mRNA isolated from the indicated cell lines as templates. The presence of two bands which are protected by the probe 7B, indicates that two species of mRNA are present in all the cell lines examined.
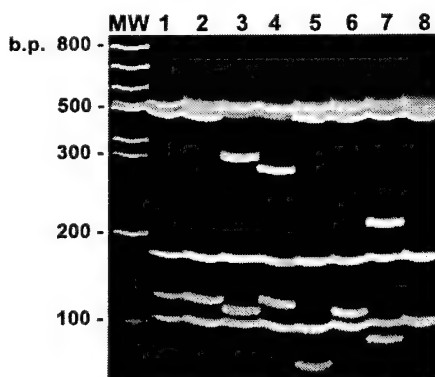
Figure 8: RT-PCR library analysis shows an equal representation of cyclin EL and its splice variants in normal and tumor cells. RT-PCR was performed on normal (76N) and tumor (MDA-MB-157) mRNA using 3' and 5' flanking oligonucleotides to cyclin EL cDNA sequence. The PCR products representing a sample of the cyclin E mRNA species, were then cloned into PCR vector, transformed into E. coli, plated, filter-lifted, probed with ^{32}P cyclin E probe, positive colonies picked, plasmid prepped, PCR was performed again to create a clean product for restriction digest with Sau 3AI, electrophoresed on 5% acrylamide gels and stained with ethidium bromide. The gel represents the different cyclin E splice variants observed in both normal and tumor cells and the identities were confirmed by sequencing. MW, 100 bp ladder. Lane 1, pLXSN-EL plasmid containing the EL form of cyclin E. Lane 2,EL, cDNA identical to pLXSN-EL. Lane 3, Δ9 + ES, cDNA containing the Δ9 splice variant in combination with the ES splice variant. Lane 4, ET, with 135 bp lost from position 706-840 (gccctt...gcagag). Lane 5, Δ48 with, with 48 bp lost from position 22-69 (cgggat...gcggag). Lane 6, Δ9. Lane 7, IN3, with 190 bp genomic sequence from intron 3 which failed to be spliced (bases 1999-2190 of genomic sequence, accgttGTGAGT...TGTTAGtttttg, [63]. Lane 8, Δ97, with 97 bp lost from position 24-120 (ggatgc...ttgcag). The numbers to the right of the gel identify the length in bp of the Sau 3AI restriction fragments from the EL cDNA PCR product.

**A)** Mass spectrometry plot with labeled peaks:
656.39(1), 700.42(2), 948.50(3), 1076.59(4), 1093.55(5), 1145.65(6), 1513.71(7), 1562.78(8), 1798.86(9), 2113.01(10)

B) Schematic of Cyclin EL (M1–A410) and Cyclin E (M16–A410).
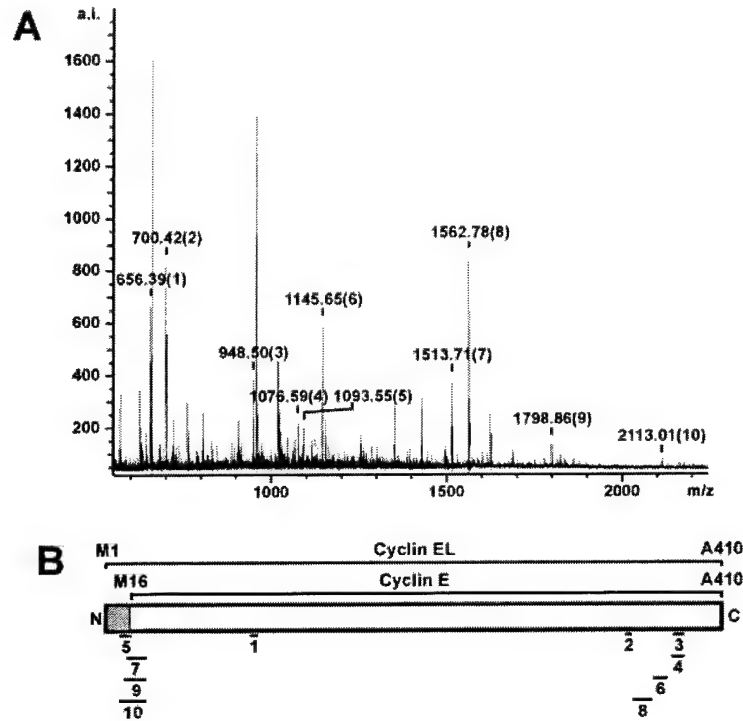
C)

#	Start	End	Peptide Sequence
1	96	101	(R)IIAPSR(G)
2	346	350	(K)LKHFT(G)
3	378	385	(K)AMLSEQNR(A)
4	377	385	(K)KAMLSEQNR(A)
5	9	17	(R)DAKERDTMK(E)
6	365	374	(R)DSLDLLDKAR(A)
7	14	27	(R)DTMKEDGGAEFSAR(S)
8	351	364	(R)GVADEDAHNIQTHR(D)
9	12	27	(K)ERDTMKEDGGAEFSAR(S)
10	9	27	(R)DAKERDTMKEDGGAEFSAR(S)

Figure 9: Mass spectrometry identifies cyclin EL as the 50 kDa cyclin found in tumor cells. A) Mass spec. analysis of the tryptic digests of purified cyclin E band excised from silver stained gel (see Fig 10A). The tryptic peptides were subjected to MALDI-TOF analysis. The major peaks identified all correspond to cyclin E when compared to the available databases through Protein Prospector via the Internet. Cyclin E peaks are designated with a number. Unlabeled peaks correspond to trypsin self-digestion products. B) Schematic representation of cyclin EL and cyclin E. Solid bars show alignments of peptides to different regions of cyclin EL. The shaded region is unique to cyclin EL C) Peptide sequences obtained from mass spectrometric sequencing of cyclin E tryptic digests, corresponding to the identified peaks in A.
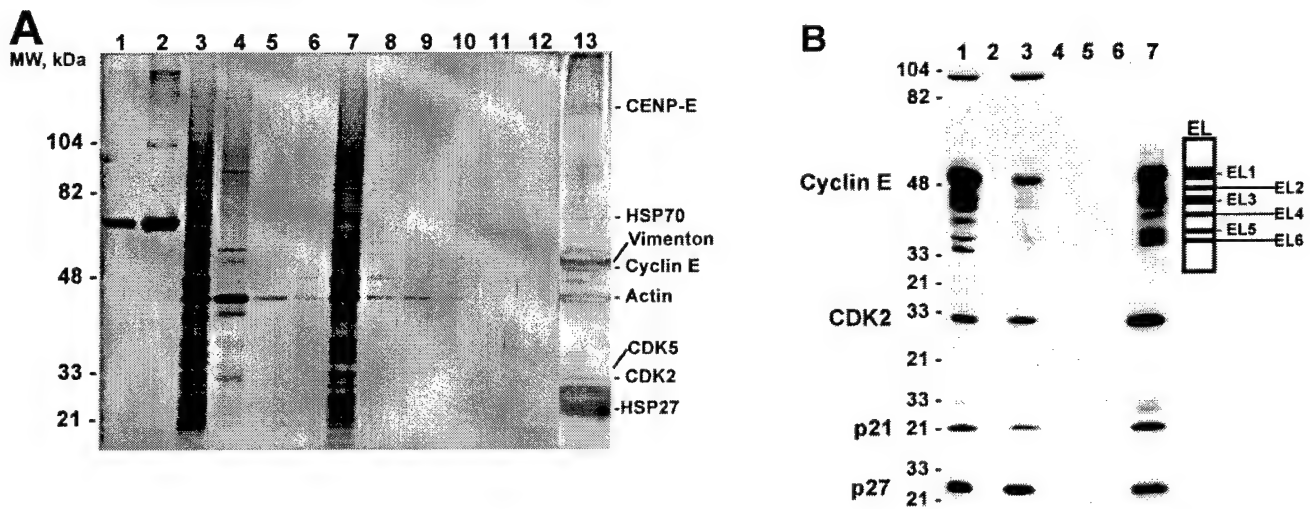
Figure 10: Purification of cyclin E and identification of cyclin E interacting proteins: (A) Silver stained SDS-PAGE showing cyclin E and associated proteins purified on monoclonal antibody affinity column. Lanes 1-2: 5 and 10 pmoles BSA; Lane 3: starting material, Lane 4: Protein A bound non-specific proteins, Lane 5 Flow through, Lanes 4-12: Different washes, Lane 13: Eluted proteins concentrated by on a Centricon 10 concentrator, boiled in reducing sample buffer. The bands labeled in the figure were identified by MALDI-TOF mass spectrometry. **(B)** Western blots of Cyclin E, CDK2, p21 and p27 from cyclin E purification Lane 1: starting material, Lane 2: Protein A bound non-specific proteins, Lane 3: Flow Through, Lanes 4-6: Washes, Lane 7, a small aliquot of the eluted proteins from lane 13 of (A). The Western blot with cyclin E also identifies the 6 isoforms of cyclin E, which were all eluted, as cyclin EL1-6, showing their relative migration on the gel.
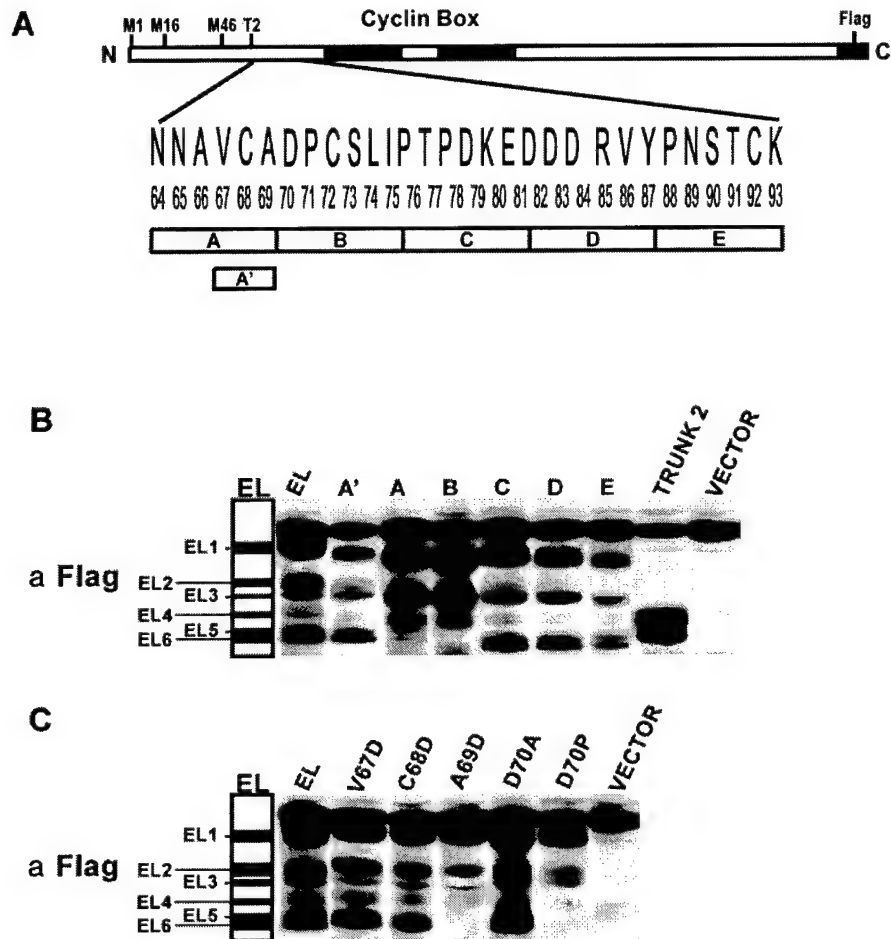
Figure 11: Deletional analysis of cyclin E identifies sequences responsible for generating the LMW forms. A) Schematic representation of cyclin EL highlighting the sequences used for deletional analysis. Five block deletions of 6 amino acids each were made in a 30 amino acid region (64-93) designated A-E. Block deletion A' contains a 3 amino acid deletion spanning from amino acid 67-69. T2 represents the start of cyclin EL-TRUNK2. All constructs were made with an 8 amino acid FLAG peptide fused at the carboxy end. **B)** The block deletions A-E, A' as well as the cyclin EL, Trunk 2 and Vector alone were transiently transfected into MDA-MB-157 cells. Protein was extracted 24 hours post transfection and subjected to Western blot analysis with an anti-FLAG antibody. Note that the block deletions A-E are each 6 amino acids shorter than EL and as such migrate faster on the gel. The band above cyclin EL-1 is a cross reactive protein to the FLAG antibody used and can be seen in all lanes including the Vector alone lane. The relative mobility of EL1-6 is schematically represented to the left of the Western blot in panels B and C. **C)** Transient transfection of cyclin EL-FLAG constructs harboring the indicated point mutations in amino acids 67-70, followed by Western blot with FLAG antibody.
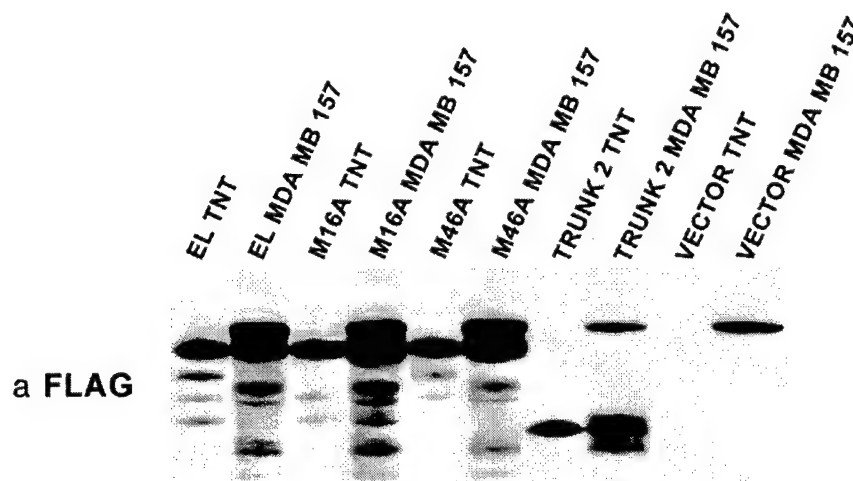
Figure 12: Identification of EL-4 by point mutation: The M16A-, Trunk 2- and M16A-FLAG constructs were transiently transfected into MDA-MB-157 cells. Protein was extracted 24 hours post transfection and subjected to Western blot analysis with an anti-FLAG antibody. The aforementioned constructs were also translated in vitro and 0.25 µl of the reaction mix was subjected to SDS-PAGE and Western blot analysis in the indicated lanes. Vector TNT and MDA-MB-157 represent in vitro translated and transfected empty vectors. The band above cyclin EL-1 is a cross reactive protein to the FLAG antibody used and can be seen in all lanes including the Vector alone lane.
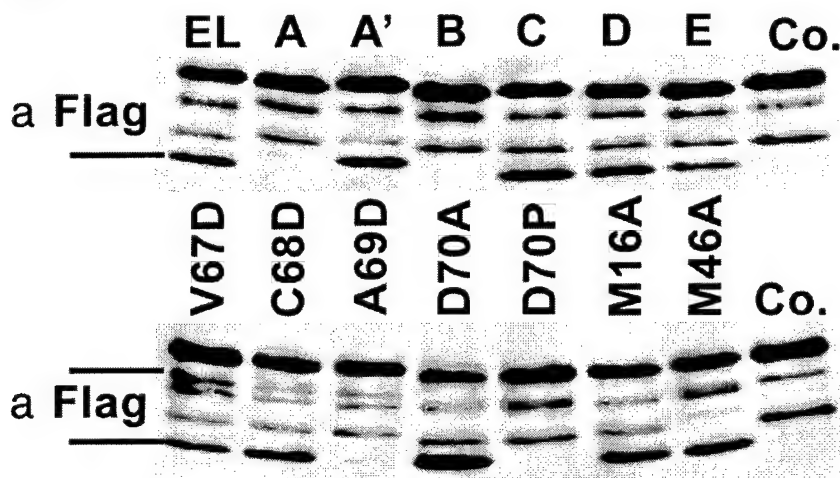
Figure 13: Cleavage of cyclin E constructs by elastase. The block deletions A-E, A' as well as the cyclin EL, Trunk 2, indicated point mutations of cyclin E FLAG tagged constructs as well as the Vector alone construct were translated in vitro using TNT kit (Promega). 10^{-4} units of the porcine pancreatic elastase were mixed with 0.25 µl of the TNT reaction mix (i.e 5 µl of a 1:20 dilution) in the elastase reaction buffer and incubated at 30°C for 5 minutes. At the end of incubation the entire reaction mix (total volume 20 µl) was subjected to SDS-PAGE and Western blot analysis with FLAG antibody. Co: Control-no elastase added to the reaction mix.   The arrows point to the elastase mediated cleavage sites.

7: Key Research Accomplishments:

- Identified the potential of cyclin E as a prognosticator of breast cancer

- Found that breast cnacer cells have lost the ability to regulate cyclin E and this deregulation leads to redundancy of cyclin E selectively in tumor cells.

- Discovered the presence of alternatively spliced variants of cyclin E

- Discovered that tumor cells have the machinery to process cyclin E into its lower molecular weight isoforms, while normal cells do not

- Discovered that lovastatin has a novel target, the proteasome and that lovastatin inhibition of this target leads to G1 arrest.

- Discovered novel treatment strategy that protects host cells to chemotherapeutic arrest by selectively arresting them in the G1 phase of the cell cycle.

- Discovered that overexpression of p21 in breast cancer cells non responsive to anti-estrogens, sensitizes these cells to the growth inhibitory effects of anti-estrogens by activating the estrogen signaling pathway.

8) Reportable Outcomes:

Manuscripts:

1. Harper, J.W., Elledge, S.J., **Keyomarsi, K.**, Dynlacht, B., Tsai, L-H., Zhang, P., Dobrowlski, S., Bai, C., Connell- Crowley, L., Swindell, E., Fox, P., and Wei, N. Analysis of p21-Cdk Interactions In vitro and In vivo: p21 and p27 can collaborate to inihibit Cdks. Mol. Biol. Cell. 6: 387-400 (1995).

2. **Keyomarsi, K.**, Conte, D., Toyofuku, W., and M. Pat Fox. Deregulation of Cyclin E in Breast Cancer. Oncogene, 11: 941-950 (1995).

3. **Keyomarsi, K.** Synchronization of Mammalian Cells by Lovastatin. Methods in Cell Science, 18: 1-6 (1996).

4. Bacus, S., Yarden, Y., Oren, M., Chin, D.M., Lyass, L., Zellnick, C.R., Kazarov, A., Toyofuku, W., Beerli, R.R., Hynes, N.E., Gudkov, A., Nikiforov, M., and **Keyomarsi K.** NEU Differentiation Factor (Heregulin) Activates a p53-Dependent Pathway in Cancer Cells. Oncogene, 12: 2535-2547 (1996).

5. Dou, Q-P., Pardee, A.B., **Keyomarsi, K.**, Cyclin E- A Better Prognostic Marker for Breast Cancer Than Cyclin D? Nature Med. 2: 254 (1996).

6. Bablin, J.G., Xalvide, J., Fox, M.P., Knickerbocker, C., DeCaprio, J., and **Keyomarsi, K.** Cyclin E, a Redundant Cyclin in Breast Cancer. Proc. Natl. Acad. Sci. USA 93: 15215-15220 (1996).

7. Bablin, J.G., Rao, S., **Keyomarsi, K.** Lovastatin Induction of cyclin-dependent-kinase inhibitors in human breast cells occurs in a cell cycle independent fashion. Cancer Research. 57: 604-609 (1997).

8. Stover, P., Chen, L.H., Suh, J.R., Stover, D.M., **Keyomarsi, K.**, Shane, B. Molecular cloning, characterization, and regulation of the human mitochondrial serine hydroxymethyltransferase gene. Journal of Biological Chemistry 272: 1842-1848 (1997).

8. **Keyomarsi, K.**, and Herliczek, T.W. The role of cyclin E in cell proliferation, development, and cancer. In Progress in Cell Cycle Research, Ed. L. Meijer, S. Guidet, and M. Philippe Volume 3: pp 171-193 (1997).

9. Rao, S., Lowe, M., Herliczek, T.W., and **Keyomarsi, K.** Lovastatin mediated G1 arrest in normal and tumor breast cells is through inhibition of CDK2 activity and redistribution of p21 and p27, independent of p53. Oncogene, 2393-2402 (1998).

10. Rao, S., Gray-Bablin, J., Herliczek, T.W., and **Keyomarsi, K.** The induction of p21 in breast cancer by modulators of cAMP is through a PKA independent mechanism. Exp. Cell Res. 252: 211-223 (1999).

11. Rao, S., Porter, D.C., Chen, X., Herliczek, T., Lowe, M., and **Keyomarsi, K.** Lovastatin induction of CKIs p21 and p27 and mevalonate reversal of lactacystin are both through modulation of the proteasome, independent of HMG-CoA reductase. Proc. Natl. Acad. Sci. USA 96: 7797-7802 (1999).

12. Chen, X., Lowe, M., and **Keyomarsi, K**. Differential sensitivity of normal and tumor breast cells to UCN-01 mediated G1 arrest is pRb dependent and p53 independent. <u>Oncogene</u>, 18: 5691-5702 (1999).

13. Harwell, R.M., Porter, D.C., Danes, C., and **Keyomarsi, K.** Processing of cyclin E differs between normal and tumor breast cells. <u>Cancer Research</u> 60: 481-489 (2000).

14. Fasco, M.J., **Keyomarsi, K.,** Arcaro, K.F., and Gierthy, J.F. Expression of an Estrogen Receptor Alpha Variant Protein in Cell Lines and Tumors. <u>Molecular and Cellular Endocrinology</u> (In Press).

15. Robertson, K.D. Keyomarsi, K., Gonzales, F.A., Velicescu, M., and Jones, P.A. Differential mRNA expression of the human DNA methyltransferases (DNMT's) 1, 3a, and 3b during the cell cycle in normal and tumor cells. Nucleic Acids Research 28: 2108-2113 (2000).

Manuscripts Submitted:

1. Chen, X., Danes, C., Lowe, M., Herliczek, T.W., and **Keyomarsi, K..** Activation of the Estrogen Signaling Pathway by p21$^{WAF1/CIP1}$ in ER Negative Breast Cancer Cells.

2. Chen, X., Lowe, M., Herliczek, T., Hall, M.J. Lawrence, D.A, and **Keyomarsi, K.** Selective killing of breast cancer cells by reversible, G1 arrest of normal cells.

3. Porter, D.C., and **Keyomarsi, K.** Identification of Novel Splice Variants of Cyclin E with altered substrate specificity.

Patents:

Keyomarsi, K. Cyclin E Variants and Use Thereof. The US Patent Application (87681.97R326) - File Date: September 5, 1996, Issued 6/9/98, Patent # 5,763,219.

Abstracts: (The following abstracts were awarded with travel grants/selected for oral presentation or poster discussion).

1.. **Keyomarsi, K.,** Conte, D., Toyofuku, W., Fox, M.P.: Deregulation of Cyclin E in Breast Cancer. **18th Annual San Antonio Breast Cancer Symposium** (1995)

2. **Keyomarsi, K.,** Gray-Bablin, J., Zalvide, J., Knickerbocker, C., DeCaprio, J., Fox, M.P.: Deregulation and Redundancy of Cyclin E in Breast Cancer. **Proc. Amer. Assoc. Cancer Res**. 38: 2932 (1997).

3. **Keyomarsi, K.,** Bacus, S., Herliczek, T., Porter, D., Rao, S., and Harwell, R. The deregulation and prognostic potential of Cyclin E in Breast Cancer. First Annual Breast Cancer Symposium held by the DOD, **"Era of Hope"**, Washington, D.C. (1997)

4. Chen, X., Lowe, M., Herliczek, T.W., and **Keyomarsi, K.** Use of Cell Cycle Checkpoint Alterations To Maximize Therapeutic Effectiveness In Breast Cancer. **Proc. Amer. Assoc. Cancer Res**. 39: 4436 (1998).

5. X. Chen, M. Lowe, C. Danes, T. W. Herliczek, and **K. Keyomarsi**. Overexpression of p21$^{WAF1/Cip1}$ activates the estrogen receptor (ER) signaling pathway in ER negative breast cancer cells. **Proc. Amer. Assoc. Cancer Res**. 40: 4196 (1999).

Funding applied for based on work supported by this award:

R01 CA87548-01 (P.I. Keyomarsi)   IRG met 1/31/00-percentile: 27.1   25%
                                                                        NCAB meeting 6/12-14/00
NCI/NIH   Direct costs recommended $900,000/ 5 years
Proteolytic processing of cyclin E in breast cancer.

Employment opportunities received on research supported by this award:

Associate Professor faculty position at the University of Texas, MD Anderson Cancer Center-Department of Experimental Radiation Oncology. Start Date 9/1/00.

9) Conclusions:

As evident we have made significant strides in completing all the proposed aims. In fact not only all the aims are completed, but we have surpassed most of them. The first aim of our studies, use of cyclin E antibody as a diagnostic prognostic marker for breast cancer is completed and we summarized most of the data in this final report. We are currently completing the 5-year survival statistics from the patients from whom we examined cyclin E expression, including those patients who were diagnosed back in 1995. In the original application we intended to examine only 150 patients, however we have surpassed our initial goal of collecting and extracting 150 tissue samples per year by increasing this number to 550 samples. We have final outcome data on 403 of these patients. We will submit our final manuscript for publication soon after compiling the final statistical data. We anticipate this task to be done by the summer of 2000. The second Aim of the application deals with utilizing the deletional mutations of cyclin E to detect early metastatic breast cancer. We have documented that these truncated forms of cyclin E are not deletional mutations and are in fact splicing variants of cyclin E found in normal and tumor cells and tissue samples. As outlined above, we have identified the lower molecular

weight forms are and have now concluded this aim. The last two aims of our proposal are also completed as have addressed how induction of the CKIs by lovastatin can lead to growth inhibition in tumor cells, even in the presence of high levels of cyclin E. We have either published or submitted manuscripts describing our results.

10. <u>References</u>

[1] Landis, S.H., Murray, T., Bolden, S. and Wingo, P.A. (1998) Cancer statistics, 1998. CA:Cancer J. Clin. 48, 6-30.

[2] Sherr, C.J. (1996) Cancer Cell Cycles. Science 274, 1672-1677.

[3] Sherr, C.J. (1994) G1 phase progression: cycling on cue. Cell 79, 551-555.

[4] Elledge, S.J. (1996) Cell cycle checkpoints: Preventing an identity crisis. Science 274, 1664-1671.

[5] Nasmyth, K. (1996) Viewpoint: Putting the cell cycle in order. Science 274, 1643-1651.

[6] Fisher, R.P. and Morgan, D.O. (1994) A novel form of cyclin associates with MO15/CDK7 to form the CDK-activating kinase. Cell 78, 713-724.

[7] Makela, T.P., Tassan, J.P., Nigg, E.A., Frutiger, S., Hughes, G.J. and Weinberg, R.A. (1994) A cyclin associates wiht the CDK-activating kinase MO15. Nature 371, 254-257.

[8] Harper, J.W. and Elledge, S.J. (1998) The role of cdk7 in CAK function, a retro-retrospective. Genes & Dev. 12, 285-289.

[9] Ewen, M.E., Sluss, H.K., Sherr, C.J., Natsushime, H., Kato, J.-Y. and Livingston, D.M. (1993) Functional interactions of the retinoblastoma protein with mammalian D-type cylins. Cell 73, 487-497.

[10] Matsushime, H., Quelle, D.E., Shurtleff, S.A., Shibuya, M., Sherr, C.J. and Kato, J.-Y. (1994) D-type cyclin-dependent kinase activity in mammalian cells. Mol. Cell. Biol. 14, 2066-2076.

[11] Bartek, J., Bartkova, J. and Lukas, J. (1997) The retinoblastoma protein pathway in cell cycle control and cancer. Exp. Cell Res. 237, 1-6.

[12] Weinberg, R.A. (1995) The retinoblastoma protein and cell cycle control. Cell 81, 323-330.

[13] Bartek, J., Bartkova, J. and Lukas, J. (1996) The retinoblastoma protein pathway and the restriction point. Curr. Opin. Cell Biol. 8, 805-814.

[14] Ikeda, M.A., Jakoi, L. and Nevins, J.R. (1996) A unique role for the Rb protein in controlling E2F accumulation during cell growth and differentiation. Proc. Natl. Acad. Sci. USA 93, 3215-3220.

[15] Pardee, A.B. (1989) G1 events and regulation of cell proliferatrion. Science 246, 603-608.

[16] Planas-Silva, M.D. and Weinberg, R.A. (1997) The restriction point and control of cell proliferation. Curr. Opin. Cell Biol. 9, 768-772.

[17] Sherr, C. and Roberts, J. (1999) CDK inhibitors: positive and negative regulators of G1-phase progression. Genes Dev. 13, 1501-1514.

[18] Elledge, S.J. and Harper, J.W. (1994) Cdk inhibitors; on the threshold of checkpoints and development. Curr. Opin Cell Biol. 6, 847-852.

[19] Harper, J.W. (1997) Cyclin Dependent Kinase Inhibitors. Cancer Surv. 29, 91-108.

[20] Elledge, S.J., Winston, J. and Harper, J.W. (1996) A question of balance: the role of cyclin-kinase inhibitors in development and tumorigenesis. Tr. Cell Biol. 6, 388-392.

[21] Toyoshima, H. and Hunter, T. (1994) p27, a novel inhibitor of G1 cyclin-cdk protein kinase activity is related to p21. Cell 78, 67-74.

[22] Harper, J.W., Adami, G.R., Wei, N., Keyomarsi, K. and Elledge, S.J. (1993) The p21 Cdk-interacting protein Cip1 is a potent inhibitor of G1 cyclin-dependent kinases. Cell 75, 805-816.

[23] El-Deiry, W.S., Tokino, T., Velculescu, V.E., Levy, D.B., Parsons, R., Trent, J.M., Lin, D., Mrcer, W.E., Kinzler, K.W. and Vogelstein, B. (1993) WAF-1, a potential mediator of p53 tumor suppression. Cell 75, 817-825.

[24] Sheikh, M.S., X., L., Chen, J., Shao, Z., Ordonez, J.V. and Fontana, J.A. (1994) Mechanisms of regulation of WAF1//Cip1 gene expression in human breast carcinoma: role of p53-dependent and independent signal transduction pathways. Oncogene 9, 3407-3415.

[25] Michieli, P., Chedid, M., Lin, D., Pierce, J.H., Mercer, W.E. and Givol, D. (1994) Induction of WAF1/CIP1 by a p53-independent pathway. Cancer Res. 54, 3391-3395.

[26] Kato, J., Matsuoka, M., Polyak, K., Massague, J. and Sherr, C.J. (1994) Cyclic AMP-induced G1 phase arrest mediated by an inhibitor (p27^{Kip1}) of cyclin-dependent kinase 4 activation. Cell 79, 487-496.

[27] Polyak, K., Kato, J.-y., Soloman, M.I., Sherr, C.J., Massague, J., Roberts, J.M. and Koff, A. (1994) p27KIP1, a cyclin-cdk inhibitor, links transforming growth factorß and contact inhibition to cell cycle arrest. Genes & Dev. 8, 9-22.

[28] Rao, S., Lowe, M., Herliczek, T. and Keyomarsi, K. (1998) Lovastatin mediated G1 arrest in normal and tumor breast cells is through inhibition of CDK2 activity and redistribution of p21 and p27, independent of p53. Oncogene 17, 2393-2402.

[29] Rao, S., Porter, D.C., Chen, X., Herliczek, T., Lowe, M. and Keyomarsi, K. (1999) Lovastatin-mediated G1 arrest is through inhibition of hte proteasome, independent of hydroxymethyl glutaryl-CoA reductase. Proc. Natl. Acad. Sci. USA 96, 7797-7802.

[30] Gao, C.Y. and Zelenka, P.S. (1996) Cyclins, cyclin-dependent kinases and differentiation. BioEssays 19, 307-315.

[31] Hunt, T. (1991) Cyclins and their partners: from a simple idea to complicated reality. Seminars in Cell Biology 2, 213-222.

[32] Hunter, T. and Pines, J. (1991) Cyclins and Cancer. Cell 66, 1071-1074.

[33] Hunter, T. and Pines, J. (1994) Cyclins and cancer II: cyclin D and cdk inhibitors come of age. Cell 79, 573-582.

[34] Matsushime, H., Roussel, M.F., Ashman, R.A. and Sherr, C.J. (1991) Colony-stimulating factor 1 regulates novel cyclins during the G1 phase of the cell cycle. Cell 65, 701-713.

[35] Lew, D.J., Dulic, V. and Reed, S.I. (1991) Isolation of three novel human cyclins by rescue of G1 cyclin (cln) function in yeast. Cell 66, 1197-1206.

[36] Xiong, Y., Connolly, T., Futcher, B. and Beach, D. (1991) Human D-type cyclin. Cell 65, 691-699.

[37] Withers, D., Harvey, R., Faust, J., Melnyk, O., Carey, K. and Meeker, T. (1991) Characterization of a candidate bcl-1 gene. Mol. Cell Biol. 11, 4846-4853.

[38] Motokura, T. and Arnold, A. (1993) Cyclin D and oncogenesis. Curr. Opin. Genet. & Devel. 3, 5-10.

[39] Motokura, T., Bloom, T., Kim, H.G., Juppner, H., Ruderman, J.V., Kronenberg, H.M. and Arnold, A. (1991) A novel cyclin encoded by a bcl-1 linked candidate oncogene. Nature 350, 512-515.

[40] Rosenberg, C.L., Wong, E., Pety, E.M., Bale, A.E., Tsujimoto, Y., Harris, N.L. and Arnold, A. (1991) PRAD1, acandidate BCL1 oncogene: mapping and expression in centrocytic lymphoma. Proc. Natl. Acad. Sci USA 88, 9638-9642.

[41] Rosenberg, C.L., Kim, H.G., Shows, T.B., Kronenberg, H.M. and Arnold, A. (1991) Rearangement and overexpression of D11S287E, a candidate oncogene on chromosome 11q13 in benign parathyroid tumors. Oncogene 6, 449-453.

[42] Bianchi, A.B., Fischer, S.M., Robles, A.I., Rinchik, E.M. and Conti, C.J. (1993) Overexpression of cyclin D1 in mouse skin carcinogenesis. Oncogene 8, 1127-1133.

[43] Buckler, A.J., Chang, D.D., Graw, S.L., Brrok, J.D., Haber, D.A., Sharp, P.A. and Housman, D.E. (1991) Exon amplification: a strategy to isolate mammalian genes based on RNA splicing. Proc. Natl. Acad. Sci. USA 88, 4005-4009.

[44] Buckley, M.F., Sweeney, K.J.E., Hamilton, J.A., Sini, R.L., Manning, D.L., Nicholson, R.I., deFazio, A., Watts, C.K.W., Musgrove, E.A. and Sutherland, R.L. (1993) Expression and amplification of cyclin genes in human breast cancer. Oncogene 8, 2127-2133.

[45] Jiang, W., Kahn, S.M., Tomita, N., Zhang, Y.-J., Lu, S.-H. and Weinstein, B. (1992) Amplification and expression of the human cyclin D gene in esophageal cancer. Cancer Res. 52, 2980-2983.

[46] Jiang, W., Kahn, S.M., Zhou, P., Zhang, Y.-J., Cacace, A.M., Infante, A.S., Doi, S., Santella, R.M. and Weinstein, I.B. (1993) Overexpression of cyclin D1 in rat fibroblasts causes abnormalities in growth control, cell cycle progresion and gene expression. Oncogene 8, 3447-3457.

[47] Lammie, A.G. and Peters, G. (1991) Chromosome 11q13 abnormalities in human cancer. Cancer Cells 3, 413-420.

[48] Leach, S.F., Elledge, S.J., Sherr, C.J., Willson, J.K.V., Markowitz, S., Kinzler, K.W. and Vogelstein, B. (1993) Amplification of cyclin genes in colorectal carcinomas. Cancer Res. 53, 1986-1989.

[49] Hinds, P.W., Dowdy, S.F., Eaton, E.N., Arnold, A. and Weinberg, R.A. (1994) Function of a human cyclin gene as an oncogene. Proc. Natl. Acad. Sci 91, 709-713.

[50] Hinds, P.W., Mittnacht, S., Dulic, V., Arnold, A., Reed, S.I. and Weinberg, R.A. (1992) Regulation of retinoblastoma protein functions by ectopic expression of human cyclins. Cell 70, 993-1006.

[51] Lovec, H., Sewing, A., Lucibello, F.C., Müller, R. and Möröy, T. (1994) Oncogenic activity of cyclin D1 revealed through cooperation with Ha-ras:link between cell cycle congrol and malignant transformation. Oncogene 9, 323-326.

[52] Musgrove, E.A., Lee, C.S.L., Buckley, M.F. and R.L., S. (1994) Cyclin D1 induction in breast cancer cells shortens G1 and is sufficient for cells arrested in G1 to complete the cell cycle. Proc. Natl. Acad. Sci. 91, 8022-8026.

[53] Quelle, D.E., Ashmun, R.A., Shurleff, S.A., Kato, J.-y., Bar-Sagi, D., Roussel, M.F. and Sherr, C.J. (1993) Overexpression of mouse D-type cyclins accelerates G1 phase in rodent fibroblasts. Genes & Dev. 7, 1559-1571.

[54] Resnitzky, D., Gossen, M., Bujard, H. and Reed, S.I. (1994) Accelaration of the G1/S phase transition by expression of cyclins D1 and E with an inducible system. Mol. Cell. Biol. 14, 1669-1679.

[55] Resnitzky, D. and Reed, S.I. (1995) Different roles for cyclins D1 and E in regulation of the G1-to-S transition. Mol. Cell. Bio. 15, 3463-3469.

[56] Sherr, C.J. (1993) Mammalian G1 cyclins. Cell 73, 1059-1065.

[57] Wang, T.C., Cardiff, R.D., Zukerberg, L., Lees, E., Arnold, A. and Schmidt, E.V. (1994) Mammary hyperplasia and carcinma in MMTV-cyclin D1 transgenic mice. Nature 369, 669-671.

[58] Ohtsubo, M. and Roberts, J.M. (1993) Cyclin-dependent regulation of G1 in mammalian fibroblasts. Science 259, 1908-1912.

[59] Keyomarsi, K., O'Leary, N., Molnar, G., Lees, E., Fingert, H.J. and Pardee, A.B. (1994) Cyclin E, a Potential Prognostic Marker for Breast Cancer. Cancer Res. 54, 380-385.

[60] Keyomarsi, K., Conte, D., Toyofuku, W. and Fox, M.P. (1995) Deregulation of cyclin E in breast cancer. Oncogene 11, 941-950.

[61] Dou, Q.-P., Levin, A.H., Zhao, S. and Pardee, A.B. (1993) Cyclin E and cyclin A as candidates for the restriction point protein. Cancer Res. 53, 1493-1497.

[62] Ohtani, K., DeGregori, J. and Nevins, J.R. (1995) Regulation of the cyclin E gene by transcription factor E2F1. Proc. Natl. Acad. Sci. 92, 12146-12150.

[63] Geng, Y., Eaton, E.N., Picon, M., Roberts, J.M., Lundberg, A.S., Gifford, A., Sardet, C. and Weinberg, R.A. (1996) Regulation of cyclin E transcription by E2Fs and retinoblastoma protein. Oncogene 12, 173-1180.

[64] Tsai, L.-H., Lees, E., Faha, B., Harlow, E. and Riabowol, K. (1993) The cdk2 kinase is required for the G1-to-S transition in mammalian cells. Oncogene 8, 1593-1602.

[65] Ohtsubo, M., Theodoras, A.M., Schumacher, J., Roberts, J.M. and Pagano, M. (1995) Human cyclin E, a nuclear protein essential for the G1-to-S phase transition. Mol. Cell. Biol. 15, 2612-2624.

[66] Resnitzky, D., M., G., Bujard, H. and Reed, S.I. (1994) Acceleration of the G1/S phase transition by expression of cyclins D1 and E with an inducible system. Mol. Cell Biol. 14, 1669-1679.

[67] Dulic, V., Drullinger, L., Lees, E., Reed, S. and Stein, G. (1993) Altered regulation of G1 cyclins in senescent human diploid fibroblasts: accumulation of inactive cyclin E-cdk2 and cyclin D1-cdk2 complexes. Proc. Natl. Acad. Sci. 90, 11034-11038.

[68] Bremner, R., Cohen, B.L., Sopta, M., Hamel, P.A., Ingles, C.J., Gallie, B.L. and Phillips, R.A. (1995) Direct transcriptional repression by pRB and its reversal by specific cyclins. Mol. Cell. Biol. 15, 3256-3265.

[69] Richardson, H., O'Keefe, L.V., Marty, T. and Saint, R. (1995) Ectopic cyclin E expression induces premature entry into S phase and disrupts pattern formation in the Drosophila eye imaginal disc. Development 121, 3371-3379.

[70] Keyomarsi, K. and Pardee, A.B. (1993) Redundant cyclin overexpression and gene amplification in breast cancer cells. Proc. Natl. Acad. Sci. USA 90, 1112-1116.

[71] Keyomarsi, K. and Herliczek, T. (1997) The role of cyclin E in cell proliferation, development and cancer. In: Progress in Cell Cycle Research (Meijer, L. et al., eds.), pp. 171-191, Plenum Press, New York.

[72] Steeg, P.S. and Zhou, Q. (1998) Cyclins and breast cancer. Breast Can. Res. & Treat. 52, 17-28.

[73] Porter, P.L., Malone, K.E., Heagerty, P.J., Alexander, G.M., Gatti, L.A., Firpo, E.J., Daling, J.R. and Roberts, J.M. (1997) Expression of cell-cycle regulators p27 and cyclin E, alone and in combination, correlate with survival in young breast cancer patients. Nat. Med. 3, 222-225.

[74] Scott, K. and Walker, R. (1997) Lack of cyclin E immunoreactivity in non-malignant breast and association with proliferation in breast cancer. Br. J Cancer 76, 1288-1292.

[75] Nielsen, N.H., Arnerlov, C., Emdin, S.O. and Landberg, G. (1996) Cyclin E overexpression, a negative prognostic factor in breast cancer with strong correlation to oestrogen receptor status. Brit. J. Canc. 74, 874-880.

[76] Gray-Bablin, J., Zalvide, J., Fox, M.P., Knickerbocker, C.J., DeCaprio, J.A. and Keyomarsi, K. (1996) Cyclin E, a redundant cyclin in breast cancer. Proc. Natl. Acad. Sci. 93, 15215-15220.

[77] Dou, Q.-P., Pardee, A.B. and Keyomarsi, K. (1996) Cyclin E- a better prognostic marker for breast cancer than cyclin D? Nature Med. 2, 254.

[78] Bortner, D.M. and Rosenberg, M.P. (1996) Induction of mammary gland hyperplasia and carcinomas in trangenic mice expressing human cyclin E. Mol. Cell. Bio. 17, 453-459.

[79] Spruck, C.H., Won, K.-A. and Reed, S.I. (1999) Deregulated cyclin E induces chromosome instability. Nature 401, 297-300.

[80] Band, V. and Sager, R. (1989) Distinctive traits of normal and tumor-derived human mammary epithelial cells expressed in a medium that supports long-term growth of both cell types. Proc. Natl. Acad. Sci. USA 86, 1249-1253.

[81] Gray-Bablin, J., Rao, S. and Keyomarsi, K. (1997) Lovastatin Induction of cyclin-dependent kinase inhibitors in human breast cells occurs in a cell cycle independent fashion. Cancer Res. 57, 604-609.

[82] Soule, H.D., Maloney, T.M., Wolman, S.R., Peterson, W.D., Jr., Brenz, R., McGrath, C.M., Russo, J., Pauley, R.J., Jones, R.F. and Brooks, S.C. (1990) Isolation and characterization of a spontaneously immortalized human breast epithelial cell line, MCF-10. Cancer Res. 50, 6075-6086.

[83] Band, V., DeCaprio, J.A., Delmolino, L., Kulesa, V. and Sager, R. (1991) Loss of p53 protein in human papillomavirus type 16 E6-immortalized human mammary epithelial cells. J. Virology 65, 6671-6676.

[84] Band, V., Zajchowski, D., Kulesa, V. and Sager, R. (1990) Human papilloma virus DNAs immortalize normal human mammary epithelial cells and reduce their growth factor requirements. Proc. Natl. Acad. Sci. USA 87, 463-467.

[85] Werness, B.A., Levine, A.J. and Howley, P.M. (1990) Association of human papillomavirus types 16 and 18 E6 proteins with p53. Science 248, 76-79.

[86] Dyson, N., Guida, P., Munger, K. and Harlow, E. (1992) Homologous sequences in adenovirus E1A and human papillomavirus E7 proteins mediate interaction with the same set of cellular proteins. J. Virol. 66, 6893-6902.

[87] Band, V., Dala, S., Delmolino, L. and Andropphy, E.J. (1993) Enhanced degradation of p53 protein in HPV-6 and BPV-1 E6-immortalized human mammary epithelial cells. EMBO J. 12, 1847-1852.

[88] Sgambato, A., Zhang, Y.J., Arber, N., Hibshoosh, H., Doki, Y., Ciaparrone, M., Santella, R., Cittadini, A. and Weinstein, I.B. (1997) Deregulated expression of p27(Kip1) in human breast cancers. Clin. Can. Res. 3, 1879-1887.

[89] Sgambato, A., Doki, Y., Schieren, I. and Weinstein, I.B. (1997) Effects of cyclin E overexpression on cell growth and response to transforming growth factor ß depend on cell context and p27kip1 expression. Cell Growth Diff. 8, 393-405.

[90] Shapiro, G.I., Edwards, C.D., Kobzik, L., Godleski, J., Richards, W., Sugarbaker, D.J. and Rollins, B.J. (1995) Recipricol Rb inactivation and p16INK4 expression in primary lung cancers and cell lines. Cancer REs. 55, 505-509.

[91] Aagaard, L., Lukas, J., Bartkovva, J., Kjerulff, A.-A., Strauss, M. and Bartek, J. (1995) Aberrations of p16INK4 and retinoblastoma tumor-suppressor genes occur in distinct sub-sets of human cancer cell lines. Int. J. Cancer 61, 115-120.

[92] Otterson, G.A., Kratzke, R.A., Coxoon, A., Kim, Y.W. and Kaye, F.J. (1994) Absence of p16INK4 protein is restricted to the subset of lung cancer lines that retains wildtype RB. Oncogene 9, 3375-3378.

[93] Parry, D., Bates, S., Mann, D.J. and Peters, G. (1995) Lack of cyclin D-cdk complexes in Rb-negative cells correlates with high levels of p16INK4/MTS1 tumour suppressor gene product. EMBO J 14, 503-511.

[94] Tam, S.W., Shay, J.W. and Pagano, M. (1994) Differential expression and cell cycle regulation of the cyclin-dependent kinase 4 inhibitor p16ink4. Cancer Res. 54, 5816-5820.

[95] Nielsen, N.H., emdin, S.O., Cajander, J. and Landberg, G. (1997) Deregulation of cyclin E and D1 in breast cancer is associaed with inactivation of the retinoblastoma protein. Oncogene 14, 295-304.

[96] Herrera, R.E., Sah, V.P., Williams, B.O., Makela, T.P., Weinberg, R.A. and Jacks, T. (1996) Altered cell cycle kinetics, gene expression, and G1 restriction point reugaltion in Rb-deficient Fibroblasts. Mol. Cell. Biol. 16, 2402-2407.

[97] Koff, A., Cross, F., Fisher, A., Schumacher, J., Leguellec, K., Philippe, M. and Roberts, J.M. (1991) Human cyclin E, a new cyclin that interacts with two members of the CDC2 gene family. Cell 66, 1217-1228.

[98] Shevchenko, A., Wilm, M., Vorm, O. and Mann, M. (1996) Mass spectrometric sequencing of proteins from silver-stained polyacrylamide gels. Anal. Chem. 68, 850-858.

[99] Jaspersen, S., Chaurand, P., van Strien, F.J., Spengler, B. and van der Greef, J. (1999) Direct sequencing of neuropeptides in biological tissue by MALDI-PSD mass spectrometry. Anal. Chem. 71, 660-666.

[100] Barrett, A.J. and Salveen, G. (1986) Proteinase Inhibitors (Research Monographs in Cell and Tissue Physiology, Volume 12), Elsevier, Cambridge.

[101] Clurman, B.E., Sheaff, R.J., Thress, K., Groudine, M. and Roberts, J.M. (1996) Turnover of cyclin E by the ubiquitin-proteosome pathway is regulated by cdk2 binding and cyclin phosphorylation. Genes & Dev. 10, 1979-1990.

[102] Wu, H., Wade, M., Krall, L., Grisham, J., Xiong, Y. and Van Dyke, T. (1996) Targeted in vivo expression of the cyclin-dependent kinase inhibitor p21 halts hepatocyte cell-cycle progression, postnatal liver development and regeneration. Genes & Dev. 10, 245-260.

[103] Choi, Y.H., Lee, S.J., Nguyen, P., Jang, J.S., Lee, J., Wu, M.L., Takano, E., Maki, M., Henkart, P.A. and Trepel, J.B. (1997) Regulation of cyclin D1 by calpain protease. J. Biol. Chem. 272, 28479-28484.

[104] Bastians, H., Townsley, F.M. and Ruderman, J.V. (1998) The cyclin-dependent kinase inhibitor p27(Kip1) induces N-terminal proteolytic cleavage of cyclin A. Proc. Natl. Acad. Sci. USA 95, 15374-15381.

[105] Read, R.J. and James, M.N.G. (1986) Introduction to the protein inhibitors: Xray crystallography (Proteinase Inhibitors, Elsevier Science Publishers BV, .

[106] Stack, J.H. and Newport, J.W. (1997) Developmentally regulated activation of apoptosis early in Xenopus gastrulation results in cyclin A degradation during interphase of the cell cycle. Development 1997, 3185-3195.

[107] Rodgers, S., Wells, R. and Rechsteiner, M. (1986) Amino acid sequences common to rapidly degraded proteins: The PEST hypothesis. Science 234, 364-369.

11) Appendices:

We have included copies of all our published and 2 submitted manuscripts listed under reportable outcomes.

12. Binding

Format outlined has been followed.

13. FINAL REPORTS

Bibliography of all publications and meeting abstracts have been provided under reprotable outcomes.

Personnel:

Julie Gray-Bablin, Ph.D	10/94 to 2/96	Post-doctoral Fellow
Wendy Toyofuku	10/94 to 2/96	Lab Technician
Donald C. Porter, Ph.D.	3/96 to 1/98	Post-doctoral Fellow
Christopher Knickerbocker	4/96 to 1/97	Chemist Aide
Sharmila Rao, Ph.D.	5/96 to 9/97	Post-doctoral Fellow
Thaddeus Herliczek	8/96 to 9/97	Lab Technician
Sheng-Kai Yang	10/96 to 2/97	Graduate Student-(rotation)
Richard Harwell	11/96 to 6/99	Graduate Student
Xiaomei Chen, Ph.D.	10/96 to 3/97	Post-doctoral Fellow
Michael D. Lowe	8/97 to 8/98	Lab Technician
Christopher Danes	9/98 to 9/99	Lab Technician

Advances in Brief

Cyclin E, a Potential Prognostic Marker for Breast Cancer[1]

Khandan Keyomarsi,[2] Nuala O'Leary, Gyongyi Molnar, Emma Lees, Howard J. Fingert, and Arthur B. Pardee

Division of Cell Growth and Regulation, Dana-Farber Cancer Institute, and Department of Biological Chemistry and Molecular Pharmacology, Harvard Medical School, Boston, Massachusetts 02115 [K. K., N. O., G. M., A. B. P.]; Massachusetts General Hospital Cancer Center, Charlestown, Massachusetts 02129 [E. L.]; and St. Elizabeth's Medical Center, Boston, Massachusetts 02135 [H. J. F.]

Abstract

A fundamental cause of cancer is changed properties of genetic material, which may deregulate normal development of the tissue or provide selective growth advantage to the tumor cell. This deregulation of cell proliferation results from altered production of a handful of proteins that play key roles in progression through the eukaryotic cell cycle. Some of these proteins include tumor suppressor genes or oncogenes.

However, no one general change or alteration of a critical gene has yet been found in all cancers. Using surgical material obtained from patients with various malignancies, we show that breast cancers and other solid tumors, as well as malignant lymphocytes from patients with lymphatic leukemia, show severe quantitative and qualitative alterations in cyclin E protein production independent of the S-phase fraction of the samples. Hence, these alterations represent a true difference between normal *versus* tumor tissue. In addition, in breast cancer, the alterations in cyclin E expression become progressively worse with increasing stage and grade of the tumor, suggesting its potential use as a new prognostic marker.

Introduction

Breast cancer is a major killer worldwide. One in eight American women may expect some form of breast cancer in their lifetime (1). Success in treatment depends greatly upon early detection. In breast cancer, the tumor size, grade, stage, lymphatic or vascular invasion, axillary node metastases, and hormone receptors are well established but not definitive prognostic factors (2). Thus, additional prognostic factors are essential.

Attention has recently focused on molecular markers, in particular genes involved in the pathogenesis of breast carcinoma. The first such marker to be tested for its clinical relevance is the c-*erb* B2/*neu* oncogene, whose activation can occur by amplification of c-*erb* B2 DNA and by overproduction of its mRNA and protein (3). Approximately 20% of breast carcinomas show evidence of c-*erb* B2 activation, which correlates with a poor prognosis primarily in patients with metastasis to axillary lymph nodes. Attempts to correlate c-*erb* B2 activation with other prognostic factors in breast carcinoma have, however, reported conflicting conclusions (4). Since it is likely that breast cancer is a result of a progressive accumulation of many different somatic mutations in diverse genes such as oncogenes and tumor suppressor genes, the clinical relevance of new markers must be examined carefully.

With the discovery of cyclins and cyclin-dependent kinases, it is now possible to specifically ask whether the deregulation of any or all of these molecules could lead to oncogenesis. The link between oncogenesis and cyclins was made with discovery of the inappropriate expression of two cyclins in tumors (5, 6): (*a*) cyclin A gene is the site of integration of a fragment of the hepatitis B virus genome in a hepatocellular carcinoma (7). Cyclin A is also associated with the adenovirus transforming protein E1A in adenovirus transformed cells (8–10); (*b*) in some parathyroid tumors, the *Prad1* (cyclin D1) locus is overexpressed as a result of a chromosomal rearrangement that translocates it to the enhancer of the parathyroid hormone gene (11–13). *Prad1* has also been found to reside near the B-lymphoid tumor-associated chromosome 11 breakpoint known as BCL1, activated by t(11;14) translocations and targeted by chromosomal translocations in centrocytic lymphomas (14). The same locus undergoes gene amplification in mouse skin carcinogenesis, as well as breast, esophageal, colorectal, and squamous cell carcinomas (15–20). These observations describe occasional changes involving only two cyclins. They do not provide a clear connection between general derangements of other cyclins or their dependent kinases in a single tumor type.

Recently, we have correlated the deranged expression of cyclins in general to loss of growth control (21). Using proliferating normal *versus* human tumor breast cell lines in culture as a model system, we have described several changes that are seen in all or most of these lines. These alterations include (*a*) increased cyclin mRNA stability, resulting in (*b*) general overexpression of mitotic cyclins and of CDC2 RNAs and proteins in 9 of 10 tumor lines, and (*c*) deranged order of appearance of cyclins in synchronized tumor *versus* normal cells, with mitotic cyclins appearing prior to G1 cyclins. The most striking abnormality in cyclin expression was that of cyclin E. We found an 8-fold amplification of cyclin E gene in one tumor line, 64-fold overexpression of its mRNA, and altered expression of its protein. In addition, cyclin E protein was not only overexpressed in all (10 of 10) breast tumor cell lines examined but was present in different sizes than found in normal cells.

In this report, we extended these observations to the *in vivo* condition by examining the pattern of cyclin E protein expression in tumor and normal adjacent tissue obtained from breast cancer patients. We find that the altered expression of cyclin E protein occurred in most of the breast tumor tissues examined, and its alterations increased with increasing grade and stage of the tumor. Cyclin E alteration was also more consistent than c-*erb* B2 overexpression in breast cancer. Furthermore, cyclin E was also altered in other types of solid tumors as well as leukemia. This alteration is a true normal *versus* tumor difference, independent of the S-phase fraction of the tumor as measured by the expression of PCNA.[3] These observations suggest that cyclin E may potentially be used as a prognostic marker in breast cancer, in addition to other markers such as c-*erb* B2 currently used in the clinic.

Materials and Methods

Western Blot Analysis of Tissue Samples. Snap frozen surgical specimens from patients diagnosed with breast cancer were obtained from the National Disease Research Interchange/Cooperative Human Tissue Network, Eastern Division. Detailed pathology/surgical reports summarize the source of specimen, clinical history and diagnosis, gross description, summary of sections, final diagnosis, and if available, estrogen/progesterone receptor status, DNA ploidy, and oncogene data. Approximately 0.5–5 g of each matched tissue (NAT and tumor tissue obtained from the same patient) were added to 1 volume of sonication buffer containing a cocktail of proteases and phosphatase inhibitors (22) in a low salt buffer, homogenized for 1 min with a hand-held homogenizer, and sonicated at 4°C using a microtip adapter for 1 min. Homogenates were centrifuged at $100,000 \times g$ for 45 min at 4°C. The supernatants were assayed for protein content (23), aliquoted, stored at −70°C, and subjected to Western blot analysis as described (21, 24). Briefly, 100 μg of protein from each tissue sample were electrophoresed in each lane of a 10% sodium dodecyl sulfate-polyacrylamide gel (cyclin E, cyclin D1, and PCNA) or 5% sodium dodecyl sulfate-polyacrylamide gel (c-*erb* B-2) and transferred to Immobilin P. Blots were incubated with blocking buffer (20 mM Tris-HCl, pH 7.5–150 mM NaCl-5% dried milk-0.2% Tween) overnight at 4°C and then incubated with various primary antibodies diluted in blocking buffer. Rabbit anti human cyclin E serum at a dilution of 1:2500 (25), monoclonal antibody HE12 to cyclin E at a dilution of 1:10 (26), polyclonal antibody to c-*erb* B2 (Oncogene Science) at a dilution of 1:30, polyclonal antibody to cyclin D1 at a dilution of 1:250 (12), and monoclonal antibody PC10 to PCNA (Santa Cruz Biochemicals) at a dilution of 1:100 were incubated for 3 h. The blots were then washed and incubated with either goat anti-mouse or anti-rabbit horse radish peroxidase conjugate at a dilution of 1:5000 in blocking buffer for 1 h, washed extensively, and developed with detection reagents (ECL) supplied by Amersham Biochemicals. ECL exposures for all Western blots were of similar duration, *i.e.*, 1–10 s.

Blood Samples. Whole blood samples were obtained from a normal volunteer and CLL/PL patients. Monocytes/lymphocytes were purified by Ficoll-Paque gradient centrifugation as described (27), homogenized by sonication, and subjected to Western blot analysis. Staining of peripheral blood lymphocyte preparation was performed by the Wright-Giemsa technique.

Results and Discussion

Abnormal Expression of Cyclin E Protein in Human Breast Tumor Tissue. An important experimental question concerns the applicability of culture studies with cell lines to the *in vivo* condition. We directly examined the relevance of cyclin derangement to *in vivo* conditions by measuring the expression of cyclin E protein as compared to c-*erb* B2 in breast tumor samples *versus* normal adjacent breast tissue obtained from patients diagnosed with breast cancer (Fig. 1). Whole cell lysates were initially prepared from nine paired cases of human breast carcinomas and adjacent nontumorous tissues and subjected to Western blot analysis using two different antibodies to cyclin E, one to c-*erb* B2 (Fig. 1*A*), one to cyclin D1, and one to the PCNA (Fig. 1*B*). These analyses revealed several findings.

(*a*) Cyclin E protein is abnormally expressed quantitatively and qualitatively in most tumor tissues compared to the NAT. In the tumor samples, cyclin E antibody reacted strongly with at least three over-expressed proteins ranging in size from M_r 35,000–50,000, whereas in the NAT samples, one major protein of $\sim M_r$ 50,000 was present at very low levels. Both the monoclonal and polyclonal antibodies specific to cyclin E recognized the same multiple cyclin E bands, even though the two anti-E antibodies recognize different epitopes on the protein (25, 26, 28). These *in vivo* observations are consistent with results obtained with cultured breast cell lines (21). Thus, abnormal

Fig. 1. Abnormal expression of cyclin E protein and c-*erb* B2 in human breast tumor *vs.* normal adjacent tissue. Whole cell lysates were extracted from nine pairs of normal adjacent and breast cancer tissues. (Each paired sample was obtained from the same patient). Breast cancer types and histological/tumor grades are: *Lane 1*, metastatic ductal carcinoma, grade IV; *Lane 2*, invasive, poorly differentiated ductal carcinoma of the breast, grade III; *Lane 3*, infiltrating ductal carcinoma, grade N/A; *Lane 4*, Poorly differentiated metastatic ductal carcinoma, grade IV; *Lane 5*, inflammatory breast cancer, grade II/III; *Lane 6*, malignant phylloides tumor, Grade II/III; *Lane 7*, infiltrating and *in situ* ductal carcinoma, Grade II; *Lane 8*, small foci of *in situ* ductal carcinoma, grade I/II; *Lane 9*, infiltrating ductal carcinoma, grade III/IV. Protein extracts were analyzed on Western blots (100 μg of protein extract/lane) and hybridized with the indicated antibodies. (*A*) *Large arrowhead*, cyclin E protein of the predicted size of $\sim M_r$ 50,000. *Small arrowheads*, the two extra cyclin E-like proteins observed in the tumor tissue samples at M_r 42,000 and 35,000. (*B*) *Arrows*, a M_r 35,000 cyclin D1 protein in the *left panel* and a M_r 36,000 PCNA protein in the *right panel*. Molecular mass standards were used on each gel to estimate the position of each band.
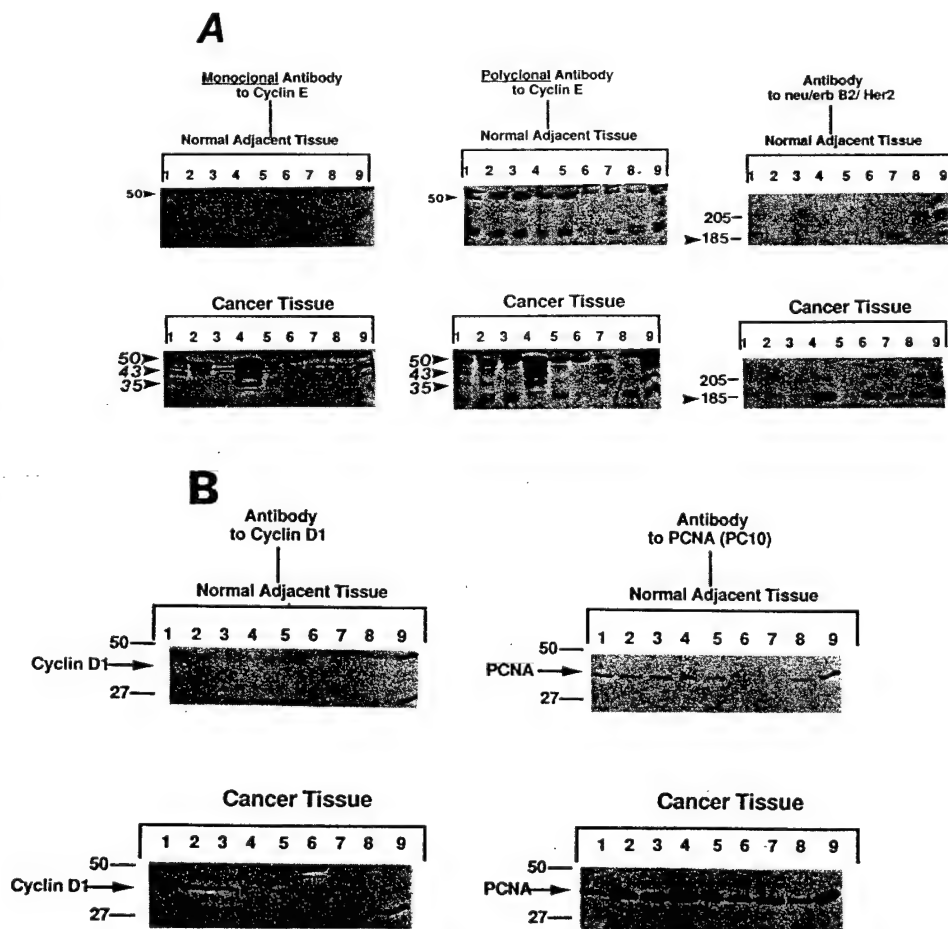
expression of cyclin E is a general phenomenon associated with oncogenesis of breast cancer.

(*b*) Cyclin E is abnormally expressed in 8 of 9 tumor tissue samples (with the exception of Fig. 1*A, Lane 8*), but c-*erb* B2 is overexpressed in only 3 of 9 of these cases (Fig. 1*A, Lanes 4, 6*, and *9*), suggesting that cyclin E is a more sensitive and consistent marker for prognosis of breast cancer than the commonly used c-*erb* B2. We found a similar overexpression of both c-*erb* B2 and cyclin E in samples 4 and 9, both from patients with advanced metastatic breast cancer.

(*c*) Analysis of cyclin D1 revealed a different pattern of overexpression in these breast tumor samples (Fig. 1*B*) as compared to cyclin E (Fig. 1*A*). The cyclin D1 locus has been shown to be amplified in 15–20% of breast cancer samples; however, no attempt has been made to correlate the overexpression of cyclin D1 protein to progression of the disease (16, 17, 29, 30). In our analysis, cyclin D1 overexpression in 2 of 9 cases (Fig. 1*B, Lanes 2* and *3*) occurs in a different subtype of breast cancers which do not correlate with overexpression of c-*erb* B2 or cyclin E (Fig. 1*A, Lanes 4* and *9*).

(*d*) Cyclins are expressed in a cell cycle regulatory manner and hence their expression is higher in proliferating than in nonproliferating quiescent cells. To determine whether the altered expression of cyclin E observed in these tissues is independent of cell proliferation, we also measured the expression of PCNA. PCNA, a M_r 36,000, nonhistone nuclear protein, is essential for cellular DNA synthesis and is closely linked to the cell cycle (31–33). The breast NAT samples have a very low cell proliferative activity as apparent by the faint PCNA signal observed on Western blots using a monoclonal antibody to PCNA (PC10; Fig. 1*B*). The expression of PCNA was much higher in the tumor samples, indicative of their high S-phase fraction. However, there was very little difference, if any, in PCNA expression among these different tumor tissue samples, regardless of the type of cancer, the stage of disease, or the degree of altered cyclin E expression. The altered expression of cyclin E seems to be distinct from the proliferative index of the tumor, and is a true normal *versus* tumor difference (see below).

Altered Expression of Cyclin E Correlates with Increased Breast Tumor Stage and Grade. To examine the likelihood that the altered expression of cyclin E is associated with high tumor stage and grade and therefore poor prognosis, we analyzed an additional seven paired samples of human breast carcinomas and NAT which are presented according to tumor stage and grade which increased correlatively (Fig. 2). Whole cell lysates from all samples were subjected to Western blot analysis. Fig. 2, *Lanes 1* and *2* were prepared from tumor

stage $T_1/N_0/M_0$ grade I patients; Fig. 2, *Lane 3* from a tumor stage $T_{1/2}/N_0/M_0$ grade I patient; Fig. 2, *Lane 4* from a tumor stage $T_2/N_0/M_0$ grade II patient, Fig. 2, *Lane 5* from a tumor stage $T_2/N_1/M_0$ grade II/III patient; Fig. 2, *Lane 6* from a tumor stage $T_3/N_0/M_0$ grade II/III patient; and Fig. 2, *Lane 7* from a tumor stage $T_4/N_0/M_0$ grade III patient. In all the NAT samples, only cyclin E protein of $\sim M_r$ 50,000 was present at very low levels. In low stage and grade tumors, cyclin E antibody recognized three proteins of low abundance ranging in size from M_r 35,000–50,000 (Fig. 2, *Lanes 1–3*). These proteins become progressively more abundant and altered with increasing tumor grade and stage (Fig. 2, *Lanes 4–7*).

To assess whether the increase in expression of cyclin E is correlated with increased proliferation rates, PCNA protein levels were also measured and revealed that there is only a minor (2–3 fold) increase in PCNA levels from low to high stage and grade tumors, not enough to account for the massive differences in cyclin E expression. Furthermore, even though cyclin E protein was altered and overexpressed in all four of the higher stage/grade tumors, c-*erb* B2 was overexpressed in only two of the samples. Thus, quantitatively and qualitatively, increased alterations of cyclin E protein correlates with increased tumor stage and grade more consistently than the proliferative index of the cells or overexpression of c-*erb* B2.

Alteration of Cyclin E Is Associated with Other Solid Tumors. Cyclin E is a cell cycle-specific protein whose normal function is thought to regulate the late G_1 to S transition in all mammalian cells, suggesting that its alterations should not be unique to breast cancer. We therefore examined whole cell lysates prepared from patients diagnosed with metastatic lung, kidney, pancreas, stomach, colon, uterus, testis, endometrial, esophagus, melanoma (spleen), and ovarian cancers (Fig. 3, *A* and *B*). In half of the cases, NAT samples were also available for analysis. Western blots were analysed using cyclin E and PCNA antibodies. In every case examined, there were severe alterations of cyclin E expression in the tumor samples compared to the NAT samples. Although the NAT samples did not contain any detectable tumor tissue, as indicated in the pathology reports, the normal tissues contained proliferating cells, probably due to local inflammation, as evident by high PCNA levels (Fig. 3*A*). Moreover, the differences in PCNA levels in NAT *versus* tumor samples were not sufficient to account for the observed severe cyclin E alterations seen in the tumor samples, most pronounced in lung, stomach, and kidney samples. Hence, as with the breast cancer specimens, cyclin E differences observed between NAT and other tumor samples is more consistent than the proliferative activity of the tissue and could represent
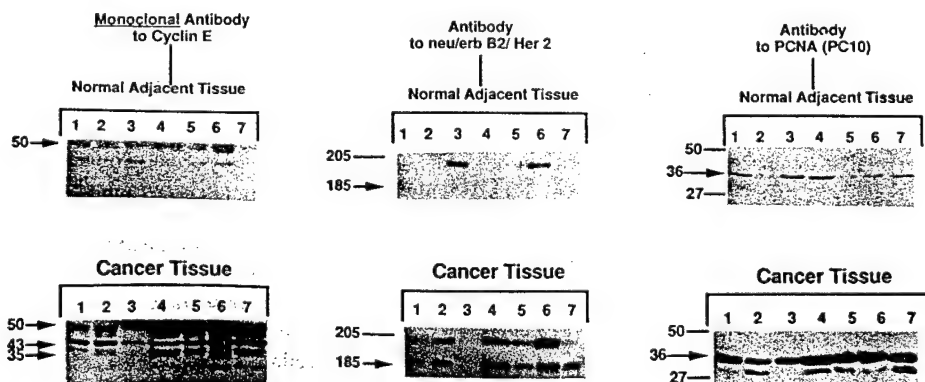

Fig. 2. The altered expression of cyclin E correlates with increased tumor grade in breast cancer. Whole cell lysates were extracted from seven pairs of adjacent normal human breast tissue samples and human breast cancer tissues. (Each paired sample was obtained from the same patient). Breast cancer types and histological/tumor grades are: *Lane 1*, intraductal carcinoma of the breast (stage $T_1/N_0/M_0$), grade I; *Lane 2*, invasive well differentiated ductal carcinoma (stage $T_1/N_0/M_0$), grade I; Lane 3, intraductal carcinoma (stage $T_{1/2}/N_0/M_0$), grade I; *Lane 4*, invasive and intraductal carcinoma (stage $T_2/N_0/M_0$), Grade II; *Lane 5, in situ* and infiltrating ductal carcinoma (stage $T_2/N_1/M_0$), grade II/III; *Lane 6*, infiltrating ductal carcinoma (stage $T_3/N_0/M_0$), grade II/III; and *Lane 7*, invasive ductal carcinoma, (stage $4/N_0/M_0$), grade III. Protein extracts were analyzed on Western blots (100 μg of protein extract/lane) and hybridized with the indicated antibodies. Arrows; predominant proteins reacting with the indicated antibodies. Molecular mass standards were used on each gel to estimate the position of each band.
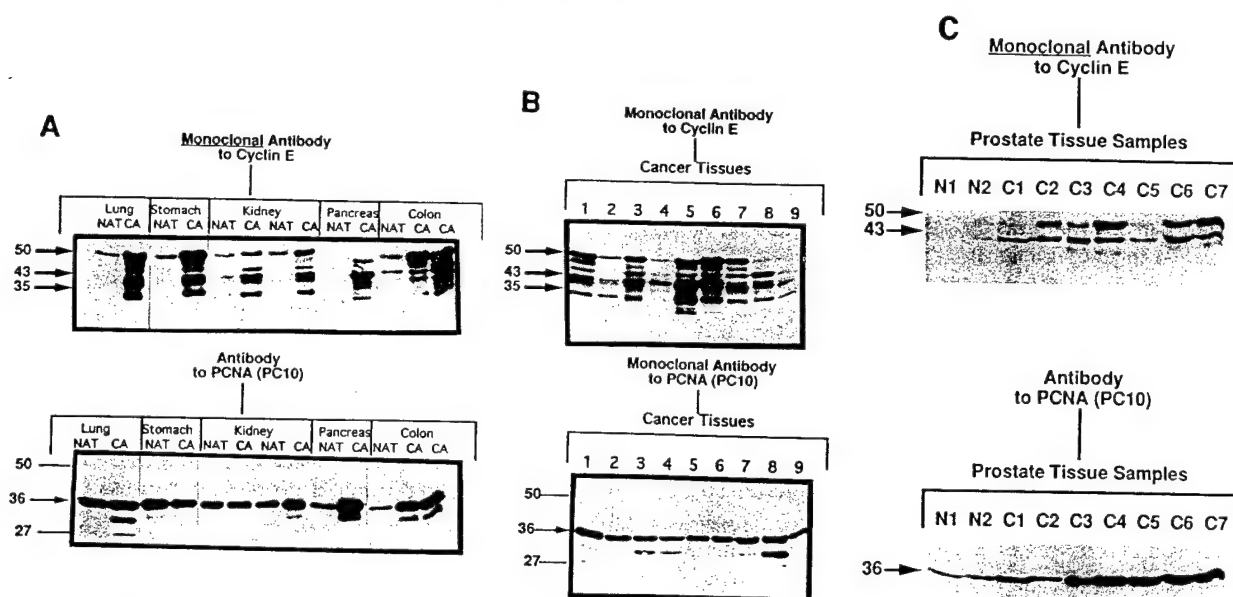
Fig. 3. Altered expression of cyclin E may be a general phenomenon in cancer. *A*, whole cell lysates were extracted from the indicated tumor tissues and normal adjacent tissue. (Each paired sample was obtained from the same patient). Cancer types are: *Lung*, adenosquamous carcinoma; *Stomach*, malignant gastrointestinal stromal tumor; *Kidney*, renal cell carcinoma (NAT samples were obtained from the surrounding kidney with mild chronic inflammation); *Pancreas*, infiltrating adenocarcinoma arising in tubular adenoma; *Colon*, invasive, poorly differentiated, mucin-secreting, signet ring adenocarcinoma. *B*, no normal adjacent tissue was available from these tumor samples. *Lane 1*, uterine leiomysarcoma, grade IV; *Lane 2*, uterine leiomysarcoma, grade II/III; *Lane 3*, moderately differentiated endometrial adenocarcinoma; *Lane 4*, well differentiated endometrial adenocarcinoma, grade II; *Lane 5*, papillary serous carcinoma of the ovary; *Lane 6*, poorly differentiated serous adenocarcinoma of ovary with psammoma bodies; *Lane 7*, testicular tumor, seminoma; *Lane 8*, metastatic esophageal adenocarcinoma; *Lane 9*, primary tumor is melanoma which has metastasized to the spleen. Protein extracts were analyzed on Western blots (100 μg of protein extract/lane) and hybridized with the indicated antibodies. *Arrows*, the predominant proteins reacting with the indicated antibodies. Molecular mass standards were used on each gel to estimate the position of each band. *C*, Cyclin E is altered in prostate cancer. Whole cell lysates were extracted from several normal and prostatic cancer samples with the following specifications and Gleason's grade. Gleason's grade is a combined score of two distinct microscopic areas of the tumor used to quantify the overall degree of histological anaplasia; a higher grade correlates with a higher risk of metastases and worse prognosis. *Lane 1*, atypical hyperplasia, normal; *Lane 2*, local-atypical hyperplasia, normal; *Lane 3*, adenocarcinoma, grade 5/10 (*Lanes 2* and *3* are a matched pair from the same patient); *Lane 4*, adenocarcinoma, grade 3/4; *Lane 5*, adenocarcinoma with mild hyperplasia, grade 3 + 2 = 5; *Lane 6*, adenocarcinoma, grade 3 + 3 = 6; *Lane 7*, adenocarcinoma with slight hyperplasia, grade 3 + 4 = 7; *Lane 8*, adenocarcinoma with moderate hyperplasia, grade 3 + 4 = 7; and *Lane 9*, adenocarcinoma with moderate hyperplasia, grade 3 + 4 = 7. Protein extracts were analyzed on Western blots (75 μg of protein extract/lane) and hybridized with the indicated antibodies. Arrows, the predominant proteins reacting with the indicated antibodies. Molecular mass standards were used on each gel to estimate the position of each band.

a true normal *versus* tumor difference. Collectively, these observations suggest that cyclin E alterations are of general occurrence, irrespective of the tumor origin.

Cyclin E alterations and PCNA levels were also examined in whole cell lysates prepared from surgical samples obtained from several prostate cancer patients and subjected to Western blot analysis and are shown according to Gleason's grade (a histological score used in the pathological description of prostate cancer due to its correlation with subsequent metastases and prognosis; Fig. 3*C*). These analyses revealed that, in the prostate NAT samples, cyclin E was present at very low to undetectable levels. However, there were at least two isoforms of cyclin E protein present in most tumor samples examined, and the expression level of these isoforms increased with increasing tumor grade (with the exception of Fig. 3, *Lane C5*). There was a high cellular proliferative activity in the hyperplastic NAT samples as evident by the PCNA levels. The PCNA levels increased with increasing tumor grade; however, the difference in cyclin E expression between NAT and tumor tissue was higher than that of PCNA. These observations suggest that cyclin E alteration is a general event which occurs in tumor and not proliferating normal cells.

Alteration of Cyclin E in Lymphatic Leukemia. In order to assess the generality of cyclin E alteration in cancer and in non-solid tumors, we next examined blood samples from leukemia patients for the presence of cyclin E alterations. Fig. 4*A* depicts Wright's stain of peripheral blood lymphocytes from a normal (*N*) volunteer and the three CLL/PL patients (*L1–3*). Whole cell lysates prepared from lymphocytes, isolated by centrifugation of whole blood through ficoll gradient, were subjected to Western blot analysis (Fig. 4*B*). In the normal volunteer, the pattern of expression of cyclin E protein is indicative of nontumorous tissue as evident by very low levels of

different cyclin E isoforms. In the CLL/PL patient with stage A form of the disease, there was a shift in the form of cyclin E protein expression but very little, if any, alterations. Only the M_r 50,000 cyclin E protein was moderately overexpressed. In the patient with stage B of the disease, however, there was a strong overexpression of the M_r 50,000 cyclin E protein and the appearance of the lower molecular weight isoforms of the protein. Finally, cyclin E alteration was most pronounced in a stage C CLL/PL patient, as evident by the overexpression of proteins ranging in size from M_r 35,000–50,000 (Fig. 4*B*, *Lane L3* and *L3 (TX)*. There was no difference in the pattern of cyclin E protein alteration before (*L3*) or 6 days into a 7-day treatment with infusion of 2-chlorodeoxy-adenosine [*L3 (TX)*], suggesting that the cyclin E producing leukemia cells were not preferentially killed during this treatment, even though the total number of lymphocytes was considerably reduced. PCNA levels in all the samples were quite similar, indicating that there are proliferating cells at every stage of the disease as well as in the normal lymphocytes. Thus, PCNA measured only cellular proliferative activity and did not differentiate between normal *versus* tumor cells.

In summary, we have examined the alterations of cyclin E protein in surgical material from 42 cancer patients and (*a*) have corroborated our previous *in vitro* observations (21) using cultured normal *versus* tumor breast cells by extending them to the *in vivo* condition. We observe that cyclin E undergoes very similar alterations *in vivo* as *in vitro*; therefore, the overexpression and alteration of cyclin E in is not an artifact of culture conditions and represents an *in vivo* phenomenon; (*b*) our data suggest that the alteration of cyclin E becomes more severe with breast tumor stage and grade and is more consistent than cell proliferation or other tumor markers such as c-*erb* B2 or cyclin D1. Hence, the altered expression of cyclin E in the breast tumor
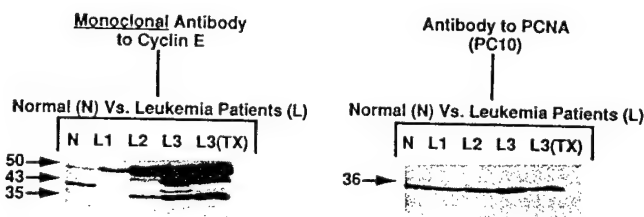
A
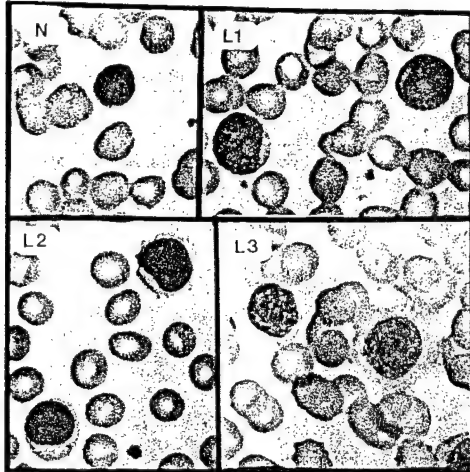
B

Fig. 4. Alteration of cyclin E in peripheral blood lymphocytes from patients with chronic lymphocytic leukemia exhibiting a prolymphocytic morphology *A*, peripheral blood lymphocytes demonstrated by Wright-Giemsa stain from normal donor (*N*) or three patients with chronic lymphocytic leukemia (*L1–3*) with predominant prolymphocytic morphology. *B*, peripheral blood mononuclear cells, containing mostly lymphocytes, were purified from whole human blood by Ficoll-Paque gradient centrifugation; whole cell lysates were extracted and subjected to Western blot analysis (at 100 μg/lane) and hybridized with the indicated antibodies. *Lane 1*, lymphocytes from a normal donor; *Lane 2*, lymphocytes from a patient with indolent CLL/PL, clinical stage A (34); *Lane 3*, lymphocytes from a patient with CLL/PL, stage B; *Lane 4*, lymphocytes from a patient with CLL/PL, stage C, before treatment with 2-chlorodeoxyadenosine; and *Lane 5*, lymphocytes from same patient as in *Lane 4* but taken 6 days after initiation of therapy with 2-chlorodeoxyadenosine given by 7-day i.v. infusion.

samples is not a mere consequence of cell proliferation and represents a true difference among NAT and low and high stage and grade tumors and as such represents a potential new prognostic marker for breast cancer; and (*c*) alteration of cyclin E is a general phenomenon which occurs in all 12 kinds of solid tumors examined as well as blood samples from patients with chronic lymphocytic leukemia exhibiting a prolymphocytic morphology.

Future studies should delineate the mechanism of this alteration in the tumor cells and examine the consequences of cyclin E alterations in the transformation process. The general alterations of cyclin E protein observed in most tumor samples examined is suggestive of its role as an oncogene. Recent *in vitro* studies propose that cyclin E alterations in tumor cells may be in part due to gene amplification and deletional mutations of the cyclin E gene (19, 21).[4] Furthermore, in synchronized populations of tumor cells which amplify the cyclin E gene, cyclin E protein is no longer cell cycle regulated and appears constitutively in the cell cycle.[4] Finally, to examine the potential use of cyclin E clinically as a prognostic marker in cancer, prospective studies with a larger number of patients are required.

---

[4] K. Keyomarsi *et al.*, unpublished observations.

References

1. Boring, C. C., Squires, T. S., and Tong, T. Cancer Statistics, 1993. CA: Cancer J. Clin., *20:* 7–26, 1993.
2. Harris, J. R., Hellman, S., Henderson, I. C., and Kinne, D. W. Breast Diseases, Ed. 2. Philadelphia: J. B. Lippincott Company, 1991.
3. Slamon, D. J., Clark, G. M., Wong, S. G., Levin, W. J., Ullrich, A., and McGuire, W. L. Human breast cancer: correlation of relapse and survival with amplification of the HER-2/*neu* oncogene. Science (Washington DC), *235:* 177–182, 1987.
4. Tiwari, R. K., Borgen, P. I., Wong, G. Y., Cordon-Cardo, C., and Osborne, M. P. HER-2/*neu* amplification and overexpression in primary human breast cancer is associated with early metastasis. Anticancer Res., *12:* 419–425, 1992.
5. Hunter, T. Oncogenes and cell proliferation. Curr. Opin. Genet. Dev., *3:* 1–4, 1993.
6. Hunter, T., and Pines, J. Cyclins and cancer. Cell, *66:* 1071–1074, 1991.
7. Wang, J., Chenivesse, X., Henglein, B., and Brechot, C. Hepatitis B virus integration in a cyclin A gene in a hepatocellular carcinoma. Nature (Lond.), *343:* 555–557, 1990.
8. Faha, B., Ewen, M. E., Tsai, L. H., Livingston, D. M., and Harlow, E. Interaction between human cyclin A and adenovirus E1A-associated p107 protein. Science (Washington DC), *255:* 87–90, 1992.
9. Giordano, A., Whyte, P., Harlow, E., Franza, B. R., Jr., Beach, D., and Draetta, G. A 60 kd cdc2-associated polypeptide complexes with the E1A protein in adenovirus-infected cells. Cell, *58:* 981–990, 1989.
10. Pines, J., and Hunter, T. Human cyclin A is adenovirus E1A-associated protein p60 and behaves differently from cyclin B. Nature (Lond.), *346:* 760–763, 1990.
11. Quelle, D. E., Ashmun, R. A., Shurleff, S. A., Kato, J-y., Bar-Sagi, D., Roussel, M. F., and Sherr, C. J. Overexpression of mouse D-type cyclins accelerates G_1 phase in rodent fibroblasts. Genes Dev., *7:* 1559–1571, 1993.
12. Motokura, T., Bloom, T., Kim, H. G., Juppner, H., Ruderman, J. V., Kronenberg, H. M., and Arnold, A. A novel cyclin encoded by a *bcl-1* linked candidate oncogene. Nature (Lond.), *350:* 512–515, 1991.
13. Matsushime, H., Roussel, M. F., Ashman, R. A., and Sherr, C. J. Colony-stimulating factor 1 regulates novel cyclins during the G_1 phase of the cell cycle. Cell, *65:* 701–713, 1991.
14. Rosenberg, C. L., Kim, H. G., Shows, T. B., Kronenberg, H. M., and Arnold, A. Rearrangement and overexpression of *D11S287E*, a candidate oncogene on chromosome 11q13 in benign parathyroid tumors. Oncogene, *6:* 449–453, 1991.
15. Bianchi, A. B., Fischer, S. M., Robles, A. I., Rinchik, E. M., and Conti, C. J. Overexpression of cyclin D1 in mouse skin carcinogenesis. Oncogene, *8:* 1127–1133, 1993.
16. Buckley, M. F., Sweeney, K. J. E., Hamilton, J. A., Sini, R. L., Manning, D. L., Nicholson, R. I., deFazio, A., Watts, C. K. W., Musgrove, E. A., and Sutherland, R. L. Expression and amplification of cyclin genes in human breast cancer. Oncogene, *8:* 2127–2133, 1993.
17. Lammie, G. A., Fantl, V., Smith, R., Shuuring, E., Brookes, S., Michalides, R., Dickson, C., Arnold, A., and Peters, G. *D11S287*, a putative oncogene on chromosome 11q13, is amplified and expressed in squamous cell and mammary carcinomas and linked to BCL-1. Oncogene, *6:* 439–444, 1991.
18. Jiang, W., Kahn, S. M., Tomita, N., Zhang, Y-J., Lu, S-H., and Weinstein, B. Amplification and expression of the human cyclin D gene in esophageal cancer. Cancer Res., *52:* 2980–2983, 1992.
19. Leach, S. F., Elledge, S. J., Sherr, C. J., Willson, J. K. V., Markowitz, S., Kinzler, K. W., and Vogelstein, B. Amplification of cyclin genes in colorectal carcinomas. Cancer Res., *53:* 1986–1989, 1993.
20. Jiang, W., Zhang, Y-J., Kahn, S. M., Hollstein, M. C., Santella, R. M., Lu, S-H., Harris, C. C., Montesano, R., and Weinstein, I. B. Altered expression of cyclin D1 and retinoblastoma genes in human esophageal cancer. Proc. Natl. Acad. Sci. USA, *90:* 9026–9030, 1993.
21. Keyomarsi, K., and Pardee, A. B. Redundant cyclin overexpression and gene amplification in breast cancer cells. Proc. Natl. Acad. Sci. USA, *90:* 1112–1116, 1993.
22. Jessus, C., Ducommun, B., and Beach, D. Direct activation of cdc2 with phosphatase: identification of p13^{suc1}-sensitive and -insensitive steps. FEBS Lett. *266:* 4–8, 1990.
23. Bradford, M. A rapid and sensitive method for the quantitation of microgram quantities of proteins using the principle of protein-dye binding. Anal. Biochem, *72:* 248–254, 1976.
24. DeCaprio, J. A., Furukawa, Y., Ajchenbaum, F., Griffin, J. D., and Livingston, D. M. The retinoblastoma-susceptibility gene product becomes phosphorylated in multiple stages during cell cycle entry and early progression. Proc. Natl. Acad. Sci. USA, *89:* 1795–1798, 1992.
25. Dulic, V., Lees, E., and Reed, S. I. Association of human cyclin E with a periodic G_1-S phase protein kinase. Science (Washington DC), *257:* 1958–1961, 1992.
26. Lees, E., Faha, B., Dulic, V., Reed, S. I., and Harlow, E. Cyclin E/cdk2 and cyclin A/cdk2 kinases associate with p107 and E2F in a temporally distinct manner. Genes Dev., *6:* 1874–1855, 1992.
27. Fazely, F., Dezube, B. J., Allen-Ryan, J., Pardee, A. B., and Ruprecht, R. M. Pen-

toxifylline (Trental) decreases the replication of the human immunodeficiency virus type I in human peripheral blood mononuclear cells and in cultured T cells. Blood, *77:* 1653–1656, 1991.

28. Tsai, L-H., Lees, E., Faha, B., Harlow, E., and Riabowol, K. The cdk2 kinase is required for the G_1-to-S transition in mammalian cells. Oncogene, *8:* 1593–1602, 1993.

29. Fantl, V., Richards, M. A., Smith, R., Lammie, G. A., Johnstone, G., Allen, D., Gregory, W., Peters, G., Dickson, C., and Barnes, D. M. Gene amplification on chromosome band 11q13 and oestrogen receptor status in breast cancer. Eur. J. Cancer, *26:* 423–429, 1990.

30. Theillet, C., Adnane, J., Szepetowski, P., Simon, M-P., Jeanteur, P., Birnbaum, D., and Gaudray, P. BCL-1 participates in the 11q13 amplification found in breast cancer. Oncogene, *5:* 147–149, 1990.

31. Prelich, G., Tan, C. K., Kostura, M., Mathews, M. B., So, A., Downey, K. M., and Stillman, B. Functional identity of proliferating cell nuclear antigen and a DNA polymerase δ auxiliary protein. Nature (Lond.), *326:* 517–520, 1987.

32. Bravo, R., and Celis, J. E. A search for differential polypeptide synthesis throughout the cell cycle of Hela cells. J. Biol. Chem., *84:* 795–802, 1980.

33. Bravo, R., Flank, R., Blundell, P. A., and Macdonaldo-Bravo, H. Cyclin/PCNA is the auxiliary protein of DNA polymerase δ. Nature (Lond.), *326:* 515–517, 1987.

34. Binet, J. L., Auquier, A., Dighiero, G., Chastang, C., Piguet, H., Goasguen, J., Vauier, G., Potron, G., Colona, P., Oberling, F., Thomas, M., Tchernia, G., Jacquillat, C., Boivin, P., Lesty, C., Duault, M. T., Monconduit, M., Belabbes, S., and Gremy, F. A new prognostic classification of chronic lymphocytic leukemia derived from a multivariate survival analysis. Cancer (Phila.), *48:* 198–206, 1981.

Deregulation of cyclin E in breast cancer

Khandan Keyomarsi, Darryl Conte Jr, Wendy Toyofuku and M Pat Fox

Division of Molecular Medicine, Laboratory of Diagnostic Oncology, Wadsworth Center, Albany, New York 12201, USA

Cyclin E, a regulatory subunit of cyclin dependent kinase-2, is thought to be rate limiting for the G1/S transition during the mammalian cell cycle. Previously, we showed severe alterations in cyclin E protein expression in human mammary epithelial cell lines and in surgical material obtained from patients with various malignancies. To understand the functional basis of these alterations we analyse here the regulation of cyclin E in breast cancer cells. We find that while cyclin E protein and its associated kinase activity in normal cells are cell cycle regulated, in tumor cells it remains in an active complex throughout the cell cycle. We also analysed cyclin E for possible deletions which could result in its constitutive function and found two novel truncated variants in its coding region. These variant forms of cyclin E were detected in several normal and tumor cell lines and tissue specimens. However, Western blot analysis indicated that only the multiple isoforms of cyclin E protein were expressed in tumor but not the normal tissue specimen, suggesting post transcriptional regulation of cyclin E. Lastly, *in vitro* analyses indicated that these truncated variant forms of cyclin E are biochemically active in their ability to phosphorylate histone H1. Collectively these observations suggest the presence of more than one form of cyclin E mRNA in all cells, normal and tumor. Once translated in tumor cells, the protein products of these truncated forms could give rise to a constitutively active form of cyclin E containing complexes.

Keywords: breast cancer; cell cycle; cyclin E; alternative splicing

Introduction

Cyclins are prime cell cycle regulators and central to the control of cell proliferation in eukaryotic cells via their association with and activation of cyclin-dependent protein kinases 1–7 (cdks) (reviewed in, Elledge and Spottswood, 1991; Heichman and Roberts, 1994; Hunter and Pines, 1994; King et al., 1994; Nurse, 1994; Sherr, 1994; Morgan, 1995). Cyclins were first identified in marine invertebrates as a result of their dramatic cell cycle expression patterns during meiotic and early mitotic divisions (Evans et al., 1983; Swenson et al., 1986; Standart et al., 1987; Sherr, 1993). Several classes of cyclins have been described and are currently designated as cyclins A-H, some with multiple members (reviewed in Draetta, 1994). Cyclins can be distinguished on the basis of conserved sequence motifs, patterns of appearance and apparent func-

tional roles during specific phases and regulatory points of the cell cycle in a variety of species.

The connection between cyclins and cancer has been substantiated with the D type cyclins (Hunter and Pines, 1991; Sherr, 1993; Draetta, 1994; Hunter and Pines, 1994). Cyclin D1 was identified simultaneously by several laboratories using independent systems: It was identified in mouse macrophages due to its induction by colony stimulating factor 1 during G1 (Matsushime et al., 1991); in complementation studies using yeast strains deficient in G1 cyclins (Lew et al., 1991; Xiong et al., 1991); as the product of the *bcl*-1 oncogene (Withers et al., 1991) and as the PRAD1 proto-oncogene in some parathyroid tumors where its locus is overexpressed as a result of a chromosomal rearrangement that translocates it to the enhancer of the parathyroid hormone gene (Matsushime et al., 1991; Motokura et al., 1991, Motokura and Arnold, 1993; Quelle et al., 1993). In centrocytic B cell lymphomas cyclin D1 (PRAD1)/BCL1 is targeted by chromosomal translocations at the BCL1 breakpoint, t(11;14) (q13;q32) (Rosenberg et al., 1991a,b). Furthermore, the cyclin D1 locus undergoes gene amplification in mouse skin carcinogenesis, as well as in breast, esophageal, colorectal and squamous cell carcinomas (Lammie et al., 1991; Jiang et al., 1992, 1993b; Bianchi et al., 1993; Buckley et al., 1993; Leach et al., 1993). Several groups have examined the ability of cyclin D1 to transform cells directly in culture with mixed results (Hinds et al., 1992, 1994; Jiang et al., 1993a; Quelle et al., 1993; Rosenwald et al., 1993; Sherr, 1993; Lovec et al., 1994; Musgrove et al., 1994; Resnitzky et al., 1994). However, the overexpression of cyclin D1 was recently observed in mammary cells of transgenic mice and results in abnormal proliferation of these cells and the development of mammary adenocarcinomas (Wang et al., 1994). This observation strengthens the hypothesis that the inappropriate expression of a G1 type cyclin may lead to loss of growth control.

Recently, we and others have reinforced the linkage between oncogenesis and the cell cycle by correlating the deranged expression of cyclins to the loss of growth control in breast cancer (Buckley et al., 1993; Keyomarsi and Pardee, 1993). Using proliferating normal *vs* human tumor breast cell lines in culture as a model system, we have described several changes that are seen in all or most of these lines. These include increased cyclin mRNA stability, resulting in overexpression of mitotic cyclins and cdc2 RNAs and proteins in 9/10 tumor lines, leading to the deranged order of appearance of mitotic cyclins prior to G1 cyclins in synchronized tumor cells.

The most striking abnormality in cyclin expression we found, was that of cyclin E. Cyclin E protein not only was overexpressed in 10/10 breast tumor cell lines but it was also present in lower molecular weight

isoforms than that found in normal cells (Keyomarsi and Pardee, 1993). We directly examined the relevance of cyclin derangement to *in vivo* conditions, by measuring the expression of cyclin E protein in tumor samples *vs* normal adjacent tissue obtained from patients with various malignancies (Keyomarsi *et al.*, 1994). These analyses revealed that breast cancers and other solid tumors, as well as malignant lymphocytes from patients with lymphatic leukemia, show severe quantitative and qualitative alteration in cyclin E protein expression independent of the S-phase fraction of the samples. In addition, the alteration of cyclin E becomes more severe with breast tumor stage and grade and is more consistent than cell proliferation or other tumor markers such as PCNA or c-*erb*B2. These observations strongly suggested the use of cyclin E as a new prognostic marker.

In this report, we have further characterized the alterations of cyclin E in breast cancer. We show that while cyclin E is cell cycle regulated in normal cells it is present constitutively and in an active cdk2 complex in synchronized populations of breast cancer cells. We also identify two novel truncated variant forms of cyclin E mRNA as detected by RT-PCR which are ubiquitously detected in normal and tumor cells and tissues. These variant forms of cyclin E can give rise to an active cyclin/cdk2 complex *in vitro*, but they do not seem to be translated in normal cells.

Results

Elevated cyclin E associated kinase activity in breast cancer cells

To test the hypothesis that the altered expression pattern of cyclin E protein found in tumor cell lines and tissue samples (Keyomarsi *et al.*, 1994) is associated with increased cyclin E kinase activity, we compared cyclin E expression and activity in two normal *vs* five breast cancer cell lines (Figure 1). The two normal cell lines are the normal cell strain, 76N (Figure 1, lane 1), obtained from reduction mammoplasty and a near diploid immortalized cell line MCF-10A (Figure 1, lane 2) (Soule *et al.*, 1990). 76N is a mortal cell strain since it rapidly proliferates (doubling time of 24–27 h) for multiple passages before senescence at around passage 20 (Band and Sager, 1989). The MCF-10A cell line is a spontaneously immortalized human breast epithelial cell line which can be cultured indefinitely. This cell line has no tumorigenicity potential but retains characteristics of a normal breast epithelial cell line (Soule *et al.*, 1990).

We examined the pattern of cyclin E protein expression in normal *vs* tumor cell lines using monoclonal and polyclonal antibodies to cyclin E on Western blots (Figure 1A). Similar immunoblot banding patterns were obtained with either the monoclonal or polyclonal antibody to cyclin E, confirming the specificity of the multiple bands. However, the patterns of cyclin E protein expression was different between normal and tumor cells. Both cyclin E antibodies recognized one major protein migrating at ~50 kDa and two much less abundant lower molecular weight forms, in the two normal cell lysates. In the tumor cell lysates on the other hand, the
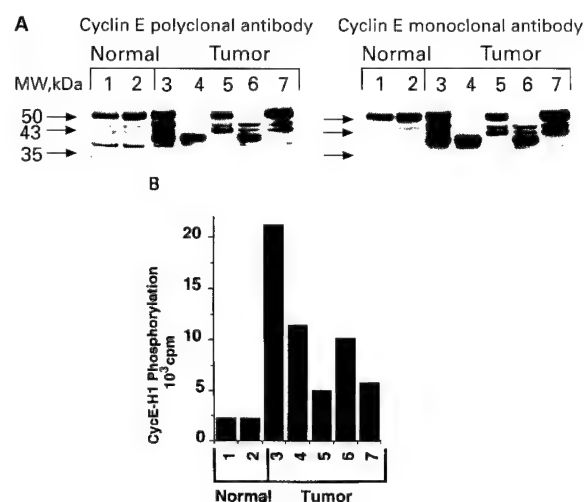
Figure 1 Correlation of cyclin E protein(s) to cyclin E associated kinase activity (**A**) Western blot analysis of cyclin E expression in normal *vs* tumor cells using two different cyclin E antibodies. Whole cell lysates were extracted from the seven cell lines, (100 μg of protein extract/lane), run on a 10% acrylamide gel and blotted as described in Materials and methods. Lane 1, 76N normal human mortal breast epithelial cell strain; lane 2, MCF-10A normal immortalized human breast epithelial cell line; (lanes 3–7 are all human breast cancer cell lines) lane 3, MDA-MB-157; lane 4, MDA-MB-436; lane 5, ZR75T; lane 6, SKBR3; lane 7, MCF-7. The 50 kDa arrowhead points to the cyclin E protein of the predicted size. The other arrowheads point to the additional cyclin E isoforms observed in the tumor cell lines ranging in molecular weight from 35 to 43 kDa. Molecular mass standards were used in each gel to estimate the position of each band. (**B**) Cyclin-E associated histone H1 kinase activity. Equal amounts of proteins from cell lysates were immunoprecipitated with anti-cyclin E coupled to protein A beads using histone H1 as substrate. The associated kinase activities were quantified by scintillation counting

same antibodies recognized three (lane 3), two (lanes 5–7) or one (lane 4) additional and highly abundant isoforms of cyclin E protein that in each case revealed a different pattern from that of the normal cells.

We next analysed the cyclin E associated protein kinase activity in all cells by measuring the phosphorylation of histone H1 in immunoprecipitates made with the polyclonal antibody to cyclin E (Figure 1B). In all of the tumor cell lysate immunoprecipitates, the activity levels of cyclin E-associated kinase were significantly higher than that of both normal cells. For example, in MDA-MB-436 and SKBR3 tumor cell lines (lanes 4 and 6) which express only the lower molecular weight isoforms of cyclin E protein, the associated kinase activity was sixfold greater than that of the normal cells which express mainly the high molecular weight, 50 kDa, form of cyclin E protein. Similarly, the other tumor lines containing altered patterns of cyclin E expression, had significantly higher cyclin E-associated H1-kinase activity as compared to the normal cell strains.

### *Lack of cell cycle regulation of cyclin E in breast cancer cells*

In one tumor line, MDA-MB-157 (Figure 1, lane 3), the level as well as the associated kinase activity of cyclin E protein was the highest of all the tumor cell lines examined. Previous studies (Keyomarsi and

Pardee, 1993) showed that this overexpression is in part due to an eightfold amplification of the cyclin E gene and 64-fold overexpression of its mRNA in this cell line. The cyclin E gene is amplified in tandem and is not associated with gross genomic rearrangements (data not shown). To investigate whether the signals required for normal regulation of cyclin E expression are altered or lost in tumor cells, the cell cycle expression of cyclin E protein and its associated kinase activities in the MDA-MB-157 cell line were compared to normal mammary epithelial 76N cells (Figure 2).

Both cell lines were synchronized in the G1/S border by double thymidine block. Synchrony of both cell types at several times after release from the block was monitored by flow cytometry * (Figure 2D). At various times after release from treatment for synchronization, cells were harvested and extracted proteins were analysed on Western blots with antibodies to cyclins E and A (Figure 2A). In normal 76N cells, the pattern of expression of cyclin E and cyclin A proteins is consistent with that seen for other normal cell types with levels rising prior to S phase and oscillating thereafter in the cell cycle (Koff et al., 1992). In addition there is only one major form (i.e., 50 kDa) of cyclin E protein detected and there is a shift in the timing of when cyclin E vs cyclin A appears in the cell cycle of these normal epithelial cells. However, in the tumor cells, cyclin E protein does not appear to be cell cycle regulated and multiple isoforms of the protein are also present with similar signal intensities and banding patterns during the time intervals examined. In addition when these tumor cells are synchronized by other agents, such as Lovastatin (Keyomarsi et al., 1991), cyclin E expression is also constitutive throughout the cell cycle, resembling a pattern identical to that shown in Figure 2A (data not shown). In the same tumor cell extracts, cyclin A protein is cell cycle regulated with peak levels coinciding with peak S and early G2/M phase. Hence, it appears that in this tumor cell line, cyclin E is abnormally regulated during the cell cycle.

In order to compare the kinase activity associated with cyclin E and cdk2 in normal and tumor cells, we measured the phosphorylation of histone H1 in immunoprecipitates prepared from synchronous cell extracts using antibody to either cyclin E or cdk2 (Figure 2B). There were two significant differences found between normal and tumor cells: First, in the length of time which an active cyclin E/cdk2 complex is present and secondly in the amount of kinase activity associated with cyclin E vs cdk2 during the normal and tumor cell cycles. In normal cells, both cyclin E associated kinase and cdk2 activities are cell cycle regulated, coinciding with the levels of cyclins E and A protein expression (Figure 2A). In addition, the cdk2 activity is one order of magnitude (i.e. 10-fold) higher than cyclin E associated activity, consistent with cdk2's ability to form an active complex with other cyclins

besides cyclin E in normal cells (Figure 2B). Hence, cyclin E in these normal cells is indeed cell cycle regulated and the signals required for such regulation are intact both at the protein expression level and kinase activity.
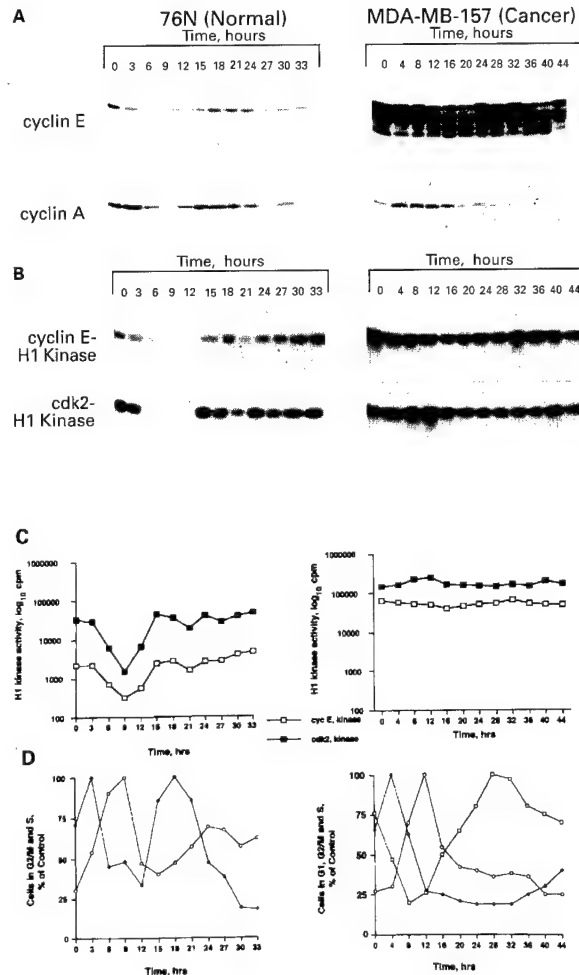
Figure 2 Expression of cyclin E in synchronized normal 76N and tumor MDA-MB-157 breast cells. Both cell types were synchronized by double thymidine block procedure (see Materials and methods). At the indicated times following release from double thymidine block, cell lysates were prepared and subjected to (**A**) Western blot and (**B**) Histone H1 kinase analysis. Protein (50 μg) for each time point was applied to each lane of a 10% acrylamide gel and blotted as described. The same blot was reacted with cyclin E monoclonal (HE12) and cyclin A affinity purified polyclonal antibodies. The blots were stripped between the two assays in 100 mm β-mercaptoethanol, 62.5 mm Tris HCl (pH 6.8) and 2% SDS for 30 min at 55°C. For Histone H1 kinase activity, equal amount of proteins (600 μg) from cell lysates prepared from each cell line at the indicated times were immunoprecipitated with anti-cyclin E (polyclonal) or anti-CDK2 (polyclonal) coupled to protein A beads using histone H1 as substrate. Panel B is the autoradiogram of the histone H1 SDS−PAGE gel and (**C**) shows the quantification of the histone H1 associated kinase activities by scintillation counting. Open symbols correspond to cyclin E associated kinase activity and closed symbols correspond to cdk2 activity (**D**). At various times after release from double thymidine block, aliquots were removed and subjected to flow cytometry analysis. Cells in S phase (◆), G2/M phase (○) and G1 phase (□), are expressed as percent of control, where control is equal to the time when the maximum number of cells enter each phase of the cell cycle

---

*The doubling times of the normal 76N and tumor MDA-MB-157 cells are 27 and 36 h, respectively, and their DNA content distribution in different cell cycle phases are as follows: 76N- G1 (75%), S (4%) and G2/M (21%); MDA-MB-157-G1 (56%), S (13%) and G2/M (31%).

In tumor cells, on the other hand, cyclin E is not cell cycle regulated and remains in a catalytically active complex throughout the cell cycle resulting in a constitutive pattern of histone H1 phosphorylation. The basal levels of cyclin E associated kinase activity during the tumor cell cycle, at any time interval examined, are at least 20 times higher than that of the normal cells (Figure 2C). Cdk2, a kinase which binds to both cyclin E and A, is also constitutively active during the cell cycle. However, cdk2 activity in this tumor cell line is only twofold higher than cyclin E associated kinase activity, presumably due to the abundance of cyclin E protein which is capable of sequestering cdk2. When cyclin A protein levels are induced in the tumor cells, there is only a 30% additional induction in cdk2 associated activity. These observations suggest that cyclin E protein, which is constitutively expressed in the cell cycle of tumor cells, also results in an active kinase complex throughout the cell cycle. Furthermore, since the same cyclin-dependent kinase can be regulated by both cyclins E and A, increased levels of cyclin E may overcompensate for cyclin A regulation, again resulting in a constitutively active and abundant cyclin E/cdk2 complex.

Isolation of variant forms of cyclin E transcripts

In an attempt to determine the presence of any potential alterations in the cyclin E gene in MDA-MB-157, we amplified the entire cyclin E coding region of this cell line by reverse transcription-polymerase chain reaction amplification (RT-PCR), cloned these products and analysed their DNA sequence (Figure 3). Using a pair of primers flanking the coding sequence of cyclin E gene, we observed at least two distinct PCR products ranging in size from 1.0 to 1.2 kb from the MDA-MB-157 RT template (Figure 3A). The product from the control (cyclin E plasmid DNA) was of 1.2 kb, corresponding to the full length cyclin E cDNA isolated from a HeLa cDNA library (Koff *et al.*, 1991; Lew *et al.*, 1991). We cloned the RT-PCR products from the MDA-MB-157 cell line and confirmed their identity by Southern blotting and by DNA sequencing (data not shown). Three independent RT-PCR reactions were performed on freshly isolated RNA from this cell line. Fifteen clones from each RT-PCR reaction were examined further. Sequence analyses revealed two types of truncated variants of the cyclin E gene, as well as an unequivocally normal sequence, from the MDA-MB-157 cell line (Figure 3).

The PCR products containing these two truncated variants were termed cyclin E-Δ9 and cyclin E-Δ148 (Figure 3B). The alteration in clone cyclin E-Δ9 is a 9 base pair in-frame deletion of nucleotides 67–75 at the 5′ end of the gene, while the alteration in clone cyclin E-Δ148 is a 148 base pair deletion of nucleotides 1000–1147 at the 3′ end of the gene resulting in a frame shift transcript. Curiously, the 148 bp deletion in cyclin E-Δ148 clone disrupts the PEST sequence motif of the gene, which is thought to be important for its role in degradation of the protein product (Koff *et al.*, 1991; Lew *et al.*, 1991). The relative positions of these two newly identified truncations to the wild type sequence of cyclin E are shown in Figure 3B. We performed *in vitro* translation studies on these clones
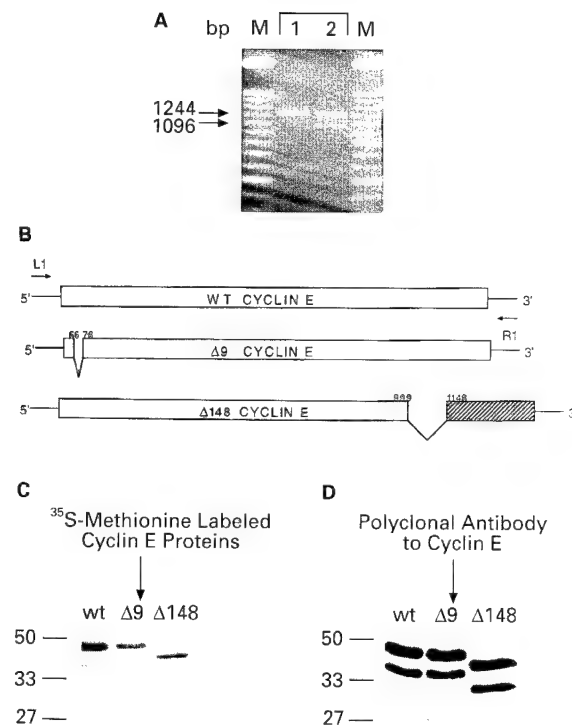
Figure 3 Identification and *in vitro* translation of cyclin E truncated transcripts. (**A**) PCR amplified cyclin E coding sequence using primers (L1CYCE and R1CYCE) flanking the entire coding region of cyclin E. Lane 1: Molecular weight standards; lane 2: control template DNA, a plasmid containing a wild type cyclin E coding sequence; lane 3: RT-PCR amplification of cyclin E using RNA from MDA-MB-157; lane 4: Molecular weight standards. PCR conditions were carried out as described in Materials and methods. PCR products were separated on a 1.5% agarose gel and stained with ethidium bromide. Molecular weight markers in base pairs are indicated (left). (**B**) Relative position of cyclin E Δ9 and Δ148 deletions to the wild type cyclin E sequence. The two arrows flanking the cyclin E coding region refer to the position of R1 (i.e., R1CYCE) and L1 (i.e.,L1CYCE) oligonucleotides used for the RT-PCR reactions. (**C**) The cDNAs of cyclin E clones were subcloned into PCR II vector and transcribed and translated *in vitro* using T7 RNA polymerase-rabbit reticulocyte lysate system in the presence of [^{35}S]methionine and products were analysed on a 10% SDS–PAGE followed by autoradiography (**D**) The *in vitro* translated cyclin E protein products from the three different clones (in the absence of radioactivity) were subjected to Western blot analysis and hybridized to a polyclonal antibody to cyclin E

using T7 RNA polymerase (Figure 3C and D). RNA was translated in the presence of [^{35}S]methionine using a rabbit reticulocyte lysate, analysed by SDS–PAGE and visualized by autoradiography. Cyclin E-wt and cyclin E-Δ9 protein products showed very similar electrophoretic mobilities (Figure 3C). [On a sequencing length SDS–PAGE, gel however, we were able to detect the slight (3 amino acids) molecular weight difference between the two clones (data not shown)]. Cyclin E-Δ148 gives rise to a protein product which is ∼5 kD smaller than the cyclin E-wt, which would correspond to the loss of the 50 amino acids. To confirm that the protein products from *in vitro* translation reactions were indeed cyclin E, the cDNAs of the three different clones were transcribed and translated in the presence of unlabeled methionine and the products were subjected to Western blot analysis
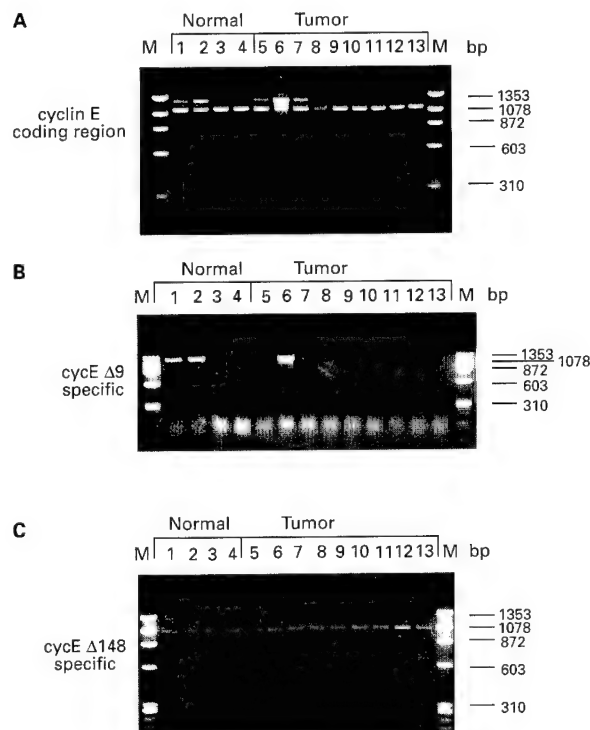
(Figure 3D). The protein products from cyclin-wt, Δ9 and Δ148 clones reacted strongly with the polyclonal antibody to cyclin E, suggesting that the *in vitro* translated products of these clones are truncated forms of cyclin E. Interestingly, all the clones gave rise to two major protein products, migrating at ~45 and ~38 kD for cyclin E-wt and Δ9 clones and ~40 and ~33 kD for cyclin E-Δ148 clone. It is not clear at this point whether the lower molecular weight protein product is a result of proteolytic cleavage, or result of translation initiation from a methionine site further downstream in the coding region.

Expression of cyclin E truncated variants in normal vs tumor cells and tissue samples

Since these two truncated forms of cyclin E cDNA were isolated from one tumor-derived cell line, we investigated the generality of expression of the cyclin E

Figure 4 RT-PCR amplification of cyclin E Δ9 and Δ148 in normal and tumor-derived breast epithelial cell lines. RT-PCR amplification of cyclin E coding sequence from normal and tumor-derived breast epithelial cell lines using (**A**) primers (L1CYCE and R1CYCE) flanking the coding region of cyclin E and amplifying wild type cyclin E sequences, as well as those containing internal deletions, (**B**) primers (LMEMARK3 and R1CYCE) spanning the Δ9 deletion and amplifying only those cyclin E sequences harboring the Δ9 internal deletion of cyclin E and (**C**) primers (L1CYCE and RMEMARK3) spanning the Δ148 internal deletion and amplifying only those cyclin E sequences containing the Δ148 deletion. The cell lines used are as follows: Lane 1, 70N; lane 2, 81N; lane 3, 76N; lane 4, MCF-10A; lane 5, MCF-7; lane 6, MDA-MB-157; lane 7, MDA-MB-231; lane 8, MDA-MB-436; lane 9, T47D; lane 10, BT-20T; lane 11, HBL-100; lane 12, Hs578T and lane 13, ZR75T. Normal cells are represented in lanes 1–4 and tumor-derived cell lines in lanes 5–13; M, Molecular weight size markers
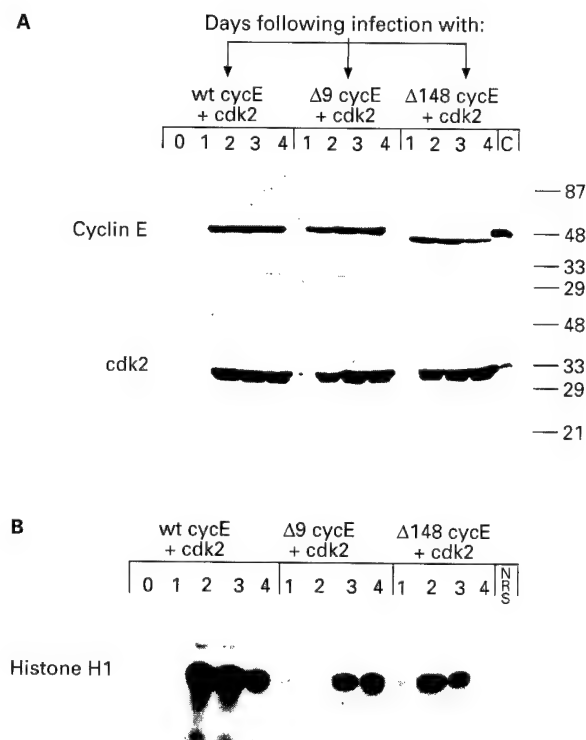
variants in a panel of 13 breast epithelial cell lines (Figure 4A). These cell lines included three normal mortal cell strains (lanes 1–3), one normal immortalized cell line (lane 4) and nine tumor-derived breast cell lines (lanes 5–13). These analyses revealed the presence of multiple transcripts of cyclin E in all cell lines examined. However, no distinct differences were observed in their pattern of expression between normal *vs* tumor cell lines. Furthermore, sequence analysis of a cloned RT-PCR product of 76N normal cells revealed that the major transcript found in this normal cell strain is the Δ148 variant of cyclin E previously identified in MDA-MB-157 tumor cell line (data not shown). These observations indicate that the Δ148 RNA is expressed in all cells examined at an apparently higher level than the wild type species of cyclin E RNA. To examine the specific expression of Δ9 and Δ148 in each cell line, we performed RT-PCR using primers that spanned the deleted sequences, such that only those cell lines containing cyclin E transcripts harboring these deletions would give rise to products. These analyses show that the Δ9 variant form of cyclin E is abundantly present in three cell lines, two of which are normal cell strains and one is the MDA-MB-157, the original cell line this variant form was isolated from (Figure 4B). In addition we find that the Δ148 is present in all cell lines examined (Figure 4C), confirming our previous observation that this variant form of cyclin E is the major transcript found in these cells (Figure 4A).

In order to apply our findings from culture studies to the *in vivo* condition, we examined whether the truncated cyclin E transcripts were also expressed in tumor tissue specimens. We performed RT-PCR using RNA isolated from seven paired samples of human breast carcinoma and normal adjacent tissue (NAT) which are presented according to increased clinical stage (Figure 5). For this experiment, we used primers flanking the entire coding region of cyclin E in order to detect all variants of cyclin E which could contain deletions in the coding region. The RT-PCR products from NAT and tumor tissue samples ranged in size from 1.0 to 1.2 kb (Figure 5A), which are consistent with products obtained with cultured breast cells (Figure 4). Surprisingly, we found that not only did both NAT and tumor tissue samples express similar RT-PCR products corresponding to the cyclin E variants, but that no distinct difference could be found among paired samples as the clinical stage of the disease increases. On the other hand, when we subjected whole cell lysates prepared from these tissue specimens to Western blot analysis, we did observe cyclin E protein alterations which increased qualitatively and quantitatively as the stage of the disease increased. In high staged tumor samples, an antibody to cyclin E reacted strongly with at least three overexpressed proteins ranging in size from 35 to 50 kDa, while in the NAT samples, one major protein of 50 kDa was present at very low levels, consistent with our previous observations (Keyomarsi *et al.*, 1994). Collectively these observations suggest that at the level of RNA there are no apparent differences between normal and tumor cells or between tissue samples in their ability to express the alternate transcripts of cyclin E. However, the alteration in cyclin E protein observed exclusively in tumor cells,

A

B

extracts were collected, homogenized and subjected to Western blot and histone H1 kinase analysis. Western blot analysis shows that there were similar levels of expression of the three cyclin E variants and cdk2 in the infected sf9 cells within one day of infection and thereafter during the course of experiment (Figure 6A). H1 kinase analysis reveal that when the cyclin E-wt/cdk2 co-infected insect cell lysates were immunoprecipitated with an antibody to cdk2, the immunoprecipitates were capable of phosphorylating histone H1 within one day of infection and an active cyclin E/cdk2 complex persisted throughout the experiment (Figure 6B, lanes 1–4). In insect cells co-infected with the two truncated variants of cyclin E, similar results were obtained illustrating that the complex which cycEΔ9 (Figure 6C, lanes 5–8) or cycEΔ148 (Figure 6C, lanes 9–12) formed with cdk2 is also active and is capable of phosphorylating histone H1. However a lower degree of activation was found compared to that with the cyclin E wild type complex. There was a twofold difference in the ability of the cycEΔ9/cdk2 or cycEΔ148/cdk2 to phosphorylate histone H1 when

Figure 5 Comparison of RT-PCR amplified products of cyclin E with their expression in breast cancer specimens. (**A**) RT-PCR amplification of cyclin E coding sequence using total RNA isolated from seven pairs of normal adjacent (NAT) and tumor tissue samples with primers (L1CYCE and R1CYCE) flanking the coding region of cyclin E as described in Figure 4A. (**B**) Western blot analysis of whole cell lysates (100 µg) were prepared from NAT and tumor tissue specimens and probed with a monoclonal antibody to cyclin E. Breast cancer types and histological/tumor grades are as follows: Lanes 1–2, intraductal carcinoma of the breast, Stage T_1, NO, MO, Grade I; Lanes 3–4, invasive well differentiated ductal carcinoma, Stage T_1, NO, MO, Grade I; Lanes 5–6, intraductal carcinoma, Stage $T_{1/2}$, NO, MO, Grade I; Lanes 7–8, invasive and intraductal carcinoma, Stage T_2, NO, MO, Grade II; Lanes 9–10, *in situ* and infiltrating ductal carcinoma, Stage T_2, N1, MO, Grade II/III; Lanes 11–12, infiltrating ductal carcinoma, Stage T_3, NO, MO, Grade II/III; Lanes 13–14, invasive ductal carcinoma, Stage T_4, NO, MO, Grade III. Molecular mass standards were used on each gel to estimate the position of each band

likely occurs post transcriptionally or translationally to result in various forms of the protein detected in tumor but not normal cells or tissues.

Cyclin E truncated variants form biochemically active complexes with cdk2

Based on the evidence that multiple cyclin E transcripts (Figures 4 and 5) are found in normal and tumor cells as well as in tissue samples and that there is an active cyclin E/cdk2 protein complex present throughout the cell cycle of the MDA-MB-157 cell line (Figure 2), we asked whether these alternate transcripts of cyclin E can give rise to a biochemically active product. To investigate this question, we overexpressed cyclin E and cdk2 in insect cells using the baculovirus expression system (Figure 6). Insect cells were co-infected with the recombinant baculovirus containing cdk2 and either cyclin E- wild type (cycE-wt), cyclin E-Δ9, (cycE-Δ9), or cyclin E-Δ148 (cycE-Δ148) cDNAs (Figure 6). At the indicated times (i.e. days) following infection, cell

A

B

Figure 6 Activation of cdk2 by cyclin E wild type and its truncated variants in insect cells. Cell lysates were prepared from insect cells co-infected with baculovirus containing the different cyclin E constructs and cdk2 at the indicated time intervals (days) following co-infection. (**A**) Equal amounts (50 µg) of protein were added to each lane; the gel was then subjected to Western blot analysis with polyclonal antibody to cyclin E or to cdk2. C: Control lane corresponding to 50 µg of extracts from insect cells infected with either cyclin E wt alone, or cdk2 alone baculovirus (**B**) Histone H1 kinase assays were also performed on the same cell extracts by immunoprecipitating equal amount of cell lysate with polyclonal antibody to cdk2 coupled to protein A beads using histone H1 as substrate. The autoradiogram of the histone H1 SDS–PAGE gel is depicted. NRS: A control immunoprecipitate performed with *N*ormal *R*abbit *S*erum in place of cdk2 antibody

compared to cyclin E wt/cdk2. These *in vitro* analyses suggest that once the cyclin E variant transcripts are translated, the protein products can give rise to a functionally active cyclin E complex capable of phosphorylating substrates such as histone H1.

Discussion

In an attempt to understand the relationship between the cell cycle and cancer, many laboratories have investigated the role cyclin/cdk complexes play in cancer. While cyclins D and A have been implicated in tumorigenesis, the role of other cyclins have been elusive and limited mainly to observations. Cyclin E is an interesting case since it shows an altered pattern of expression in all breast cancer cell lines and tumor tissue samples we have examined to date (Keyomarsi *et al.*, 1994). The cyclin E alterations include over-expression of the authentic-sized protein as well as expression of lower molecular weight isoforms found in tumor cells or tissues. We set out to decipher the mechanism responsible for these alterations by initially correlating the activity of cyclin E/cdk2 complexes with the expression pattern and level of cyclin E protein, both in exponentially growing and synchronized population of normal *vs* tumor cells. We find that regardless of which combination of the cyclin E (50 kDa) and its lower molecular weight isoforms are expressed in these tumor cell lines, the associated kinase activity is much higher in tumor than normal cells. Furthermore, we find that in synchronized populations of tumor cells, cyclin E is present in altered forms throughout the cell cycle and the kinase activity associated with it, or with cdk2, is also constitutively active. In addition the abundant and constitutive expression of cyclin E in these tumor cells result in sequestering of cdk2 away from other cyclins, such as cyclin A. This suggests that, there is a cyclin E/cdk2 complex which is abundantly and uniformly active in the tumor but not the normal cell cycle.

In order to determine whether the multiple forms of the cyclin E protein detected in tumor cells originate from different transcripts of cyclin E RNA, we performed RT-PCR and found two different truncated variants of cyclin E (i.e. Δ9 and Δ148) expressed in MDA-MB-157 tumor cell line. Further analysis revealed that the most intriguing feature of the Δ9 and Δ148 variant forms of cyclin E is that there is no distinct difference in their mRNA expression in normal *vs* tumor cells or tissue samples. In addition there is little correlation between expression of these cyclin E variants at the level of RNA *vs* protein. Yet, we show here that at the level of protein in tumor cells, (a) cyclin E isoforms ranging in size from 35 to 50 kDa are abundantly expressed (Figures 1, 2 and 5) and that (b) these protein isoforms of cyclin E are not subject to cell cycle regulation and may constitutively interact with cdk2 resulting in an active complex (Figure 2). Lastly (c) we also show that once Δ9 and Δ148 transcripts of cyclin E are allowed to express their protein products, the resulting proteins can bind to cdk2 and form active complexes *in vitro* (Figure 6). Collectively, based on these observations we suggest that the multiple protein isoforms of cyclin E detected in tumor cells are a result of altered post-transcrip-

tional and/or translational regulation of cyclin E mRNAs. Hence, there may be a translational fidelity that has been altered/lost in tumor cells, allowing for the translation of these truncated variants of cyclin E to occur and once translated, they can form active complexes with cdk2 throughout the cell cycle (see Figures 2 and 6). Alternatively, there may be post-translational modification of cyclin E which is also altered or lost in tumor cells. The presence of lower molecular weight protein isoforms of cyclin E, barely detectable in normal cell lysates (Figure 1, lanes 1 and 2) could also suggest that these isoforms of cyclin E are in fact translated in normal cells as well, but they are rapidly degraded. In tumor cells, the protein turnover is much longer and as a result we can readily detect lower molecular weight isoforms of cyclin E which are highly abundant and functionally active.

One possibility for the presence of multiple transcripts of cyclin E is due to alternative splicing. Precedent for alternative splicing of cyclin E has recently been reported by Ohtsubo *et al.* (1995) where they identified a longer form of cyclin E (cyclin E-L) which contains 15 amino acids at the amino terminus which through alternative splicing, is absent in the original form of cyclin E (cyclin E wt) (Ohtsubo *et al.*, 1995). In addition Sewing *et al.* (1994) also identified another splice variant of cyclin E, termed cyclin Es. Like cyclin E-L and Es, there is a strong possibility that both cyclin EΔ9 and cyclin EΔ148 reported here, are results of alternative splicing as we find potential splice donor and acceptor sites at the deleted junctions of each transcript. However, the cyclin Es variant differs from those we report here in that cyclin Es lacks 49 amino acids within the cyclin box and is 90% less abundant than the wild type cyclin E sequence. This form is unable to associate with cdk2, is inactive in histone H1 kinase assays and is unable to rescue a triple CLN mutation of *S. cerevisiae* (Sewing *et al.*, 1994). Unlike cyclin Es, neither the cyclin EΔ9 nor the Δ148 transcripts disrupts the cyclin box, the consensus region which confers activity by its association to a cdk (Lees *et al.*, 1992). As a result, both Δ9 and Δ148 variants of cyclin E retain the ability to functionally bind to cdk2 and phosphorylate histone H1 in insect cells (Figure 6). The ability of these novel variants of cyclin E to form an active complex with cdk2 has implications for their biological functions. The Δ148 variant has another interesting feature in that the PEST sequence important for its degradation has been disrupted by this 148 base pair deletion. It is possible that the deletion of a PEST sequence may have an effect on turnover of Δ148 cyclin E, allowing it to remain active for a longer duration than the wild type form.

The data presented here suggest that the mechanisms responsible for the presence of the multi isoforms of cyclin E protein in tumor cells may be due to a number of factors, one of which is the altered post-transcriptional or translation regulation of the truncated variants of cyclin E. However a question can be raised whether these two novel variant forms of cyclin E attribute to the cancer phenotype. We present data that these two variants are not a result of deletional mutations in the cyclin E gene as they are expressed in both normal and tumor cells as well as tissue samples. However, they are not readily detected in normal cells

either due to their lack of translation or rapid degradation. There is evidence that when the wild type cyclin E is overexpressed in normal cells the length of G1 is decreased, but cells are not transformed (Ohtsubo and Roberts, 1993; Resnitzky et al., 1994). With the discovery of the cyclin E variants that may be translated in tumor but not normal cells, the oncogenecity of these cyclin E forms can now be directly deciphered. A second question that our data has raised, is whether the lower molecular weight isoforms of cyclin E detected mainly in tumor cells are the protein products of the cyclin EΔ9 and/or Δ148 variant transcripts of cyclin E. By identification of these two variants, we can now utilize them as molecular probes to identify their protein products in tumor cells and tissues. Identification of the multiple protein isoforms of cyclin E will give us insight as to the regulation of this protein, which when complexed with cdk2 is thought to be rate limiting for the G1/S transition during the mammalian cell cycle. With an active cyclin E/cdk2 complex, substrates may be phosphorylated at altered points in the cell cycle resulting in loss of checkpoint control during the progression of G1 to S in tumor cells.

Materials and methods

Cells lines, culture conditions and tissue samples

The culture conditions for 70N, 81N and 76N normal cell strains and MCF-7, MDA-MB-157, MDA-MB-231, MDA-MB-436, T47D, BT-20, HBL100, Hs578T, SKBR3 and ZR75T tumor cell lines were described previously (Keyomarsi and Pardee, 1993). MCF-10A is a normal human mammary epithelial cell line which is spontaneously immortalized and does not grow in soft agar and is not tumorigenic in nude mice (Soule et al., 1990). This cell line was obtained from ATCC and is cultured in DFCI-1 (Band and Sager, 1989). All cells were cultured and treated at 37°C in a humidified incubator containing 6.5% CO_2 and maintained free of Mycoplasma as determined by the MycoTect Kit (Gibco). Snap frozen surgical specimens from patients diagnosed with breast cancer were obtained from the National Disease Research Interchange/Co-operative Human Tissue Network, Eastern Division. The clinical stage and grade of the tissue samples used were obtained from pathology/surgical reports and indicated in the figure legend.

Synchronization and flow cytometry

76N normal mammary epithelial cell strain and MDA-MB-157 tumor cell line were synchronized at the G1/S boundary by a modification of the double thymidine block procedure (Rao and Johnson, 1970). Briefly, 48 h after the initial plating of cells, the medium was replaced with fresh medium containing 2 mM thymidine for either 24 h (76N cells) or for 36 h (MDA-MB-157 cells). This medium was then removed, the cells were washed three times and subsequently incubated in fresh medium lacking thymidine for 12 h (76N cells) or 24 h (MDA-MB-157 cells). Next cells were re-incubated in medium containing 2 mM thymidine, as above, washed with fresh medium and incubated in thymidine free medium for the rest of the experiment. Cells were harvested at the indicated times, cell density was measured electronically using a Coulter Counter (Hialeah, Florida) and flow cytometry analysis was performed. For flow cytometry studies, 10^6 cells were centrifuged at $1000 \times g$ for 5 min, fixed with ice-cold 70%

ethanol (30 min at 4°C) and washed with phosphate buffered saline (Crissman and Tobey 1974). Cells were suspended in 5 ml of phosphate-buffered saline containing 10 µg ml⁻¹ RNase, incubated at 37°C for 30 min, washed once with phosphate buffered saline and resuspended in 1 ml of 69 µM propidium iodide in 38 mM sodium citrate. Cells were then incubated at room temperature in the dark for 30 min and filtration through a 75 mm Nitex mesh. DNA content was measured on a FACScan flow cytometer system (Becton Dickinson, San Jose, CA) and data were analysed using CELLFIT software system (Becton Dickinson).

Western blot and H1 kinase analysis

Cell lysates and tissue homogenates were prepared and subjected to Western blot anaylsis as previously described (Keyomarsi and Pardee, 1993; Keyomarsi et al., 1994). Briefly, 100 µg of protein from each tissue sample or cell line (for sf9 extracts, 50 µg) were electrophoresed in each lane of a 10% sodium dodecyl sulfate-polyacrylamide gel (SDS–PAGE) (cyclin E and cyclin A), or a 13% SDS–PAGE (cdk2 and all Sf9 cell extracts) and transferred to Immobilon P. Blots were blocked with 20 mM Tris-HCl, pH 7.5, 150 mM NaCl, 5% dried milk, 0.2% Tween overnight at 4°C and were incubated with various primary antibodies diluted in blocking buffer for 3 h. Primary antibodies used were rabbit anti-human cyclin E serum at a dilution of 1:2500 (gift from A Koff and J Roberts, Fred Hutchinson Cancer Research Center), monoclonal antibody HE12 to cyclin E at a dilution of 1:10 (a gift of E Lees and E Harlow, Massachusetts General Hospital [MGH] Cancer Center), affinity-purified rabbit anti-human p33^{cdk2} kinase antibody at a dilution of 1:2000 (a gift from L-H Tsai and E Harlow, MGH Cancer Center) and affinity-purified rabbit anti-human cyclin A antibody at a dilution of 1:20 000 (a gift from JW Harper, Baylor College of Medicine). Following primary antibody incubation, the blots were washed and incubated with either goat anti-mouse or anti-rabbit horseradish peroxidase conjugate at a dilution of 1:5000 in blocking buffer for 1 h and finally washed and developed with detection reagents (ECL) supplied by Amersham biochemicals. ECL exposures for all Western blots are of similar duration, i.e. 1–10.

For H1 kinase assays, 250 µg of protein (unless otherwise indicated in the figure legend) were used per immunoprecipitation with either polyclonal antibody to cyclin E or CDK2 in lysis buffer containing 50 mM Tris HCl pH 7.5, 250 mM NaCl, 0.1% NP-40, 25 µg ml⁻¹ leupeptin, 25 µg ml⁻¹ aprotinin, 10 µg ml⁻¹ pepstatin, 1 mM benzamidine, 10 µg ml⁻¹ soybean trypsin inhibitor, 0.5 mM PMSF, 50 mM NaF, 0.5 mM Sodium Ortho-Vanadate. The protein/antibody mixture was incubated with protein A Sepharose for 1 h and the immunoprecipitates were then washed twice with lysis buffer and four times with kinase buffer (50 mM Tris HCl pH 7.5, 250 mM NaCl, 10 mM MgCl₂, 1 mM DTT and 0.1 mg ml⁻¹ BSA). Immunoprecipitates were then incubated with kinase buffer containing 5 µg histone H1, 60 µM cold ATP and 5 µCi of [³²P]γATP in a final volume of 50 µl at 37°C for 30 min. The products of the reaction were then analysed on a 13% SDS–PAGE gel. The gel was then stained, destained, dried and exposed to X-ray film. For quantitation, the protein bands corresponding to histone H1 were excised and radioactivity was measured by scintillation counting.

Reverse transcription-polymerase chain reaction amplification (RT-PCR)

RNA was isolated from cell lines and tissue samples as previously described (Keyomarsi and Pardee, 1993). To

remove chromosomal DNA contamination from RNA, 50 μg of total cellular RNA was incubated for 30 min at 37°C with 10 units of RNasin (Promega) and 20 units of RQI DNase (Promega) in 10 mM Tris HCl, pH 8.3, 50 mM KCl, 1.5 mM MgCl$_2$. After extraction with phenol/CHCl$_3$ (1:1) followed by CHCl$_3$, the supernatant was ethanol precipitated in the presence of 0.3 M NaOAC and RNA was redissolved in 0.1 × Tris-EDTA in diethyl pyrocarbonate-treated water. Reverse transcription was performed by incubating 1 μg of the DNase treated RNA with 300 units of Moloney Murine Leukemia Virus reverse transcriptase (MMLV RT) (Gibco/BRL) in the presence of 15 μM oligo-dT (12–18) (Pharmacia) as a primer and 20 μM dNTP for 10 min at room temperature, 45 min at 42°C, 5 min at 99°C and 5 min at 5°C in the Gene Amp PCR system 9600 (Perkin Elmer Cetus, San Diego, CA). One half of the reaction was subsequently used for 30 cycles of PCR amplifications using GeneAmp PCR reagent kit (Perkin Elmer Cetus). PCR cycles include denaturation for 40 s at 94°C, annealing for 1 min at 61°C and polymerization for 1 min at 72°C. A minimum of three independent PCR amplifications from each specimen, for each experiment, were performed to guard against potential errors due to Taq polymerase misincorporation.

Oligonucleotides, cloning and sequencing of RT-PCR products

A pair of primers L1CYCE: 5′-GGGATGCGAAGGA-GCGGGACA-3′ and R1CYCE: 5′-AGCGGCGCAAC-TGTCTTTGGT-3′ based on the mRNA sequence of cyclin E (Koff et al., 1991; Lew et al., 1991) were designed to amplify the entire cyclin E coding sequence of human cyclin E cDNA (1250 bp, i.e. from nucleotide −23 to +1227). To specifically amplify the cyclin E transcripts harboring the Δ9 and Δ148 deletion, the following sets of primers were used respectively: LMEMARK3: 5′-GC-AAACGTGACCGTTG-3′ and R1CYCE: 5′-AGCGGCG-CAACTGTCTTTGGT-3′; L1CYCE: 5′-GGGATGCGA-AGGAGCGGGACA-3′ and RMEMARK3: 5′-ACCG-CTCTGTGCTTCATC-3′. The PCR products were visualized by fractionating 1/5th of each reaction on a 1.5% agarose gel stained with ethidium bromide. A fraction of each reaction was then used to clone the RT-PCR products into the PCR II vector using the TA cloning system from Invitrogen (San Diego, CA). Plasmid DNA sequencing of cloned cDNA products with either T7 of SP6 primer was carried out using Sequenase 2.0 sequencing kit from United States Biochemicals Co (Cleveland, OH). Fifteen clones from each independent RT-PCR reaction (at least three) were completely sequenced in both orientations to confirm the sequences for Δ9 and Δ148 variants of cyclin E.

In vitro translation

To transcribe and translate the cyclin E cDNAs cloned in the PCR II vector we used the TNT coupled Reticulocyte Lysate system (Promega). Briefly, 1 μg of PCR II vector containing either cyclin E-wt, cyclin E-Δ9 or cyclin E-Δ148 was added to rabbit reticulocyte lysate (50% of total volume) in the presence of T7 RNA polymerase, 1 mM amino acid mixture minus methionine, 40 μCi [^{35}S]methionine (Dupont), RNasin ribonuclease inhibitor and the TNT reaction buffer (Promega) in a total volume of 50 μl. For non-radioactive reactions, unlabeled methionine was added to the mix and radioactivity was excluded. The reactions were then incubated at 30°C for 2 h and the translated radioactive products were separated by SDS–PAGE. The gels were then stained, destained, fluorographed, dried and the protein products were visualized by autoradiography. For visualization of the non-radioactive samples, the translation products were subjected to Western blot analysis using a polyclonal antibody specific to cyclin E.

Production of cyclins and kinases in insect cells

The cDNAs of cyclin E wild type, cyclin E-Δ9, cyclin E-Δ148 and cdk2 were subcloned into pMP3 (Pharmingen) plasmid containing the Basic Protein promoter that is active during and after viral DNA synthesis when the cell is producing baculovirus components to assemble the virus particles. At this stage there are larger numbers of modifying enzymes present which will increase the effectiveness of post-translational modification of the gene product of interest. Once the plasmids were constructed, they were individually co-transfected in sf9 insect cells with the linearized BaculoGold (Pharmingen) virus DNA (containing a lethal deletion), which through recombination would only produce viable recombinant baculovirus expressing our clones. The titer of all the supernatants were determined and insect cells were then infected with a plaque-forming unit/cell number of 1.

References

Band V and Sager R. (1989). *Proc. Natl. Acad. Sci. USA*, **86**, 1249–1253.

Bianchi AB, et al. (1993). *Oncogene*, **8**, 1127–1133.

Buckley MF, et al. (1993). *Oncogene*, **8**, 2127–2133.

Crissman HA and Tobey RA. (1974). *Science*, **184**, 1287–1298.

Draetta GF. (1994). *Curr. Opin. Cell Biol.*, **6**, 842–846.

Elledge SJ and Spottswood MR. (1991). *EMBO J.*, **10**, 2643–2659.

Evans T, et al. (1983). *Cell*, **33**, 389–396.

Heichman, KA and Roberts JM. (1994). *Cell*, **79**, 557–562.

Hinds PW, et al. (1994). *Proc. Natl. Acad. Sci. USA*, **91**, 709–713.

Hinds PW, et al. (1992). *Cell*, **70**, 993–1006.

Hunter T and Pines J. (1991). *Cell*, **66**, 1071–1074.

Hunter T and Pines J. (1994). *Cell*, **79**, 573–582.

Jiang W, et al. (1992). *Cancer Res.*, **52**, 2980–2983.

Jiang W, et al. (1993a). *Oncogene*, **8**, 3447–3457.

Jiang W, et al. (1993b). *Proc. Natl. Acad. Sci. USA*, **90**, 9026–9030.

Keyomarsi K, et al. (1994). *Cancer Res.*, **54**, 380–385.

Keyomarsi K and Pardee AB. (1993). *Proc. Natl. Acad. Sci. USA*, **90**, 1112–1116.

Keyomarsi K, Sandoval L, Band V and Pardee AB. (1991). *Cancer Res.*, **51**, 3602–3609.

King RW, Jackson PK and Kirschner MW. (1994). *Cell*, **79**, 563–571.

Koff A, *et al.* (1991). *Cell*, **66**, 1217–1228.

Koff A, *et al.* (1992). *Science*, **257**, 1689–1694.

Lammie GA, *et al.* (1991). *Oncogene*, **6**, 439–444.

Leach SF, *et al.* (1993). *Cancer Res.*, **53**, 1986–1989.

Lees E, *et al.* (1992). *Genes Dev.*, **6**, 1874–1855.

Lew DJ, Dulic V and Reed SI. (1991). *Cell*, **66**, 1197–1206.

Lovec H, *et al.* (1994). *Oncogene*, **9**, 323–326.

Matsushime H, Roussel MF, Ashman RA and Sherr CJ. (1991). *Cell*, **65**, 701–713.

Morgan DO. (1995). *Nature*, **374**, 131–134.

Motokura T and Arnold A. (1993). *Curr. Opin. Genet. & Devel.*, **3**, 5–10.

Motokura T, *et al.* (1991). *Nature,* **350**, 512–515.

Musgrove EA, Lee CSL, Buckley MF and Sutherland RL. (1994). *Proc. Natl. Acad. Sci. USA*, **91**, 8022–8026.

Nurse P. (1994). *Cell*, **79**, 547–550.

Ohtsubo M and Roberts JM. (1993). *Science*, **259**, 1908–1912.

Ohtsubo M, *et al.* (1995). *Mol. Cell. Biol.*, **15**, 2612–2624.

Quelle DE, *et al.* (1993). *Genes & Dev.*, **7**, 1559–1571.

Rao PN and Johnson RT. (1970). *Nature*, **225**, 159–164.

Resnitzky D, Gossen M, Bujard H and Reed SI. (1994). *Mol. Cell. Biol.*, **14**, 1669–1679.

Rosenberg CL, *et al.* (1991a). *Oncogene*, **6**, 449–453.

Rosenberg CL, *et al.* (1991b). *Proc. Natl. Acad. Sci. USA*, **88**, 9638–9642.

Rosenwald IB, Lazaris-Karatzas A, Sonenberg N and Schmidt EV. (1993). *Mol. Cell. Biol.*, **13**, 7358–7363.

Sewing A, *et al.* (1994). *J. Cell Sci.*, **107**, 581–588.

Sherr CJ. (1993). *Cell*, **73**, 1059–1065.

Sherr CJ. (1994). *Cell*, **79**, 551–555.

Soule HD, *et al.* (1990). *Cancer Research*, **50**, 6075–6086.

Standart N, Minshull J, Pines J and Hunt T. (1987). *Dev. Biol.*, **124**, 248–258.

Swenson KI, Farrell KM and Ruderman JV. (1986). *Cell*, **47**, 861–870.

Wang TC, *et al.* (1994). *Nature*, **369**, 669–671.

Withers D, *et al.* (1991). *Mol. Cell Biol.*, **11**, 4846–4853.

Xiong Y, Connolly T, Futcher B and Beach D. (1991). *Cell*, **65**, 691–699.

Cyclin E, a redundant cyclin in breast cancer

(cell cycle/retinoblastoma/p16/redundancy)

JULIE GRAY-BABLIN*, JUAN ZALVIDE†, M. PAT FOX*, CHRIS J. KNICKERBOCKER*, JAMES A. DECAPRIO†,
AND KHANDAN KEYOMARSI*‡

*Division of Molecular Medicine, Laboratory of Diagnostic Oncology, Wadsworth Center, Albany, NY 12201; and †Division of Neoplastic Disease Mechanisms, Dana–Farber Cancer Institute, Boston, MA 02146

ABSTRACT   Cyclin E is an important regulator of cell cycle progression that together with cyclin-dependent kinase (cdk) 2 is crucial for the G_1/S transition during the mammalian cell cycle. Previously, we showed that severe overexpression of cyclin E protein in tumor cells and tissues results in the appearance of lower molecular weight isoforms of cyclin E, which together with cdk2 can form a kinase complex active throughout the cell cycle. In this study, we report that one of the substrates of this constitutively active cyclin E/cdk2 complex is retinoblastoma susceptibility gene product (pRb) in populations of breast cancer cells and tissues that also overexpress p16. In these tumor cells and tissues, we show that the expression of p16 and pRb is not mutually exclusive. Overexpression of p16 in these cells results in sequestering of cdk4 and cdk6, rendering cyclin D1/cdk complexes inactive. However, pRb appears to be phosphorylated throughout the cell cycle following an initial lag, revealing a time course similar to phosphorylation of glutathione *S*-transferase retinoblastoma by cyclin E immunoprecipitates prepared from these synchronized cells. Hence, cyclin E kinase complexes can function redundantly and replace the loss of cyclin D-dependent kinase complexes that functionally inactivate pRb. In addition, the constitutively overexpressed cyclin E is also the predominant cyclin found in p107/E2F complexes throughout the tumor, but not the normal, cell cycle. These observations suggest that overexpression of cyclin E in tumor cells, which also overexpress p16, can bypass the cyclin D/cdk4·cdk6/p16/pRb feedback loop, providing yet another mechanism by which tumors can gain a growth advantage.

Progression through the eukaryotic cell cycle is mediated both positively and negatively by a variety of growth regulatory proteins (1–3). Cyclins and their catalytic cyclin-dependent kinase (cdk) partners act positively to propel a cell through the proliferative cycle (4, 5). Activation of cyclin-cdk complexes results in a cascade of protein phosphorylations that ultimately induce cell cycle progression (1, 4). Although the identity of downstream substrates and effectors of cyclin-cdks remains to be firmly established, it is commonly believed that cdk-mediated phosphorylations manifest cell cycle regulation via inhibition of growth inhibitory signals and activation of proteins necessary for each stage of the cell cycle (6). A putative, well-characterized substrate for the G1 cyclins is retinoblastoma susceptibility gene product (pRb; refs. 7 and 8). This protein is sequentially phosphorylated during the cell cycle presumably through the concerted activity of different cyclin-cdk complexes (9–11). This phosphorylation is required for cell cycle progression, and the hypophosphorylated form of pRb inhibits cell cycle progression by tethering and inactivating transcription factors of the E2F family, which are required for the transactivation of S phase-specific proteins, including dihydrofolate reductase, cyclin A, and thymidylate synthase (12–14). The phosphorylation of pRb results in the

release of E2F transcription factors, freeing them to stimulate transcription of growth-promoting target genes.

Inhibition of pRb phosphorylation, therefore, represents a potent form of growth inhibition. Such inhibition has recently been exemplified through the characterization of cyclin-dependent kinase inhibitor proteins (reviewed in refs. 15 and 16). To date, these proteins exist as two functionally and structurally distinct groups typified by p21 and its homologues p27 and p57, as well as p16 and p15 and their related homologues (17, 18). As potential tumor suppressors, the cyclin-dependent kinase inhibitor genes have been studied extensively to evaluate the possible contribution of cyclin-dependent kinase inhibitor-specific genomic mutations to neoplastic transformation (17). In particular, the gene encoding p16, or multitumor suppressor 1, on chromosome 9p21 has been postulated to encode a tumor suppressor and has been demonstrated to be mutated in a wide variety of tumor-derived cell lines (19–22).

A curious finding has ensued from the analysis of p16 in cancer; although both pRb and p16 are often mutated in human cancers, these mutations seem mutually exclusive (23–26). This inverse correlation has been established in various tumor cell types both *in vitro* and *in vivo*. A logical conclusion then is that these proteins, which act similarly to inhibit cell cycle progression, are differentially regulated by a common pathway, perhaps involving a negative feedback loop. In fact, the growth suppression mediated via p16 overexpression has been shown to be definitively correlated with pRb status (27, 28). Thus, p16 inhibition of cell proliferation is evident only in cells expressing wild-type pRb. As an inhibitor of the putative pRb kinases cdk4 and cdk6, p16 is thought to bind, inhibit, and sequester these cdks, thereby rendering cyclin-D orphan with respect to cdk association. Some groups have postulated that p16 expression is regulated by pRb or by a feedback mechanism involving pRb (29), and it has been demonstrated by others that p16 is transcriptionally regulated by pRb (30). Such a mechanism would permit high levels of p16 to be expressed only when pRb is inactivated, by hyperphosphorylation, genomic mutation, or association with transforming viral oncoproteins. Although not without exception, the inverse correlation of these two proteins, particularly in breast epithelial cells, may represent a tightly regulated feedback mechanism.

In this report, we have identified and characterized an exception to the pRb/p16 inverse correlation rule. In the cell line MDA-MB-157, pRb is wild-type and phosphorylated, and p16 is significantly overexpressed and effectively binds cdk4 and cdk6, thus preventing cyclin D1 from binding to these kinases. We also have demonstrated that although cyclin D1-cdk4 and cyclin D1-cdk6 complexes are inactivated by p16, pRb is progressively synthesized and phosphorylated during the cell cycle. Cyclin D1, cdk4, and cdk6 are not overexpressed in this cell line; however, cyclin E is overexpressed, and its

---

Abbreviations: cdk, cyclin-dependent kinase; pRb, retinoblastoma susceptibility gene product; GST-Rb, glutathione *S*-transferase retinoblastoma.
‡To whom reprint requests should be addressed at: Wadsworth Center, Empire State Plaza, P.O. Box 509, Albany, NY 12201. e-mail: keyomars@wadsworth.org.

levels and associated kinase activity remain constitutively high during all phases of the cell cycle. In addition, cyclin E-cdk2 complex can phosphorylate glutathione *S*-transferase retinoblastoma (GST-Rb) throughout the cell cycle. We conclude, therefore, that there exists a functional redundancy among the cyclins such that overexpression of cyclin E may compensate for the inactivation of cyclin D complexes by p16 with respect to the pRb phosphorylation and cell cycle progression.

METHODS

Cells Lines, Culture Conditions, and Tissue Samples. The culture conditions for all cell lines used in this study were described previously (31, 32). Snap-frozen surgical specimens from patients diagnosed with breast cancer were obtained from the Quantitative Diagnostic Laboratories (Almhurst, IL). 76N normal mammary epithelial cell strain and MDA-MB-157 tumor cell line were synchronized at the G_1/S boundary by a modification of the double thymidine block procedure (33) as described (32). For each time interval, 10^6 cells were subjected to FACScan analysis as described (32, 34).

Western Blot and Immune Complex Kinase Analysis. Cell lysates and tissue homogenates were prepared and subjected to Western blot analysis as described (31, 35). Primary antibodies used were monoclonal antibodies to cyclins E and D1 (Santa Cruz Biochemicals), cdk4 (Transduction Laboratories, Lexington, KY), pRb (PharMingen), and p16 (J.A.D.); and polyclonal antibodies to cdk6 (Santa Cruz Biochemicals) and cyclin A (a gift from J. W. Harper, Baylor College of Medicine, Houston). Immunoprecipitations and H1 kinase assays were performed as described (32, 36). Briefly, for H1 kinase and GST-Rb kinase assays, 500 μg of protein (unless otherwise indicated in the figure legend) were used per immunoprecipitation with polyclonal antibody to cyclin E. Immunoprecipitates were then incubated with kinase buffer containing either 5 μg of histone H1 or 1 μg of purified GST-Rb, 60 μM cold ATP, and 5 μCi of [γ-^{32}P]ATP in a final volume of 50 μl at 37°C for 30 min. The products of the reaction were then run on a SDS/13% PAGE gel. The gel was then stained, destained, dried, and exposed to x-ray film.

For immunoprecipitation followed by Western blot analysis, 250 μg of protein (unless otherwise indicated in the figure legend) were used per immunoprecipitation with either monoclonal antibody to p16, polyclonal antibody to cyclin D1 obtained from M. Pagano (Mitotix, Cambridge, MA) (37), or monoclonal antibody to cyclin D1-clone HD33 (a gift from E. Harlow and C. Ngwu, Massachusetts General Hospital Cancer Center, Boston) in lysis buffer as described above. The immunoprecipitates were then electrophoresed on a SDS/13% PAGE, transferred to Immobilon P, blocked, and incubated with either polyclonal antibody to cdk4 obtained from M. Pagano (Mitotix) (37) or cdk6 as described in the figure legend.

Gel Retardation Assays. Whole-cell extracts were prepared as described (31, 35), and 15 μg of protein were used per lane. Binding reactions were performed as described elsewhere (13, 38). The oligonucleotide used as a labeled DNA probe includes the E2F binding site of the human dehydrofolate reductase promoter (DHFR WT) (13). For antibody perturbation experiments, 2 μl (200 ng) of rabbit polyclonal antibody to cyclin E (Upstate Biotechnology, Lake Placid, NY) was added.

RESULTS

Overexpression of p16 and Absence of Cyclin D1/cdk4-D1/cdk6 Complexes in a Breast Cancer Cell Line with Functional Rb Protein. A panel of 13 breast cell lines was surveyed for the correlation of p16 and Rb status, as well as association of p16 and cyclin D1 with cdks 4 and 6 (Fig. 1). The cell lines used include three proliferating normal mammary epithelial cell strains obtained from reduction mammoplasties and used at early passages, one near diploid normal-immortalized breast epithelial cell line and nine tumor cell lines with different cyclin E levels, estrogen receptor, and p53 status as outlined in Table 1.
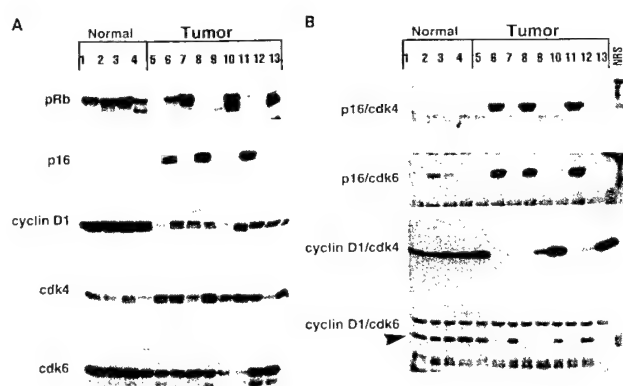
FIG. 1. Expression and complex formation of p16/pRB pathway proteins in normal and tumor-derived breast epithelial cells. (*A*) Western blot analysis: exponentially growing normal and tumor cells were subjected to Western blot analysis using 50 μg of protein for each cell line in each lane of either a 6% (pRb), 13% (cyclin D1, cdk4, and cdk6), or 15% (p16) acrylamide gel and blotted as described. The same blot was reacted with cyclin D1, cdk4, and cdk6 affinity-purified antibodies. The blots were stripped between the three antibodies in 100 mM 2-mercaptoethanol, 62.5 mM Tris·HCl (pH 6.8), and 2% SDS for 30 min at 55°C. (*B*) Immune-complex formation: for immunoprecipitation followed by Western blot analysis, equal amounts of protein (500 μg) from cell lysates prepared from each cell line were immunoprecipitated with either monoclonal antibody to p16 (p16/cdk4 and p16/cdk6), polyclonal antibody to cyclin D1 (cyclin D1/cdk4), or a monoclonal antibody to cyclin D1 (cyclin D1/cdk6), coupled to protein A/G beads, and the immunoprecipitates were washed, boiled for 3 min, separated by SDS/13% PAGE, blotted to Immobilon membranes, and hybridized with either polyclonal antibody to cdk4 (p16/cdk4), polyclonal antibody to cdk6 (p16/cdk6 and cyclin D1/cdk6; arrow pointing to the complexed protein), or monoclonal antibody to cdk4 (cyclin D1/cdk4). The list of normal and tumor cell lines is presented in Table 1 using identical numbers.

We examined the expression of pRb by direct immunoblotting with a monoclonal antibody in which the presence of functional pRb is inferred from the presence of higher molecular weight-hyperphosphorylated forms of the protein. This analysis revealed that besides three tumor cell lines (Fig. 1*A*, lanes 8, 11, and 12; i.e., MDA-MB-436, HBL-100, and Hs-578T) in which pRb is either mutated (42), inactive due to its binding to simian virus 40 large T antigen, or not expressed, pRb is present and functional in all of the other cell lines examined. Furthermore, in all of the pRB-positive cell lines, there are at least two pRb bands present representing different phosphorylation states of pRb. (Due to different levels of pRb expression in each of the cell lines, longer exposures were used to evaluate presence of slower migrating, functional form of pRb, specifically in lanes 1, 2, and 5; data not shown). Next, we correlated the expression of p16 levels with pRb status and found that p16 is overexpressed in three cell lines (Fig. 1*A*, lanes 6, 8, and 11), two of which Rb has been functionally compromised (i.e., MDA-MB-436 and HBL-100). It is curious that in MDA-MB-157, which contains a wild-type pRb, p16 is also markedly overexpressed (Fig. 1*A*, lane 6). Hence, MDA-MB-157, in which cyclin E is severely overexpressed (Table 1; refs. 31, 32), is one exception to the reciprocal p16/Rb correlation rule.

Because overexpression of cdk4, cdk6, or cyclin D1 could counteract the inhibitory effect caused by the overabundance of p16, we also measured the relative levels of these proteins in all 13 cell lines (Fig. 1*A*). Western blot analysis with cyclin D1, cdk4, and cdk6 revealed that these proteins were not overexpressed in MDA-MB-157 cell line relative to the other 12 cell lines examined, suggesting that the overexpressed p16 may adequately sequester cdk4 and cdk6 away from cyclin D1, rendering it inactive. To test this hypothesis, we performed a series of two-step immunoprecipitations followed by Western blot analysis (Fig. 1*B*). When p16 immunoprecipitates were separated on denaturing gels, transferred to poly(vinylidene

Table 1. Characterization of normal and tumor-derived breast epithelial cells

Cell lines	Cell types	Estrogen receptor (31)	p53	Cyclin E (31, 32)	pRb*
1. 70N	N-mortal	−	+ (39)	+	+
2. 81N	N-mortal	−	+ (39)	+	+
3. 76N	N-mortal	−	+ (39)	+	+
4. MCF-10-A	N-immortalized	−	+ (40)	+	+
5. MCF-7	A (pe)	+	+ (40)	+ + +	+
6. MDA-MB-157	C (pe)	−	− (40)	+ + + + + +	+
7. MDA-MB-231	A (pe)	−	− (40)	+ + + +	+
8. MDA-MB-436	A	−	− (41)	+ + + + +	−
9. T47D	DC (pe)	+	− (40)	+ +	+
10. BT20	C	+	+ (40)	+ +	+
11. HBL-100	T (bm) SV40 transformed	−	− (40)	+ + +	−
12. HS-578T	DC	−	− (40)	+ + + +	−
13. ZR75T	IDC	+	+ (40)	+ + +	+

Cell type, estrogen receptor (ER), p53, and cyclin E status as determined in indicated references. +, wild type; + +(+ + + +), varying degrees of overexpression with MDA-MB-157 showing the highest degree (64-fold, hence 6 + s) of cyclin E overexpression. N, normal breast cells from reduction mammoplasty; A, adenocarcinoma; pe, pleural effusion; C, carcinoma; DC, ductal carcinoma; T(bm), tumor breast milk; SV40, simian virus 40; IDC, infiltrating DC; −, mutant or not expressed.
*pRb status is adopted from Fig. 1, in which + indicates wild type and present in hypo- and hyperphosphorylated forms, and − indicates mutated or virally bound and inactive.

difluoride) membrane, and blotted with antiserum to cdk4 or cdk6, p16 was capable of forming a complex with both cdk4 and cdk6 in the three tumor cell lines in which p16 is overexpressed. Curiously, p16 was also capable of forming a complex with cdk6 in normal breast cell strains in which no overexpression of p16 or cdk6 was noted. However, cyclin D1 immunoprecipitates that were separated and blotted with antibodies to cdk4 or cdk6 revealed that, in the normal cell strains, cyclin D1 formed a complex with cdk4 and cdk6, suggesting that p16 did not completely sequester these kinases from cyclin D1. On the other hand, in tumor cells in which p16 is overexpressed, no complexes were formed between cyclin D1 and cdk4 or cdk6, suggesting that in these three tumor cell lines enough p16 is overexpressed to sufficiently sequester cdk4 and cdk6 away from cyclin D1, preventing it from forming complexes with these kinases (Fig. 1B). Collectively, these data provide evidence for the absence of cyclin D1/cdk complexes in a breast cancer cell line with a functional Rb protein.

Cyclin E-Associated Kinase Phosphorylates pRb in the Absence of Cyclin D1/cdk4 or Cyclin D1/cdk6 Complexes in Tumor Cells. To examine the cell cycle regulation of pRb in normal and tumor cells, we synchronized both cell lines by double thymidine block and analyzed the pattern of pRb expression and phosphorylation by Western blot analysis (Fig. 2A). Synchrony of both cell types at several times after release from the block was monitored by flow cytometry (Fig. 2C). At various times after release from treatment for synchronization, cells were harvested, and extracted proteins were analyzed on Western blots with antibodies to pRb and cyclins E and A (Fig. 2A). In normal 76N cells, the pattern of synthesis and phosphorylation of pRb, as well as expression of cyclin E and cyclin A proteins, is consistent with that seen for other normal cell types, with levels rising before S phase and oscillating thereafter in the cell cycle (8, 43, 44). In addition, pRb is present mainly in the hyperphosphorylated form at G_1/S boundary up to G2, where the levels drop to resume again at G_1. Furthermore, there is only one major form (i.e., 50 kDa) of cyclin E protein detected. However, in the tumor cells, pRb and cyclin E proteins do not appear to be cell cycle-regulated. pRb is induced and phosphorylated shortly after release from thymidine block and remains in that phosphorylated state throughout the cell cycle. In addition, multiple isoforms of cyclin E protein are present with similar signal intensities and banding

patterns during the time intervals examined. In the same tumor cell extracts, cyclin A protein is cell cycle-regulated with peak levels coinciding with peak S and early M phase. Hence, it appears that in this tumor cell line, pRb and cyclin E are abnormally regulated during the cell cycle.

To decipher whether cyclin E-associated kinase is responsible for the phosphorylation of pRb, cells were immunoprecipitated with cyclin E antibody and used in kinase assays with either histone H1 or a recombinant GST-Rb fusion protein as substrates (Fig. 2B). In normal cells, cyclin E-associated kinase is capable of phosphorylating histone H1 and is cell cycle-regulated, coinciding with the levels of cyclin E protein expression (Fig. 2A). However, the same cyclin E immunoprecipitates prepared from normal cells were not capable of phosphorylating GST-Rb (Fig. 2B). In tumor cells, on the other hand, cyclin E is not cell cycle-regulated and remains in a catalytically active complex throughout the cell cycle, resulting in a constitutive pattern of histone H1 and GST-Rb phosphorylation. Finally, the timing of pRb expression in the tumor cell cycle (Fig. 2A) is similar to the timing of phosphorylation of GST-Rb by cyclin E immunoprecipitates (Fig. 2B). These observations suggest that overexpression of cyclin E results in an active kinase complex throughout the cell cycle capable of phosphorylating not only histone H1, but also GST-Rb. Hence, in tumor cells that overexpress p16, resulting in the inactivation of cyclin D1/cdk4 or cyclin D1/cdk6 complexes, pRb can still get phosphorylated by cyclin E-associated kinase.

Overexpression of Cyclin E and p16 in Breast Tumor Tissues Is Correlated with Functional pRb. Because the lack of inverse association of pRb and p16 was observed in only one of three breast tumor cell lines overexpressing p16 (Fig. 1A), we were interested in deciphering the frequency at which such a phenomenon would occur in breast tissue samples. Therefore, we examined 20 tumor tissue specimens obtained from breast cancer patients. Table 2 lists estrogen and progesterone status, ploidy, and proliferation index expression as measured by immunofluorescence with the respective antibodies followed by image analysis as described (45, 46). We also analyzed the expression of cyclin E, p16, and pRb in these samples by Western blot analysis. The results revealed that cyclin E was severely overexpressed and present in lower molecular weight forms in 18 of 20 tissue samples, which is consistent with the role of cyclin E as a prognosticator for breast cancer (31, 35, 48). The pattern of cyclin E expression observed in these tumor specimens was similar to those used in a previous
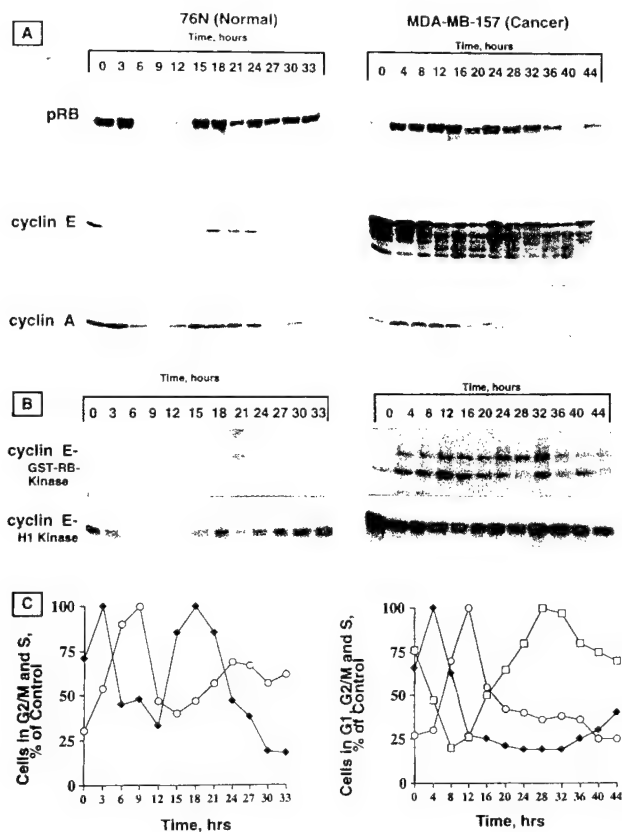
FIG. 2. Phosphorylation of pRb in synchronized population of tumor versus normal cells. Both cell types were synchronized by double thymidine block procedure. At the indicated times after release from double thymidine block, cell lysates were prepared and subjected to Western blot analysis (*A*) and histone H1 or GST-Rb kinase analysis (*B*). Protein (50 μg) for each time point was applied to each lane of either a 6% (pRb) or 10% (cyclins E and A) acrylamide gel and blotted as described. The same blot was reacted with cyclin E monoclonal (HE12) and cyclin A affinity-purified polyclonal antibodies. The blots were stripped between the two assays as described for Fig. 1. For kinase activity, equal amounts of proteins (600 μg) from cell lysates prepared from each cell line at the indicated times were immunoprecipitated with anti-cyclin E (polyclonal) coupled to protein A beads using either histone H1 or purified GST-Rb as substrates. (*C*) The relative percentage of cells in different phases of the cell cycle for each cell line at various times after release from double thymidine block was calculated from flow cytometric measurements of DNA content. ♦, cells in S phase; ○, cells in G_2/M phase; □, cells in G_1 phase.

study (49) showing presence of lower molecular weight forms of cyclin E with increasing stage of the disease. It is interesting that most of the tumor specimens that showed an overexpression of cyclin E also were negative for estrogen and progesterone receptors. A negative steroid receptor status is indicative of poor response to endocrine and cytotoxic chemotherapy characteristics of very aggressive breast tumors (50). Furthermore, p16 was overexpressed in 7 (i.e., KK-005, 086, 147, 173, 190, 369, and 399) of the 20 samples examined. Three of these seven samples had a defect in pRb expression, whereas in the remaining four samples (i.e., KK-005, 147, 173, and 369), pRb was expressed and present in multiple bands, suggesting a functional protein. In addition, cyclin E was severely overexpressed in all four p16/pRb double-positive samples. Hence, these observations suggest that *in vivo*, in breast cancer tissues that overexpress cyclin E, overexpression of p16 is not always accompanied by a defect in pRb, consistent with results obtained with MDA-MB-157 cell line. Cyclin E, which is overexpressed and present in lower molecular weight forms in these tumor tissue samples, may be capable of phosphorylating pRb in the absence of functional cyclin D-containing complexes *in vivo* as well as in cell lines.

Cyclin E Is Present in E2F Complexes Throughout the Cell Cycle of Tumor, but Not Normal, Cells. One of the major targets of growth regulation by pRb is the E2F family of transcription factors. During the G1 phase of the cell cycle, underphosphorylated pRB binds to E2F and represses its transcriptional activity. Phosphorylation of pRb by cyclins during late G_1 and S phase release E2F, which in turn leads to activation of the transcription of genes important for cell cycle progression. Similarly, p107 and p130, two pRb-related proteins, regulate the transcriptional activity of E2F. In addition, both cyclins A and E can bind to p107 and p130 while in complex with E2F. Although the significance of this association is not known, it has been suggested that it regulates the transcriptional activity of E2F.

To determine whether the cyclin E overexpression in the tumor cell lines affected the E2F DNA binding complexes throughout the cell cycle, we performed bandshift assays using an oligonucleotide with an E2F binding site as a probe (Fig. 3). As a control, extracts from a synchronized population of normal cells were prepared. As described (13), normal cells contained several E2F complexes that were present at various times in the cell cycle. The disappearance of E2F complexes at 6, 9, and 12 h after release from the thymidine block occurred when the cells were enriched for G_2/M (Fig. 3*A*; ref. 13). The complex marked with an arrow contained the pRB-related protein p107 and cyclin A, as determined by antibody supershift analysis (data not shown). Addition of cyclin E antibody did not have any effect on the mobility of this complex (Fig. 3*A*), suggesting that cyclin E is not the predominant cyclin in the p107/E2F complex in normal cells. On the other hand, in extracts prepared from tumor cells, E2F complexes were present throughout the cell cycle, and no loss of these complexes was observed during G_2/M. The complex marked with an arrow could be disturbed with anti-p107 and partially with anti-cyclin A antibodies (data not shown). The addition of an anti-cyclin E antibody resulted in a supershift of a large proportion of the complex, suggesting that most of the p107-E2F complex contained cyclin E (Fig. 3*B*). Addition of antibodies to cyclin A and cyclin E to the same extract did not result in the appearance of any different complexes than when both antibodies were added independently (data not shown), suggesting that both cyclins did not form part of the same complex. The association of cyclin E with the E2F complexes in tumor cells paralleled the constitutive expression of cyclin E throughout the cell cycle (Fig. 2*A*, *Right*). Hence, overexpression of cyclin E in tumor cells was capable of forming a major complex with p107 and E2F. This is a second example of how overexpression and constitutive expression of cyclin E could result in a dual role for this cyclin allowing redundancy in function.

DISCUSSION

The interplay between cyclin D1/cdk4-cdk6/p16/pRb has been implicated as a crucial G_1 phase-controlling pathway that becomes frequently deregulated in many types of cancer. Any mutations giving rise to an imbalance in any one of these proteins may therefore result in a cell growth advantage leading to tumorigenesis. In this model, overexpression of p16 would prevent cdk4/cdk6 from phosphorylating pRb, and lead to a G_1 block (27–29). Thus, p16 is thought to negatively regulate the cell cycle (51). In fact, several studies have documented that primary tumors that showed expression of functional pRb protein did not express p16 protein (due to mutations in the gene) and, conversely, cells that expressed p16 protein did not have a detectable pRb protein (23–26). These studies suggest a link between D-type cyclins, cdk4/cdk6, pRb, and p16, such that overexpression of cyclin D1, inactivation of pRb, or loss of p16 may have equivalent consequences for loss of normal growth control. In addition, this model predicts a lack of functional redundancy of this pathway with other cell cycle regulatory proteins.

Even though many studies have corroborated the p16/pRb inverse correlation model, there also has been documentation to the contrary. For example, in their analysis of pRb and p16 expression in lung cancers, Otterson *et al.* (25) reported that 14%

Table 2.   Correlation of p16 and pRb status in a series of breast carcinomas

Patient ID no.	ER/PR*	DNA index/ploidy*	Proliferation index (%)*	Cyclin E†	p16†	pRb†
KK005	−/−	1.18/Aneuploid	12.2 (H)	+ + +	+ + + +	+
KK017	−/−	1.72/Aneuploid	1.5 (L)	+ + + + + +	±	+
KK020	−/−	1.73/Aneuploid	14.1 (H)	+ + + + +	−	−
KK036	+/−	1.84/Tetraploid	3.3 (L)	+ +	±	+
KK061	−/−	ND	ND	+ + + +	±	−
KK070	+/+	ND	ND	+	±	−
KK076	−/−	2.08/Tetraploid	12.5 (H)	+ + +	±	−
KK086	−/−	1.50/Aneuploid	36.0 (H)	+ + + + +	+ +	−
KK147	ND	ND	ND	+ + + + +	+ + +	+
KK173	+/−	1.91/Tetraploid	30.2 (H)	+ + + + + + +	+ + + +	+
KK190	−/−	2.09/Tetraploid	31.8 (H)	+ + + + + + +	+ + +	−
KK322	+/−	2.70/Aneuploid	30.0 (H)	+ + +	−	+
KK369	ND	ND	40.0 (H)	+ + + + + + +	+ + + +	+
KK399	−/−	ND	ND	+ + + +	+ + + +	−
KK400	+/−	ND	ND	+ + + +	±	−
KK407	−/−	1.89/Tetraploid	18.0 (H)	+ + + +	−	−
KK428	−/−	1.75/Aneuploid	27.0 (H)	+ + + +	−	−
KK429	−/−	1.71/Aneuploid	28.0 (H)	+ + + + +	−	−
KK457	ND	ND	ND	+ + + + + +	−	+
KK458	−/−	1.96/Tetraploid	11.3 (H)	+	−	+

*Quantitation of immunohistochemical staining by image analysis was performed on sections stained with either the monoclonal antibody to estrogen receptor H222 (ER-ICA kit, Abbott), monoclonal antibody to progesterone receptor mPRI (Cell Analysis Systems, Lombard, IL), or monoclonal antibody to Ki67 (Dako) as described (45, 46). Ki67 staining determined growth fraction of the tumor. Values indicate percentage of positive staining: 1.0–7.0% is indicative of low (L) proliferation index, 7.1–11.9 is indicative of moderate (M) proliferation index, and >12.0% is indicative of high (H) proliferation index. For each case, the DNA ploidy was determined by quantitation of the DNA Feulgen stain by computerized microdensitometry as described (47). ND, not determined.

†Cyclin E, p16, and pRb levels were measured using Western blot analysis with HE12 monoclonal antibody to cyclin E (Santa Cruz Biotechnology) as described (31, 32), monoclonal antibodies to p16, and pRb as described in text. Levels of cyclin E in tumor tissue samples were correlated with 76N normal (+) and MDA-MB-157 (+ + + + + +) tumor cell lines. For example, cyclin E in MDA-MB-157 cell line is 64-fold (i.e., + + + + + +) overexpressed compared with 76N cell line (i.e., +) (31). Any tumor tissue overexpressing cyclin E more than MDA-MB-157 received seven +s (i.e., + + + + + + +). p16 levels also were correlated with MDA-MB-157 (+ + + +) cell line. Equal protein loading was monitored by reprobing blots with actin, and all blots were analyzed by densitometry using AGFA scanner and IP Lab Gel software.

of small cell lung cancers and 15% of non-small cell lung cancers examined were p16 and pRb double positives, and Sakaguchi *et al.* (52) reported that 16.4% of non-small cell lung cancers studied immunohistochemically also stained positively for both p16 and Rb protein. In addition, Gerardts *et al.* (53) report that in 43% of all carcinomas examined (breast: 5 of 20; bladder: 7 of 19; colon: 16 of 19; lung: 4 of 17), both pRb and p16 could be detected, suggesting that in common human malignancies, p16 and pRb expression is not mutually exclusive. Furthermore, Musgrove *et al.* (54) report that in 50% of breast cancer cell lines examined, INK4^{p16} mRNA was expressed in the absence of any pRb mutations. Finally, Ueki *et al.* (49) show that 13% of glioblastoma cell lines examined showed neither p16 nor RB alterations, and Wang *et al.* (55) report that regardless of the status of p16 protein, all 15 melanoma cell lines examined showed the presence of pRb protein, ruling out an inverse correlation between the expression of p16 and pRb in these particular cell lines.

One possible explanation for the lack of inverse correlation between p16 and pRb may be due to overexpression of cyclin E, which could act redundantly and replace cyclin D/cdk complexes for phosphorylating pRb. In accordance with this redundancy hypothesis, Hinds *et al.* (56) first demonstrated that overexpression of several different cyclins, including cyclin E, could override the growth arrest properties of pRb in SaOS-2 cells. In addition, we had reported previously that cyclin E is severely overexpressed in all breast cancer cell lines examined (31), and overexpression of cyclin E is accompanied by its constitutive expression and activity throughout the tumor cell cycle (32). Because cyclin E is overexpressed and forms a complex with cdk2 constitutively, the active complex can act upstream of pRb and phosphorylate it even when cyclin D is inactive due to overexpression of p16. To test this model, in this study we used a breast cancer cell line that exemplified an exception to the inverse correlation rule of p16/pRb. In this tumor cell line (MDA-MB-157), cyclin E is markedly overexpressed and

present in lower molecular weight isoforms, p16 is also overexpressed, and pRb is not mutated and detectable in both its hypo- and hyperphosphorylated forms. Under these conditions, we show that p16 binds to both cdk4 and cdk6 and inhibits the binding of cyclin D1 to these cdks. We also provide evidence that, in synchronized populations of MDA-MB-157 cells, pRb is phosphorylated throughout the cell cycle following an initial lag, revealing a time course similar to phosphorylation of GST-Rb by cyclin E immunoprecipitates prepared from these synchronized cells. This analysis suggests that cyclin E/cdk2, and not cyclin D/cdk4-cdk6, is a candidate kinase complex capable of phosphorylating pRb throughout the cell cycle of this tumor cell line.

To directly examine the lack of inverse correlation of p16 and pRb *in vivo*, we document in Table 2 that in breast tumor specimen obtained from breast cancer patients in whom cyclin E is markedly overexpressed and p16 also is overexpressed, pRb is detectable in both its hypo- and hyperphosphorylated forms. These studies suggest that phosphorylation of pRb under conditions in which cyclin D/cdk complexes are rendered inactive is not an artifact of the culture conditions and occurs *in vivo*.

Because cyclin E is constitutively expressed in MDA-MB-157 cancer cells and is present during times in the cell cycle when cyclin A is not detected (see Fig. 2), it followed that cyclin E could also replace cyclin A-containing complexes. In fact, as displayed in Fig. 3, cyclin E can function redundantly and replace cyclin A in E2F complexes with cdk2 and p107 in tumor cells. In normal cells, cyclin E was not detected in complex with the pRb-related proteins p107 and p130 and with E2F during the late G$_1$ and early S phase of the cell cycle. We have found that while this cyclin was a minor component of E2F DNA binding complexes in normal cells, it was a major component of this complex in MDA-MB-157 cells. It is interesting that although normal cells display a down-regulation of E2F DNA binding activity in the G$_2$/M phases of the cell cycle, MDA-
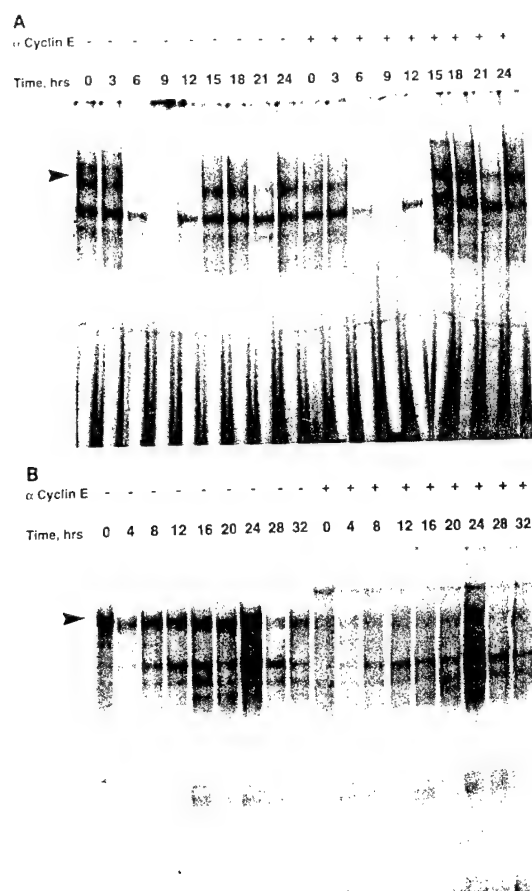
A

B

Fɪɢ. 3.   Cyclin E is the predominant cyclin in p107/E2F complexes in tumor cells. E2F complexes were analyzed by gel retardation assays using cell lysates (15 μg) prepared from synchronized populations (see Fig. 2) of normal 76N cells (*A*) and tumor MDA-MB-157 cells (*B*). The oligonucleotide used as a labeled DNA probe includes the E2F binding site of the human dehydrofolate reductase promoter. The anti-cyclin E antibody (200 ng) was used to disrupt the E2F complexes.

MB-157 cells show constitutive E2F DNA binding complexes through the cell cycle. This raises the possibility that overexpression of cyclin E perturbed the regulation of E2F activity not only by promoting the hyperphosphorylation of pRb but also by perturbing the cell cycle regulation of E2F by p107.

Based on our observations in breast cancer cell lines and tumor tissue samples, we suggest an alternative order of events along the G_1 phase-controlling pathway culminating in phosphorylation of pRb. In this pathway, cyclin E would act upstream of pRb bypassing cyclin D/cdk4 and giving the tumor cells a selective growth advantage even in the presence of high levels of p16. Hence, abrogation of cyclin D1, cdk4/cdk6, or p16 will not have any effect on the phosphorylation of pRb, which will be accomplished by cyclin E/cdk2 in these cells leading to a deregulated progression through G_1. Our data also demonstrate that cyclin D1 is not required for G_1 progression in tumor cells that exhibit an overexpressed cyclin E and a wild-type pRb. As a result, the function of cyclin D1 is dispensable not only in cell lines in which pRb is inactivated as described (57), but also in cell lines in which cyclin E is overexpressed and constitutively active (ref. 58 and this study). Finally, this study provides evidence for a lack of functional link between p16 and pRb, suggesting that in subpopulations of breast cancers, pRb is not a major substrate for the inhibitory activity of the p16 product. Hence, certain populations of tumor cells can overcome the role of p16 as a tumor suppressor protein by providing a redundant pathway to inactivate pRb and provide a growth advantage to the cells.

1.   Hartwell, L. H. & Kastan, M. B. (1994) *Science* **266**, 1821–1828.
2.   Elledge, S. J. & Harper, J. W. (1994) *Curr. Opin. Cell Biol.* **6**, 847–852.
3.   Morgan, D. O. (1995) *Nature (London)* **374**, 131–134.
4.   Sherr, C. J. (1994) *Cell* **79**, 551–555.
5.   Nasmyth, K. (1993) *Curr. Opin. Cell Biol.* **5**, 166–179.
6.   Nigg, E. A. (1993) *Curr. Opin. Cell Biol.* **5**, 187–193.
7.   Ludlow, J. W., DeCaprio, J. A., Huang, C., Lee, W.-H., Paucha, E. & Livingston, D. M. (1989) *Cell* **56**, 57–65.
8.   DeCaprio, J. A., Ludlow, J. W., Lynch, D., Furukawa, Y., Griffin, J., Piwnica-Worms, H., Huang, C.-M. & Livingston, D. M. (1989) *Cell* **58**, 1085–1095.
9.   Hatakeyama, M., Brill, J. A., Fink, G. R. & Weinberg, R. A. (1994) *Genes Dev.* **8**, 1759–1771.
10.   Ludlow, J. W., Glendening, C. L., Livingston, D. M. & DeCaprio, J. A. (1993) *Mol. Cell Biol.* **13**, 367–372.
11.   DeCaprio, J. A., Furukawa, Y., Ajchenbaum, F., Griffin, J. D. & Livingston, D. M (1992) *Proc. Natl. Acad. Sci. USA* **89**, 1795–1798.
12.   Nevins, J. R. (1992) *Science* **258**, 424–429.
13.   Shirodkar, S., Ewen, M., DeCaprio, J. A., Morgan, J., Livingston, D. M. & Chittenden, T. (1992) *Cell* **68**, 157–166.
14.   Lam, E. W.-F. & La Thangue, N. B. (1994) *Curr. Opin. Cell Biol.* **6**, 859–866.
15.   Hunter, T. (1993) *Cell* **75**, 839–841.
16.   Sherr, C. J. & Roberts, J. M. (1995) *Genes Dev.* **9**, 1149–1163.
17.   Kamb, A. (1995) *Trends Genet.* **11**, 136–140.
18.   Grana, X. & Reddy, E. P. (1995) *Oncogene* **11**, 211–219.
19.   Otsuki, T., Clark, H. M., Wellmann, A., Jaffe, E. S. & Raffeld, M. (1995) *Cancer Res.* **55**, 1436–1440.
20.   Nabel, G. & Baltimore, D. (1987) *Nature (London)* **326**, 711–713.
21.   Nobori, T., Miura, K., Wu, D., Lois, A., Takabayashi, K. & Carson, D. A. (1994) *Nature (London)* **368**, 753–756.
22.   Kamb, A., Gruis, N. A., Weaver-Feldhaus, J., Liu, Q., Harshman, K., Tavtigian, S. V., Stockert, E., Day, F. S., Johnson, B. E. & Skolnick, M. H. (1994) *Science* **264**, 436–440.
23.   Shapiro, G. I., Edwards, C. D., Kobzik, L., Godleski, J., Richards, W., Sugarbaker, D. J. & Rollins, B. J. (1995) *Cancer Res.* **55**, 505–509.
24.   Aagaard, L., Lukas, J., Bartkova, J., Kjerulff, A.-A., Strauss, M. & Bartek, J. (1995) *Int. J. Cancer* **61**, 115–120.
25.   Otterson, G. A., Kratzke, R. A., Coxon, A., Kim, Y. W. & Kaye, F. J. (1994) *Oncogene* **9**, 3375–3378.
26.   Parry, D., Bates, S., Mann, D. J. & Peters, G. (1995) *EMBO J.* **14**, 503–511.
27.   Medema, R. H., Herrera, R. E., Lam, F. & Weinberg, R. A. (1995) *Proc. Natl. Acad. Sci. USA* **92**, 6289–6293.
28.   Lukas, J., Parry, D., Aagaard, L., Mann, D. J., Bartkova, J., Strauss, M., Peters, G. & Bartek, J. (1995) *Nature (London)* **375**, 503–506.
29.   Koh, J., Enders, G. H., Dynlacht, B. D. & Harlow, E. (1995) *Nature (London)* **375**, 506–510.
30.   Li, Y., Nichols, M. A., Shay, J. W. & Xiong, Y. (1994) *Cancer Res.* **54**, 6078–6082.
31.   Keyomarsi, K. & Pardee, A. B. (1993) *Proc. Natl. Acad. Sci. USA* **90**, 1112–1116.
32.   Keyomarsi, K., Conte, D., Toyofuku, W. & Fox, M. P. (1995) *Oncogene* **11**, 941–950.
33.   Rao, P. N. & Johnson, R. T. (1970) *Nature (London)* **225**, 159–164.
34.   Crissman, H. A. & Tobey, R. A. (1974) *Science* **184**, 1287–1298.
35.   Keyomarsi, K., O'Leary, N., Molnar, G., Lees, E., Fingert, H. J. & Pardee, A. B. (1994) *Cancer Res.* **54**, 380–385.
36.   Bacus, S. S., Yarden, Y., Oren, M., Chin, D. M., Lyass, L., Zelnick, C. R., Kazarov, A., Toyofuku, W., Gray-Bablin, J., Beerli, R. R., Hynes, N. E., Nikiforov, M., Haffner, R., Gudkov, A. & Keyomarsi, K. (1996) *Oncogene* **12**, 2535–2547.
37.   Tam, S. W., Theodoras, A. M., Shay, J. W., Draetta, G. & Pagano, M. (1994) *Oncogene* **9**, 2663–2674.
38.   Zalvide, J. & DeCaprio, J. A. (1995) *Mol. Cell. Biol.* **15**, 5800–5810.
39.   Delmolino, L., Band, H. & Band, V. (1993) *Carcinogenesis* **14**, 827–832.
40.   Gudas, J., Nguyen, H., Li, T., Hill, D. & Cowan, K. H. (1995) *Oncogene* **11**, 253–261.
41.   Runnebaum, I. B., Nagarajan, M., Bowman, M., Soto, D. & Sukumar, S. (1991) *Proc. Natl. Acad. Sci. USA* **88**, 10657–10661.
42.   Lee, E. Y.-H. P., To, H., Shew, J.-Y., Bookstein, R., Scully, P. & Lee, W.-H. (1988) *Science* **241**, 218–221.
43.   Koff, A., Giordano, A., Desia, D., Yamashita, K., Harper, J. W., Elledge, S. J., Nishomoto, T., Morgan, D. O., Franza, R. & Roberts, J. M. (1992) *Science* **257**, 1689–1694.
44.   Buchkovich, K., Dufy, L. A. & Harlow, E. (1989) *Cell* **58**, 1097–1105.
45.   Bacus, S. S. & Ruby, S. G. (1993) *Pathol. Annu.* **28**, 179–204.
46.   Bacus, S. S., Chin, D., Ortiz, R., Potocki, D. & Zelnick, C. (1994) *Comp. Cytol. Hist. Lab.* 143–156.
47.   Bacus, S. S., Goldschmidt, R., Chin, D., Moran, G., Weinberg, D. & Bacus, J. W. (1989) *Am. J. Pathol.* **135**, 783–792.
48.   Dou, Q.-P., Pardee, A. B. & Keyomarsi, K. (1996) *Nat. Med.* **2**, 254.
49.   Ueki, K., Ono, Y., Henson, J. W., Efird, J. T., von Deimling, A. & Louis, D. N. (1996) *Cancer Res.* **56**, 150–153.
50.   Lippman, M. E. & Allegra, J. C. (1980) *Cancer* **46**, 2829–2834.
51.   Serrano, M., Hannon, G. J. & Beach, D. (1994) *Nature (London)* **366**, 704–707.
52.   Sakaguchi, M., Fujii, Y., Hirabayashi, H., Yoon, H.-E., Komoto, Y., Oue, T., Kusafuka, T., Okada, A. & Matsuda, H. (1996) *Int. J. Cancer* **65**, 442–445.
53.   Gerardts, J., Kratzke, R. A., Niehans, G. A. & Linclon, C. E. (1995) *Cancer Res.* **55**, 6006–6011.
54.   Musgrove, E. A., Lilischkis, R., Cornish, A. L., Lee, C. S. L., Setlur, V., Seshadri, R. & Sutherland, R. L. (1995) *Int. J. Cancer* **63**, 584–591.
55.   Wang, Y. & Becker, D. (1996) *Oncogene* **12**, 1069–1075.
56.   Hinds, P. W., Mittnacht, S., Dulic, V., Arnold, A., Reed, S. I. & Weinberg, R. A. (1992) *Cell* **70**, 993–1006.
57.   Lukas, J., Bartkova, J., Rohde, M., Strauss, M. & Bartek, J. (1995) *Mol. Cell. Biol.* **15**, 2600–2611.
58.   Resnitzky, D. M. G., Bujard, H. & Reed, S. I. (1994) *Mol. Cell. Biol.* **14**, 1669–1679.

PI: Keyomarsi, K.

Appendix

Ref. #4

Processing of Cyclin E Differs between Normal and Tumor

Richard M. Harwell, Donald C. Porter, Christopher Danes, and Khandan Keyomarsi

Division of Molecular Medicine, Wadsworth Center, Albany, New York 12201-0509 [R. M. H., D. C. P., C. D., K. K.], and Department of Biomedical Sciences, State University of New York, Albany, New York 12222 [R. M. H., K. K.]

ABSTRACT

Cyclin E is a G_1 cyclin essential for G_1 to S-phase transition of the cell cycle with a profound role in oncogenesis. In tumor cells and tissues, cyclin E is overexpressed and present in its lower molecular weight (LMW) isoforms, and it can be used as a prognosticator for poor patient outcome. In this study, we have examined differences in the processing of cyclin E between normal mammary epithelial and breast cancer cell lines. Five NH_2-terminally deleted epitope-tagged (FLAG) cyclin E vectors were constructed spanning the range of LMW forms observed in tumor cells. These constructs were transfected into normal and tumor cells and analyzed for the production of cyclin E-FLAG protein products by Western blot analysis with FLAG and cyclin E antibodies. Our results show that only tumor cells had the machinery to process these cyclin E-FLAG constructs to their LMW forms, whereas normal cells mainly expressed the full-length unprocessed form of each protein. Tumor and normal cells always process the cyclin E-FLAG protein in the same way as endogenously expressed cyclin E. This phenomenon is consistent with all of the cell lines used, regardless of transfection efficiency, time of processing posttransfection, or method of transfection. Furthermore, measurement of FLAG-associated kinase activity in the transfectants revealed that the protein products of the cyclin E-FLAG constructs are 10 times more active in tumor cells than in normal cells. These studies suggest that the LMW forms of cyclin E detected at a much higher level in tumor cells arise from posttranslational action of a protease.

INTRODUCTION

Progression through the cell cycle, the sequence of events between two cell divisions, is governed by the actions of positive and negative regulators in the eukaryotic cell. Cyclins and CDKs[3] serve as positive regulators, whereas CKIs serve as negative regulators of the cell cycle. To date, 10 different classes of cyclins (A-J, and L), 9 classes of CDKs (CDK1–9), and 2 classes of CKIs (CIP/KIP and INK) have been described, some of which have multiple members (1–3). In normal cells, the cyclins, CDKs, and CKIs work in concert to ensure a regulated transition from one phase of the cell cycle to the next. The level and pattern of expression of these regulators during the normal cell cycle are critical for the regulated progression through the cell cycle. In tumor cells, this exquisite balance between the positive and negative regulators is not maintained, thus contributing to the transformed phenotype.

The connection between cancer and the cell cycle has been established in part due to the alteration in the expression and function of G_1 cyclins in cancer cells and tissues. For example, cyclin D1, a G_1 cyclin that forms complexes with CDK4 and CDK6 (4) and whose major function is the phosphorylation of the retinoblastoma gene product pRb (5–7), was initially cloned as the PRAD1 proto-oncogene in some

parathyroid tumors, where its locus is overexpressed as a result of a chromosomal rearrangement (8, 9). Cyclin D1 undergoes gene amplification and/or overexpression in a number of other tumors, including breast, colon, and ovarian cancers (10, 11). Cyclin D1 is also overexpressed in mammary cells of transgenic mice and results in abnormal proliferation of these cells and the development of mammary adenocarcinomas (12).

Cyclin E, another G_1 cyclin that forms complexes with CDK2 and is essential for S-phase entry (13, 14), also has a profound role in oncogenesis (15, 16). Cyclin E expression occurs during a brief window of time from late G_1 into early S phase, with a peak expression level near the restriction point (17, 18). Kinase activities of cyclin E/CDK2 complexes are also at maximum levels before S-phase entry (19). Functional knockout of cyclin E by injection of anti-cyclin E antibodies into fibroblast cells causes cell arrest in the G_1 phase (20). Conversely, the overexpression of cyclin E protein causes acceleration through G_1 along with a decreased cell size (20, 21). In addition to its requirement for DNA synthesis, cyclin E also plays a key role in senescence (22), development (23, 24), and modulation of downstream signals involving pRb (7) and E2F (25, 26). Due to the crucial role played by normal cyclin E expression and activity in cell proliferation, any defects in its expression could have a critical effect on oncogenesis.

The linkage between oncogenesis and cyclin E has been reinforced by correlating the altered expression of cyclin E to the loss of growth control in breast cancer (27–29). Furthermore, several tumor cohort studies (reviewed in Ref. 11) have documented a strong correlation between cyclin E overexpression and poor patient disease-free or overall survival (15, 30) and lack of estrogen receptor expression (31–33). In addition, patients with high cyclin E levels in their tumors had a significantly increased risk of death and/or relapse from breast cancer, even if they were node negative (30, 32). In our own studies (34)[4], in which we examined tumor specimens from 403 breast cancer patients, we observe that cyclin E protein is the most consistent marker for determining the prognosis of early-stage node-negative breast carcinoma. Lastly, examination of the oncogenic potential of cyclin E in transgenic mice under the control of the bovine β-lactoglobulin promoter revealed a corroborating role for cyclin E in mammary tumorigenesis (35). Lactating mammary glands of the transgenic mice contained hyperplasia, and >10% of female transgenic mice also developed mammary carcinomas up to 13 months later (35). Collectively, these data provide strong support for the role of cyclin E overexpression in breast cancer tumorigenesis.

There are three main alterations in cyclin E expression that are seen in tumor cells, but not in normal cells: (*a*) amplification of the cyclin E gene and overexpression of cyclin E mRNA by 64-fold in a subset of breast cancer cell lines (27, 28); (*b*) cell cycle regulation of cyclin E expression is lost in some tumor cells, leading to constitutive cyclin E expression and activity throughout the cell cycle (16, 36). Such constitutive overexpression and activation of cyclin E also results in the functional redundancy of cyclin E/CDK2 in breast cancer cells because this complex has the ability to phosphorylate pRb under conditions in which cyclin D/CDK4/CDK6 complexes have been

rendered inactive by overexpression of p16 (33); and (c) cyclin E expression in tumor cells is commonly characterized by the overexpression of the wild-type form and the appearance of LMW isoforms that are not present in normal cells or tissues (15, 27). The LMW isoforms of cyclin E usually appear as bands migrating between M_r 49,000 and M_r 34,000 as detected by Western blot analysis, whereas the wild-type cyclin E migrates at M_r 51,000 (15, 27). These isoforms are found in breast cancer cell lines as well as tumor tissue specimens from breast cancer patients (15, 29, 32). The expression of these cyclin E isoforms correlates very strongly with the stage, severity, and outcome of breast cancer (15, 32). The LMW isoforms of cyclin E that are linked to poor prognosis are also observed in other tumors such as colon cancer and hematological malignancies (Refs. 37 and 38; reviewed in Ref. 39). However, despite the tumor-specific expression of the LMW forms of cyclin E and the compelling prognostic evidence, very little is known about what gives rise to these isoforms.

We previously reported that the generation of LMW forms of cyclin E is not a result of genomic rearrangements of the cyclin E gene (16, 27). We and others have also identified several alternative splice variants of cyclin E (16, 20, 40). In addition to the authentic cyclin E, referred to as the wild-type form, there are four additional splice variants of cyclin E representing: (a) a variant termed E-L that adds 15 amino acids to the NH$_2$ terminus of cyclin E (20); (b) a rare form of cyclin E termed E-S that lacks 49 amino acids containing the cyclin box motif (40); (c) a 9-bp in-frame deletion at the 5' end of the gene termed Δ9 variant (16); and (d) a 148-bp deletion in the 3' end of the gene termed Δ148 resulting in a frameshift of cyclin E (16). Both normal and tumor cells contain these variants; however, cyclin E protein expression clearly shows overexpression of the LMW isoforms in tumor cells, but not in normal cells (16). Because the LMW forms of cyclin E protein are only found in tumor cells, and the five cyclin E splice variants are found in normal and tumor cells, it suggests that the splice variants, by themselves, do not give rise to the cyclin E isoforms.

In this report, we have explored the hypothesis that a posttranslational proteolytic cleavage event is responsible for the LMW forms of cyclin E in tumor cells. We examined the possibility that tumor cells contain the machinery to process a full-length cyclin E protein into LMW forms, whereas normal cells do not. We introduced a full-length cyclin E cDNA that has been COOH-terminally tagged with FLAG sequence into tumor and normal cells and examined its pattern of expression/processing using antibodies against FLAG and cyclin E. These studies show that there is a profound difference in cyclin E processing between normal and tumor cells. Tumor cells process the FLAG-tagged cyclin E into LMW isoforms, identical to the endogenous cyclin E, whereas normal cells were unable to process the FLAG-tagged cyclin E to the LMW isoforms at high levels. Furthermore, the cyclin E processing is taking place at the NH$_2$ terminus, most likely by a protease that is more active in tumor cells.

MATERIALS AND METHODS

Vector Construction. Cyclin E-L, cyclin E, and three NH$_2$-terminally truncated FLAG-tagged constructs were engineered by fusing the cloned cyclin E cDNA sequences at the COOH terminus to the sequence coding for the FLAG peptide. FLAG is an 8-amino acid peptide (N-Asp-Tyr-Lys-Asp-Asp-Asp-Asp-Lys-C) that is immunogenic to a commercially available FLAG antibody (Santa Cruz Biotechnology, Santa Cruz, CA). The 5' primers used to create the constructs presented in Fig. 1B are as follows: cyclin E-L, 5'-GAGCGGGACACCATGC-CGAGGGAGCGCAGG-3'; cyclin E, 5'-GAGCGGGACACCATGCGAAG-GAGCGGGACA-3'; Trunk 1, 5'-GAGCGGGACACCATGGATCCAGAT-GAAGAA-3'; Trunk 2, 5'-GAGCGGGACACCATGGCAGTCTGTGCAGAC-3'; and Trunk 3 5'-GAGCGGGACACCATGTGGAAAAATCATGTTA-3'. The 3' primer containing the <u>FLAG</u> sequence is FLAGCE 5'-GCAAGCTTTTCA*CTT-GTCATCGTCGTCCTTGTAGTC*CGCCATTTCCGGCCCGCT-3'. The template

used is cyclin E-L cDNA (20). The FLAG-cyclin E PCR product was ligated directly into the TA cloning vector, pCRII (Invitrogen, Carlsbad, CA). For each of the constructs, a cyclin E primer was used that added an identical Kozak ribosome binding site and start codon to allow for equal expression levels *in vitro* and in cells. Each truncated cyclin E PCR product was cloned directly into TA cloning vector PCRII (Invitrogen). Each FLAG-tagged cyclin E was then cloned into the mammalian expression vector pCDNA3.1 (Invitrogen) under the control of a cytomegalovirus promoter. This vector system was used to allow for constitutive, transient expression of high levels of FLAG-tagged cyclin E in mammalian cells.

In Vitro **Transcription and Translation.** To transcribe and translate the cyclin E-FLAG constructs cloned in pcDNA3.1 vector, we used the TNT-coupled reticulocyte lysate system (Promega, Madison, WI). Briefly, 1 μg of pCDNA3.1 plasmid containing either the cyclin E-FLAG inserts or no insert was added to rabbit reticulocyte lysate in the presence of T7 RNA polymerase and 1 mM complete amino acid mixture in a total volume of 50 μl and incubated at 30°C for 90 min. One μl of each of the translation products containing both the rabbit reticulocyte lysate and the synthesized cyclin E protein was then separated on a SDS-PAGE gel and subjected to Western blot analysis using either a monoclonal antibody to cyclin E (clone HE-12) or a polyclonal antibody to FLAG (both from Santa Cruz Biotechnology).

Transfection. Transfection by electroporation was carried out on the tumor cell lines MDA-MB-157 and MDA-MB-436, the normal immortalized cell line MCF-10A, and the normal mortal cell strain 76N. All cells were cultured to 70% confluence in media as described previously (16). Voltages used for transfection were as follows: (a) MDA-MB-157, 0.28 kV; (b) MDA-MB-436, 0.23 kV: (c) MCF-10A, 0.3 kV; and (d) 76N, 0.32 kV (all at 960 μF capacitance). For each cell line, 1×10^7 cells were suspended in 0.5 ml of media, with 40 μg of plasmid (cyclin E-FLAG + pEGFPC-1) in a 0.4 cm gap cuvette. The pEGFPC-1 vector (CLONTECH, Palo Alto, CA) was cotransfected along with the cyclin E-FLAG vectors with a 1:4 ratio of GFP vector:cyclin E vector; the total DNA introduced was maintained at 40 μg. For MDA-MB-157 and MDA-MB-436 tumor cells, transfection was carried out in serum-free α-MEM; for MCF-10A cells and 76N normal cells, transfection was carried out in complete D medium (41) with 1% serum. After transfection, cells were plated with complete medium and harvested 24 h after transfection for analysis. The transfection time course analysis was performed on MDA-MB-157 and MCF-10A cells. Transfection conditions were identical, except that cells were harvested at time intervals of 12, 24, 48, and 72 h after transfection.

Flow Cytometry. Flow cytometry was performed to analyze transfection efficiency by examining GFP expression. After transfection, $1–5 \times 10^6$ live cells were harvested by centrifugation at $1000 \times g$ for 10 min and resuspended in PBS. GFP expression was measured on a Becton Dickinson FACScan flow cytometer (Becton Dickinson, San Jose, CA) using an excitation wavelength of 350 nm and absorbance at 485 nm. Data were analyzed using the CellQuest program (Becton Dickinson), and efficiency was measured as a percentage of cells expressing GFP over background fluorescence.

Western Blotting and Kinase Assays. Cell lysates from transfected cells were prepared and subjected to Western blot analysis as described previously (42). Briefly, 50 μg of protein from each condition were electrophoresed in each lane of a 10% SDS-polyacrylamide gel (SDS-PAGE) and transferred to Immobilon P overnight at 4°C at 35 mV constant voltage. The blots were blocked overnight at 4°C in Blotto [5% nonfat dry milk in 20 mM Tris, 137 mM NaCl, and 0.25% Tween (pH 7.6)]. After six 10-min washes in TBST [20 mM Tris, 137 mM NaCl, and 0.05% Tween (pH 7.6)], the blots were incubated in primary antibodies for 3 h. Primary antibodies used were cyclin E monoclonal antibody (Santa Cruz Biotechnology) at 1 μg/ml, anti-FLAG polyclonal antibody (Santa Cruz Biotechnology) at 0.25 μg/ml, and actin monoclonal antibody (Boehringer Mannheim, Indianapolis, IN) at 0.63 μg/ml. All dilutions were made in Blotto. After primary antibody incubation, the blots were washed and incubated with the appropriate goat antimouse or antirabbit horseradish peroxidase conjugate at a dilution of 1:5000 in Blotto for 1 h and then washed and developed with the Renaissance chemiluminescence system as directed by the manufacturer (NEN Life Sciences Products, Boston, MA).

For histone H1 kinase assay, 100 μg of cell extracts were used per immunoprecipitation with polyclonal antibody to FLAG or CDK2 (42) in lysis buffer containing 50 mM Tris buffer (pH 7.5), 250 mM NaCl, 0.1% NP40, 25 μg/ml leupeptin, 25 μg/ml aprotinin, 10 μg/ml pepstatin, 1 mM benzamidine, 10 μg/ml soybean trypsin inhibitor, 0.5 mM phenylmethylsulfonyl fluoride, 50 mM NaF, and 0.5 mM sodium orthovanadate. The protein/antibody mixture was incubated with
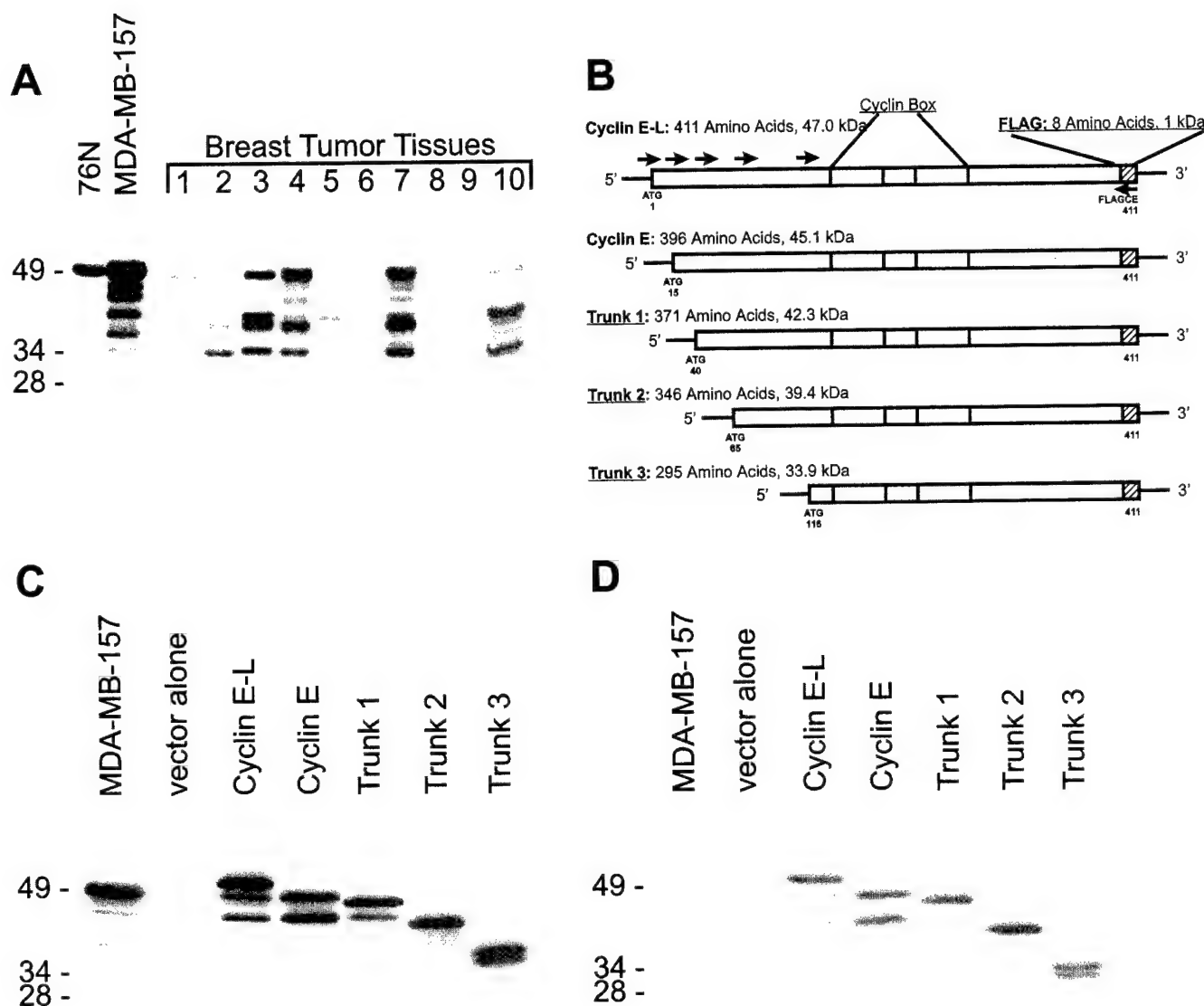
Fig. 1. Generation of cyclin E-FLAG constructs. *A*, tumor cells and tissue overexpress the LMW isoforms of cyclin E. Whole cell lysates were extracted from 10 breast cancer tissues as well as 76N normal and MDA-MB-157 tumor cell lines. Breast cancer types and tumor stages are as follows: *Lane 1*, infiltrating ductal carcinoma, stage 2A; *Lane 2*, infiltrating ductal carcinoma, stage 2B; *Lane 3*, infiltrating, poorly differentiated carcinoma, stage 3A; *Lane 4*, infiltrating ductal carcinoma, stage 3A; *Lane 5*, infiltrating ductal carcinoma, stage 1; *Lane 6*, infiltrating ductal carcinoma, stage 1; *Lane 7*, infiltrating ductal carcinoma, stage 2B; *Lane 8*, infiltrating ductal carcinoma, stage 1; *Lane 9*, infiltrating, well-differentiated ductal carcinoma, stage 1A; and *Lane 10*, infiltrating ductal carcinoma, stage 3A. Patients whose tumors were analyzed in *Lanes 3, 4, 7,* and *10* had poor outcomes (*i.e.,* death due to disease or lack of disease-free survival). Protein extracts were loaded (50 µg/lane) on a 10% SDS-PAGE and subjected to Western blot analysis with anti-cyclin E antibody. *B*, schematic representation of FLAG-tagged cyclin E constructs. All cyclin E vectors were engineered with a 3' FLAG sequence (*FLAGCE*; ←), and the five different 5' PCR primers used are shown as five sequential arrows (→) representing the five different constructs. The FLAG tag region is shown as a *hatched box*, and the cyclin box (CDK binding) region is shown as *shaded boxes*. The predicted molecular weight of each construct is listed, minus the M_r 1,000 from the FLAG tag. *C* and *D*, *in vitro* translation products of the cyclin E-FLAG constructs. Cyclin E-FLAG constructs were subjected to *in vitro* translation using the rabbit reticulocyte lysate TNT expression system with a T7 promoter. A 1-µl aliquot of the translation product was then subjected to Western blot analysis with either (*C*) anti-cyclin E or (*D*) anti-FLAG antibody. For both Western blots, *Lane 1* is 50 µg of MDA-MB-157 cell extract. *Vector alone*, the pCDNA3.1 vector with no insert incubated with the TNT reaction and used as a negative control.

protein A-Sepharose for 1 h, and the immunoprecipitates were then washed twice with lysis buffer and washed four times with kinase buffer [50 mM Tris-HCl (pH 7.5), 250 mM NaCl, 10 mM MgCl₂, 1 mM DTT, and 0.1 mg/ml BSA]. The immunoprecipitates were then incubated with kinase buffer containing 60 µM cold ATP and 5 µCi of [^{32}P]ATP in a final volume of 50 µl at 37°C for 30 min. The products of the reaction were then analyzed on a 13% SDS-PAGE gel. The gel was then stained, destained, dried, and exposed to X-ray film. For quantitation, the protein bands corresponding to histone H1 were excised, and the radioactivity of each band was measured by Cerenkov counting.

RESULTS

Generation of LMW Cyclin E Constructs. A Western blot analysis of cyclin E illustrating the pattern of cyclin E LMW isoforms

detected in breast tumor cells and tissue samples from breast cancer patients is shown in Fig. 1A. The MDA-MB-157 breast cancer cell line and several tumor tissues obtained from breast cancer patients with different stages of the disease (see Fig. 1 legend) overexpress the LMW forms of cyclin E. The electrophoretic mobility of the LMW forms of cyclin E is similar in both the MDA-MB-157 cell line and the tumor tissue samples. The normal, human mammary epithelial cell strain 76N, on the other hand, expresses predominantly the full-length form of cyclin E. The appearance of the LMW forms of cyclin E in breast tumor tissues and cell lines is predictive of their physiological roles in tumors but not normal cells or tissues.

To investigate the proteolytic processing of cyclin E in normal and

tumor cells creating the LMW isoforms, a series of cyclin E constructs were engineered with the epitope FLAG sequence at the COOH terminus (Fig. 1B). Five different FLAG-tagged cyclin E constructs were engineered and are schematically presented in Fig. 1B. These constructs include cyclin E-L-FLAG (the splice variant with a 15-amino acid insertion at the 5' end; Ref. 20), E-FLAG (the wild-type cyclin E), and three NH$_2$-terminal truncated cyclin E constructs designated Trunk 1–3-FLAG constructs (Fig. 1B). These five cyclin E constructs were created to serve two purposes: (a) the E-L-FLAG and E-FLAG constructs will be used to determine whether a full-length cyclin E can give rise to the LMW forms in tumor or normal cells. In addition, these two constructs show that the E-L form is the predominant cyclin expressed in both normal and tumor cells (see Fig. 1A); and (b) the smaller trunks will be used to bracket the LMW forms expressed in tumor cells. Our previous studies suggest that the endogenous LMW isoforms of cyclin E found in tumor cells are a result of NH$_2$-terminal deletions of the protein (Ref. 16; data not shown). By comparing the mobility of the cyclin E trunk forms with the cyclin E LMW forms on a Western blot, the sizes of the isoforms can be more accurately determined.

The expression of the truncated cyclin E cDNAs was first examined by *in vitro* transcription/translation to analyze the sizes of their respective protein products. FLAG-tagged cyclin E-L, E, and Trunks 1–3 as well as the pCDNA3.1 vector with no insert were synthesized by *in vitro* transcription/translation and then subjected to Western blot analysis with both cyclin E (Fig. 1C) and FLAG (Fig. 1D) antibodies. In both Western blots, *Lane 1* represents 50 μg of MDA-MB-157 total cell extract, which was used as a positive control for the cyclin E antibody (Fig. 1C) detecting endogenous cyclin E. *Lane 1* also serves as a negative control for the FLAG antibody (Fig. 1D). *Lane 2* is the negative control for vector pCDNA3.1 with no insert in the transcription/translation reaction and shows no cyclin E protein as detected by the cyclin E or FLAG antibodies. *Lanes 3–7* are the *in vitro* translated products of the five different cyclin E-FLAG constructs. The size difference for each trunk can clearly be seen as each lane shows a smaller sized cyclin E band (Fig. 1, C and D). The predicted sizes of the cyclin E-FLAG Trunk forms determined by sequence information of the proteins produced by the constructs are between M_r 48,000 for E-L-FLAG and M_r 34,800 for Trunk 3-FLAG. The FLAG tag adds an additional M_r 1,000 to the size of the cyclin E protein (Table 1). However, the actual sizes of the *in vitro* transcribed trunks, as determined by gel migration, are quite different and range from M_r 52,000 for E-L-FLAG to M_r 34,000 for Trunk 3-FLAG (Table 1). The differences in cyclin E molecular weight determined by Western blotting of the *in vitro* translated constructs *versus* those predicted from the amino acid sequence suggest that cyclin E protein migrates anomalously on an SDS-PAGE. In addition, smaller forms of cyclin E are detected on the Western blots, probably as the result of alternate translation start sites present within the cyclin E cDNA. For example, cyclin E-L-FLAG also produced a M_r 46,000 band that comigrates with cyclin E-FLAG at M_r 46,300. In addition, cyclin E-L-, E-, and Trunk-1-FLAG constructs all synthesized a protein migrating at ~ M_r 41,000; this is most likely a translation start site at bp 136–138, which is close to Trunk 2-FLAG migrating at M_r 41,200. Trunk 3-FLAG produces an additional band at M_r 30,600 that may be from a translation start site at bp 358–361 within the middle of the cyclin E gene. The cyclin E constructs used in this study span the entire range of cyclin E LMW forms from about M_r 51,000 to M_r 34,000 detected in MDA-MB-157 (Fig. 1A, Lane 2 and Fig. 1C, Lane 1) and tumor tissue samples (Fig. 1A, Lanes 1–5, 7, and 10).

Differential Processing of Cyclin E in Normal *versus* Tumor Cells. The *in vitro* translation of the cyclin E constructs generated only the full-length and the alternative start site protein products (Fig. 1). However, the pattern of cyclin E expression in breast cancer cells

Table 1 *Predicted versus actual molecular weight of cyclin E-FLAG constructs translated in vitro or transfected into MDA-MB-157 or MCF-10 A cells*

The molecular weight of *in vitro* translated and transfected protein products of the constructs was analyzed from Western blot analysis performed with anti-FLAG antibody as presented in Figs. 1–4. The gels were then scanned, and Kodak Digital Science 1D software (Eastman Kodak Company, New Haven, CT) was used to estimate the actual molecular weight of each protein product detected on Western blot relative to molecular weight standards run on each gel.

Constructs	Predicted M_r	In vitro translated M_r	MDA-MB-157 transfected M_r	MCF-10A transfected M_r
Cyclin E-L-FLAG	48,000	52,000	51,900	52,000
		46,000	49,700	
		41,800	45,800	
			42,600	
			39,300	
			37,300	
Cyclin E-FLAG	46,100	46,300	45,800	46,000
		41,500	42,600	
			41,200	
			38,700	
Trunk 1-FLAG	43,300	45,500	45,500	45,500
		41,100	43,700	43,700
			41,200	
			38,700	
Trunk 2-FLAG	40,400	41,200	42,000	41,900
			40,300	
			38,700	
Trunk 3-FLAG	34,900	34,000	34,500	34,500
		36,000	36,000	36,000

and tissues is indicative of a more complex processing of cyclin E (Fig. 1A). To compare normal and tumor processing, we transfected two different sets of normal and tumor cells with the cyclin E-FLAG constructs and examined the expression and associated kinase activity of the protein products from these constructs (Fig. 2).

The two normal cell lines and the two tumor cell lines used for these study are the tumor cell lines MDA-MB-157 and MDA-MB-436 and normal cell lines MCF-10A (immortalized) and 76N (mortal) cell strain. All cells were transfected with either the vector backbone, cyclin E-L-FLAG, or cyclin E-FLAG constructs. Because differences in transfection efficiencies could account for differential processing of cyclin E between cells, we monitored transfection efficiencies by cotransfection with the GFP-expressing vector pEGFPC-1, and the percentage of efficiency was determined by measuring GFP expression by flow cytometry (see "Materials and Methods"). Table 2 lists the transfection efficiencies of the four cell lines used in this study.

After transfection with the indicated vectors and determination of transfection efficiency, cell extracts were prepared and subjected to Western blot analysis with FLAG antibody (Fig. 2, A and B). The results revealed that in both MDA-MB-157 and MDA-MB-436 tumor cells, cyclin E-L-FLAG and cyclin E-FLAG were processed into several LMW isoforms as well as the full-length form, generating a pattern of cyclin E-FLAG expression similar to endogenously expressed cyclin E (Fig. 2A and B, Lanes 3 and 4). [The generation of these LMW forms of cyclin E in tumor cells is independent of the method of cell lysis, protein, extraction, or buffer used to lyse cells before Western blotting (data not shown)]. This result suggests that a single full-length cyclin E has the ability to give rise to LMW forms in tumor cells. Moreover, these forms most likely arise from a post-translational processing event, because the cyclin E cDNA used was isolated from a mature mRNA that was already spliced (17, 20). The LMW forms produced from the full-length cyclin E-L-FLAG and cyclin E-FLAG range from M_r 51,000 to M_r 34,000, which is the same range as endogenous LMW forms detected in nontransfected cells.

The pattern of expression of cyclin E-L-FLAG and cyclin E-FLAG in normal cells is quite different than that observed in tumor cells (Fig. 2, A and B). Transfection of either cyclin E-L-FLAG or cyclin E-FLAG into either MCF-10A or 76N cells results mainly in the expression of the
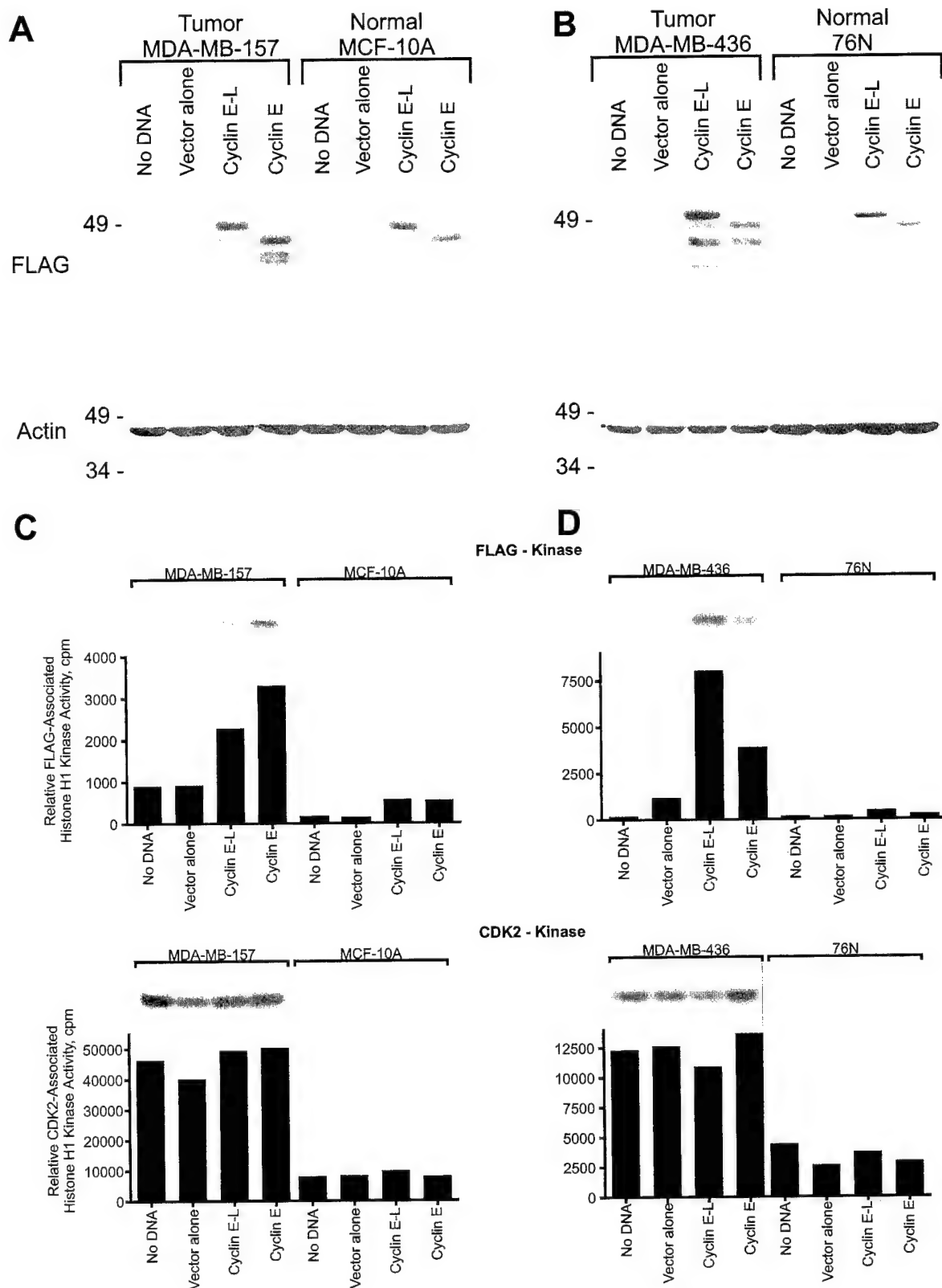
Fig. 2. Cyclin E-FLAG is processed into its LMW forms in tumor cells but not in normal breast cells. Cyclin E-L-FLAG and cyclin E-FLAG constructs were transfected into (*A* and *C*) MDA-MB-157 and MCF-10A cells or (*B* and *D*) MDA-MB-436 and 76N cells, harvested 24 h after transfection, and subjected to (*A* and *B*) Western blot analysis with anti-FLAG and anti-actin antibodies or (*C* and *D*) histone H1 kinase analysis. For Western blot analysis, 50 μg of protein extract from each condition were analyzed with the indicated antibodies, and actin was used to confirm equal protein loading. The blots were developed by chemiluminescence reagents. The same blots were sequentially hybridized with different antibodies (see "Materials and Methods"). The blots were stripped between the antibodies in 100 mM 2-mercaptoethanol, 62.5 mM Tris-HCl (pH 6.8), and 2% SDS for 10 min at 55°C. For kinase activity, equal amounts of protein (100 μg) from cell lysates were prepared from each condition and immunoprecipitated with anti-FLAG or anti-CDK2 antibodies (polyclonal) coupled to protein A beads using histone H1 as substrate. For each condition, we show the resulting autoradiogram of the histone H1 SDS-PAGE and the quantitation of the histone H1-associated kinase activities by Cerenkov counting.

Table 2 *Flow cytometric analysis of GFP expression of transfected cells*

Tumor (MDA-MB-157, MDA-MB-436) and normal (MCF-10A, 76N) cell lines were cotransfected with cyclin E-FLAG vectors and the pEGFPC-1 vector harboring the GFP cDNA. Forty μg of total DNA were transfected, and the cyclin E-FLAG:GFP vector ratio is 4:1. All cells were transfected by electroporation (see text for voltages used). Percentage of GFP expression is measured as a percentage of cells above background fluorescence of cyclin E-FLAG alone. Percentage of GFP expression is referred to as percentage of transfection efficiency throughout the text. Mean values from the indicated totals (n) are presented.

Cell lines	% GFP expression
MDA-MB-157	55% ($n = 10$)
MCF-10A	68.4% ($n = 10$)
MDA-MB-436	14% ($n = 5$)
76N	13% ($n = 5$)

full-length protein products (Fig. 2, *A* and *B*, *Lanes 7* and *8*). There was a slight expression of LMW forms in normal cells after transfection with cyclin E-FLAG; however, the levels of these proteins were much lower than those of the LMW forms expressed by tumor cells. The inability of normal cells to express high levels of LMW forms of cyclin E-L-FLAG or cyclin E-FLAG proteins from the full-length form shows that the LMW processing is much less active in normal cells than in tumor cells. The similar Western blot pattern of expression between endogenous and transfected cyclin E in normal cells again shows that the transfected cyclin E-FLAG constructs are being expressed similarly to the endogenous cyclin E. The levels of expression of the LMW forms of both the endogenous and transfected cyclin E in normal cells are always much lower than the levels exhibited by tumor cells (Fig. 1*A*, *Lanes 1* and *2*). This suggests that the machinery to process cyclin E may be present in both normal and tumor cells; however, this processing machinery is more active in tumor cells.

We found that transiently expressed cyclin E-L-FLAG and cyclin E-FLAG can activate CDK2, and the kinase activation is greater in tumor cells (Fig. 2, *C* and *D*). Cyclin E-associated kinase activity was measured by the phosphorylation of histone H1 in immunoprecipitates prepared from transfected normal and tumor cells using an antibody to FLAG. This analysis revealed that cyclin E-FLAG-associated kinase activity was 10-fold higher in tumor cells than in normal cells. This was surprising because equal amounts of cyclin E-L-FLAG or cyclin E-FLAG constructs were transfected into the cell lines as determined by efficiency studies (Table 2). The increased kinase activity associated with FLAG in tumor cells may be due not only to the processing of cyclin E-FLAG into its LMW forms but also to its overexpression. Furthermore, the high kinase activity in tumor cells suggests that the LMW isoforms of cyclin E-FLAG products can activate the kinase and that there is more CDK2 present in tumor cells. We also measured CDK2-associated kinase activity in both normal and tumor cells and found that tumor cells harbor a higher level of CDK2 activity than normal cells (Fig. 2, *C* and *D*). Transfection of cyclin E-L-FLAG and cyclin E-FLAG in normal and tumor cells increases cyclin E-FLAG-associated kinase activity in tumor cells due to the increased processing of these constructs and the greater amount of CDK2 in tumor cells.

Processing of Cyclin E in Tumor Cells Is Independent of Time, Transfection Efficiency, Cell Lines Used, or Method of Transfection. To examine changes in the pattern of cyclin E processing in tumor and normal cells over time, cyclin E-L-FLAG and cyclin E-FLAG constructs were transfected into MDA-MB-157 and MCF-10A cells. Protein was extracted at 12, 24, 48, and 72 h after transfection and subjected to Western blot analysis with antibodies to cyclin E and FLAG (Fig. 3). The decreasing expression of cyclin E-L-FLAG and cyclin E-FLAG can be seen over the time course examined in both MDA-MB-157 (Fig. 3*A*) and MCF-10A (Fig. 3*B*) cells. The maximum level of expression peaks between 12 and 24 h and then drops steadily in both cell lines. Again, fewer cyclin E LMW forms are found in the MCF-10A cells (Fig. 3*B*) than in MDA-MB-157 tumor cells (Fig. 3*A*). Tumor cells process cyclin E into LMW forms as early as 12 h after transfection. Furthermore, at every time interval examined, the relative levels of the isoforms and the full-
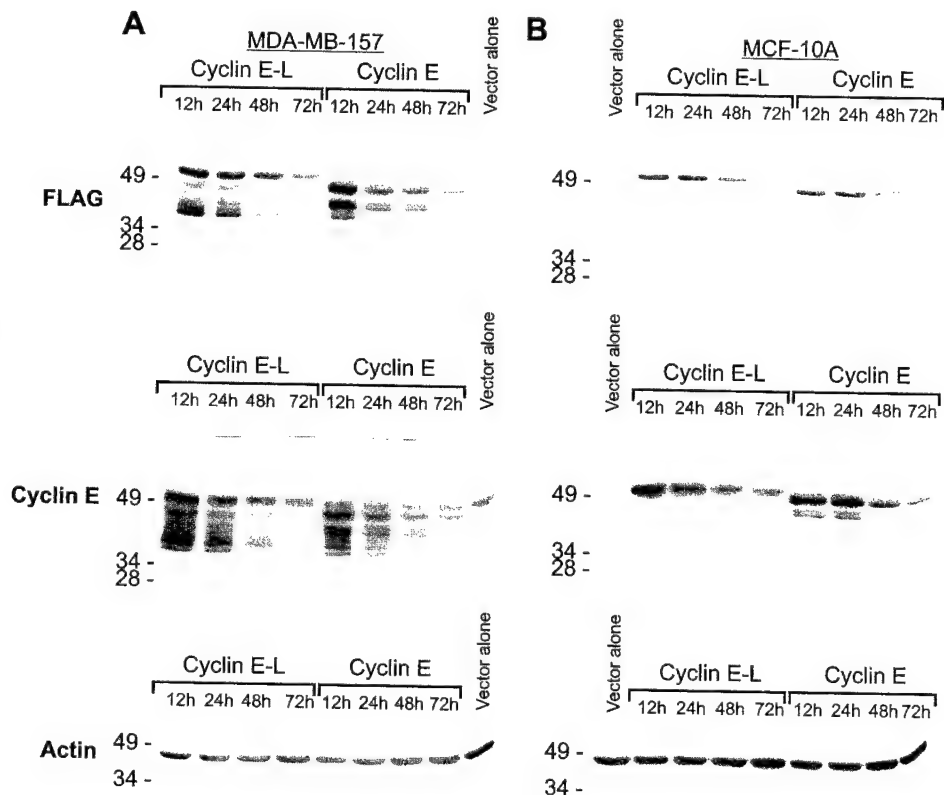

Fig. 3. Processing of cyclin E-FLAG in tumor cells is independent of transfection time. Cyclin E-L-FLAG and cyclin E-FLAG constructs were transfected into (*A*) MDA-MB-157 tumor cells or (*B*) MCF-10 A normal cells, harvested at the indicated times, and subjected to Western blot analysis with the indicated antibodies (actin was used for equal protein loading). The blots were developed by chemiluminescence reagents. The same blots were sequentially hybridized with different antibodies (see Fig. 2 legend). *Vector alone,* the pCDNA3.1 backbone.
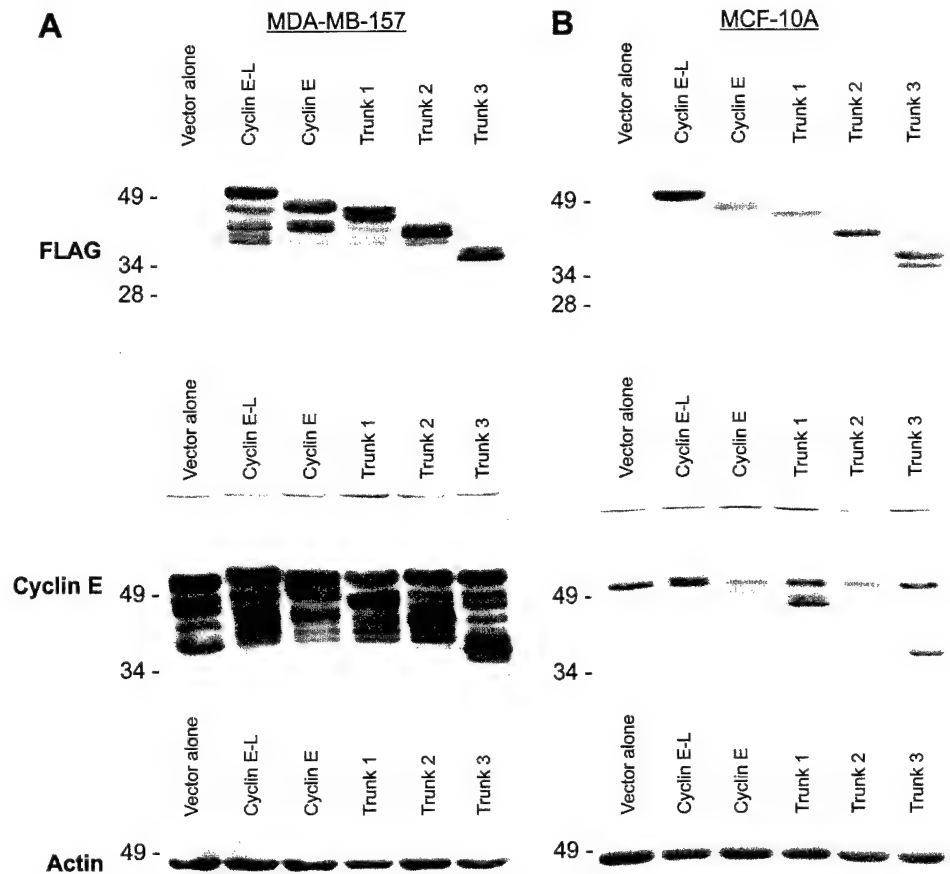
Fig. 4. Processing of all of the cyclin E-FLAG constructs in tumor cells but not in normal cells. The five different cyclin E-FLAG constructs (see Fig. 1) or vector alone was transfected into (A) MDA-MB-157 tumor cells or (B) MCF-10 A normal cells, harvested 24 h after transfection, and subjected to Western blot analysis with the indicated antibodies (actin was used for equal protein loading). The same blots were sequentially hybridized with different antibodies (see Fig. 2 legend). *Vector alone*, the pCDNA3.1 backbone.

length form do not change in the tumor cells, revealing a persistent pattern of cyclin E-FLAG overexpression over the time of transfection. These results suggest that there is a balance between steady-state synthesis and proteolysis of cyclin E over time and that this balance is maintained regardless of time or the degree of transfection.

The overexpression of transfected cyclin E-L-FLAG and cyclin E-FLAG in both cell lines is evident in the total cyclin E expressed (*i.e.,* endogenous plus transfected) using an antibody to cyclin E that reacts to both forms of cyclin E (Fig. 3, *A* and *B, middle panel*). The vector alone (*i.e.,* mock-transfected) lanes in Fig. 3, *A* and *B*, establish the endogenous baseline amount of cyclin E in each cell line. Although cyclin E-FLAG is significantly overexpressed transiently in normal cells, it does not give rise to the LMW isoforms. The amount of cyclin E overexpressed is similar between normal and tumor cells, as reflected by the similar transfection efficiencies in these two cell lines (55–68%; Table 2). The processing of cyclin E in tumor cells is independent of transfection efficiency and of the expression level of cyclin E. However, it is possible that although the same amount of plasmid was delivered into each cell type, tumor cells may express cyclin E-FLAG at a higher level than normal cells. Nonetheless, we have found that even when very low amounts of plasmid are delivered to tumor cells (*i.e.,* 10–15% transfection efficiency), the tumor cells process cyclin E-FLAG into its LMW forms (data not shown). In fact, we have investigated the effect of transfection efficiency on the processing of cyclin E in tumor and normal cells and have found that tumor cells with a wide range of transfection efficiencies (*i.e.,* 10–70%) always process cyclin E into its LMW forms, whereas normal cells, even those with the highest transfection efficiency (*i.e.,* 80%) never process cyclin E into its LMW forms (data not shown). Therefore the appearance of the LMW form of cyclin E is independent of the amount of cyclin E-FLAG expression. In Fig. 2, we also show that the

processing of cyclin E occurs similarly in tumor cell lines MDA-MB-157 and MDA-MB-436. The transfection efficiency in these two cell lines is very different (Table 2); however, the pattern of cyclin E processing is always similar to the pattern of endogenous cyclin E, suggesting that the transfected cyclin E is treated the same as the endogenous form. Lastly, the processing of cyclin E is independent of the method of transfection used. For all of the experiments depicted in this study, we have used the electroporation method of transfection. However, identical patterns of cyclin E processing in tumor cells were seen when other methods of transfection were used; such as lipofection, calcium phosphate, or GenePORTER (data not shown). Collectively, our data suggest that the processing of cyclin E in tumor cells is independent of time, transfection efficiency, cell lines used, or method of transfection.

Differential Processing of All Cyclin E-FLAG Constructs in Normal *versus* Tumor Cells. Because tumor cells are able to process the full-length cyclin E into LMW forms, the next step was to determine more precisely which region of the cyclin E protein is subject to the processing. Transfection of all five cyclin E-FLAG vectors (see Fig. 1*B*) into normal and tumor cells will bracket the endogenous LMW forms of cyclin E found in tumor cells and define their approximate mass. MDA-MB-157 and MCF-10A cells were transfected with each of the five cyclin E-FLAG constructs (presented schematically in Fig. 1*B*) and the vector backbone, harvested 24 h after transfection, and subjected to Western blot analysis with FLAG and cyclin E antibodies (Fig. 4).

Transfection of each of the cyclin E-FLAG constructs into tumor cells resulted in their processing into LMW forms that fell within the range of M_r 52,000 to M_r 36,000 (Table 1). The largest protein produced from each construct migrated with a mobility similar to that observed by *in vitro* translation (Table 1). However, MDA-MB-157

cells were able to further generate LMW forms from all of the constructs. For example, cyclin E-L-FLAG expressed *in vitro* generated one major protein migrating at M_r 52,000 and two minor bands at M_r 46,000 and M_r 41,800, detected by a FLAG antibody (see Fig. 1, *C* and *D*; Table 1). However, the same construct transfected in tumor cells generated six major proteins migrating between M_r 37,000 and M_r 52,000 (Fig. 4*A*; Table 1). This result indicates that alternate translational start sites active in the *in vitro* translation system do not account for all of the LMW forms of cyclin E produced by tumor cells. Additionally, each of the constructs transfected in the tumor cells is also processed into the next series of LMW forms, and the LMW isoforms common between all constructs comigrate (Fig. 4*A*, *Lanes 2–6*; Table 1). Because the FLAG tag is on the COOH end of each construct, these data provide additional evidence that the processing of cyclin E occurs from the NH_2-terminal end of the cyclin E protein and that the COOH terminus remains intact.

Transfection of MCF-10A cells with each of the cyclin E-FLAG constructs results mainly in the expression of the full-length form of each construct with minimal processing (Fig. 4*B*, *Lanes 2–6*). This is consistent with the results obtained in the transfection of cyclin E-L-FLAG and cyclin E-FLAG constructs into MCF-10A and 76N cells (Fig. 2). The protein products of each MCF-10A transfected cyclin E-FLAG construct migrated with the same mobility as the *in vitro* synthesized form as well as the longest form of each construct after transfection in MDA-MB-157 cells (Table 1). Based on these comparisons, the sizes of all of the cyclin E processed proteins detected in MDA-MB-157 cells were estimated within 6 amino acids and listed in Table 1.

Lastly, expression of total cyclin E (*i.e.*, endogenous + transfected), as detected by cyclin E antibody, highlights the levels of overexpression of transfected cyclin E-FLAG in both cell lines (Fig. 4, *middle panels*). These results show that although the cyclin E-FLAG constructs were overexpressed in both normal and tumor cells to the same extent, only tumor cells can process cyclin E into LMW isoforms, whereas normal cells have a reduced capacity for further processing.

DISCUSSION

In this study, we provide evidence that a tumor-specific proteolytic activity generates the LMW forms of cyclin E detected in tumor cells. The physiological relevance of the LMW forms of cyclin E unique to tumor cells has been substantiated by their role in the prognosis of breast cancer and their constitutive expression and activation throughout the tumor but not the normal cell cycle (see "Introduction"). The generation of LMW forms of cyclin E could potentially occur at several different levels including alternative splicing of the cyclin E gene. Although five different splice variants of cyclin E have been identified to date (16, 20, 40), all splice variants are present at similar levels in normal and tumor cells and cannot account for the generation of the LMW isoforms of cyclin E protein detected in tumor cells and tissues. Other translational or posttranslational events that could give rise to the LMW isoforms of cyclin E include alternative translation start or stop sites and proteolytic cleavage of cyclin E. Analysis of the cyclin E sequence reveals that there are simply not enough start codons that lie within the size range of the gene, which could give rise to all LMW forms of cyclin E between M_r 51,000 and M_r 35,000. Premature termination of translation of cyclin E would give rise to LMW forms of cyclin E but would not contain the COOH terminus sequence required for antibody detection (43). Although posttranslational modification of cyclin E such as glycosylation or phosphorylation could potentially account for the LMW forms of cyclin E, such a possibility is unlikely. Glycosylation of cyclin E has never been detected and cannot result in faster migration of proteins. The full-length form of cyclin E is already hyperphosphorylated, and although

autophosphorylation of cyclin E at Thr^{380} occurs (44), it cannot account for a M_r 16,000 difference in molecular weight (*i.e.*, between M_r 51,000 and M_r 35,000) forms of cyclin E detected in tumor cells. Posttranslational proteolytic cleavage seems reasonable for generating tumor cell-specific LMW forms of cyclin E.

As a strategy to study the processing of cyclin E in normal and tumor cells, we introduced full-length cyclin E cDNA tagged with FLAG into normal cells and tumor cells and examined the transfected cyclin E-FLAG for processing into LMW forms. This strategy was used to determine whether the processing occurs posttranslationally and to reveal any processing differences between normal and tumor cells. We found that tumor cells processed the full-length cyclin E-FLAG into its LMW isoforms, and normal cells predominantly expressed the full-length form. Furthermore, cyclin E-FLAG protein products have a much higher associated kinase activity in tumor cells than in normal cells. This increased cyclin E activity is due to increased free CDK2 in tumor cells (data not shown) and the increased ability of the LMW forms of cyclin E to form active complexes with CDK2.

The processing of the transfected cyclin E-FLAG seen in normal and tumor cells always reflects the processing of endogenous cyclin E. This similarity suggests that the same machinery that processes the endogenous cyclin E is also processing the transfected cyclin E. Furthermore, the processing occurs at a low level in normal cells, which suggests that it is an overactive mechanism in tumor cells, acting to cleave the full-length cyclin E into its LMW forms. Although tumor cells express high levels of cyclin E, the processing is not a function of overexpression because normal cells do not process cyclin E, even when it is transiently overexpressed to the same extent as in tumor cells. These results suggest that overburdening the cell with cyclin E does not, by itself, result in the generation of the LMW forms. Both 76N and MCF-10A cells can accommodate overexpression of cyclin E proteins without processing them to their LMW forms. Hence, the difference in processing of cyclin E detected between tumor and normal cells is not a result of overexpression of cyclin E but is more likely due to the action of proteases active in tumor cells that can process cyclin E to its LMW forms.

The cyclin E processing event seems to involve a cleavage of the NH_2-terminal end of cyclin E, yielding LMW isoforms that span the region of M_r 51,000 to M_r 35,000. There is already some evidence that the processing event is occurring at the NH_2 terminus of cyclin E. The antibodies used to detect the LMW forms of cyclin E (*i.e.*, clone HE-12 or FLAG) both recognize the COOH terminus of cyclin E, suggesting an intact COOH terminus. Based on these findings, we hypothesize that tumor cells may overexpress or activate a protease that could cleave the NH_2-terminal region of cyclin E at several specific sites to generate the LMW forms. Additionally, the NH_2-terminal secondary structure of cyclin E is not critical for the processing of cyclin E. The results from Fig. 4 clearly show that transfection of Trunk 3-FLAG, the smallest construct made (Fig. 1*B*), results in its cleavage very close to its NH_2 terminus. The proximity of the Trunk-3 cleavage site to its NH_2 terminus is not likely to allow for a significant NH_2-terminal secondary structure.

Based on the unique pattern of cyclin E processing observed in tumor cells but not in normal cells and the definitive role of cyclin E for DNA replication, we propose that tumor cells harbor proteases that cleave cyclin E into its LMW forms. These proteases have to be localized in the nucleus and act independently of the proteasome. Localization of the cyclin E protease to the nucleus is necessary because cyclin E immunostaining with antibodies that detect the LMW forms always shows nuclear localization of the cyclin E signal (Refs. 20 and 29; data not shown). The appearance of both the LMW forms and the unprocessed full-length forms of cyclin E in tumor cells provide evidence for a non-proteasome-mediated cleavage of cyclin E. Although the proteasome pathway

has been implicated for the degradation of cyclin E (44, 45), it is not likely to be responsible for the generation of the LMW forms of cyclin E observed in tumor cells. The manner by which the proteasome proteolytic machinery degrades proteins is either all or none. Once a protein has been tagged for proteasome degradation, it is completely degraded. Because the LMW forms of cyclin E are present constitutively in the tumor cells (16), they do not represent the intermediate proteolytic products of degradative machinery. These LMW forms of cyclin E are more likely due to the action of a protease. In fact, the analysis of the molecular weights generated by the different cyclin E-FLAG constructs used in this study helped to identify two regions in the NH_2 terminus of cyclin E that are cleaved to give rise to the LMW forms of cyclin E detected in tumor cells. These two motifs in the cyclin E sequence are potential protease cleavage sites. Current biochemical and molecular approaches have identified these sites as target sequences for a serine protease with high activity in tumor cells.[5]

In summary, we show that tumor cells contain the machinery to process epitope-tagged cyclin E-FLAG constructs into LMW isoforms, identical to the endogenous cyclin E, at a much higher degree than normal cells. The processing of cyclin E is independent of the amount of cyclin E, takes place at the NH_2 terminus, and is most likely performed by the action of a nonproteasome nuclear protease with high activity in tumor cells.

ACKNOWLEDGMENTS

REFERENCES

1. Gao, C. Y., and Zelenka, P. S. Cyclins, cyclin-dependent kinases and differentiation. Bioessays, *19:* 307–315, 1996.
2. Harper, J. W. Cyclin dependent kinase inhibitors. Cancer Surv., *29:* 91–108, 1997.
3. Sherr, C. J. Cancer cell cycles. Science (Washington DC), *274:* 1672–1677, 1996.
4. Hunter, T., and Pines, J. Cyclins and cancer II: cyclin D and cdk inhibitors come of age. Cell, *79:* 573–582, 1994.
5. Hinds, P. W., Mittnacht, S., Dulic, V., Arnold, A., Reed, S. I., and Weinberg, R. A. Regulation of retinoblastoma protein functions by ectopic expression of human cyclins. Cell, *70:* 993–1006, 1992.
6. Kato, J-Y., Matsushime, H., Hiebert, S. W., Ewen, M. E., and Sherr, C. J. Direct binding of cyclin D to the retinoblastoma gene product (pRb) and pRb phosphorylation by the cyclin D-dependent kinase, CDK4. Genes Dev., *7:* 331–342, 1993.
7. Weinberg, R. A. The retinoblastoma protein and cell cycle control. Cell, *81:* 323–330, 1995.
8. Motokura, T., Bloom, T., Kim, H. G., Juppner, H., Ruderman, J. V., Kronenberg, H. M., and Arnold, A. A novel cyclin encoded by a bcl-1 linked candidate oncogene. Nature (Lond.), *350:* 512–515, 1991.
9. Rosenberg, C. L., Wong, E., Pety, E. M., Bale, A. E., Tsujimoto, Y., Harris, N. L., and Arnold, A. PRAD1, a candidate BCL1 oncogene: mapping and expression in centrocytic lymphoma. Proc. Natl. Acad. Sci. USA, *88:* 9638–9642, 1991.
10. Marone, M., Scambia, G., Giannitelli, C., Ferrandina, G., Masciullo, V., Bellacosa, A., Benedetti-Panici, P., and Mancuso. S. Analysis of cyclin E and cdk2 in ovarian cancer: gene amplification and RNA overexpression. Int. J. Cancer, *75:* 34–39, 1998.
11. Steeg, P. S., and Zhou, Q. Cyclins and breast cancer. Breast Cancer Res. Treat., *52:* 17–28, 1998.
12. Wang, T. C., Cardiff, R. D., Zukerberg, L., Lees, E., Arnold, A., and Schmidt, E. V. Mammary hyperplasia and carcinoma in MMTV-cyclin D1 transgenic mice. Nature (Lond.), *369:* 669–671, 1994.
13. Ohtsubo, M., and Roberts, J. M. Cyclin-dependent regulation of G_1 in mammalian fibroblasts. Science (Washington DC), *259:* 1908–1912, 1993.
14. Resnitzky, D., and Reed, S. I. Different roles for cyclins D1 and E in regulation of the G_1-to-S transition. Mol. Cell. Biol., *15:* 3463–3469, 1995.
15. Keyomarsi, K., O'Leary, N., Molnar, G., Lees, E., Fingert, H. J., and Pardee, A. B. Cyclin E, a potential prognostic marker for breast cancer. Cancer Res., *54:* 380–385, 1994.
16. Keyomarsi, K., Conte, D., Toyofuku, W., and Fox, M. P. Deregulation of cyclin E in breast cancer. Oncogene, *11:* 941–950, 1995.
17. Lew, D. J., Dulic, V., and Reed, S. I. Isolation of three novel human cyclins by rescue of G_1 cyclin (cln) function in yeast. Cell, *66:* 1197–1206, 1991.
18. Dou, Q-P., Levin, A. H., Zhao, S., and Pardee, A. B. Cyclin E and cyclin A as candidates for the restriction point protein. Cancer Res., *53:* 1493–1497, 1993.
19. Koff, A., Giordano, A., Desia, D., Yamashita, K., Harper, J. W., Elledge, S. J., Nishomoto, T., Morgan, D. O., Franza, R., and Roberts, J. M. Formation and activation of a cyclin E-cdk2 complex during the G_1 phase of the human cell cycle. Science (Washington DC), *257:* 1689–1694, 1992.
20. Ohtsubo, M., Theodoras, A. M., Schumacher, J., Roberts, J. M., and Pagano, M. Human cyclin E, a nuclear protein essential for the G_1-to-S phase transition. Mol. Cell. Biol., *15:* 2612–2624, 1995.
21. Resnitzky, D. M. G., Bujard, H., and Reed, S. I. Acceleration of the G_1/S phase transition by expression of cyclins D1 and E with an inducible system. Mol. Cell. Biol., *14:* 1669–1679, 1994.
22. Dulic, V., Drullinger, L., Lees, E., Reed, S., and Stein, G. Altered regulation of G_1 cyclins in senescent human diploid fibroblasts: accumulation of inactive cyclin E-cdk2 and cyclin D1-cdk2 complexes. Proc. Natl. Acad. Sci. USA, *90:* 11034–11038, 1993.
23. Bremner, R., Cohen, B. L., Sopta, M., Hamel, P. A., Ingles, C. J., Gallie, B. L., and Phillips, R. A. Direct transcriptional repression by pRB and its reversal by specific cyclins. Mol. Cell. Biol., *15:* 3256–3265, 1995.
24. Richardson, H., O'Keefe, L. V., Marty, T., and Saint, R. Ectopic cyclin E expression induces premature entry into S phase and disrupts pattern formation in the *Drosophila* eye imaginal disc. Development (Camb.), *121:* 3371–3379, 1995.
25. Ohtani, K., DeGregori, J., and Nevins, J. R. Regulation of the cyclin E gene by transcription factor E2F1. Proc. Natl. Acad. Sci. USA, *92:* 12146–12150, 1995.
26. Geng ,Y., Eaton, E. N., Picon, M., Roberts, J. M., Lundberg, A. S., Gifford, A., Sardet, C., and Weinberg, R. A. Regulation of cyclin E transcription by E2Fs and retinoblastoma protein. Oncogene, *12:* 173–1180, 1996.
27. Keyomarsi, K., and Pardee, A. B. Redundant cyclin overexpression and gene amplification in breast cancer cells. Proc. Natl. Acad. Sci. USA, *90:* 1112–1116, 1993.
28. Buckley, M. F., Sweeney, K. J. E., Hamilton, J. A., Sini, R. L., Manning, D. L., Nicholson, R. I., deFazio, A., Watts, C. K. W., Musgrove, E. A., and Sutherland, R. L. Expression and amplification of cyclin genes in human breast cancer. Oncogene, *8:* 2127–2133, 1993.
29. Keyomarsi, K., and Herliczek, T. The role of cyclin E in cell proliferation, development and cancer. *In:* L. Meijer, S. Guidet, and M. Philippe, (eds.), Progress in Cell Cycle Research, Vol. 3, pp. 1–20. New York: Plenum Press, 1997.
30. Porter, P. L., Malone, K. E., Heagerty, P. J., Alexander, G. M., Gatti, L. A., Firpo, E. J., Daling, J. R., and Roberts, J. M. Expression of cell-cycle regulators p27 and cyclin E, alone and in combination, correlates with survival in young breast cancer patients. Nat. Med., *3:* 222–225, 1997.
31. Scott, K., and Walker, R. Lack of cyclin E immunoreactivity in non-malignant breast and association with proliferation in breast cancer. Br. J. Cancer, *76:* 1288–1292, 1997.
32. Nielsen, N. H., Arnerlov, C., Emdin, S. O., and Landberg, G. Cyclin E overexpression, a negative prognostic factor in breast cancer with strong correlation to oestrogen receptor status. Br. J. Cancer, *74:* 874–880, 1996.
33. Gray-Bablin, J., Zalvide, J., Fox, M. P., Knickerbocker, C. J., DeCaprio, J. A., and Keyomarsi, K. Cyclin E, a redundant cyclin in breast cancer. Proc. Natl. Acad. Sci. USA, *93:* 15215–15220, 1996.
34. Dou, Q-P., Pardee, A. B., and Keyomarsi, K. Cyclin E: a better prognostic marker for breast cancer than cyclin D? Nat. Med., *2:* 254, 1996.
35. Bortner, D. M., and Rosenberg, M. P. Induction of mammary gland hyperplasia and carcinomas in trangenic mice expressing human cyclin E. Mol. Cell. Biol., *17:* 453–459, 1996.
36. Sgambato, A., Doki, Y., Schieren, I., and Weinstein, I. B. Effects of cyclin E overexpression on cell growth and response to transforming growth factor β depend on cell context and $p27^{kip1}$ expression. Cell Growth Differ., *8:* 393–405, 1997.
37. Wang, A., Yoshimi, N., Suzui, M., Yamauchi, A., Tarao, M., and Mori, H. Different expression patterns of cyclins A, D1, and E in human colorectal cancer. J. Cancer Res. Clin. Oncol., *122:* 122–126, 1996.
38. Scuderi, R., Palucka, K. A., Pokrovskaja, K., Bjorkholm, M., Wiman, K. G., and Pisa, P. Cyclin E overexpression in relapsed adult acute lymphoblastic leukemias of B-cell lineage. Blood, *8:* 3360–3367, 1996.
39. Donnellan, R., and Chetty, R. Cyclin E in human cancers. FASEB J., *13:* 773–780, 1999.
40. Sewing, A., Ronicke, V., Burger, C., Funk, M., and Muller, R. Alternative splicing of human cyclin E. J. Cell Sci., *107:* 581–588, 1994.
41. Band, V., and Sager, R. Distinctive traits of normal and tumor-derived human mammary epithelial cells expressed in a medium that supports long-term growth of both cell types. Proc. Natl. Acad. Sci. USA, *86:* 1249–1253, 1989.
42. Rao, S., Lowe, M., Herliczek, T., and Keyomarsi, K. Lovastatin mediated G_1 arrest in normal and tumor breast cells in through inhibition of CDK2 activity and redistribution of p21 and p27, independent of p53. Oncogene, *17:* 2393–2402, 1998.
43. Lees, E., Faha, B., Dulic, V., Reed, S. I., and Harlow, E. Cyclin E/cdk2 and cyclin A/cdk2 kinases associate with p107 and E2F in a temporally distinct manner. Genes Dev., *6:* 1874–1885, 1992.
44. Won, K-A., and Reed, S. I. Activation of cyclin E/cdk2 is coupled to site-specific autophosphorylation and ubiquitin-dependent degradation of cyclin E. EMBO J., *15:* 4182–4193, 1996.
45. Clurman, B. E., Sheaff, R. J., Thress, K., Groudine, M., and Roberts, J. M. Turnover of cyclin E by the ubiquitin-proteosome pathway is regulated by cdk2 binding and cyclin phosphorylation. Genes Dev., *10:* 1979–1990, 1996.

---

[5] D. C. Porter, C. Danes, and R. H. Harwell. Elastase proteolysis of cyclin E in breast cancer cells, manuscript in preparation.

Lovastatin mediated G1 arrest in normal and tumor breast cells is through inhibition of CDK2 activity and redistribution of p21 and p27, independent of p53

Sharmila Rao[1], Michael Lowe[1], Thaddeus W Herliczek[1] and Khandan Keyomarsi[1,2]

[1]Laboratory of Diagnostic Oncology, Division of Molecular Medicine, Wadsworth Center, Albany, New York 12201-0509;
[2]Department of Biomedical Sciences, State University of New York, Albany, New York 12222, USA

Previously, we reported that lovastatin, a potent inhibitor of the enzyme HMG CoA reductase also acts as an antimitogenic agent by arresting cells in the G1 phase of the cell cycle resulting in cell cycle-independent alteration of cyclin dependent kinase inhibitors (CKIs). In the present study we have investigated the nature of the CKIs (p21 and p27) alterations resulting in G1 arrest in both normal and tumor breast cell lines by lovastatin. We show that even though lovastatin treatment causes G1 arrest in a wide variety of normal and tumor breast cells irrespective of their p53 or pRb status, the p21 and p27 protein levels are not increased in all cell lines treated suggesting that the increase in p21 and p27 protein expression per se is not necessary for lovastatin mediated G1 arrest. However, the binding of p21 and p27 to CDK2 increases significantly following treatment of cells with lovastatin leading to inhibition of CDK2 activity and a subsequent arrest of cells in G1. The increased CKI binding to CDK2 is achieved by the redistribution of both p21 and p27 from CDK4 to CDK2 complexes subsequent to decreases in CDK4 and cyclin D3 expression following lovastatin treatment. Lastly, we show that lovastatin treatment of 76N-E6 breast cell line with an altered p53 pathway also results in G1 arrest and similar redistribution of CKIs from CDK4 to CDK2 as observed in other breast cell lines examined. These observations suggest that lovastatin induced G1 arrest of breast cell lines is through a p53 independent pathway and is mediated by decreased CDK2 activity through redistribution of CKIs from CDK4 to CDK2.

Keywords: lovastatin; cell cycle; cyclins; CKIs; CDKs; adaptor molecule

Introduction

The mammalian cell cycle, defined as a sequence of events between two cell divisions, is positively regulated by cyclins and cyclin dependent kinases (CDKs) which associate to form hetrodimeric complexes (Sherr, 1994, 1996; Elledge et al., 1996; Nasmyth, 1996). Mitogenic stimuli results in the phosphorylation and thereby activation of cyclin-CDK complexes by CDK activating kinase, CAK (Fisher and Morgan, 1994; Makela et al., 1994; Harper and Elledge, 1998). The activated

cyclin/CDK complexes in turn sequentially phosphorylate substrates such as the retinoblastoma protein (pRb) throughout the cell cycle (Ewen et al., 1993a; Matsushime et al., 1994; Sherr, 1996). Phosphorylation of pRb which is necessary for the progression through G1 is regulated primarily by cyclin D/CDK4/CDK6 complexes while the cyclin E/CDK2 complex regulates the passage of cells from late G1 to S phase and further contribute to pRb hyper-phosphorylation (Sherr, 1994, 1996; Bartek et al., 1997). The hypophosphorylated pRb serves as a tumor suppressor by interacting with and inhibiting cellular proteins such as E2F-DP heterodimeric transcription factors which activate many genes required for DNA replication pivotal for G1/S transition (Weinberg, 1995; Bartek et al., 1996, 1997; Ikeda et al., 1996). The complete hyperphosphorylation of pRb by cyclin E/CDK2 complexes and consequent activation of E2F-DP transcription complex are thought to play a major role in overcoming of the restriction point (Pardee, 1989; Planas-Silva and Weinberg, 1997b).

Progression through the cell cycle and the restriction point is also negatively regulated through the association with CDK inhibitors, CKIs (Elledge and Harper, 1994; Sherr and Roberts, 1995; Harper and Elledge, 1996; Harper, 1997). There are two families of structurally distinct CKIs, the CIP/KIP family which inhibit a broad range of CDKs by selectively binding and inhibiting the fully associated cyclin/CDK complexes and the INK family which bind specifically to CDK4 and/or CDK6 and inhibit complex formation with cyclin D (Elledge et al., 1996; Sherr, 1996; Harper, 1997). The CKI p21 (CIP1/ WAF1), the first mammalian CKI to be identified was simultaneously characterized by several laboratories as the major p53 inducible gene (WAF1) (El-Deiry et al., 1993) as a CDK inhibitor protein (CIP1, p21 and p20CAP1) (Gu et al., 1993; Harper et al., 1993; Xiong et al., 1993) as a protein highly expressed in senescent fibroblasts (SDI) (Noda et al., 1994), and as a melanoma differentiation associated gene (mda 6) (Jiang and Fisher, 1993). p27 (KIP1), similar in amino acid sequence and inhibitory specificity to p21, was identified as a protein associated with inactive cyclin E/CDK2 complexes in TGF-β1 treated and contact inhibited cells (Polyak et al., 1994a,b), as a protein that interacts with cyclin D1/CDK4 complexes (Toyoshima and Hunter, 1994), and in cells arrested in G1 (Hengst et al., 1994). Although p21 is induced by p53 in response to DNA damage resulting in CDK inhibition and G1 growth arrest (Dulic et al., 1994), it can also be induced by p53

independent mechanisms; by serum, PDGF and EGF in embryonic fibroblasts from p53 knockout mice (Michieli et al., 1994), by serum starvation in p53 mutant human breast carcinoma cells (Sheikh et al., 1994), by EGF in squamous carcinoma cells (Jakus and Yeudall, 1996), by TGF-β1 in p53 mutant cells (Elbendary et al., 1994; Datto et al., 1995; Reynisdottir et al., 1995) and by lovastatin in breast cancer cells (Gray-Bablin et al., 1997). p27 is similarly induced by lovastatin (Hengst et al., 1994; Hengst and Reed, 1996; Gray-Bablin et al., 1997), by TGF-β1 (Polyak et al., 1994a), following cell to cell contact inhibition, by rapamycin and by agents that induce cAMP mediated growth arrest (Kato et al., 1994; Nourse et al., 1994; Polyak et al., 1994b; Toyoshima and Hunter, 1994). Hence, p21 and p27 may function similarly to inhibit CDK activity and proliferation in response to different environmental stimuli. Furthermore, removal by degradation/inactivation of p27 may be necessary for proliferation (Pagano et al., 1995).

We and others have previously reported that treatment of mammary epithelial cells or HeLa cells by lovastatin results in the induction of p21 and p27 in mammary cells (Gray-Bablin et al., 1997) and p27 in HeLa cells (Hengst et al., 1994; Hengst and Reed, 1996). Lovastatin is an inhibitor of HMG COA reductase which is the rate limiting enzyme of the cholesterol biosynthesis pathway (Alberts et al., 1980). Though lovastatin has been primarily prescribed for patients with high cholesterol levels (Rettersol et al., 1996) it has also been used as an effective agent in cell synchronization for both tumor and normal cells (Keyomarsi et al., 1991; Keyomarsi, 1996). The inhibition of the cholesterol biosynthesis pathway by lovastatin not only blocks mevalonate synthesis (the product of HMG COA reductase) but also prevents the farnesylation and geranylgeranylation (intermediate products of the cholesterol pathway) of several signal transduction proteins such as Ras, Rap and many G proteins, thereby preventing their proper intracellular localization and function (Goldstein and Brown, 1990; Maltese, 1990). The induction of p21 and p27 by lovastatin in breast cancer cells seems to be independent of the Ras pathway (Keyomarsi et al., 1991). Furthermore, the lovastatin mediated CKI induction is also through cell cycle independent mechanisms, distinct from other G1 arresting agents/ conditions such as serum starvation or double thymidine block (Gray-Bablin et al., 1997).

In this study, we have investigated the nature of induction of p21 and p27 by lovastatin in both normal and tumor-derived mammary epithelial cells. We show that lovastatin is capable of inducing G1 arrest in both normal and tumor breast cells. Furthermore, we provide evidence that it is not the increase in protein levels of the p21 and p27 per se, but the increase in binding of both p21 and p27 to CDK2 complexes and the resulting decrease in activity of cyclin/CDK2 complexes that is essential for lovastatin mediated G1 arrest of normal and tumor cells. We also show that the increased binding of CKIs to CDK2 correlates with decreased CDK4 and cyclin D3 levels and the subsequent release of p21 and p27 from the cyclin D/ CDK4 complex, providing evidence for the redistribution of both p21 and p27 under physiological conditions in vivo. Lastly, we show that binding of CKIs to CDK2 or the switching of partners from CDK4 to CDK2 following lovastatin treatment is through a p53 independent pathway.

Results

Lovastatin synchronizes a broad range of tumor and normal breast cancer cells

In order to determine whether lovastatin would have a differential affect of G1 mediated arrest of normal versus tumor breast cells, three normal and six tumor cell lines were treated with lovastatin at the same dose of duration (i.e. 40 μM for 36 h) (Table 1). The normal cells examined were 76N and 70N (both mortal) and MCF-10A (immortalized). The tumor cells used were classified on their ability to express tumor suppressor genes p53, pRb and estrogen receptor (ER). The ER positive tumor cells are MCF-7, ZR75T, and T47D and the ER negative tumor cells are MDA-MB-157, MDA-MB-231 and Hs578T. In the ER positive group all 3 tumor cell lines are also wild type for pRb and p53, except for T47D, which has a p53 mutant phenotype. In the ER negative group all three tumor cell lines are negative for p53 and pRb except for MDA-MB-157 which has a wild type pRb. However, the pRb in these cells is expressed at very low levels (see Figure 1) and is inactive because of high levels of p16 and overexpression of cyclin E (Keyomarsi et al., 1995). p16 has been shown to transcriptionally down regulate pRb expression (Fang et al., 1998) while the overexpression of cyclin E results in constitutive hyperphosphorylation of pRb rendering it inactive as a tumor-suppressor (Gray-Bablin et al., 1996). In the case of Hs578T, it too is pRb negative as published

Table 1 Cell cycle profiles of lovastatin treated normal and tumor (RB and p53 positive and negative) breast cells

Cell lines	Lovastatin, 40 μM h	ER	p53	pRb	%G1	%S	%G2
76N	0	−	+	+	56.6	12.1	31.3
	36				72	1.2	27
MCF-10A	0	−	+	+	65	12	23
	36				90	1.6	8.4
70N	0	−	+	+	60	13	27
	36				78	1.2	21
MCF-7	0	+	+	+	77	11	12
	36				82	4	14
ZR75T	0	+	+	+	67	19	14
	36				85	6	9
T47D	0	+	−	+	73	13	14
	36				86	4	10
Hs578T	0	−	−	−	62	16	20
	36				83	5	12
MDA-MB-157	0	−	−	±	55	12	32
	36				60	4.3	36
MDA-MB-231	0	−	−	−	54	22	24
	36				80	7	13

Estrogen Receptor (ER), p53 and pRb status of cell lines were determined previously (Gray-Bablin et al., 1996, and references within). + indicates wild-type, − indicates mutant or deleted, $\pm$ indicates wild-type but functionally inactive (see text). Percentages of cells in different phases of the cell cycle for each cell line following lovastatin treatment were obtained from flow cytometric measurements of DNA contents from three separate experiments and the average of the values are indicated

previously (Gray-Bablin *et al.*, 1996). In this cell line the pRb protein, although expressed at very low levels (Figure 1), is highly susceptible to degradation (data not shown). Therefore, Hs578T, MDA-MB-231 and MDA-MB-157 cell lines are considered functionally pRb negative as we previously described (Gray-Bablin *et al.*, 1996).

These studies revealed that lovastatin treatment for 36 h resulted in G1 arrest in both tumor and normal cell lines irrespective of their p53, pRb, or ER status (Table 1). However, the percent S phase decrease may be dependent on the expression of the aforementioned proteins. For example, treatment of normal breast epithelial cells with lovastatin resulted in the largest S phase decrease (89% drop from untreated cells) while the S phase in p53/pRb/ER positive or negative cells dropped by 68% from the untreated controls. Furthermore, no changes in cell cycle distribution were observed after 36 h in untreated control cultures (data not shown). These observations suggest that although lovastatin is capable of arresting both normal and tumor cells in G1, the degree of synchronization is more profound in normal cells. Next, we examined the pattern of expression of key cell cycle regulators in these three classes of cell lines following treatment of cells with lovastatin (Figure 1).

Lovastatin treatment causes a decrease in the levels of CDK4 and cyclin D3 in both normal and tumor cells

To determine which key cell cycle regulators were required for lovastatin mediated G1 arrest, we examined the expression of several positive and negative cell cycle proteins in both normal and tumor cells. A subset of the cell lines from Table 1 consisting of two normal cell lines, 76N and MCF-10A, two tumor cell lines which are p53, pRb and ER positive, MCF-7, ZR75T and two tumor cell lines which are p53, pRb and ER negative, Hs578T and MDA-MB-157 cell lines were analysed. The 76N and MCF-10A cells were chosen as they represented normal cells obtained from two different lineages, 76N cell lines are normal mortal cells obtained from reduction mammoplasty while MCF-10A cell lines were immortalized from normal breast epithelial cell strain, MCF-10, after cultivation in medium containing low calcium concentrations (Soule *et al.*, 1990).

All cells within each category were treated with 40 μM lovastatin for 36 h and at the indicated times following treatment, cells were harvested and subjected to Western blot analysis with antibodies to p27, p21, p16, pRb, p53, CDK2, CDK4, cyclin D1 and cyclin D3 (Figure 1). These analyses revealed that the total protein levels of p21 and p27 were induced significantly only in the cells with pRb/p53/ER negative status suggesting that lovastatin causes an induction of these CKI's through a p53 independent mechanism. In p53 and pRb positive cells (MCF-7 and ZR75T) the basal levels of p21 and p27 were very high and no subsequent increase in these CKI's were seen when examining total protein levels. Normal cells on the other hand show an increase in p27 but a decrease in p21 following lovastatin treatment. The p27 levels accumulate by sixfold in MCF-10A cells and 2.5-fold in 76N cells reproducibly. INK CKI, p16 was expressed only in MDA-MB-
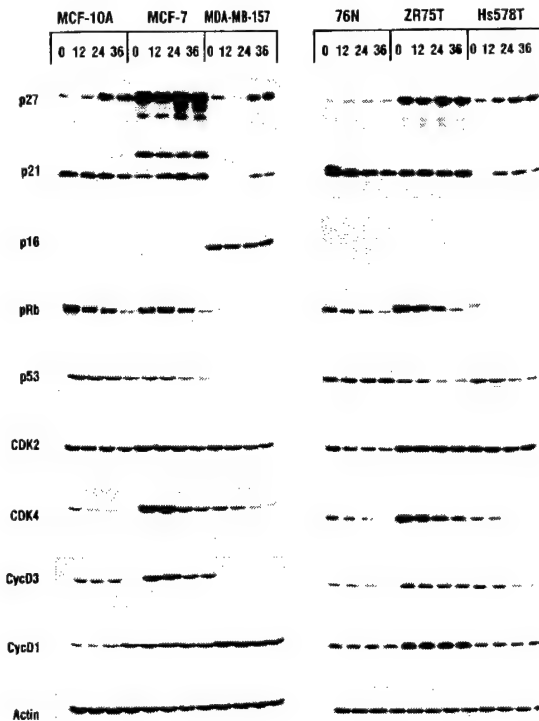
Figure 1 Expression of positive and negative cell cycle regulators in normal and tumor breast cells following lovastatin treatment. All cells were cultured in medium containing 40 μM lovastatin. At the indicated times following treatment cells were harvested, cell lysates prepared and subjected to Western blot analysis: 50 μg of protein extract from each condition was analysed by Western blot analysis with the indicated antibodies or actin used for equal loading. The blots were developed by chemiluminescence reagents. The same blots were sequentially hybridized with different antibodies (see Materials and methods). The blots were stripped between the antibodies in 100 mM 2-mercaptoethanol, 62.5 mM Tris-HCl (pH 6.8), and 2% SDS for 10 min at 55°C

157 cells and its levels did not change following lovastatin treatment.

The levels of p53 and pRb tumor suppressor protein decreased in both normal and ER/p53/pRb positive tumor cell lines. The simultaneous decrease in p53 and p21 in normal cells suggest that in normal cells p21 expression may be strongly influenced by p53. A similar decrease in p21 is not noticed in p53 positive tumor cell lines (MCF-7 and ZR75T) even though p53 levels decreased, suggesting that the p53-p21 pathway in these tumor cell lines is not as tightly controlled as seen in normal. Analysis of cyclins and CDKs revealed that following lovastatin treatment CDK4 and cyclin D3 protein levels decreased in all cell lines while cyclin D1 and CDK2 levels remained relatively unchanged. Collectively these results reveal that the only cell cycle regulators which consistently decrease in response to lovastatin are CDK4 and cyclin D3. Furthermore, the increases of p21 and p27 at the protein levels were only apparent in ER/p53/pRb negative cell tumor cell lines and were not universally observed in lovastatin induced G1 arrest which occurred in all cells regardless of their p53 or pRb status (Table 1). Lastly, the arrest of MDA-MB 157 and Hs578T cells which are p53 and pRb negative implies that the activity of the tumor

suppressors is not required for lovastatin mediated G1 arrest. This analysis raised the question if and how p21 and p27 could play a role in lovastatin mediated G1 arrest and how the decrease in the CDK4 and cyclin D3 in response to lovastatin could contribute to this arrest?

Inactive cyclin CDK2 complexes in lovastatin treated cells are due to increased p21 and p27 binding

A likely explanation for lovastatin mediated G1 arrest in the different cell types is that lovastatin treatment of cells results in the inhibition of CDK2 activity which is necessary for cells to overcome the restriction point in the G1 phase of the cell cycle. In order to examine the kinase activity associated with CDK2 in normal and tumor cells, we measured the phosphorylation of histone H1 in immunoprecipitates prepared from lovastatin treated cells using an antibody to CDK2 (Figure 2a). This analysis revealed that treatment of all cells by lovastatin resulted in a rapid decrease of CDK2 activity and by 36 h, the time when G1 arrest fully manifests itself in cells, the level of CDK2 activity reaches its nadir in all cells examined. These data suggest that lovastatin mediated G1 arrest results in lowered CDK2 activity in all cells regardless their p53, pRb, normal or tumor status.

To determine if the decreased activity of the CDK2 is due to its association with CKIs, a two step experiment consisting of an immunoprecipitation with anti-CDK2 antibody followed by Western blot analysis with p21 or p27 was performed (Figure 2b). These analyses revealed that the decreased CDK2 activity observed (Figure 2a) was concomitant with increased binding of p27 to CDK2 in all normal and tumor cell lines treated with lovastatin. Furthermore, all tumor cell lines treated with lovastatin exhibited increased binding of p21 to CDK2 as well. In normal cells however, not only were the p21 total protein levels decreased by lovastatin treatment (Figure 1), but the binding of p21 to CDK2 also decreased (Figure 2b), despite complete inhibition of the CDK2 activity (Figure 2a). Collectively these results suggest that the G1 arrest induced by lovastatin is concomitant with decreased activity of CDK2 mediated by increased binding of p27 (in all cells) and p21 (only in tumor cells) to CDK2. Interestingly, MCF-7 and ZR75T which exhibited no increases in p21 or p27 expression (Figure 1) revealed a clear increase in binding of both these CKIs to CDK2 (Figure 2b). These observations raise the question that if the total levels of p21 and p27 are not induced by lovastatin (Figure 1) what accounts for the increased binding of these inhibitors to CDK2 in MCF-7 and ZR75T cells (Figure 2b)?

Lovastatin treatment causes the CKIs to switch from binding to CDK4 to CDK2

It has been proposed that cyclin D/CDK4 complexes play a critical role in titrating p21 and p27 by binding to them, resulting in decreased amounts of p21 and p27 which would otherwise bind to and inhibit cyclin/CDK2 complex activity (LaBaer et al., 1997). At low concentrations, the binding of p21 and p27 to CDK4 will not inhibit cyclin D/CDK4 activity but rather promote efficient binding of cyclin D with CDK4, and
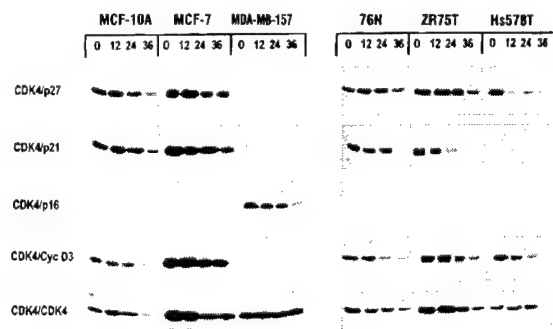
Time, hours of Lovastatin Treatment
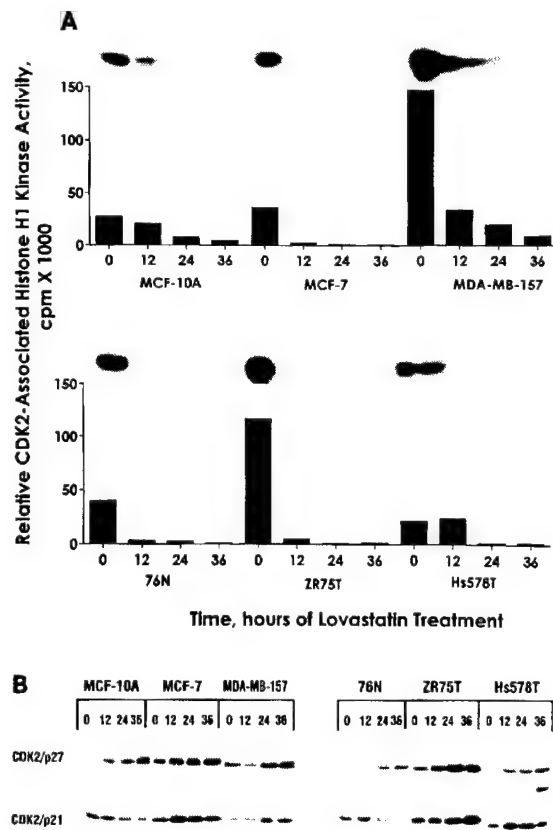
Figure 2 Lovastatin treatment reduces CDK2 activity by increased p21 and p27 binding. All cells were cultured in medium containing 40 μM lovastatin. At the indicated times following treatment cells were harvested, cell lysates prepared and subjected to (**a**) Histone H1 kinase analysis or (**b**) Immune-complex formation. For kinase activity, equal amounts of protein (300 μg) from cell lysates were prepared from each cell line at the indicated times following lovastatin treatment and immunoprecipitated with anti-CDK2 antibody (polyclonal) coupled to protein A beads using histone H1 as substrate. For each cell line we show the resulting autoradiogram of the histone H1 SDS–PAGE and the quantitation of the histone H1 associated kinase activities by scintillation counting. For immunoprecipitation followed by Western blot analysis, equal amounts of protein (300 μg) from cell lysate prepared from each cell lines were immunoprecipitated with anti-CDK2 (polyclonal) coupled to protein A beads and the immunoprecipitates were subjected to Western blot analysis with the indicated antibodies

as such function as adaptor molecules (LaBaer et al., 1997). Since lovastatin causes the synchronization of cells apparently by increasing binding of p21 (tumor cells) and p27 (normal and tumor cells) to CDK2 complexes, it can be hypothesized that this increased binding of CKI's to CDK2 may be due to the switching of the CKI's from CDK4 to CDK2, mediated by lovastatin. To test this hypothesis and to examine this adaptor molecule theory we examined the association of p21 and p27 to CDK4 following lovastatin treatment (Figure 3). Our results clearly demonstrate that in untreated normal and ER/p53/pRb positive tumor cells, p21 and p27 bind to CDK4, and upon treatment with lovastatin, both p21 and p27 are released from CDK4 in a time dependent fashion (Figure 3) which corresponds to their binding (i.e.

switching partners) to CDK2 (Figure 2b). The apparent increase in p27 levels observed in 76N cells following lovastatin treatment seems to be the primary event leading to CDK2 inactivation; primary to redistribution of p27 from CDK4 to CDK2. However, in MCF-7 and ZR75T cells, where no detectable increase in the levels of p21 and p27 following lovastatin treatment is observed, the switching of these CKIs from CDK4 to CDK2 occurs concomitantly with decrease in CDK2 activity, suggesting that in these ER/p53/pRb positive tumor cells the p21 and p27 switch from CDK4 to CDK2 is the primary event leading to CDK2 inactivation. In both sets of cell lines we show that lovastatin creates a signal for these CKIs to switch partners from CDK4 to CDK2 and such switching of partners is concurrent with G1 arrest. The signal that initiates the switching may be the decrease in CDK4 and cyclin D3 protein levels observed in all cells examined following treatment with lovastatin (Figure 1).

The p53/pRb/ER negative tumor cell lines reveal a different pattern of CKI/CDK4 binding than either the normal cells or the p53/pRb/ER positive tumor cell lines (Figure 3). MDA-MB-157 cells which have very low levels of p21 and p27 show no binding of these proteins to CDK4. In fact CDK4 is bound to p16 which is expressed in high quantities in this cell line and can titrate and thus prevent any CDK4 complex formation with p21 or p27. In the Hs578T cell line which do not express detectable p16 levels, CDK4 is not titrated and binds only to p27 in untreated cells and treatment of cells with lovastatin decreases the binding of p27 to CDK4. Collectively, these observations support the validity of the adaptor molecule theory where p21 and p27 switch partners from CDK4 to CDK2 specifically for ER/p53/pRb positive cells which have endogenously high levels of p21 and p27. Furthermore, the decreased binding of the CKIs to CDK4 also suggest that lovastatin affects the cellular pathways that provide the switching signal for CKIs to redistribute from cyclin/CDK4 complex to cyclin/CDK2 complexes.

CDK2 is completely sequestered by p21 and p27 following lovastatin treatment

To determine whether the increased binding of p21 and p27 to CDK2 is sufficient to inactivate CDK2, we examined the proportion of CDK2 bound to p21 and p27 following lovastatin treatment. For these experiments MCF-7 and ZR75T cell lines were chosen as the basal levels p21 and p27 are very high in these cell lines (Figure 1) and treatment with lovastatin results in increased binding of both CKIs to CDK2 (Figure 2). To evaluate the proportion of CDK2 in complex with p21 and p27 we immunodepleted cell extracts with anti-p21 and anti-p27 antibodies. These extracts were prepared from both cell lines before and after lovastatin treatment. Following immunodepletion, the final supernatant was subjected to Western blot analysis with antibodies to p21, p27, CDK2, CDK4 and actin (Figure 4). These results revealed that upon immunodepletion of cells of p21 and p27, there is little or no CDK2 present following lovastatin treatment. CDK4 levels were also not detectable following p21 and p27 immunodepletion in lovastatin treated cells (Figure 4) partly due to the decrease in total CDK4


Figure 3 Redistribution of p21 and p27 from CDK4 to CDK2 following lovastatin treatment. All cells were cultured in medium containing 40 μM lovastatin. At the indicated times following treatment cells were harvested, cell lysates prepared and subjected to Immune-complex formation. Equal amounts of protein (300 μg) from cell lysate prepared from each cell line was immunoprecipitated with anti-CDK4 (polyclonal) coupled to protein A beads and the immunoprecipitates were subjected to Western blot analysis with the indicated antibodies

Figure 4 Immunodepletion of p21 and p27 in lovastatin treated cells also depletes the cells of CDK2. Cells were cultured in medium 40 μM lovastatin for 0 and 36 h. Following treatment cells were harvested, cell extracts prepared and immunodepleted with antibodies against p21 and p27. Following three rounds of immunodepletion with anti-p21 and anti-p27 coupled to protein A beads, or protein A beads alone, the remaining supernatant (50 μg/lane) were subjected to Western blot analysis with the indicated antibodies

2398

levels following treatment (Figure 1). Hence, upon lovastatin treatment, CDK4 levels decrease, p21 and p27 levels do not change yet their binding to CDK2 increase, and CDK2 activity greatly declines. Furthermore lovastatin results in sequestering of CDK2 by these CKIs suggesting that p21 and p27 alone will inhibit CDK2 activity. These observations also suggest that the amounts of p21 and p27 released from CDK4 complexes in lovastatin treated cells is sufficient to block the CDK2 activity in these cells.

Lovastatin mediated G1 arrest is through a p53 independent pathway

To directly examine the role of p53 in the G1 arrest induced by lovastatin in breast epithelial cells, we investigated perturbation of the cell cycle by lovastatin in 76N cells transformed by the human papilloma virus E6 (76N-E6) (Band et al., 1991). Initially, we examined the expression of key cell cycle regulatory proteins in 76N-E6 as compared to 76N parental cell line (Figure 5b, right panel). This analysis showed that aside from lack of expression of p53 and p21 in 76N-E6 cell line, the other cell cycle regulatory proteins are similarly expressed between 76N-E6 and the parental 76N cells. Next, to examine the effects of lovastatin on 76N-E6 cells we treated them with 40 μM lovastatin for 36 h. Such treatment resulted in a G1 arrest of 76N-E6 cells despite the absence of p53 (Figure 5a). At the indicated times following treatment, cells were harvested and subjected to Western blot analysis with antibodies to key cell cycle regulators (Figure 5b). These analyses reveal that as expected the cells did not express any p53 due to its rapid degradation by the transfected E6 oncogene. However, both p27 and p21 levels were induced following lovastatin treatment (Figure 5b) which is unlike what was observed in the 76N parental p53 wild-type cells (Figure 1) or HeLa cells where only p27 was shown to be induced by lovastatin (Hengst et al., 1994; Hengst and Reed, 1996). These results suggest that the elimination of p53 in 76N-E6 cells results in induction of p21 by lovastatin through a p53 independent mechanism and that p53 expression is not critical for lovastatin mediated G1 arrest.

All the other cell cycle regulatory proteins examined in 76N-E6 cells revealed a similar pattern of alteration following lovastatin treatment as observed in normal 76N cells (Figure 1); i.e. the expression of hyperphosphorylated pRb, CDK4 and cyclin D3 decreased rapidly and significantly in response to lovastatin while the levels of CDK2 and cyclin D1 remain relatively unchanged (Figure 5b). Similarly, CDK2 activity also decreased profoundly in 76N-E6 cells following lovastatin treatment and G1 arrest (Figure 5c). We also examined the association of p21 and p27 with CDK2 following lovastatin treatment and found that the binding of both p21 and p27 to CDK2 increased significantly during the course of lovastatin treatment, suggesting that p21 and p27 are indeed acting as inhibitors of CDK2 leading to G1 arrest in 76N-E6 cells independent of p53 (Figure 5d). Lastly, we examined the association of p21 and p27 with CDK4 following lovastatin treatment and found that in untreated 76N-E6 cells both p21 and p27 bind to CDK4 only to redistribute from CDK4 to CDK2 upon treatment with lovastatin (Figure 5e). These results
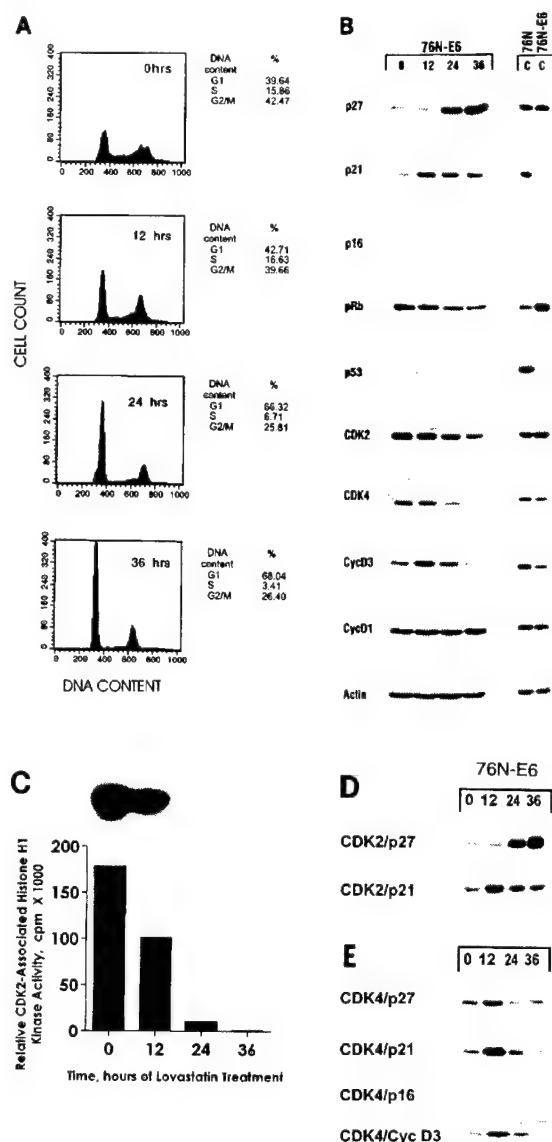
Figure 5 Induction of CKIs in 76N-E6 cells following lovastatin mediated GI arrest. 76N-E6 cells treated with 40 μM lovastatin. At the indicated times following treatment cells were harvested and subjected to (a) Flow cytometry. Percentages of cells in different phases of the cell cycle for 76N-E6 were determined from flow cytometric measurements of DNA content. (b) Western blot analysis. Fifty μg of protein extracts from each condition was analysed by Western blot analysis with the indicated antibodies or actin used for equal loading and the blots were developed using the chemiluminescence reagents. The right panel shows Western blot analysis using cell extracts from untreated 76N parental and 76N-E6 cell lines on the same blot with identical exposure times. (c) Histone H1 kinase analysis. Equal amounts of protein (300 μg) from cell lysates were prepared at the indicated times following lovastatin treatment and immunoprecipitated with anti-CDK2 antibody (polyclonal) coupled to protein A beads using histone H1 as substrate. The autoradiogram of the histone H1 SDS–PAGE and the quantitation of the histone H1 associated kinase activities by scintillation counting are presented. (d) CDK2 Immune-complex formation and (e) CDK4 Immuno-complex formation. For immunoprecipitation followed by Western blot analysis, equal amounts of protein (300 μg) from cell lysates prepared from lovastatin treated cells were immunoprecipitated with anti-CDK2 (polyclonal) (d) or anti-CDK4 (polyclonal) (e) coupled to protein A beads and the immunoprecipitates were subjected to Western blot analysis with the indicated antibodies

suggest that the lovastatin mediated G1 arrest in 76N-E6 cells, the concomitant decrease in CDK2 activity, the increased expression of p21 and p27, the increased association of these CKIs to CDK2, and lastly the redistribution of CKIs from CDK4 to CDK2 are all independent of p53.

Discussion

The outcome of CKI induction in most cells is the cessation of cell proliferation, differentiation or even cell death. In tumor cells the regulation of the CKIs is altered leading to either lack of function, or expression. Hence, if the CKIs could be induced consistently in tumor cells, and their induction lead to G1 arrest the goal of controlling the proliferation of cancer cells could be achieved. As shown in this study we observe that lovastatin can cease cell proliferation in a wide variety of normal and tumor breast cells, independent of their p53, pRb or ER status. We also provide evidence that it is not the increase in the levels of the CKIs per se but the increased binding of p21 and p27 to CDK2 and the consequent reduction of CDK2 activity that is actually responsible for the G1 arrest caused by lovastatin in both normal and tumor breast cell lines. The increased binding of CKIs to CDK2 is through a p53 independent pathway. Our results also reveal that lovastatin like other growth arresting agents such as TGF-β (Reynisdottir and Massague, 1997) use the switching of CKI from CDK4 complex to CDK2 as a method to initiate growth arrest.

Redistribution of both p21 and p27 from CDK4 complexes to CDK2 complexes following lovastatin treatment

Recently a new functional role has been assigned to p21 and p27, that of facilitating cyclin D/CDK4 assembly *in vitro* or acting as adaptor molecules (Poon *et al.*, 1995; LaBaer *et al.*, 1997; Planas-Silva and Weinberg, 1997a; Prall *et al.*, 1997). Adaptor molecules facilitate the association or complex formation between proteins without hindering in the function of the complex. Both *in vitro* studies using purified p21, p27 or p57 (KIP2) and *in vivo* studies using cells transiently transfected with p21, CDK4 and cyclin D1, showed an abundance of assembled CDK4/cyclin D1 complex which increased directly with increasing inhibitor levels. In fact, the addition of p21, p27 and p57 were able to promote assembly of the cyclin CDK4 complexes by 35–80-fold without inhibiting the activity of the complex (LaBaer *et al.*, 1997). Hence, at low concentrations p21 and p27 can act as adaptor molecules, facilitate the binding of cyclin D/CDK4 complexes, promote the phosphorylation of pRb and progression through G1, while at higher concentrations, the CKIs can switch partners bind to CDK2 and inhibit cell cycle progression. Similarly, other studies examining the effect of estrogen on the cell cycle of ER positive MCF-7 cells revealed that the addition of β-estradiol or estrogen were able to rescue synchronized cells and induce progression through the cell cycle by increasing the level of cyclin D and increased binding of p21 and p27 to the cyclin D/CDK4 complexes from the cyclin E/CDK2 complexes (Planas-Silva and Weinberg, 1997a;

Prall *et al.*, 1997). This redistribution of p21 caused a marked induction of the cyclin E/CDK2 kinase activity. Similarly, studies with the growth inhibitor TGF-β also showed redistribution of the cyclin kinase inhibitors, i.e. CKIs switch from CDK4 to CDK2 in response to growth inhibitory activity of TGF-β. In addition TGF-β resulted in the reduced synthesis of CDK4 and cyclin D leading to the subsequent dissociation of cyclin D/CDK4 complexes and redistribution of p27 from cyclin D/CDK4 complex to cyclin E/CDK2 leading to a G1 arrest (Ewen *et al.*, 1993b). Subsequent studies have suggested that the redistribution of p27 following TGF-β treatment was due to the increased binding of p15 to cyclin D/CDK4 complexes in Mink Lung cells (Reynisdottir *et al.*, 1995; Reynisdottir and Massague, 1997). It therefore has been proposed that cyclin D/CDK4 complexes apart from phosphorylating pRb, titer the p21 and p27 in the cells and hence prevent the binding of the CKIs to cyclin/CDK2 complexes.

In the present study we also observe that treatment of cells with lovastatin induce a cascade of events leading to cessation of cell proliferation through the redistribution of the CKIs from cyclin D/CDK4 complexes to cyclin E/CDK2 complexes. We observed that lovastatin treatment of all cells examined, normal or tumor caused a reduced synthesis of both cyclin D3 and CDK4 but not cyclin D1. A similar decrease in CDK4 and cyclin D3 but not D1 was seen in retinoic acid arrested MCF-7 cell (Zhu *et al.*, 1997) and glucocorticoids arrested U2OS and SAOS2 cells (Rogatsky *et al.*, 1997) suggesting that the rapid reduction in cyclin D3 or CDK4 levels may be the key signal for redistribution of the CKIs. In the present study we observed that the CKI binding to CDK4 complexes reduced rapidly and significantly following lovastatin treatment (Figure 4). This reduction was seen in both normal and ER/p53/pRb positive tumor cell lines. Hence, the redistribution of both p21 and p27 from CDK4 complexes to CDK2 complexes, apparently signaled by a decrease in the expression of CDK4 and cyclin D3, leads to G1 arrest caused by lovastatin treatment. This switching also explains the increased binding of the CKI's to CDK2 complexes that is observed in ER/p53/pRb positive cells (Figure 2) without the corresponding increase in CKI levels, as these cell lines have a high basal levels of these CKIs (Figure 1). The high levels of both CKIs could be attributed to increase cyclin D/CDK4 activity required to phosphorylate pRb in these cells and thereby giving these tumor cells a growth advantage. We also show that when cell extracts prepared from lovastatin treated cultures of ER/p53/pRb positive tumor cell lines (i.e. MCF-7 and ZR75T) are immunodepleted of both p21 and p27, there is little to no CDK2 or CDK4 left in the final supernatant. These results suggest that CDK2 is completely sequestered by p21 and p27 following lovastatin treatment in the absence of any CKI accumulation. Furthermore, the amounts of p21 and p27 released from CDK4 complexes which then associate with CDK2 complexes in lovastatin treated cells are sufficient to block the CDK2 activity in these cells.

Lovastatin mediated G1 arrest is p53 independent

In this study we analysed the effect of lovastatin on a broad range of breast cells, normal and tumor with

different p53 status. We found that whether a cell is p53 wild-type or mutant the effect of lovastatin was the same in all cells and resulted in G1 arrest suggesting that the p53 pathway is not involved in the G1 arrest induced by lovastatin. We observed this p53 independence under three different conditions. First, the protein levels and CDK2 binding of p21 and p27 in p53/Rb negative cells, (MDA-MB 157 and Hs578T) increased dramatically following lovastatin treatment, resulting in the G1 arrest of these cells. MDA-MB-157 is null for p53 while Hs578T harbors a mutant p53. Hence, the increase in p21 levels following lovastatin treatment in these cells is independent of p53. Secondly, MCF-7 and ZR75T cells which are p53 and pRb positive tumor cells showed a decrease in p53 levels following treatment with lovastatin (Figure 1) even though the binding of p21 and p27 to CDK2 increased resulting in inhibition of CDK2 activity and subsequent G1 arrest (Figure 2). In these cells the increased binding of p21 to CDK2 was independent of p53, due to decrease in p53 levels in response to lovastatin (Figure 1). Finally, and most directly, we show that 76N-E6 cells, stably transformed by the human papilloma virus E6 which renders p53 inactive (Band *et al.*, 1990; 1991), not only were G1 arrested by lovastatin treatment but also revealed an induction of p21 and p27 expression followed by increased binding of p21 (and p27) to CDK2. The above results using three different cell types which are either p53/pRb wild-type, or p53/pRb mutant, or harbor an inactive p53 (i.e. 76N-E6) clearly reveal that the p21 induction and subsequent G1 arrest mediated by lovastatin is p53 independent.

Lovastatin is a widely used drug for patients suffering from hypercholesterolemia (Rettersol *et al.*, 1996). Investigators attempted to use lovastatin as an agent for treatment of cancer because it inhibits the cholesterol biosynthesis pathway and tumor cells have an increased level of cholesterol synthesis (Bernstein and Ross, 1993). However, these studies and recent clinical trials were inconclusive in providing a role for lovastatin as an anti-cancer agent (Thibault *et al.*, 1996). On the other hand, it is reasonable to evaluate the chemo-preventative effect of this drug since data from a large clinical trial of lovastatin for reducing serum cholesterol produced the unexpected finding of a 33% decrease in cancer incidence (Stein *et al.*, 1993). Furthermore, lovastatin has also been shown to inhibit metastasis of highly metastatic B16F10 mouse melanoma in nude mice (Jani *et al.*, 1993). Lastly, in the present study we show that lovastatin treatment of cells leading to G1 arrest is through the induction of p21 and p27 and subsequent inhibition of CDK2 activity. Collectively the above studies suggest that lovastatin may have chemo-preventative properties by inducing the inhibitory activity of the negative regulators of the cell cycle. It therefore is quite pertinent to investigate the direct mechanism by which lovastatin activates the CKIs in the cells, whether by inducing their expression in otherwise CKI negative cells, or mediating their redistribution to cyclin/CDK complexes which inhibit progression through the cell cycle. The universality and the p53 independent action of lovastatin in cessation of cell proliferation, also make it a very attractive agent for use as a potential chemo-preventative agent.

Materials and methods

Materials, cell lines and culture conditions

Lovastatin was kindly provided by William Henkler (Merck, Sharp and Dohme Research Pharmaceuticals, Rathway, NJ, USA). Serum was purchased from Hyclone Laboratories (Logan, Utah, USA) and cell culture medium from Life Technologies, Inc. (Grand Island, NY, USA). All other chemicals used were reagent grade. Before addition to cultures, lovastatin was converted from its inactive lactone prodrug form to its active dihydroxy-open acid as described previously (Keyomarsi *et al.*, 1991; Keyomarsi, 1996). The culture conditions for 76N, 70N normal cell strains, MCF-10A immortalized cell line, and MCF-7, ZR75T, MDA-MB-157, Hs578T, T47D, and MDA-MB-231 breast cancer cell lines were described previously (Keyomarsi and Pardee, 1993; Keyomarsi *et al.*, 1995). 76N-E6 cell line (a gift from Dr V Band, Tufts Medical Institute, Boston, MA, USA) were immortalized and cultured as described previously (Band *et al.*, 1990, 1991). All cells were cultured and treated at 37°C in a humidified incubator containing 6.5% CO_2 and maintained free of mycoplasma as determined by Hoechst staining (Hessling *et al.*, 1980).

Synchronization and flow cytometry

Synchronization by lovastatin treatment was performed as described previously (Keyomarsi *et al.*, 1991). Briefly medium was removed 24–36 h after the initial plating, replaced with fresh medium plus 40 μM lovastatin for 0–36 h. Cells were harvested at the indicated times and flow cytometry analysis was performed. For Fluorescence-Activated Cell Sorter (FACS) analysis 10^6 cells were centrifuged at 1000 *g* for 5 min, fixed by the gradual addition of ice cold 70% ethanol (30 min at 4°C) and washed with phosphate buffered saline. Cells were then treated with RNAse (10 ug/ml) for 30 min at 37°C, washed once with phosphate buffered saline and resuspended and stained in 1 ml of 69 μM propidium iodide in 38 mM sodium citrate for 30 min at room temperature. The cell cycle phase distribution was determined by analytical DNA Flow cytometry as described previously (Keyomarsi *et al.*, 1995).

Western blot and immune complex kinase analysis

Cell lysates were prepared and subjected to Western blot analysis as previously described (Keyomarsi *et al.*, 1995). Briefly, 50 μg of protein from each condition was electrophoresed in each lane of either a 7% sodium dodecyl sulfate-polyacrylamide gel (SDS–PAGE) (pRb), 10% SDS–PAGE (p53, cyclin A, cyclin D1, cyclin D3), 13% SDS–PAGE (p21, p27, CDK2, CDK4), or a 15% SDS–PAGE (p16), and transferred to Immobilon P overnight at 4°C at 35 mV constant volts. The blots were blocked overnight at 4°C in Blotto (5% nonfat dry milk in 20 mM Tris, 137 mM NaCl, 0.25% Tween, pH 7.6). After six, 10 min washes in TBST (20 mM Tris, 137 mM NaCl, 0.05% Tween, pH 7.6), the blots were incubated in primary antibodies for 3 h. Primary antibodies used were pRb monoclonal antibody (PharMingen, San Diego, CA, USA), at a dilution of 1:100, monoclonal antibody to p16 (a gift from Jim DeCaprio, Dana Farber Cancer Institute) at a dilution of 1:20, CDK2, CDK4 and p27, monoclonal antibodies (Transduction Laboratories, Lexington, KY, USA) each at a dilution of 1:100, p21 and p53 monoclonal antibodies (Oncogene Research Products/Calbiochem, San Diego, CA, USA) at a dilution of 1:100 cyclin D1 monoclonal antibody (Santa Cruz Biochemicals, Santa Cruz, CA, USA) at a dilution of 1:100, and actin

monoclonal antibody (Boehringer-Mannheim, Indianapolis, IN, USA) at 0.63 µg/ml in Blotto. Following primary antibody incubation, the blots were washed and incubated with goat anti-mouse horseradish peroxidase conjugate at a dilution of 1:5000 in Blotto for 1 h and finally washed and developed with the Renaissance chemiluminescence system as directed by the manufacturers (NEN Life Sciences Products, Boston, MA, USA).

For immunoprecipitations followed by Western blot analysis 300 µg of cell extracts were used per immunoprecipitation with polyclonal antibody to CDK2 [CDK2 antibody was generated by immunizing rabbits with multiple antigenic peptide (MAP peptides) (Posnett *et al.*, 1988) consisting of the 30 amino acids of the N terminal region of the CDK2 protein. MAP peptides consist of branched lysines, with each lysine directly attached to the peptide. Rabbits were primed and boosted subcutaneously, with 2 mg of MAP peptide without a carrier protein and emulsified in complete or incomplete (four boosts) adjuvant, respectively. The rabbits were boosted in 3 week intervals and the titer and the specificity of the serum was monitored by ELISA (Enzyme-linked immunosorbent assay) following each boost.] or CDK4 (a gift from Dr M Pagano, New York University Medical Center, NY, New York) (Tam *et al.*, 1994) in lysis buffer containing 50 mM Tris buffer pH 7.5, 250 mM NaCl, 0.1% NP-40, 25 µg/ml leupeptin, 25 µg/ml aprotinin, 10 µg/ml pepstatin, 1 mM benzamidine, 10 µg/ml soybean trypsin inhibitor, 0.5 mM PMSF, 50 mM NaF, 0.5 mM Sodium Ortho-Vanadate. The protein/antibody mixture was incubated with protein A Sepharose for 1 h and the immunoprecipitates were then washed twice with lysis buffer and four times with kinase buffer (50 mM Tris HCL pH 7.5, 250 mM NaCl, 10 mM MgCl$_2$, 1 mM DTT and 0.1 mg/ml BSA). The immunoprecipitates were then electrophoresed on 10%

(cyclin D3) 13% (p21, p27, CDK4 and CDK2) and 15% gels (p16) transferred to Immobolin P, blocked and incubated with the indicated antibodies at dilutions described above. For Histone H1 kinase assay the immunoprecipitates were incubated with kinase assay buffer containing 60 µM cold ATP and 5 µCi of [^{32}P]ATP in a final volume of 50 µl at 37°C for 30 min. The products of the reaction were then ana-lysed on a 13% SDS−PAGE gel. The gel was then stained, destained, dried and exposed to X-ray film. For quantitation, the protein bands corresponding to histone H1 were excised and radioactivity was measured by scintillation counting.

For immunodepletion, three sequential immunodepletions were carried out with 500 µg of each cell extract using either anti-p21 and anti-p27 polyclonal antibodies (Santa Cruz Biochemicals, Santa Cruz, CA, USA) bound to protein A beads or protein A beads alone. Fifty µg aliquots of the remaining supernatant were subjected to Western blot analysis as described above to analyse the presence of remaining proteins.

References

Alberts AW, Chen J, Kuron G, Hunt V, Hoffman C, Rothrock J, Lopez M, Joshua H, Harris E, Patchett A, Monaghan R, Currie S, Stapley E, Albers-Schonberg G, Hensens O, Hirshfield G, Hoogsteen K. Liesch J and Springer J. (1980). *Proc. Natl. Acad. Sci. USA*, **77**, 3957−3961.

Band V, DeCaprio JA, Delmolino L, Kulesa V and Sager R. (1991). *J. Virol.*, **65**, 6671−6676.

Band V, Zajchowski D, Kulesa V and Sager R. (1990). *Proc. Natl. Acad. Sci. USA*, **87**, 463−467

Bartek J, Bartkova J and Lukas J. (1996). *Curr. Opin. Cell Biol.*, **8**, 805−814

Bartek J, Bartkova J and Lukas J. (1997). *Exp. Cell Res.*, **237**, 1−6.

Bernstein L and Ross RK. (1993). *Epidemiology Rev.*, **15**, 48−65.

Datto MB, Li Y, Panus JF, Howe DJ, Xiong Y and Wang X-F. (1995). *Proc. Natl. Acad. Sci. USA*, **92**, 5545−5549.

Dulic V, Kaufman WK, Wilson S, Tlisty TD, Lees E, Harper JW, Elledge SJ and Reed SI. (1994). *Cell*, **76**, 1013−1023.

El-Deiry WS, Tokino T, Velculescu VE, Levy DB, Parsons R, Trent JM, Lin D, Mercer WE, Kinzler KW and Vogelstein B. (1993). *Cell*, **75**, 817−825.

Elbendary A, Berchuck A, Davis P, Havrilesky L, Bast J, Iglehart RCJD and Marks JR. (1994). *Cell Growth & Diff.*, **5**, 1301−1307.

Elledge SJ and Harper JW. (1994). *Curr. Opin Cell Biol.*, **6**, 847−852.

Elledge SJ, Winston J and Harper JW. (1996). *Trend Cell Biol.*, **6**, 388−392.

Ewen ME, Sluss HK, Sherr CJ, Natsushime H, Kato J-Y and Livingston DM. (1993a). *Cell*, **73**, 487−497.

Ewen ME, Sluss HK, Whitehouse LL and Livingston DM. (1993b). *Cell*, **74**, 1009−1020.

Fang X, Jin X, Xu H-J, Liu L, Peng H-Q, Hogg D, Roth JA, Yu Y, Xu F, Blast RC and Mills GB. (1998). *Oncogene*, **16**, 1−8.

Fisher RP and Morgan DO. (1994). *Cell*, **78**, 713−724.

Goldstein JL and Brown MS. (1990). *Nature*, **343**, 425−430.

Gray-Bablin J, Rao S and Keyomarsi K. (1997). *Cancer Res.*, **57**, 604−609.

Gray-Bablin J, Zalvide J, Fox MP, Knickerbocker CJ, DeCaprio JA and Keyomarsi K. (1996). *Proc. Natl. Acad. Sci.*, **93**, 15215−15220.

Gu Y, Turck CW and Morgan DO. (1993). *Nature*, **366**, 707−710.

Harper JW. (1997). *Cancer Surv.*, **29**, 91−108.

Harper JW, Adami GR, Wei N, Keyomarsi K and Elledge SJ. (1993). *Cell*, **75**, 805−816.

Harper JW and Elledge SJ. (1996). *Curr. Opin. Gene & Dev.*, **6**, 56−64.

Harper JW and Elledge SJ. (1998). *Genes & Dev.*, **12**, 285−289.

Hengst, L, Dulic V, Slingerland JM, Lees E and Reed SI. (1994). *Proc. Natl. Acad. Sci.*, **91**, 5291−5295.

Hengst L and Reed SI. (1996). *Science*, **271**, 1861−1864.

Hessling JJ, Miller SE and Levy NL. (1980). *J. Immunol. Meth.*, **38**, 315−324.

Ikeda MA, Jakoi L and Nevins JR. (1996). *Proc. Natl. Acad. Sci. USA*, **93**, 3215−3220.

Jakus J and Yeudall WA. (1996). *Oncogene*, **12**, 2369−2376.

Jani JP, Specht S, Stemmler N, Blanock K, Singh SV, Gupta V and Katoh A. (1993). *Inv. Metas.*, **13**, 314−324.

Jiang H, Fisher PB. (1993). *Molec. and Cell. Differen.*, **3**, 285−299.

Kato J, Matsuoka M, Polyak K, Massague J and Sherr CJ. (1994). *Cell*, **79**, 487−496.

Keyomarsi K. (1996). *Methods in Cell Science,* i18, 109 – 114.

Keyomarsi K, Conte D, Toyofuku W and Fox MP. (1995). *Oncogene,* **11,** 941 – 950.

Keyomarsi K and Pardee AB. (1993). *Proc. Natl. Acad. Sci. USA,* **90,** 1112 – 1116.

Keyomarsi K, Sandoval L, Band V and Pardee AB. (1991). *Cancer Res.,* **51,** 3602 – 3609.

LaBaer J, Garrett MD, Stevenson LF, Slingerland J, Sandhu C, Chou HS, Fattaey A and Harlow E. (1997). *Genes & Dev.,* **11,** 847 – 862.

Makela TP, Tassan JP, Nigg EA, Frutiger S, Hughes GJ, Weinberg RA. (1994). *Nature,* **371,** 254 – 257.

Maltese WA. (1990). *FASEB J.,* **4,** 3319 – 3328.

Matsushime H, Quelle DE, Shurtleff SA, Shibuya M, Sherr CJ, Kato J-Y. (1994). *Mol. Cell. Biol.,* **14,** 2066 – 2076.

Michieli P, Chedid M, Lin D, Pierce JH, Mercer WE and Givol D. (1994). *Cancer Res.,* **54,** 3391 – 3395.

Nasmyth K. (1996). *Science,* **274,** 1643 – 1651.

Noda AF, Ning Y, Venable S, Pereira-Smith OM and Smith JR. (1994). *Exp. Cell. Res.,* **211,** 90 – 98.

Nourse J, Firpo E, Flanagan M, Coats S, Polyak C, Lee M, Massague J, Crabtree G and Roberts J. (1994). *Nature,* **372,** 570 – 573.

Pagano M, Tam SW, Theodoras AM, Beer-Romero P, Del Sal, G, Chau V, Yew RP, Draetta GF and Rolfe M. (1995). *Science,* **269,** 682 – 685.

Pardee AB. (1989). *Science,* **246,** 603 – 608.

Planas-Silva MD and Weinberg RA. (1997a). *Mol. Cell. Biol.,* **17,** 4059 – 4069.

Planas-Silva MD and Weinberg RA. (1997b). *Curr. Opin. Cell Biol.,* **9,** 768 – 772.

Polyak K, Kato J-Y, Soloman MI, Sherr CJ, Massague J, Roberts JM and Koff A. (1994a). *Genes & Dev.,* **8,** 9 – 22.

Polyak K, Lee M-H, Erdjument-bromage H, Tempst P and Massaague J. (1994b). *Cell,* **78,** 59 – 66.

Poon RYC, Toyoshima H and Hunter T. (1995). *Mol. Biol. Cell,* **6,** 1197 – 1213.

Posnett DN, McGrath H and Tam JP. (1988). *J. Biol. Chem.,* **263,** 1719 – 1725.

Prall OWJ, Sarcevic B, Musgrove EA, Watts CKW and Sutherland RL. (1997). *J. Biol. Chem.,* **272,** 10882 – 10894.

Rettersol K, Stuggard M, Gorbitz C and Ose L. (1996). *Am. J. Card.,* **78,** 1369 – 1374.

Reynisdottir I and Massague J. (1997). *Genes & Dev.,* **11,** 492 – 503.

Reynisdottir I, Polyak K, Iavarone A and Massague J. (1995). *Genes & Dev.,* **9,** 1831 – 1845.

Rogatsky I, Trowbridge JM and Garabedian MJ. (1997). *Mol. Cell. Biol.,* **17,** 3181 – 3193.

Sheikh MS, Li X, Chen J, Shao Z, Ordonez JV and Fontana JA. (1994). *Oncogene,* **9,** 3407 – 3415.

Sherr CJ. (1994). *Cell,* **79,** 551 – 555.

Sherr CJ. (1996). *Science,* **274,** 1672 – 1677.

Sherr CJ. and Roberts, J. M. (1995). *Genes & Dev.,* **9,** 1149 – 1163.

Soule HD, Maloney TM, Wolman SR, Peterson SR, Jr, Brenz R, McGrath CM, Russo J, Pauley RJ, Jones, RF and Brooks SC. (1990). *Cancer Res.,* **50,** 6075 – 6086.

Stein EA, Lazkarzewski P, Steiner P and Lovastatin Study Groups I through IV. (1993). *Arch. Intern. Med.,* **153,** 1079 – 1087.

Tam SW, Theodoras AM, Shay JW, Draetta G and Pagano M. (1994). *Oncogene,* **9,** 2663 – 2674.

Thibault A, Samid D, Tompkins AC, Figg WD, Cooper M., Hohl RJ, Trepel J, Liang B, Patronas N, Venzon DJ, Reed E and Myers CE. (1996). *Clin. Can. Res.,* **2,** 483 – 491.

Toyoshima H and Hunter T. (1994). *Cell,* **78,** 67 – 74.

Weinberg RA. (1995). *Cell,* **81,** 323 – 330.

Xiong Y, Hannon GJ, Zhang GJ, Gasso D, Kobayashi R and Beach D. (1993). *Nature,* **366,** 710 – 714.

Zhu W-Y, Jones CS, Kiss A, Matsukuma K, Amin S and De Luca LM. (1997). *Exp. Cell Res.,* **234:** 293 – 299.

The Biphasic Induction of p21 and p27 in Breast Cancer Cells by Modulators of cAMP Is Posttranscriptionally Regulated and Independent of the PKA Pathway

Sharmila Rao,[*,1] Julie Gray-Bablin,[*,1] Thaddeus W. Herliczek,[*] and Khandan Keyomarsi[*,†,2]

*Laboratory of Diagnostic Oncology, Division of Molecular Medicine, Wadsworth Center, Albany, New York 12201-0509;
and †Department of Biomedical Sciences, State University of New York, Albany, New York 12222

Cyclic AMP (cAMP) elevation affects growth arrest and differentiation in a wide variety of breast cell lines; however, the mechanisms associated with this process are poorly understood. Previous studies linked cAMP-mediated growth arrest in breast tumor cells to increased levels of cyclin kinase inhibitor (CKI), p21. In the present study we examined the role of cAMP-dependent protein kinase (PKA) on p21 and p27 induction in the breast cancer cell line, MDA-MB-157. The induction of the CKIs by modulators of cAMP such as cholera toxin (CT) + 1-isobutyl-3-methylxanthine (IBMX) and lovastatin fluctuates with biphasic kinetics (although the kinetics of CKI induction with CT + IBMX treatment are different from that of lovastatin) and is depicted by the periodic accumulation of lower molecular weight forms of p21 and p27 which also correlate with fluctuations in CDK2 activity. Using three different approaches we show that the cAMP-mediated induction of CKIs is independent of PKA activity. In the first approach we treated MDA-MB-157 cells with a variety of cAMP modulators such as CT + IBMX, and forskolin in the presence or absence of H-89, a potent PKA inhibitor. This analysis revealed that the cAMP activators were capable of inducing p21 even though PKA activity was completely eliminated. In the second approach PKA dominant negative stable clones of MDA-MB-157 treated with CT + IBMX or forskolin also resulted in p21 induction, in the absence of any PKA activity. Last, treatment of MDA-MB-157 cells with lovastatin, another known cAMP modulator which also causes growth arrest, resulted in the induction of p21 and p27 without any increase in PKA activity. Collectively, the above results suggest that the induction of p21 by cAMP is through a novel pathway, independent of PKA activity.   © 1999 Academic Press

Key Words: PKA; cAMP; cell cycle; p21; CKIs; CDKs.

[1] S. R. and J. G. B. contributed equally to the paper.
[2] To whom correspondence and reprint requests should be addressed at Wadsworth Center, Room C-400, Empire State Plaza, P.O. Box 509, Albany, NY 12201-0509. Fax: (518) 486-5798. E-mail: keyomars@wadsworth.org.

INTRODUCTION

The mammalian cell cycle is positively regulated by complexes of stable kinases termed cyclin-dependent kinases (CDKs) and unstable regulatory subunits called cyclins which act to phosphorylate appropriate substrates within the cell [1–4]. Progression through the cell cycle is also negatively regulated through the association of cyclin/CDK complexes with CDK inhibitors, CKIs [5–8]. There are two families of structurally distinct CKIs, (i) the CIP/KIP family, including p21^{CIP1}, p27^{KIP1}, and p57^{KIP2}, which inhibits a broad range of CDKs by selectively binding and inhibiting the fully associated cyclin/CDK complexes and (ii) the INK family, including p15^{INK4a} and p16^{INK4b}, which binds specifically to CDK4 and/or CDK6 and inhibits complex formation with cyclin D [1, 3, 8, 9].

The CKI p21 (CIP1/WAF1), the first mammalian CKI to be identified, was simultaneously characterized by several laboratories [10–15] and is an important mediator of signals which block proliferation or lead to differentiation. p21 can inhibit the activity of CDK2, CDK4, and cdc2 cyclin complexes *in vitro* and *in vivo* as demonstrated in transgenic mice hepatocytes overexpressing p21 [16]. DNA damage presumably triggers p53 induction of p21 and results in CDK inhibition and G1 growth arrest [17]. However, p21 can be induced by p53-independent mechanisms, by serum, PDGF, and EGF in embryonic fibroblasts from p53 knockout mice [18], by serum starvation in p53 mutant human breast carcinoma cells [19], by TGF-β1 in human ovarian cancer cells [20], and by lovastatin in a variety of cell lines [21, 22]. p27 (KIP1), similar in amino acid sequence and inhibitory specificity to p21, was identified as a protein associated with inactive cyclin E/CDK2 complexes in TGF-β1-treated and contact-inhibited cells [23, 24]. p27 also interacts with cyclin D1/CDK4 complexes [25] and is accumulated in cells arrested in G1 or by lovastatin [21, 26, 27]. Hence, p21 and p27 may function similarly to inhibit CDK activity and proliferation in response to different environmental

stimuli. Conversely, removal by degradation or inactivation of p27 may be necessary for proliferation [28].

One pathway which has been thought to have profound effects on the regulation of the CKIs is the cyclic adenosine 3':5'-monophosphate (cAMP)-protein kinase (PKA) pathway. Changes in the intracellular levels of cAMP have a variety of effects on cell growth, stimulating the growth of some cell lines like epithelial cells [29] and Swiss 3T3 cells [30], while inhibiting the growth of others such as breast tumor cells [31], gliomas (A-172), melanomas [32], and macrophages [33]. Early studies suggested that cAMP suppresses proliferation of some cell lines by either inhibiting growth-associated genes such as c-myc or transferrin receptor [34, 35] or by activating negative growth regulators such as TGF-β, cyclin D1, and p27 [36–38].

Most of these cAMP-dependent events are mediated by cAMP-dependent protein kinase [39]. Activation of cAMP by the membrane-bound adenyl cyclase results in the binding of cAMP to the regulatory subunit of PKA and the subsequent release of the catalytic subunit of PKA. The released PKA catalytic subunit phosphorylates a specific class of nuclear proteins belonging to the cAMP response element binding/activating transcription factor family [39]. These nuclear proteins recognize and bind to specific DNA regulatory regions known as cAMP-responsive elements, located in the promoter region of cAMP responsive genes and thereby regulate the activity of the gene [39].

cAMP levels are modulated by several agents such as forskolin [40], cholera toxin (CT) [41], 1-isobutyl-3-methylxanthine (IBMX) [42], and 8-Br-cAMP. All these cAMP modulators have the ability to inhibit cell proliferation in certain cell types. For example CT has been shown to inhibit growth and trigger apoptosis in small cell lung carcinomas [41, 43]. IBMX, forskolin, and 8Br-cAMP have also been found to cause G1 arrest in macrophages by increasing cAMP levels [24, 33]. This G1 arrest has been related to the induction of the cyclin kinase inhibitor p27 (KIP1) [24, 33] and inhibition of CDK-activating kinase (CAK) by cAMP [33]. The inhibition of CAK by cAMP was mediated directly neither by PKA nor by phosphorylation of PKA substrates *in vitro*. Thus, even though changes of intracellular cAMP have been associated with G1 arrest, the role of PKA activity in cell cycle arrest induced by cAMP is still unknown.

Another agent which has been shown to modulate cAMP levels both in cultured cells [44, 45] and in patients [46] is lovastatin, a widely used drug for the treatment of hypercholesterolemia [47]. Previously we reported that lovastatin can be used as an effective agent in cell synchronization for both tumor and normal cells [48, 49], arresting cells in G1. We have shown that treatment of mammary epithelial cells by lovastatin results in the induction of p21 and p27 [21]. Furthermore these increases seem to be mediated by

mechanisms independent of other standard G1 arresting agents/conditions such as serum starvation or double thymidine block [21]. Lovastatin treatment of HeLa, HL60, normal fibroblasts [26, 27], mesangial [50], and rat FRTL-5 cells [51] also results in the induction of p27 while treatment of PC-3M human prostate carcinoma cells [52], metastatic melanoma cells [53], A-253 head and neck, Calu-1 lung, or T-24 bladder carcinoma cells [54] all result in the induction of p21 protein levels. Furthermore, we have shown that the induction of CKIs by lovastatin leads to increased p21/CDK2 and p27/CDK2 complexes and such complex formation is sufficient to completely inactivate CDK2 and lead to G1 arrest in breast epithelial cells [22].

Since increased levels of cAMP have been associated with G1 arrest, and G1 arrest is a direct result of induction of CKIs p21 and p27 [6], we examined the link between cAMP modulation, PKA activation, and increased levels of cyclin kinase inhibitors p21 and p27 in cultured breast cancer cells. We hypothesized that the mechanism by which lovastatin and other inducers of cAMP result in CKI induction and subsequent G1 arrest is through the activation of the PKA pathway. We show that treatment of breast tumor cells, MDA-MB-157 with cAMP modulators CT + IBMX, and forskolin as well as lovastatin resulted in increased levels of p21 and p27. Such an induction is biphasic only at the protein level. The increased biphasic induction of the CKIs leads to increased binding of these CKIs to CDK2 and concomitant inhibition of the CDK2 activity. However, the CKI induction by CT + IBMX, forskolin, or lovastatin is not due to the activation in the PKA pathway. This novel finding was revealed when we inhibited PKA activity (during treatment by the cAMP modulators) by two different means: first, we used a dominant negative PKA mutant to eradicate endogenous PKA activity in stably transfected cells. Additionally we used a pharmacological inhibitor of PKA, H89. Our results indicate that the induction of CKIs by cAMP modulators occurs through a PKA-independent mechanism.

MATERIALS AND METHODS

Materials, cell cultures, and transfections. Forskolin, CT, and IBMX were purchased from Sigma Chemical Co. (St Louis, MO). The PKA inhibitor H-89 was procured from L.C Laboratories (Woburn, MA). Lovastatin was a gift from William Henckler (Merck, Sharp, and Dohme Research Pharmaceuticals, Rahway, NJ). Serum was purchased from Sigma Chemical Co. Before addition to cultures lovastatin was converted from its lactone or pro-drug form to its active dihydroxy-open acid as described previously [49]. The breast tumor cell line MDA-MB-157 cells were cultured as previously described [55] in a 37°C incubator containing 6.5% CO_2. The MDA-MD-157 cells were transfected by the calcium phosphate method with the Mt-Rev (AB) Neo expression plasmid [56], a gift from Dr G. S. McKnight (Univ. of Washington, Seattle, WA). Following transfection cells were cultured in G418 (400 μg/ml) containing medium. Five pools and 10 colonies from each pool were selected. Treatment of these pools with cAMP modulators was performed in the presence of

10 μM ZnCl$_2$ or ZnSO$_4$ as the mutated regulatory region of PKA in the MT-Rev-Neo plasmid is under the influence of a metallothionine promoter.

cAMP-dependent protein kinase assay. Soluble protein extracts were prepared from MDA-MB-157 cells after treatment by sonicating the cells in homogenization buffer (0.25 mM Tris, pH 6.8, 1 mM DTT, 5 mM EDTA, 10 μg aprotinin, 1 μm PMSF, 20 μm leupeptin, 1 μm pepstatin, 1 μM okadiac acid) and centrifuging at 45000 rpm for 1 h at 4°C to remove cell debris. Protein concentration was determined by the Bradford assay (Bio-Rad). PKA activity was measured by a colorometric, nonradioactive assay (Pierce) which utilizes a synthetic fluorescent substrate, kemptide. Quantitation of the phosphorylated product is accomplished by measuring its absorbance at 570 nm. This assay is highly sensitive with a working range from approximately 0.03 to 1.0 units of cAMP-dependent protein kinase A activity. The PKA activity in cell extracts was calculated according to absorbance obtained from appropriate PKA standard with a known activity. The assay is also highly specific and only recognizes cAMP-associated PKA activity recognizing both PKA RI- and RII-mediated activity with no cross-reactions with PKC or other kinase activities. The experiments were performed in triplicates. Values are expressed as units of kinase activity per milligram of protein.

Western blot analysis and immune complex kinase analysis. MDA-MB-157 cells were treated with CT (1 μg/ml) + IBMX (10^{-4} M), forskolin (10 μM), or lovastatin (40 μM) for the indicated time intervals. Cell lysates were prepared and subjected to Western blot analysis as previously described [55]. Briefly, 50 μg of protein from each condition was electrophoresed in each lane of a 13% sodium dodecyl sulfate–polyacrylamide gel (SDS-PAGE) and transferred to Immobilon P overnight at 4°C at 35 mV constant volts. The blots were blocked overnight at 4°C in Blotto (5% nonfat dry milk in 20 mM Tris, 137 mM NaCl, 0.25% Tween, pH 7.6). After six 10-min washes in TBST (20 mM Tris, 137 mM NaCl, 0.05% Tween, pH 7.6), the blots were incubated in primary antibodies for 3 h. Primary antibodies used were p27 (Transduction Laboratories, Lexington, KY) and p21 monoclonal antibodies (Oncogene Research Products/Calbiochem, San Diego, CA) at a dilution of 1:100 and actin monoclonal antibody (Boehringer Mannheim, Indianapolis, IN) at 0.63 μg/ml in Blotto. Following primary antibody incubation, the blots were washed and incubated with goat anti-mouse horseradish peroxidase conjugate at a dilution of 1:5000 in Blotto for 1 h and finally washed and developed with the Renaissance chemiluminesence system as directed by the manufacturers (NEN Life Sciences Products, Boston, MA).

For immunoprecipitations followed by Western blot analysis 300 μg of cell extracts was used per immunoprecipitation with polyclonal antibody to CDK2 [22] in lysis buffer containing 50 mM Tris buffer, pH 7.5, 250 mM NaCl, 0.1% NP-40, 25 μg/ml leupeptin, 25 μg/ml aprotinin, 10 μg/ml pepstatin, 1 mM benzamidine, 10 μg/ml soybean trypsin inhibitor, 0.5 mM PMSF, 50 mM NaF, and 0.5 mM sodium orthovanadate. The protein/antibody mixture was incubated with protein A Sepharose for 1 h and the immunoprecipitates were then washed twice with lysis buffer and four times with kinase buffer (50 mM Tris–HCl, pH 7.5, 250 mM NaCl, 10 mM MgCl2, 1 mM DTT, and 0.1 mg/ml BSA). The immunoprecipitates were then electrophoresed on 13% gels, transferred to Immobolin P, blocked, and incubated with the indicated antibodies at dilutions described above. For histone H1 kinase assay the immunoprecipitates with either cyclin E or CDK2 antibody [22] were incubated with kinase assay buffer containing 60 μM cold ATP and 5 μCi of [^{32}P]ATP in a final volume of 50 μl at 37°C for 30 min. The products of the reaction were then analyzed on a 13% SDS–PAGE gel. The gel was then stained, destained, dried, and exposed to X-ray film. For quantitation, the protein bands corresponding to histone H1 were excised and radioactivity was measured by scintillation counting.

RNA isolation and Northern blot hybridization. Total cellular RNA was extracted from normal and tumor cells by guanidinium isothiocyanate and subjected to cesium chloride gradient purification. For Northern blot analysis, 20 μg of total RNA was fractionated under denaturing conditions on a 1.2% agarose/0.66 M formaldehyde gel and transferred to a Nytran filter (Schleicher & Schell) for subsequent hybridization. The DNA probes were prepared by random-primed labeling (Boehringer Mannheim). Vector containing p21 was provided by S. Elledge and W. Harper and cDNA to p27 was provided by Joan Massague. All cDNA inserts were labeled with [α-^{32}P]dCTP to a specific activity of 1×10^9 dpm/μg of DNA.

RESULTS

Posttranscriptional, biphasic regulation of p21 and p27 in response to CT + IBMX and lovastatin. Initially, we examined the temporal effects of cAMP modulators on the expression and activity of p21 and p27 in MDA-MB-157 cells. The results are shown in Fig. 1. For this experiment cells were treated simultaneously with CT and IBMX as these agents act synergistically to raise cAMP levels. Briefly, MDA-MB-157 tumor cells were treated with 1 μg/ml CT and 10^{-4} M IBMX for several time intervals up to 48 h (Fig. 1). Treatment of cells with CT + IBMX results in G1 arrest following 36 h of treatment (data not shown). At the indicated time intervals, cells were harvested and protein and RNA extracted and analyzed by Northern and Western blot analysis (Figs. 1A and 1B), immunecomplex formation (Fig. 1C), and kinase assays (Fig. 1D). Northern blots of CT + IBMX-treated cells reveal that the p21 and p27 mRNA levels peak at 4 and 6 h and gradually diminish returning to basal levels by 12 h (Fig. 1A) and stay at basal levels for the duration of the experiment (data not shown). Western blot analysis (Fig. 1B) indicates that the CT + IBMX treatment dramatically modulates the levels of the CKIs examined. Curiously the induction of p21 and p27 protein is biphasic. Levels rapidly increase beginning at 15 min following treatment with CT + IBMX, peaking at 1 h, and then gradually decreasing such that at 4 h no intact p21 or p27 proteins are detected. This pattern then repeats with levels increasing dramatically at 6 h and diminishing again at 20 h. In untreated cells [lanes 0 and 0E (E = ethanol)], a specific monoclonal antisera to p27 detects p27 protein migrating at 27 kDa as well as an additional lower molecular weight form of this protein which is migrating at 15 kDa. As p27 is induced there is a rapid shift from the 15-kDa lower molecular weight form to the intact 27-kDa form such that at 30 min and 1 h following the CT + IBMX treatments, only the 27-kDa form of this protein is present. We detected a very similar pattern of a shift from low to high/intact molecular weight form of p21 following treatment with CT + IBMX when we exposed the blots for longer duration (data not shown). As the intact form of these proteins diminishes, a ladder of lower molecular weight forms is detected and at 4 and 20 h only the lowest molecular weight band for each of the proteins is visible. Probing blots with an anti-actin antiserum indicates that equal amounts of protein were loaded onto each lane of the gels used for Western blot anal-
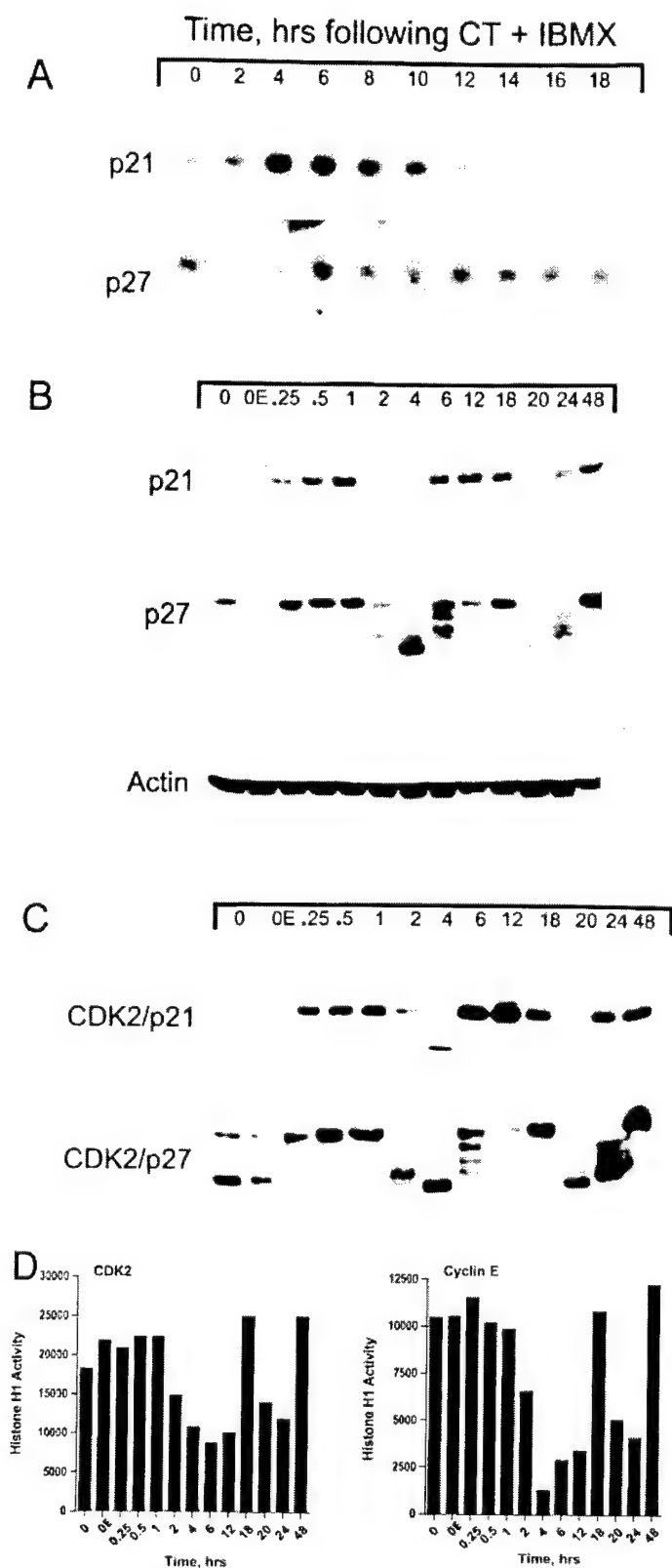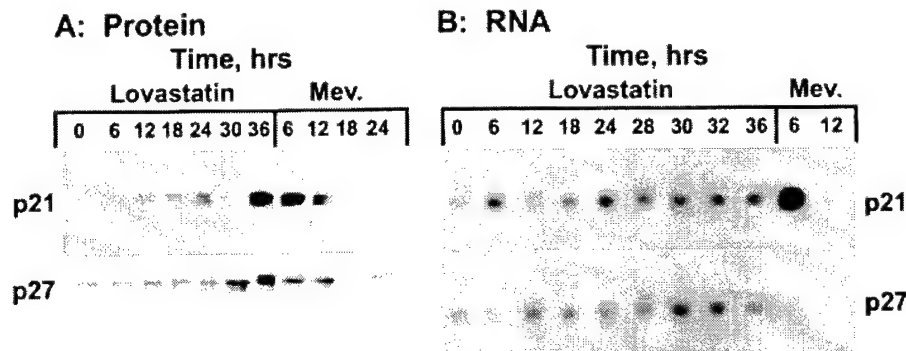
FIG. 1. Cholera toxin (CT) and iso-1-butyl-3-methylxanthine (IBMX) treatment results in the biphasic induction of p21 and p27. MDA-MB-157 cells were cultured in medium containing CT (1 μg/ml) and IBMX (10^{-4} M). At the indicated times following treatment cells were harvested and cell lysates were prepared and subjected to (A) Northern blot analysis: 20 μg of total RNA from each condition was analyzed by Northern blot analysis with the indicated cDNAs as probes. (B) Western blot analysis: 50 μg of protein extract from each condition was analyzed by Western blot analysis with the indicated antibodies. (0E is the cells treated with ethanol for 48 h—IBMX was made in ethanol.) The blots were developed by chemiluminescence reagents. (C) Immunecomplex formation. For immunoprecipitation followed by Western blot analysis, equal amounts of protein (300 μg) from cell lysate prepared from each condition were immunoprecipitated with anti-CDK2 (polyclonal) coupled to protein A beads and the immunoprecipitates were subjected to Western blot analysis with the indicated antibodies. (D) Histone H1 kinase analysis assays. For kinase activity, equal amounts of protein (300 μg) from cell lysates were prepared from each condition and immunoprecipitated with either anti-CDK2 or anti-cyclin E antibodies (polyclonal). The antibodies were coupled to protein A beads. Histone H1 was used as a substrate. The phosphorylated H1 band was cut from the SDS–PAGE and quantitated by scintillation counting.

ysis. To determine whether the low-molecular-weight forms of p21 and p27 are capable of complex formation with CDK2 we performed a two-step experiment consisting of an immunoprecipitation with anti-CDK2 antibody followed by Western blot analysis with p21 and p27 (Fig. 1C). These results revealed that the lower molecular weight forms of p21 and p27 are capable of forming complexes with CDK2 with a very similar pattern to the total levels of these CKIs (Fig. 1B). We observed a slight difference in the levels of p27 in 0E compared to 0 controls (Fig. 1B); however, both forms of p27 in 0E controls bind to CDK2 with a similar pattern to that of 0 control (Fig. 1C). To investigate whether the binding of these lower molecular forms of p21 and p27 to CDK2 had an effect in inhibiting the kinase activity of CDK2 and cyclin E we measured the phosphorylation of histone H1 in immunoprecipitates prepared from treated cells using antibodies to both CDK2 and cyclin E (Fig. 1D). These results surprisingly revealed that maximal inhibition of CDK2- and cyclin E-associated activities occurs at 4–6 h, the time intervals when the low-molecular-weight forms of p21 and p27 accumulate. These low-molecular-weight forms of p21 and p27 seem to inhibit the CDK2-associated H1 kinase activity better than the intact p21 and p27 (Fig. 1D). In fact the lower molecular weight forms of p27 are able to cause a decrease in CDK2 activity seen at 6 h even in the presence of p21/CDK2 complexes (Figs. 1C and 1D). Collectively, the data from this experiment suggest that the induction of intact p21 and p27 proteins precedes the induction of their mRNAs and that the disappearance of p21 and p27 proteins and the biphasic pattern of their expression occurs posttranscriptionally. Furthermore, the low-molecular-weight forms of p21 and p27 bind to and inhibit the associated kinase activity of CDK2 and cyclin E.

Next, we examined the kinetics of CKI modulation by lovastatin. Our previous work had established that lovastatin is capable of inducing both CKIs and that

FIG. 2. Lovastatin treatment of breast cancer cells results in the biphasic induction of p21 and p27. MDA-MB-157 cells were treated with 20 μM lovastatin. Protein and RNA was extracted after 0, 6, 12, 18, 24, 30, and 36 h of lovastatin treatment. Protein and RNA levels were also analyzed from MDA-MB157 cells cultured with lovastatin (20 μM) for 36 h, at which time lovastatin was removed and replaced with fresh medium containing mevalonate (200 μM) for 6, 12, 18, and 24 h for protein and 6 and 12 h for RNA. (A) Western blot: 50 μg of extracts of cells treated with lovastatin alone or lovastatin followed by mevalonate at indicated time intervals was analyzed by SDS–PAGE. Proteins were transferred and blots probed with antisera specific for the indicated CKI. (B) Northern blot: 20 μg of total RNA from lovastatin-treated cells was analyzed by Northern analysis and probed with the cDNA corresponding to the indicated CKI.

such induction is sufficient to lead to G1 arrest [21, 22]. The purpose of this experiment was to determine whether the temporal pattern of CKI induction of lovastatin, another cAMP modulator, is similar to that of CT + IBMX. The results are shown in Fig. 2. Cells were treated with lovastatin for 36 h, at which time they were washed and incubated with fresh medium containing mevalonate (mevalonate is routinely used to reverse the lovastatin-mediated G1 arrest [48]). Cells were treated with mevalonate for an additional 24 h in A or 12 h in B. At various times (6 h intervals) during lovastatin/mevalonate treatments, cells were harvested and extracted protein and RNA were analyzed on Western and Northern blots with the indicated CKI cDNAs and antisera as probes (Fig. 2). Western blot analysis reveals that both p21 and p27 are induced by lovastatin with p21 showing a biphasic pattern of induction, while p27 protein was induced continuously. Upon longer exposures at 24- and 30-h time points lower molecular weight proteins were detected for both p21 and p27 proteins (data not shown). Furthermore, although the induction of these proteins correlates with an induction of their mRNAs, the disappearance and biphasic kinetics are a posttranscriptional event as mRNA levels do not disappear with similar kinetics as protein levels (Fig. 2B). This biphasic pattern of CKI induction is very consistent and reproducible in several other mammary epithelial cells examined (data not shown). Last, CDK2 H1 kinase assays performed with the treated cells show that maximal kinase inhibition is achieved starting at 30 h post lovastatin treatment (data not shown). Collectively the results from Figs. 1 and 2 suggest that both CT + IBMX and lovastatin induce the CKIs with a biphasic, posttranscriptionally regulated kinetics and that induction of these CKIs leads to inhibition of CDK2 activity.

Induction of p21 by CT and IBMX is independent of PKA activity. In order to more fully characterize the induction of p21 and p27 by CT and IBMX, which act to elevate intracellular cAMP levels, we investigated the involvement of PKA. Since most cAMP-mediated affects in cells are thought to be through the activation of PKA it was reasonable to assume that induction of p21 by CT and IBMX is also through activation of the PKA pathway. We chose to limit the following studies to p21 since the pattern of its biphasic pattern of induction is more pronounced than that of p27 in both lovastatin- and CT + IBMX-treated cells. To directly assess the involvement of PKA in the induction of p21 by CT and IBMX we made use of a commonly used dominant negative mutant of PKA [56–58]. MDA-MB-157 cells deficient for PKA activity were generated via stable transfection with the MT-rev-Neo vector which contains the mutated regulatory region of the PKA enzyme under the influence of a metallothionine promoter [56]. The mutated regulatory regions of PKA do not bind cAMP and therefore do not dissociate from and activate the catalytic subunits. Thus the PKA enzyme is rendered catalytically inactive and insensitive to increases in intracellular cAMP [56].

MDA-MB-157 cells were transfected with MT-Rev-Neo and selected with G418 for 2–3 weeks. Following stable selection numerous stable clones and pooled populations of transfected cells were analyzed for p21 expression following cAMP induction. For this experiment 5 stably MT-Rev-Neo-transfected pooled populations of MDA-MB-157 cells were treated with CT and IBMX for 6 h, a time interval which allows for significant induction of both p21 and p27 and maximal inhibition of CDK2 activity (Fig. 3). Cellular extracts were prepared from CT + IBMX-treated parental cells and the pooled transfectant populations cultured in both the presence and the absence of ZnSO4 and ZnCl2
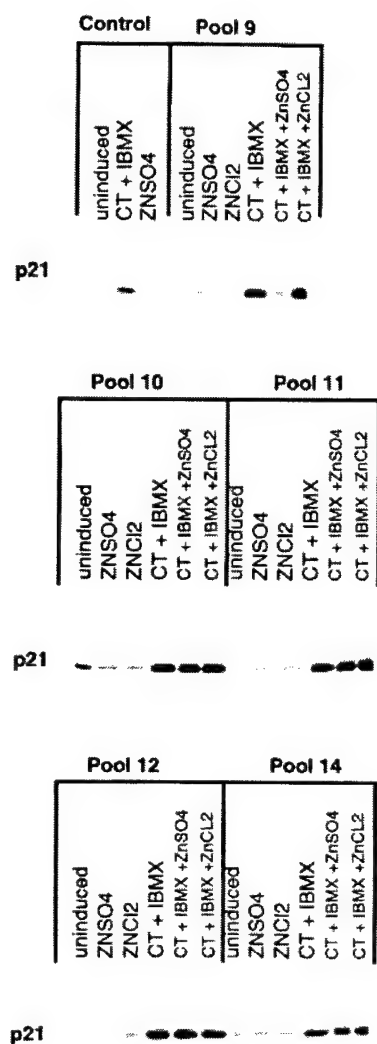
FIG. 3. p21 induction by CT and IBMX does not require the activity of PKA. Five pools (9, 10, 11, 12, 14) of the MDA-MB-157 cells transfected with the PKA dominant negative mutants along with the parental (i.e., untransfected) MDA-MB 157 cell lines were subjected to treatment with CT (1 μg/ml) and IBMX (10^{-4}) in the presence or absence of 10 μm ZnSo4 or ZnCl2 for 24 h. G418 (400 μg/ml) was present in the medium at all times to maintain the selection conditions. Transfections were performed as described under Materials and Methods. Following treatments cells were harvested and cell lysates prepared and subjected to Western blot analysis: 50 μg of protein extract from each condition was analyzed by Western blot analysis with the p21 antibody.

(since transcription of the PKA construct is regulated by the Zn inducible metallothionine promoter) (Fig. 3). CT + IBMX treatment induced a dramatic increase in p21 levels in control untransfected (Fig. 3), mock-transfected (data not shown), and MT-Rev-Neo-transfected cells regardless of the presence of Zn (Fig. 3). Furthermore the CT + IBMX-mediated induction of p21 in all the stable clones (except for pool 9 treated with CT + IBMX in the presence of ZnCl2) is more pronounced than the p21 induction in mock-trans-

fected cells (Fig. 3, top). This experiment was repeated three times with these pooled transfected cells at different passages with similar results as those presented in Fig. 3 (data not shown). Additionally, a similar CT + IBMX induction of p21 was observed in 12 different stable clonal populations isolated from the pools in Fig. 3 (data not shown). These results were the first indication that induction of p21 following CT + IBMX treatment is independent of the PKA pathway as cells with either an active (i.e., parental cells or mock-transfected cells) or inactive PKA (i.e., cells transfected with dominant negative mutant form of PKA) showed similar p21 induction.

p21 induction by forskolin and CT + IBMX occurs in the presence of PKA inhibitor H-89. The above findings suggest that induction of p21 by two cAMP modulators, CT and IBMX, did not require the activity of PKA, at least in cells transfected with the dominant negative mutant form of PKA. To further examine the validity of this hypothesis a pharmacological approach was used. H-89, a serine/threonine protein kinase inhibitor with selectivity toward cAMP-dependent protein kinase routinely used to inhibit PKA activity, was used to examine the role of PKA in p21 induction in cells treated with cAMP modulators. In addition, cells were treated with forskolin, another commonly used modulator of cAMP modulator, to determine whether p21 induction is a direct result of cAMP modulation or due to an unspecified effect of CT and IBMX treatment (Fig. 4). We found that treatment of cells with forskolin also resulted in G1 arrest similar to arrest following CT + IBMX treatment (data not shown). Forskolin increases cAMP levels by directly activating adenyl cyclase, while CT and IBMX raise cAMP levels by activating Gs proteins and inhibiting phosphodiesterase activity, respectively.

Western blot analysis of extracts from MDA-MB-157 treated with forskolin (10 μM) for different time intervals revealed an induction of p21 levels (Fig. 4B). This increase was seen as soon as 3 min following forskolin treatment and remained elevated even after 6 h of treatment. To determine the kinetics of PKA activity in relation to p21 induction following forskolin treatment, PKA activity was measured in cells treated with forskolin. Figure 4A shows that PKA activity initially increased above basal levels 4 min after treatment with forskolin and showed a maximum 2.5-fold induction after 10 min of treatment; by 30 min the PKA activity returned to basal levels. The kinetics of PKA activity following forskolin treatment is highly reproducible as very similar results were obtained from three experiments and the mean of these three experiments is presented in Fig. 4A. The increase in PKA activity is highly suggestive of the increase in cAMP levels due to forskolin treatment of MDA-MB-157 cells. Although an increase in both PKA activity and p21 levels was seen

A

B

Time of Exposure
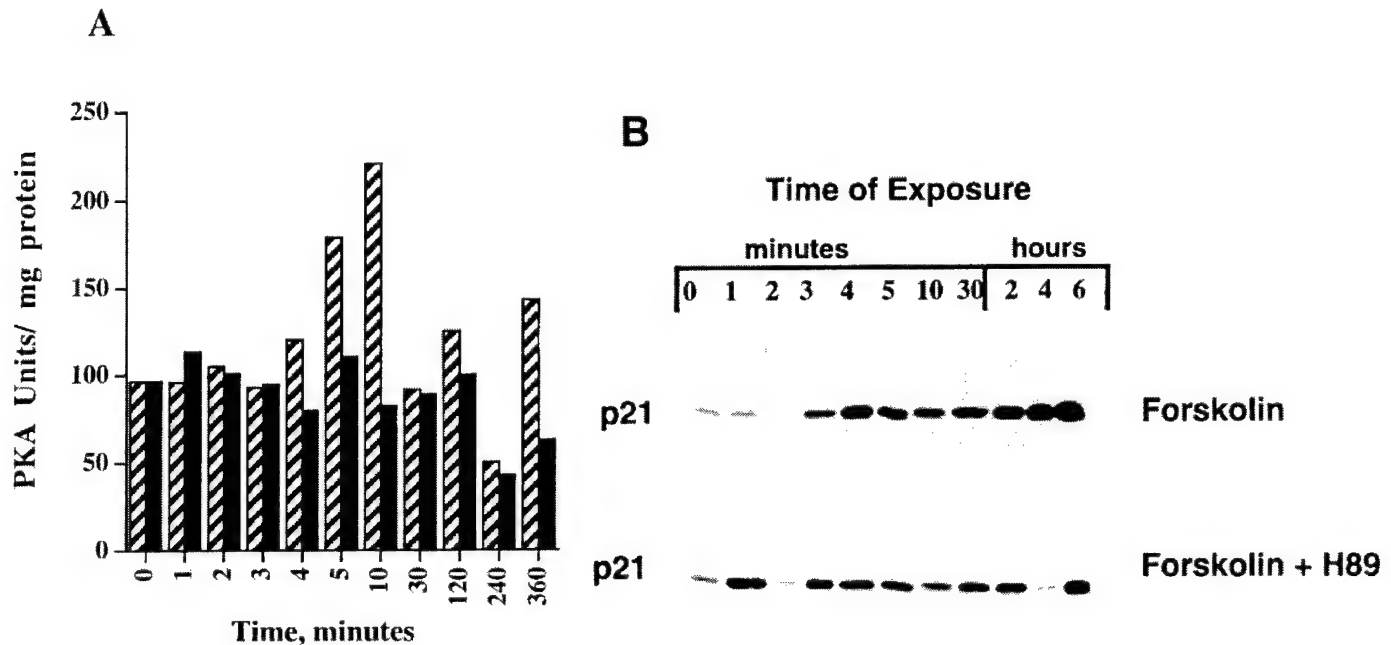
FIG. 4. PKA inhibitor H-89 does not affect p21 induction mediated by forskolin. MDA-MB-157 cells were treated with 10 μM forskolin in the presence or absence of the potent PKA inhibitor H-89 for the indicated times. H-89 (10 μM was added to the cells 6 h prior to the addition of forskolin. (A) Protein extracts from the treated cells were analyzed for PKA activity by its ability to phosphorylate a fluorescent peptide as described under Materials and Methods. Forskolin, hatched bars. Forskolin + H89, solid bars. (B) Cellular extracts (50 μg) from forskolin- and forskolin + H-89-treated MDA-MB-157 cells were analyzed by Western analysis and probed with anti-p21 antibody as described for Fig. 1.

in cells treated with forskolin, kinetics of the induction of p21 did not correspond to PKA activity, suggesting that either PKA activity is not required for p21 induction or PKA affects pathways upstream of p21. To further elucidate the role of PKA activity in p21 induction following forskolin treatment, MDA-MB-157 cells were treated with a potent inhibitor of PKA, H-89 (10 μM) for 6 h prior to treatment with forskolin.

Measurement of PKA activity in cells treated with forskolin and H-89 showed that H-89 was able to completely prevent the induction of PKA activity by forskolin (Fig. 4A). However, the analysis of p21 levels in cells treated with forskolin and H-89 showed that the presence of the PKA inhibitor resulted only in a shift of the biphasic pattern of p21 induction but had no affect on the extend of induction of p21 by forskolin (Fig. 4B), even though the induction of PKA activity was completely inhibited by H-89. The differences seen between p21 induction under forskolin and forskolin + H-89 treatments are the loss of p21 at 4 h and the faster induction of p21 after forskolin and H-89 treatment, suggesting that the presence of H-89, which blocks the PKA pathway, might be accelerating the activation of the PKA-independent pathway. The presence of H-89 also might be responsible for the biphasic induction of p21 (the loss of p21 at 4 h), which is not seen after the treatment of cells with only forskolin. Similar induction of p21 was seen in cells treated with CT + IBMX in the presence of H-89 (data not shown). Collectively

the results from Figs. 3 and 4 suggest that the induction of the CKI p21 by forskolin or by CT + IBMX in MDA-MB-157 cells in the presence or absence of PKA inhibitor H-89 or in cells transfected with dominant negative PKA mutant is independent of PKA.

Forskolin also induces p21 expression in dominant negative mutants for PKA. Even though the above results suggest that cAMP modulators, forskolin and CT + IBMX, induce p21 in breast tumor cells through a cAMP-dependent, PKA-independent pathway, it can be argued that pharmacological agents such as H-89, although effective in reducing PKA activity, might also affect other cellular pathways. Hence to further determine the role of PKA activity in p21 induction following forskolin treatment, we treated dominant negative mutants of PKA with forskolin. For this experiment we used a PKA dominant negative mutant stable clone (No. 12). Western blot analysis with an anti-PKA antibody revealed the expression of the dominant negative protein in all transfectants used in this study (data not shown). Forskolin treatment of this stable clone resulted in only slight and delayed induction of PKA activity, with increased PKA activity <1.5-fold seen only after 30 min of forskolin treatment (Fig. 5A). The above results suggest that although the dominant negative mutant clone was able to reduce PKA activity (from 2.5- to less than 1.5-fold) and delay the increase in PKA activity (from 10 to 30 min following drug
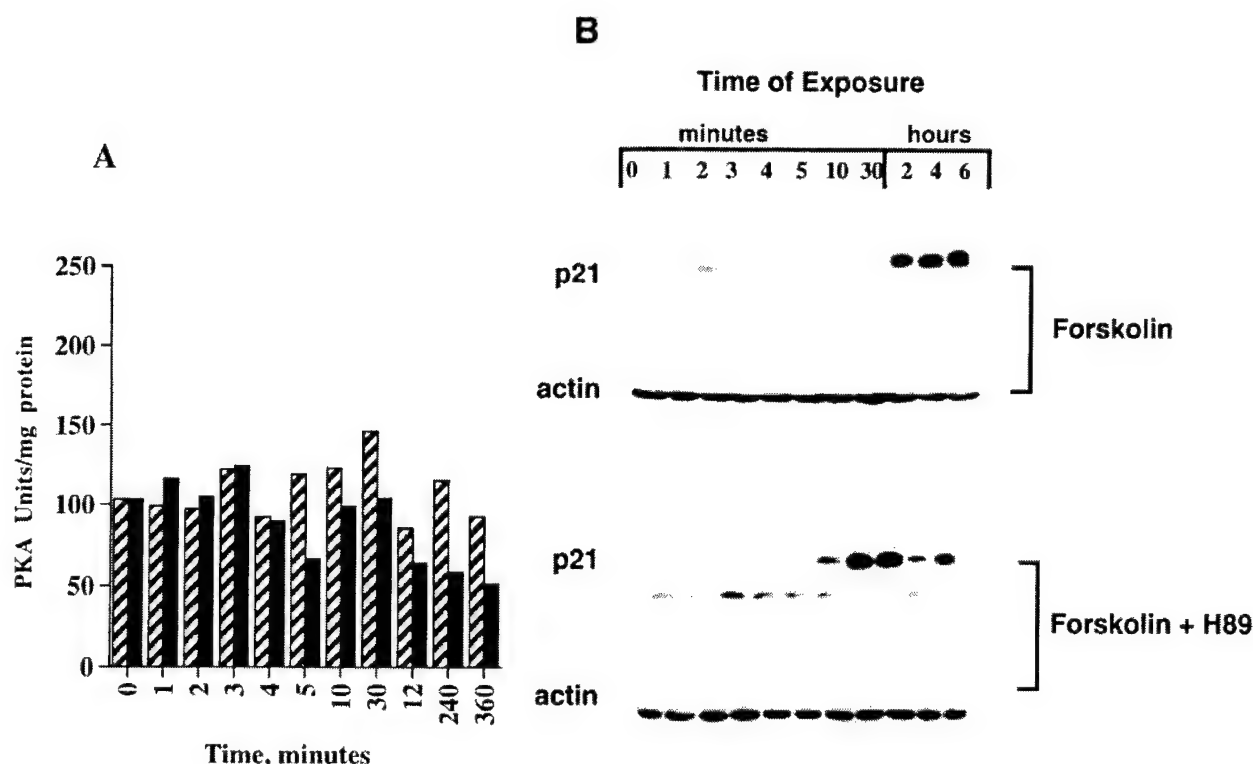
FIG. 5. P21 is induced by forskolin in dominant negative PKA mutants. MDA-MB-157 cells (pool 12) transfected with dominant negative PKA were treated with 10 μM forskolin in the presence or absence of the potent PKA inhibitor H-89 for the indicated times. H-89 (10 μM was added to the cells 6 h prior to the addition of forskolin. Protein extracts from treated cells were analyzed for (A) PKA activity. (forskolin, hatched bars, forskolin + H89, solid bars) and (B) Western blot analysis as described in Fig. 3.

treatment) it did not completely inhibit the PKA enzyme activity in the presence of forskolin, suggesting that the stably transfected cells still have low levels of PKA activity. These low levels of inducible PKA activity could account for p21 induction by forskolin or CT + IBMX. To rule out this possibility, H-89 was used to completely inactivate PKA in these cells transfected with the dominant negative PKA. Addition of H-89 6 h prior to forskolin to the dominant negative PKA mutants was able to completely eliminate the PKA activity in these cells even in the presence of forskolin (Fig. 5A). However, Western blot analysis of these PKA mutant clones treated in the presence or absence of H-89 revealed that p21 expression is increased by forskolin regardless of PKA activity (Fig. 5B). These results corroborate our earlier observations (Figs. 3 and 4), suggesting that p21 induction by forskolin is independent of PKA activity.

Lovastatin, an inducer of both p21 and p27 in MDA-MB-157 cells, does not activate PKA. The above results indicate that both cAMP and lovastatin induce p21 with a similar and biphasic pattern of induction and that the cAMP-mediated induction is by a PKA-independent mechanism. Recent studies suggest that lovastatin modulates cAMP levels in both cells [59] and in patients [46] and decreases prolactin and growth hormone gene expression in GH4C1 cells by decreasing cAMP levels [44]. Additionally lovastatin suppresses protein prenylation and hence affects the proper localization of several G proteins (including Ras) which in turn can affect the activation of adenyl cyclase [44]. Hence, a mechanism by which lovastatin induces p21 may be through the modulation of intracellular cAMP levels and activation of PKA. We directly examined this hypothesis by measuring PKA activity during the lovastatin-mediated induction of p21 and p27 both in

FIG. 6. Lovastatin-mediated induction of p21 is not PKA dependent. MDA-MB-157 cells were cultured in medium containing 40 μM lovastatin. At the indicated times cell extracts were prepared and assayed for (A) PKA activity and (B) Western blot analysis with the indicated antibodies. (C) To examine the effect of H89 on lovastatin-mediated induction of p21 and p27, MDA-MB-157 cells were cultured in medium containing 40 μM lovastatin in the presence or absence of 10 μM H89 (PKA inhibitor). At the indicated times cell extracts were prepared and subjected to Western blot analysis with the indicated antibodies. The same blots were sequentially hybridized with different antibodies (see Materials and Methods). The blots were stripped between the antibodies in 100 mM 2-mercaptoethanol, 62.5 mM Tris–HCl (pH 6.8), and 2% SDS for 10 min at 55°C.
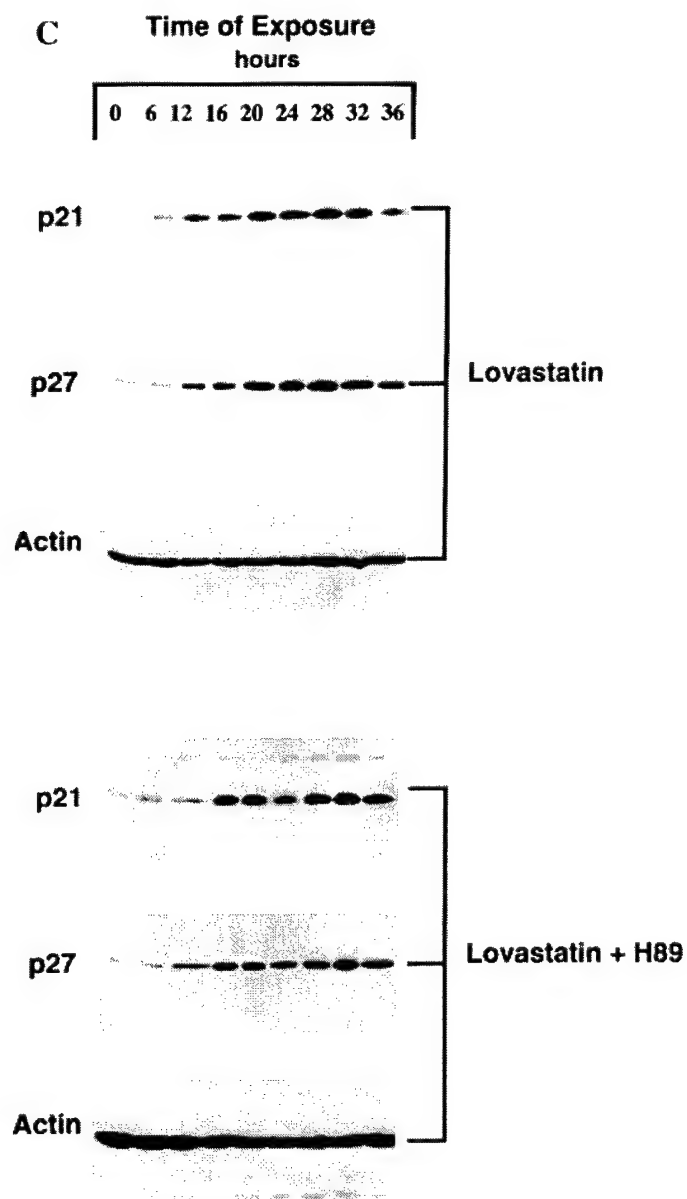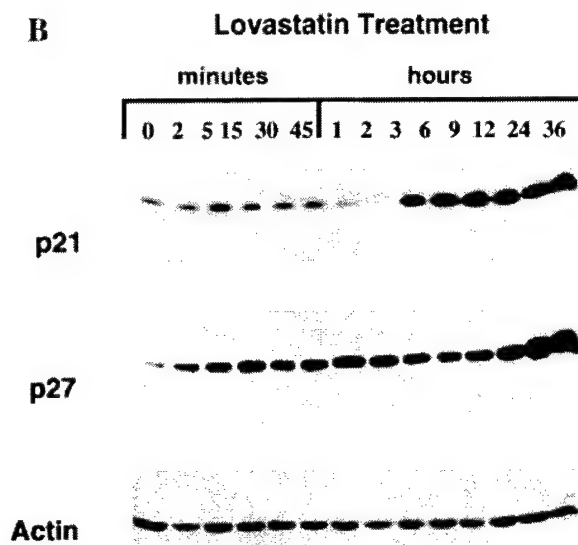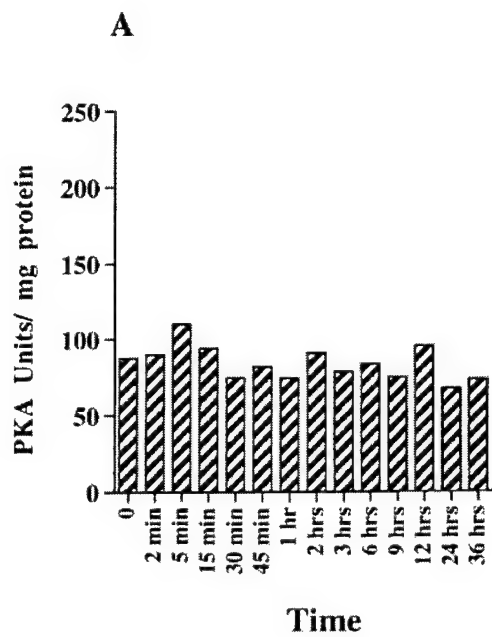
the presence and in the absence of the PKA inhibitor, H-89 (Fig. 6).

We measured PKA activity as well as p21 and p27 levels in the presence or absence of H-89 as shown in Fig. 6. PKA activity in MDA-MB-157 cells did not increase following treatment with 40 μM lovastatin at any of the time intervals examined (i.e., 0, 2, 5, 15, 30, and 45 min and 1, 2, 3, 6, 9, 12, 24, and 36 h) (Fig. 6A). The different time intervals were chosen as cAMP-PKA activity occurs extremely rapidly after treatment, while lovastatin induction of p21 and p27 occurs following several hours of treatment. Western blot analysis of cell extracts from cells treated with lovastatin revealed that p21 levels increased after 3 h and p27 levels increased after 12 h of treatment (Fig. 6B). The addition of H-89 with lovastatin to MDA-MB-157 cells did not alter the lovastatin-mediated induction of p21 and p27 at any time interval examined in these cells (Fig. 6C). Upon longer exposure, the low-molecular-weight forms of both p21 and p27 were apparent in lovastatin-treated cell extracts (data not shown). These results confirm that lovastatin-mediated induction of p21 and p27 is also through a pathway independent of PKA activity.

DISCUSSION

Increased intracellular levels of cAMP have been associated with the inhibition of cell growth in a number of different breast epithelial cells [31, 42], yet the mechanism of growth arrest is poorly understood. In the present study we investigated the pathway by which cAMP modulators, CT, IBMX, forskolin, and lovastatin induced the expression of the cyclin kinase inhibitor p21 in MDA-MB-157 breast tumor cell lines. The induction of the CKIs by lovastatin and CT + IBMX fluctuates with biphasic kinetics and is depicted by the periodic accumulation of lower molecular weight forms of p21 and p27 which correlate with fluctuations in CDK2 activity. Using three different approaches we also show that the cAMP-mediated induction of CKIs is independent of PKA activity. First, the addition of H-89, a PKA inhibitor which eliminated PKA activity in forskolin-treated MDA-MB-157 cells, was unable to affect p21 induction by forskolin or CT + IBMX. However, treatment of MDA-MB-157 cells with forskolin elevated PKA activity, suggesting modulation of the cAMP levels. Second, dominant negative mutants for PKA were able to respond to forskolin, CT, and IBMX by inducing p21 even in the absence of PKA activity. Finally, lovastatin, which also modulates cAMP levels and is a mediator of p21 and p27 induction, did not require the activity of PKA in the induction of the CKIs. These results taken together suggest that CKI induction mediated by cAMP modulators does not require the activity of PKA.

Although most of cAMP-associated events are a di-

rect result of PKA, there are examples of processes that are cAMP mediated but independent of PKA. For example, cAMP has been shown to directly activate a specific type of ion channel, the cyclic nucleotide-gated (CNG) ion channels without the activation of PKA [60–62]. This hypothesis has been substantiated by other studies showing that cAMP mediates the opening of Ca^{2+} and K^+ ion channels in cardiac pacemaker cells by directly binding to the channels and opening of these channels independent of PKA activity [61]. The activation of CNG channels by cAMP in a PKA-independent fashion has also been demonstrated in olfactory sensory neuronal cells and more recently in mammalian sperm [63, 64]. Additionally, the CNG channel identified in sperm has been demonstrated to be directly opened to cAMP and cGMP and are thought to mediate Ca^{2+} entry [63]. Similarly the secretion of β-endorphin by AtT20 cells following stimulation by vasoactive intestinal peptide is cAMP dependent, but does not require the presence of PKA or protein kinase C [65]. Last, a recent study [60] also showed that the inward current (which is sodium ion dependent), generated by oxytocin, a neuromodulator, in rat vagal neurons was cAMP dependent but PKA independent.

We postulate that in our cells the cAMP modulators CT + IBMX may act on a similar Ca^{2+} CNG in order to effect the observed cellular response and induction of p21 and p27. We base this hypothesis on two observations: First, the induction of CKIs by cAMP modulators is PKA independent, and second, the induction of the CKIs by both CT + IBMX and lovastatin is characterized by a biphasic pattern of accumulation and degradation. It is important to note that although forskolin was able to induce p21-like CT + IBMX and lovastatin, it did not do so in a biphasic manner or with the accumulation of lower molecular weight forms, suggesting that forskolin might not be as potent an activator of the Ca^{2+} CNG channels as CT + IBMX or that it may not inhibit the proteasome as readily as lovastatin (see below). The biphasic pattern of CKI expression seen with CT + IBMX and lovastatin seems to be mediated by posttranscriptional mechanism which is capable of generating lower molecular weight fragments of p21 and p27. Both these CKIs are regulated by the ubiquitin/proteasome degradation pathway [28, 66, 67]. Differences in ubiquitination activity observed in proliferating and quiescent cells contribute to the observed differences in p27 half-life [28, 67].

Recently, we have determined that the mechanism by which lovastatin mediates the induction of p21 and p27 is via proteasome inhibition, independent of the cholesterol biosynthesis pathway [68]. We show that the β-lactone, closed ring of lovastatin directly inhibits the proteasome multienzyme complex both *in vivo* and *in vitro,* and this inhibition fully accounts for the accumulation of both p21 and p27 following lovastatin treatment [68]. In the present study, we also show that

following lovastatin or CT + IBMX treatment, there is a significant accumulation of both p21 and p27, which appears with a biphasic kinetics posttranscriptionally. Furthermore, we show that following the accumulation of p21 and p27 there is a periodic accumulation of lower molecular weight forms of these CKIs which can bind to and inhibit CDK2 activity. We propose that the appearance of the lower molecular weight forms of p21 and p27 is a result of proteolytic degradation of these CKIs which can now be detected since the proteasome pathway has been inhibited by either lovastatin or CT + IBMX treatment. The proteasome activity responsible for the degradation of p21 and p27 not only is modulated by a cAMP mediated pathway but also could be regulated by the Ca^{2+} CNG channels. There are several examples of proteasome modulation by Ca^{2+} CNG channels: (A) The osteoblast proliferation is modulated by parathyroid hormone by enhancing the ubiquitinylation of protein substrates and stimulating proteasome activity through a cAMP-dependent mechanism [69]. (B) The proteasome regulation of the dynein light chain responsible for the motility of samonid fish sperm is through a cAMP-dependent phosphorylation of this protein [70]. (C) Increases in pineal serotonin N-acetyltransferase activity, responsible for the regulation of melatonin in vertebrates, is modulated by selective proteasomal proteolysis, regulated by cAMP [71]. (D) The intracellular levels of cAMP responsible for the regulation of cAMP-dependent transcriptional response itself is regulated by degradation via the ubiquitin–proteasome pathway [72]. Last, the CNG channels which regulate the cAMP levels intracellularly are also regulated by the ubiquitination/proteasome pathway [73]. For example, an activator of the 20S proteasome, REG, has been shown to bind calcium and subsequently regulate proteasome activity [74].

We postulate that modulation of cAMP pathway by CT + IBMX, forskolin, or lovastatin is via the CNG channels' ability to modify the proteasome activity. Treatment of cells by these agents results in accumulation of the CKIs in their intact and proteolyzed low-molecular-weight states. Intact CKIs may have either a stimulating or an inhibiting effect on CDK activity as previously reported [75]. The data presented here suggest that an additional determinant designating the potency of CKI inhibitory function is the size of the CKIs, intact versus the lower molecular weight form observed in cells treated with wither CT + IBMX or lovastatin. Both p21 and p27 proteins contain distinct functional domains regulating PCNA binding, CDK binding, and nuclear localization. It has been suggested that the amino- and carboxy-terminus domains of p27 function distinctly with the amino-terminus inhibiting and carboxy-terminus activating CDK complex activities [76]. We propose that the proteolyzed fragments of p21 and p27 may act as superinhibitory molecules as CDK2 complexes containing these frag-

ments possess extremely low levels of H1 kinase activity. Our data suggest the novel finding that p21 and p27 are subject to proteasome-mediated proteolysis which renders them more potent CDK inhibitor molecules.

In summary, we show that inducers of cAMP levels such as CT + IBMX, forskolin, or lovastatin are capable of inducing p21 and p27 in a biphasic pattern, posttranscriptionally. We also show that knocking out the activity of PKA either by transfection with a dominant negative PKA cDNA or pharmacologically by a specific and potent PKA inhibitor failed to block induction of p21 by inducers of cAMP. These results suggest that the cAMP induction of p21 is independent of PKA activity. We suggest that one possible mechanism which could give rise to the cAMP-dependent, PKA-independent biphasic and posttranscriptional regulation of CKIs in breast cancer could be via inhibition of the proteasome pathway through modulation of the CNG channels.

REFERENCES

1. Sherr, C. J. (1996). Cancer cell cycles. *Science* **274**, 1672–1677.
2. Sherr, C. J. (1994). G1 phase progression: Cycling on cue. *Cell* **79**, 551–555.
3. Elledge, S. J. (1996). Cell cycle checkpoints: Preventing an identity crisis. *Science* **274**, 1664–1671.
4. Nasmyth, K. (1996) Viewpoint: Putting the cell cycle in order. *Science* **274**, 1643–1651.
5. Elledge, S. J., and Harper, J. W. (1994) Cdk inhibitors; On the threshold of checkpoints and development. *Curr. Opin. Cell Biol.* **6**, 847–852.
6. Sherr, C. J., and Roberts, J. M. (1995) Inhibitors of mammalian G1 cyclin-dependent kinases. *Genes Dev.* **9**, 1149–1163.
7. Harper, J. W., and Elledge, S. J. (1996) CDK inhibitors in development and cancer. *Curr. Opin. Genes Dev.* **6**, 56–64.
8. Harper, J. W. (1997) Cyclin dependent kinase inhibitors. *Cancer Surv.* **29**, 91–108.
9. Elledge, S. J., Winston, J., and Harper, J. W. (1996). A question of balance: The role of cyclin-kinase inhibitors in development and tumorigenesis. *Tr. Cell Biol.* **6**, 388–392.
10. El-Deiry, W. S., Tokino, T., Velculescu, V. E., Levy, D. B., Parsons, R., Trent, J. M., Lin, D., Mrcer, W. E., Kinzler, K. W., and Vogelstein, B. (1993) WAF-1, a potential mediator of p53 tumor suppression. *Cell* **75**, 817–825.
11. Gu, Y., Turck, C. W., and Morgan, D. O. (1993) Inhibition of cdk2 activity *in vivo* by an associated 20K regulatory subunit. *Nature* **366**, 707–710.
12. Harper, J. W., Adami, G. R., Wei, N., Keyomarsi, K., and Elledge, S. J. (1993) The p21 Cdk-interacting protein Cip1 is a potent inhibitor of G1 cyclin-dependent kinases. *Cell* **75**, 805–816.

13. Xiong, Y., Hannon, G. J., Zhang, G. J., Gasso, D., Kobayashi, R., and Beach, D. (1993) p21, a universal inhibitor of cyclin kinases. *Nature* **366,** 710–704.

14. Noda, A. F., Ning, Y., Venable, S., Pereira-Smith, O. M., and Smith, J. R. (1994) Cloning of senescent cell-derived inhibitors of DNA synthesis using an expression screen. *Exp. Cell. Res.* **211,** 90–98.

15. Jiang, H., and Fisher, P. B. (1993) Use of a sensitive and efficient subtraction hybridization protocol for the identification of genes differentially regulated during the induction of differentiation in human melanoma cells. *Mol. Cell. Diff.* **3,** 285–299.

16. Wu, H., Wade, M., Krall, L., Grisham, J., Xiong, Y., and Van Dyke, T. (1996) Targeted *in vivo* expression of the cyclin-dependent kinase inhibitor p21 halts hepatocyte cell-cycle progression, postnatal liver development and regeneration. *Genes Dev.* **10,** 245–260.

17. Dulic, V., Kaufman, W. K., Wilson, S., Tlisty, T. D., Lees, E., Harper, J. W., Elledge, S. J., and Reed, S. I. (1994) p53-dependent inhibition of cyclin dependent kinase activities in human fibroblasts during radiation-induced G1 arrest. *Cell* **76,** 1013–1023.

18. Michieli, P., Chedid, M., Lin, D., Pierce, J. H., Mercer, W. E., and Givol, D. (1994) Induction of WAF1/CIP1 by a p53-independent pathway. *Cancer Res.* **54,** 3391–3395.

19. Sheikh, M. S., X., L., Chen, J., Shao, Z., Ordonez, J. V., and Fontana, J. A. (1994) Mechanisms of regulation of WAF1/Cip1 gene expression in human breast carcinoma: Role of p53-dependent and independent signal transduction pathways. *Oncogene* **9,** 3407–3415.

20. Elbendary, A., Berchuck, A., Davis, P., Havrilesky, L., Bast, J., R. C., Iglehart, J. D., and Marks, J. R. (1994) Transforming growth factor B1 can induce CIP1/WAF1 expression independent of the p53 pathway in ovarian cancer cells. *Cell Growth Diff.* **5,** 1301–1307.

21. Gray-Bablin, J., Rao, S., and Keyomarsi, K. (1997) Lovastatin induction of cyclin-dependent kinase inhibitors in human breast cells occurs in a cell cycle independent fashion. *Cancer Res.* **57,** 604–609.

22. Rao, S., Lowe, M., Herliczek, T., and Keyomarsi, K. (1998) Lovastatin mediated G1 arrest in normal and tumor breast cells in through inhibition of CDK2 activity and redistribution of p21 and p27, independent of p53. *Oncogene* **17,** 2393–2402.

23. Polyak, K., Lee, M.-H., Erdjument-bromage, H., Tempst, P., and Massaague, J. (1994) Cloning of p27KIP1, a cyclin-dependent kinase inhibitor and potential mediator of extracellular antimotogenic signals. *Cell* **78,** 59–66.

24. Polyak, K., Kato, J.-Y., Soloman, M. I., Sherr, C. J., Massague, J., Roberts, J. M., and Koff, A. (1994) p27KIP1, a cyclin-cdk inhibitor, links transforming factorβ and contact inhibition to cell cycle arrest. *Genes Dev.* **8,** 9–22.

25. Toyoshima, H., and Hunter, T. (1994) p27, a novel inhibitor of G1 cyclin-cdk protein kinase activity, is related to p21. *Cell* **78,** 67–74.

26. Hengst, L., Dulic, V., Slingerland, J. M., Lees, E., and Reed, S. I. (1994) A cell cycle-regulated inhibitor of cyclin-dependent kinases. *Proc. Natl. Acad. Sci. USA* **91,** 5291–5295.

27. Hengst, L., and Reed, S. I. (1996) Translational control of p27Kip1 accumulation during the cell cycle. *Science* **271,** 1861–1864.

28. Pagano, M., Tam, S. W., Theodoras, A. M., Beer-Romero, P., Del Sal, G., Chau, V., Yew, R. P., Draetta, G. F., and Rolfe, M. (1995) Role of the ubiquitin–proteosome pathway in regulating abundance of the cyclin-dependent kinase inhibitor p27. *Science* **269,** 682–685.

29. Starzec, A. B., Spanakis, E., Nehme, A., Salle, V., Veber, N., Mainguene, C., Planchon, P., Valette, A., Prevost, G., and Israel, L. (1994) Proliferative responses of epithelial cells to 8-bromo-cyclic AMP and to a phorbol ester change during breast pathogenesis. *J. Cell. Phys.* **161,** 31–38.

30. Mann, D. J., Higgins, T., Jones, N. C., and Rozengurt, E. (1997) Differential control of cyclins D1 and D3 and the cdk inhibitor p27Kip1 by diverse signalling pathways in Swiss 3T3 cells. *Oncogene* **14,** 1759–1766.

31. Revillion, F., Vandewalle, B., Lassalle, B., and Lefebvre, J. (1992) cAMP effect on extracellular matrix synthesis in human breast cancer cells. *Cell Prol.* **25,** 633–642.

32. Agarwal, K. C., and Parks, R. E. (1983) Forskolin: A potential antimetastatic agent. *Int. J. Cancer* **32,** 801–804.

33. Kato, J., Matsuoka, M., Polyak, K., Massague, J., and Sherr, C. J. (1994) Cyclic AMP-induced G1 phase arrest mediated by an inhibitor (p27^{Kip1}) of cyclin-dependent kinase 4 activation. *Cell* **79,** 487–496.

34. Trepel, J. B., Colamonici, O. R., Kelly, K., Schwab, G., Watt, R. A., Sausville, E. A., Jaffe, E. S., and Neckers, L. M. (1987) Transcriptional inactivatio of -myc and the transferrin receptor in dibutyryl cyclic AMP-treated HL-60 cells. *Mol. Cell. Biol.* **7,** 2644–2648.

35. Slungaard, A., Confer, D. L., and Schubach, W. H. (1987) Rapid transcriptional down-regulation of c-myc expression during cyclic adenosine monophosphate-promoted differentiation of leukemic cells. *J. Clin. Invest.* **79,** 1542–1547.

36. Bang, Y. J., Kim, S. J., Danielpour, D., O'Reilly, M. A., Kim, K. Y., Myers, C. E., and Trepel, J. B. (1992) Cyclic AMP induces transforming growth factor β2 gene expression and growth arrest in the human androgen-independent prostate carcinoma cell line PC-3. *Proc. Natl. Acad. Sci. USA* **89,** 3556–3560.

37. Sewing, A., Burger, C., Brusselbach, S., Schalk, C., Lucibello, F. C., and Muller, R. (1993) Human cyclin D1 encodes a labile nuclear protein whose synthesis is directly induced by growth factors and suppressed by cyclic AMP. *Cell Sci.* **104,** 545–554.

38. Friessen, A. J., Miskimins, W. K., and Miskimins, R. (1987) Cyclin-dependent kinase inhibitor p27kip1 is expressed at high levels in cells that express a myelinating phenotype. *J. Neuro. Res.* **50,** 373–382.

39. Vallejo, M., and Habener, J. F. (1994) Mechanisms of transcriptional regulation by cAMP. *In* "Transcription: Mechanisms and Regulation," pp. 353–368, Raven Press, Ltd., New York.

40. Laurenza, A., Sutkowski, E. M., and Seamon, K. B. (1989) Forskolin: A specific stimulator of adenylyl cyclase or a diterpene with multiple sites of action? *Trends Pharmacol. Sci.* **10,** 442–447.

41. Viallet, J., Sharoni, Y., Frucht, H., Jensen, R. T., Minna, J. D., and Sausville, E. A. (1990) Cholera toxin inhibits signal transduction by several mitogens and the *in vitro* growth of human small-cell lung cancer. *J. Clin. Invest.* **86,** 1904–1912.

42. Drees, M., Zimmermann, R., and Eisenbrand, G. (1993) 3′,5′-Cyclic nucleotide phosphodiesterase in tumor cells as potential target for tumor growth inhibition. *Cancer Res.* **53,** 3058–3061.

43. Kaur, G., Stetler-Stevenson, M., Sebers, S., Worland, P., Sedlacek, H., Myers, C., Czech, J., Naik, R., and Sausville, E. (1992) Growth inhibition with reversible cell cycle arrest of carcinoma cells by falvone L86-8275. *J. Natl. Cancer Inst.* **84,** 1736–1740.

44. Lasa, M., Chiloeches, A., Garcia, N., Montes, A., and Toro, M. J. (1997) Lovastatin decreases prolactin and growth hormone gene expression in GH4C1 cells through a cAMP dependent mechanism. *Mol. Cell. Endocrinol.* **130,** 93–100.

45. Ecay, T. W., and Valentich, J. D. (1993) Lovastatin inhibits cAMP- and calcium-stimulated chloride secretion by T84 cells. *Am. J. Physiol.* **265,** C422–C431.

46. Kaczmarek, D., Hohfeld, T., Wambach, G., and Schror, K. (1993) The actions of lovastatin on platelet function and platelet eicosanoid receptors in type II hypercholesterolaemia. A double-blind, placebo-controlled, prospective study. *Eur. J. Clin. Pharmacol.* **45,** 451–457.

47. Retterstol, K., Stuggard, M., Gorbitz, C., and Ose, L. (1996) Results of intensive long term treatment of familial hypercholesterolemia. *Am. J. Cardiol.* **78,** 1369–1374.

48. Keyomarsi, K., Sandoval, L., Band, V., and Pardee, A. B. (1991) Synchronization of tumor and normal cells from G1 to multiple cell cycles by lovastatin. *Cancer Res.* **51,** 3602–3609.

49. Keyomarsi, K. (1996) Synchronization of mammalian cells by lovastatin. *Methods Cell Sci.* **18,** 109–114.

50. Terada, Y., Inoshita, S., Nakashima, O., Yamada, T., Kuwahara, M., Sasaki, S., and Marumo, F. (1998) Lovastatin inhibits mesangial cell proliferation via p27 Kip1. *J. Am. Soc. Nephrol.* **9,** 2235–2243.

51. Hirai, A., Nakamura, S., Noguchi, Y., Yasuda, T., Kitagawa, M., Tatsuno, I., Oeda, T., Tahara, K., Terano, T., Narumiya, S., Kohn, L. D., and Saito, Y. (1997) Geranylgeranylated rho small GTPase(s) are essential for the degradation of p27Kip1 and facilitate the progression from G1 to S phase in growth-stimulated rat FRTL-5 cells. *J. Biol. Chem.* **272,** 13–16.

52. Lee, S. J., Ha, M. J., Lee, J., Nguyen, P. M., Choi, Y. H., Pirnia, F., Kang, W.-K., Wang, X.-F., Kim, S.-J., and Trepel, J. B. (1998) Inhibition of the 3-hyroxy-3-methylglutaryl-coenzyme A reductase pathway induces p53-independent transcriptional regulation of p21 in human prostatic carcinoma cells. *J. Biol. Chem.* **273,** 10618–10623.

53. Arita, Y., Buffolino, P., and Coppock, D. L. (1998) Regulation of the cell cycle at the G2/M boundary in metastatic melanoma cells by 12-*O*-tetradecanoyl phorbol-13-acetate (TPA) by blocking p34cdc kinase activity. *Exp. Cell Res.* **242,** 381–390.

54. Vogt, A., Sun, J., Qian, Y., Hamilton, A. D., and Sebti, S. M. (1997) The geranylygeranyltransferase-I inhibitor GGTI-298 arrests human tumor cells in G0/G1 and induces p21 in a p53-independent manner. *J. Biol. Chem.* **272,** 27224–27229.

55. Keyomarsi, K., Conte, D., Toyofuku, W., and Fox, M. P. (1995) Deregulation of cyclin E in breast cancer. *Oncogene* **11,** 941–950.

56. Rogers, K. V., Goldman, P. S., Frizzell, R. A., and McKnight, G. S. (1990) Regulation of C1-transport of T84 cell clones expressing a mutant regulatory subunit of cAMP-dependent protein kinase. *Proc. Natl. Acad. Sci. USA* **87,** 8975–8979.

57. Clegg, C. H., Correll, L. A., Cadd, G. C., and McKnight, G. S. (1987) Inhibition of intracellular cAMP-dependent protein kinase using mutant genes of regulatory type I subunit. *J. Biol. Chem.* **262,** 13111–13119.

58. Steinberg, R. A., O'Farrell, P. H., Fiedrich, U., and Coffino, P. (1977) Mutations causing charge alterations in regulatory subunits of the cAMP-dependent protein kinase of cultured S49 lymphoma cells. *Cell* **10,** 381–391.

59. Ecay, T. W., and Valentich, J. D. (1993) Lovastatin inhibits cAMP- and calcium-stimulated chloride secretion by T84 cells. *Am. J. Physiol.* **265** (*Cell. Physiol.* **34**), C422–C431.

60. Alberi, S., Dreiguss, J., and Raggenbass, M. (1997) The oxytocin-induced inward current in bagal neurons of the rat is mediated by G protein activation but not by an increase in the intracellular calcium concentration. *Eur. J. Neuro.* **9,** 2605–2612.

61. DiFrancesco, D., and Tortora, P. (1991) Direct activation of cardiac pacemaker channels by intracellular cyclic AMP. *Nature* **351,** 145–147.

62. Nakamura, T., and Gold, G. H. (1987) A cyclic nucleotide-gated conductance in olfactory receptor cilia. *Nature* **325,** 442–444.

63. Wiesner, B., Weiner, J., Middendorff, R., Hagen, V., Kaupp, U. B., and Weyand, I. (1998) Cyclic nucleotide-gated channels on the flagellum control Ca2+ entry into sperm. *J. Cell Biol.* **142,** 473–484.

64. Weyand, I., Godde, M., Fringe, S., Weiner, J., Altenhofen, W., Hatt, H., and Kaupp, U. B. (1994) Cloning and functional expression of a cyclic-nucleotide-gated channel from mammalian sperm. *Nature* **368,** 859–863.

65. Schecterson, L. C., and McKnight, G. S. (1991) Role of cyclic adenosine 3′,5′-monophosphate-dependent protein kinase in hormone-stimulated β-endorphin secretion in AtT20 cells. *Mol. Endocrinol.* **5,** 170–178.

66. Blagosklonny, M. V., Wu, G. S., Mura, S., and Eldeiry, W. S. (1996) Proteosome dependent regulation of p21 expression. *Biochem. Biophys. Res. Commun.* **227,** 564–569.

67. Pagano, M. (1997) Cell cycle regulation by the ubiquitin pathway. *FASEB J.* **11,** 1067–1075.

68. Rao, S., Porter, D. C., Chen, X., Herliczek, T., Lowe, M., and Keyomarsi, K. (1999) Lovastatin-mediated G1 arrest is through inhibition of the proteasome, independent of hydroxymethyl glutaryl-CoA reductase. *Proc. Natl. Acad. Sci. USA* **96,** 7797–7802.

69. Murray, E. J., Bentley, G. V., Grisanti, M. S., and Murray, S. S. (1998) The ubiquitin–proteasome system and cellular proliferation and regulation in osteoblastic cells. *Exp. Cell Res.* **242,** 460–469.

70. Inaba, K., Morisawa, S., and Morisawa, M. (1998) Proteasomes regulate the motility of salmonid fish sperm through modulation of cAMP-dependent phosphorylation of an outer arm dynein light chain. *J. Cell Sci.* **111,** 1105–1115.

71. Gastel, J. A., Roseboom, P. H., Rinaldi, P. A., Weller, J. L., and Klein, D. C. (1998) Melatonin production: Proteasomal proteolysis in serotonin *N*-acetyltransferase regulation. *Science* **279,** 1358–1360.

72. Falco, E. J., and Koren, G. (1997) Degradation of the inducible cAMP early repressor (ICER) by the ubiquitin–proteasome pathway. *Biochem. J.* **328,** 37–43.

73. Staub, O., Gautschi, I., Ishikawa, T., Breitschopf, K., Ciechanover, A., Schild, L., and Rotin, D. (1997) Regulation of stability and function of the epithelial Na+ channel (ENaC) by ubiqitination. *EMBO J.* **16,** 6325–6336.

74. Realini, C., and Rechsteiner, M. (1995) A proteasome activator subunit binds calcium. *J. Biol. Chem.* **270,** 29664–29667.

75. LaBaer, J., Garrett, M. D., Stevenson, L. F., Slingerland, J., Sandhu, C., Chou, H. S., Fattaey, A., and Harlow, E. (1997) New functional activities for the p21 family of cdk inhibitors. *Genes Dev.* **11,** 847–862.

76. Font de Mora, J., Uren, A., Heidaran, M., and Santos, E. (1997) Biological activity of p27kip1 and its amino- and carboxy-terminal domains in G2/M transition of Xenopus oocytes. *Oncogene* **15,** 2541–2551.

Lovastatin-mediated G₁ arrest is through inhibition of the proteasome, independent of hydroxymethyl glutaryl-CoA reductase

SHARMILA RAO*, DONALD C. PORTER*, XIAOMEI CHEN*, THADDEUS HERLICZEK*, MICHAEL LOWE*, AND KHANDAN KEYOMARSI*†‡

*Laboratory of Diagnostic Oncology, Division of Molecular Medicine, Wadsworth Center, Albany, NY 12201-0509; and †Department of Biomedical Sciences, State University of New York, Albany, NY 12222

ABSTRACT   In this paper we present the finding that lovastatin arrests cells by inhibiting the proteasome, which results in the accumulation of p21 and p27, leading to G_1 arrest. Lovastatin is an inhibitor of hydroxymethyl glutaryl (HMG)-CoA reductase, the rate-limiting enzyme in cholesterol synthesis. Previously, we reported that lovastatin can be used to arrest cultured cells in the G_1 phase of the cell cycle, resulting in the stabilization of the cyclin-dependent kinase inhibitors (CKIs) p21 and p27. In this report we show that this stabilization of p21 and p27 may be the result of a previously unknown function of the pro-drug, β-lactone ring form of lovastatin to inhibit the proteasome degradation of these CKIs. The lovastatin mixture used in this study is 80% open-ring form and 20% pro-drug, β-lactone form. We show that while the lovastatin open-ring form and pravastatin (a lovastatin analogue, 100% open ring) inhibit the HMG-CoA reductase enzyme, lovastatin pro-drug inhibits the proteasome but does not inhibit HMG-CoA reductase. In addition, many of the properties of proteasome inhibition by the pro-drug are the same as the specific proteasome inhibitor lactacystin. Lastly, mevalonate (used to rescue cells from lovastatin arrest) unexpectedly abrogates the lactacystin and lovastatin pro-drug inhibition of the proteasome. Mevalonate increases the activity of the proteasome, which results in degradation of the CKIs, allowing lovastatin- and lactacystin-arrested cells to resume cell division. The lovastatin-mediated inhibition of the proteasome suggests a unique mechanism for the chemopreventative effects of this agent seen in human cancer.

Metabolic and cellular processes that require exquisite temporal precision, like the cell cycle, often involve selective proteolytic degradation of regulated proteins (1). One major degradative pathway capable of such activity is the proteasome pathway (2, 3). This pathway is involved in the regulation of diverse processes including embryogenesis, signal transduction, and cell cycle progression (2, 4). For example, degradation of several proteins involved in cell cycle regulation such as Clns, Clbs, cyclins A, B, D, E, p53, and pRb are via ubiquitin-mediated proteolysis (2, 4). The ubiquitin pathway also regulates the levels of cyclin-dependent kinase inhibitors (CKIs) p27 and p21 (5–7).

Proteasome activity is inhibited by several peptide aldehydes (e.g., LLnL) and compounds like 3,4-dichloroisocoumarin and lactacystin (8). Lactacystin, a Streptomyces metabolite containing a β-lactone ring, selectively inhibits proteolytic activities of the proteasome (8, 9). The moiety crucial for inhibition of the proteasome activity is the β-lactone electrophilic car-

bonyl, which targets enzymes containing a catalytic nucleophile such as a protease. In contrast, the dihydroxy acid form of lactacystin is essentially inert to nucleophilic attack and is incapable of inhibiting the proteasome (10). These findings suggest that the pro-drug form of another β-lactone, lovastatin, similar in structure to lactacystin, may inhibit the ubiquitin-mediated proteolysis of key regulatory proteins such as the cyclins and CKIs.

Lovastatin is used for the treatment of hypercholesterolemia (11) because it inhibits hydroxymethyl-glutaryl (HMG)-CoA reductase, and thus prevents HMG-CoA's conversion into mevalonic acid (12, 13). When mevalonate levels decrease as a response to lovastatin, isoprenylation of key signal transduction proteins (e.g., Ras, Rap, etc.) is prevented, their subcellular localization is disrupted, and they are inactivated as signal transducers (14). Administration of lovastatin to cells in culture impacts cell cycle progression. We have reported that lovastatin effectively synchronizes both tumor and normal cells (15) and arrests cells in G_1 (16, 17). The cell cycle pathways perturbed by lovastatin have been shown by several laboratories to result in the induction of CKIs p21 and/or p27 (16–21) independent of other standard G_1-arresting agents/conditions such as serum starvation or double thymidine block (17). Additionally, the lovastatin-mediated G_1 arrest and p21/p27 induction occur independently of the ras signaling pathway/function (22, 23).

How lovastatin induces G_1 arrest and simultaneously increases p21 and/or p27 currently is undefined. One simple explanation is that decreased cholesterol and/or its intermediary metabolites prevent cell cycle progression and that the induction of p21/p27 is a secondary event. Indeed because mevalonate releases arrested cells from G_1 block, it has been assumed that the target of lovastatin action is within the mevalonate/cholesterol pathway and that mevalonate or one of its downstream products is essential for cell division (20, 24).

The studies presented here suggest that alternative pathways may be targeted by lovastatin; these pathways may mediate the lovastatin effects on cell proliferation. We show that lovastatin in its pro-drug form (β-lactone) is entirely responsible for the effects on p21 and p27 leading to G_1 arrest. We identified the ubiquitin-proteasome pathway as an alternative, HMG-CoA independent, pathway and show that the pro-drug inhibits the proteasome both *in vitro* and *in vivo*. Our studies also suggest that an additional role for mevalonate is to abrogate the effects of both lactacystin and the pro-drug form of lovastatin by increasing the activity of the proteasome.

Abbreviations: HMG, hydroxymethyl glutaryl; CKI, cyclin-dependent kinase inhibitor.
‡To whom reprint requests should be addressed at: Wadsworth Center, Room C-400, Empire State Plaza, P.O. Box 509, Albany, NY 12201-0509. e-mail: keyomars@wadsworth.org.
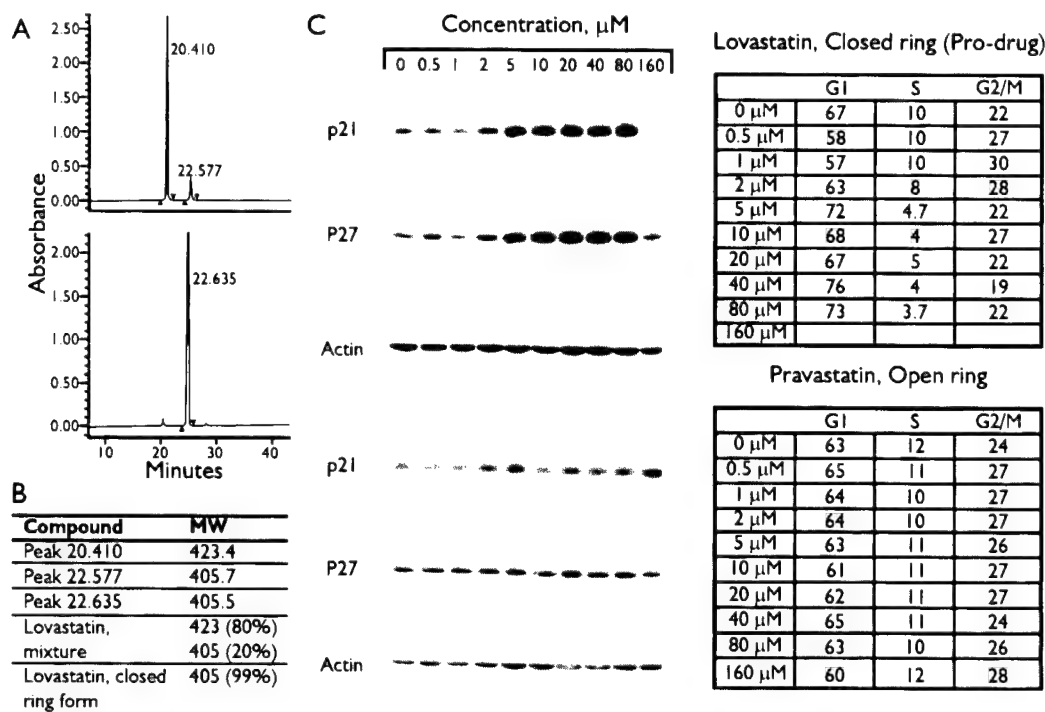
Lovastatin, Closed ring (Pro-drug)

	GI	S	G2/M
0 µM	67	10	22
0.5 µM	58	10	27
1 µM	57	10	30
2 µM	63	8	28
5 µM	72	4.7	22
10 µM	68	4	27
20 µM	67	5	22
40 µM	76	4	19
80 µM	73	3.7	22
160 µM			

Pravastatin, Open ring

	GI	S	G2/M
0 µM	63	12	24
0.5 µM	65	11	27
1 µM	64	10	27
2 µM	64	10	27
5 µM	63	11	26
10 µM	61	11	27
20 µM	62	11	27
40 µM	65	11	24
80 µM	63	10	26
160 µM	60	12	28

B

Compound	MW
Peak 20.410	423.4
Peak 22.577	405.7
Peak 22.635	405.5
Lovastatin, mixture	423 (80%) 405 (20%)
Lovastatin, closed ring form	405 (99%)

FIG. 1. Induction of CKIs by the β-lactone form of lovastatin. (*A*) Chromatographic separation of lovastatin mixture (*Upper*) and closed-ring form (*Lower*) by HPLC analysis as described (15, 25). (*B*) Fractions corresponding to each HPLC peak were collected and subjected to mass determination by electrospray ionization quadrupole mass spectrometry analysis as described (26). The lovastatin mixture and closed-ring forms also were subjected to mass spectrometry analysis to determine the components of each reagent. (*C*) MDA-MB-157 tumor cells were treated with the indicated concentrations of lovastatin pro-drug or pravastatin for 36 hr. Cells were harvested and subjected to either flow cytometry (*Right*) or Western blot analysis with the indicated antibodies (*Left*).

METHODS

Materials, Cell Lines, and Culture Conditions. Lovastatin was provided by William Henckler (Merck, Sharp, and Dohme Research Pharmaceuticals, Rahway, NJ) and was converted from its pro-drug form to its dihydroxy-open acid form as described (15). The pro-drug was soluble in 60% ethanol, and pravastatin was soluble in water. Treatments of MDA-MB-157 with lovastatin, its pro-drug form, pravastatin, LLnL, or lactacystin and Western blot analysis were performed as described (15, 16).

HPLC Analysis of Pro-Drug, Lovastatin, and Pravastatin. RP-HPLC using a Waters 625 chromatography system was performed as described (25). Briefly, a C 18 Novopac column was equilibrated with the stationary phase of 0.1% trifluoroacetic acid (TFA) and 90% acetonitrile as the mobile phase. Ten micrograms of lovastatin mixture or β-lactone (diluted 0.1% TFA) was analyzed by HPLC, and the eluted fractions were subjected to mass spectrometry as described (26).

Assay for HMG-CoA Reductase Activity. The HMG-CoA reductase assays in MDA-MB-157 cells were performed as described (27). Briefly, cells were homogenized by sonication in the reaction buffer (200 mM phosphate buffer pH 7.4/20 mM DTT/40 mM glucose-6-phosphate/3 mM β-NADPH/2 units/ml glucose-6-phosphatase), and the 20,000 $\times$ g supernatant was incubated with the pro-drug, lovastatin, or pravastatin at 37°C, followed by the addition of the [^{14}C] HMG-CoA. Samples were subjected to TLC with [^{14}C] mevalolactone (MVA) as standard and analyzed by PhosphorImager scanning. The efficiency of the enzymatic reaction is a measure of conversion of [^{14}C] HMG-CoA into [^{14}C] MVA formed and expressed as percent conversion per mg of microsomal protein.

Proteasome Activity Assay. For measurement of the proteasome chymotrypsin peptidase activity, 10 μl of cellular extract (100 μg, prepared by brief sonication of cells and fractionation at 16,000 $\times$ g) was diluted in a cuvette containing

2 ml of 20 mM Hepes, 0.5 M EDTA, pH 8, 0.035% SDS with the indicated concentrations of lactacystin, pro-drug, lovastatin, and pravastatin. The cell extracts contain a mixture of 26S and 20S proteasomes. (The proteasome assays of the pretreated cells were performed after treatment of MDA-MB-157 cells with the indicated drugs, and the medium was removed and the cells were washed several times before they were lysed to removed excess inhibitor). The above mixture was incubated at 37°C before the addition of the fluorogenic substrate, 10 μM succinyl-Leu-Leu-Val-Tyr-7-amido-4-methylcoumarin. Substrate hydrolysis was measured by continuous monitoring of fluorescence (emission at 440 nm, excitation at 380 nM) of the liberated 7-amido-4-methylcoumarin for 15 min as described (9).

^{35}S Metabolic Labeling for MDA-MB-157 Cells. Pulse–chase experiments with MDA-MB-157 were performed as described (18) with the following modifications. Cells were incubated in DMEM without methionine and cysteine and with β-lactone or no drug for 2 hr. EXPRESS [^{35}S]protein labeling mix (0.2 mCi; NEN/DuPont) was added, and the cells were pulse-labeled for 4 hr.

RESULTS

Lovastatin-Mediated Induction of p21 and p27 Is Independent of the HMG-CoA Reductase Block. Our hypothesis is that the induction of CKIs by lovastatin is not solely through inhibition of the HMG-CoA reductase pathway, but also through the inhibition of the proteasome pathway. We base this hypothesis on the structural similarities between the pro-drug form of lovastatin and lactacystin, a proteasome inhibitor. The chemical form of lovastatin likely to inhibit the proteasome pathway is the closed β-lactone ring (referred to herein as pro-drug) form, whereas the open-ring form inhibits the HMG-CoA reductase. The pro-drug form of lovastatin is routinely modified to its open dihydroxy acid form chemically as described (15) before treatment of cells. By using RP-HPLC
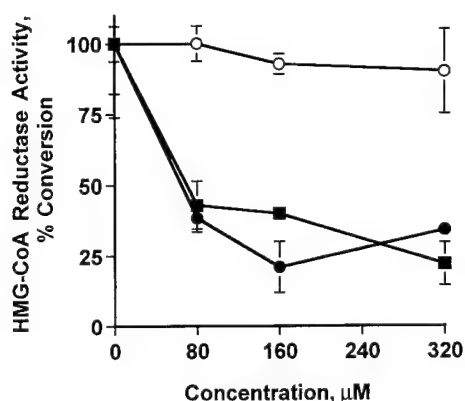
FIG. 2. Inactivation of HMG-CoA reductase enzyme by lovastatin. Microsomes (100 μg) prepared from subconfluent cultures of MDA-MB-157 were incubated at 37°C in the presence of the indicated concentrations of lovastatin, pro-drug, or pravastatin followed by the addition of ^{14}C-HMG-CoA. After the lactonization of the reaction with HCL, the samples were resolved by TLC and analyzed by PhosphorImaging. The activity of HMG-CoA reductase is a measure of the percent conversion of ^{14}C-HMG-CoA into mevalolactone, the end product of the HMG-CoA reductase. ●, lovastatin mixture; ○, pro-drug; ■, pravastatin.

we found that the chemical conversion of lovastatin from its pro-drug to open-ring form was 80% efficient; 20% of the lovastatin mixture after preparation remained in the unmodified pro-drug form (Fig. 1*A, Upper*). The pro-drug form of lovastatin elutes with the same HPLC retention time as the second peak of the modified lovastatin (Fig. 1*A, Lower*), showing that the actual prepared form of lovastatin used in our studies contains both forms. Electrospray ionization mass spectrometry analysis confirmed the identity of the eluted HPLC peaks (Fig. 1*B*). The first peak of the lovastatin mixture is the open-ring form, with a mass of 423 (and was 80% of the mixture), whereas the second peak had an identical mass as the pro-drug (i.e., 405), suggesting that they are the same compound. The ratio of the two forms is constant over time and not affected by the medium used (data not shown).

To determine which form of lovastatin (open or closed) is responsible for CKI induction cells were treated with either the pro-drug form of lovastatin or an analogue of lovastatin, called pravastatin, present only in its open-ring form. (Lovastatin cannot be prepared entirely as the open-ring form.) Pravastatin is similar in structure and potency to the open-ring form of lovastatin and does not require modification to inhibit HMG-CoA reductase activity. MDA-MB-157 cells were treated with the indicated concentrations of these two agents for 36 hr and analyzed by flow cytometry and Western blot (Fig. 1*C*). Treatment of cells with the pro-drug form of lovastatin resulted in inhibition of cell proliferation and pronounced CKI induction in a dose-dependent manner (Fig. 1*C*). The flow cytometric data shows that after treatment of cells with only 5 μM pro-drug the cells accumulate in the G_1 phase with a concomitant reduction in S phase. To achieve the same degree of growth inhibition, 40 μM of the chemically modified lovastatin (a mixture of open and closed forms) had to be used (data not shown and ref. 16). The highest concentrations of the pro-drug, i.e., 160 μM, resulted in apoptosis of most of the cells. Pravastatin, on the other hand, does not induce the CKIs or arrest cells at any concentration examined (Fig. 1*C*). Collectively these studies suggest that the pro-drug, closed-ring form of lovastatin, but not the open-ring form is responsible for the induction of p21 and p27. These observations also raise the hypothesis that the mechanism of CKI induction by lovastatin is not through the inhibition of the HMG-CoA reductase enzyme.
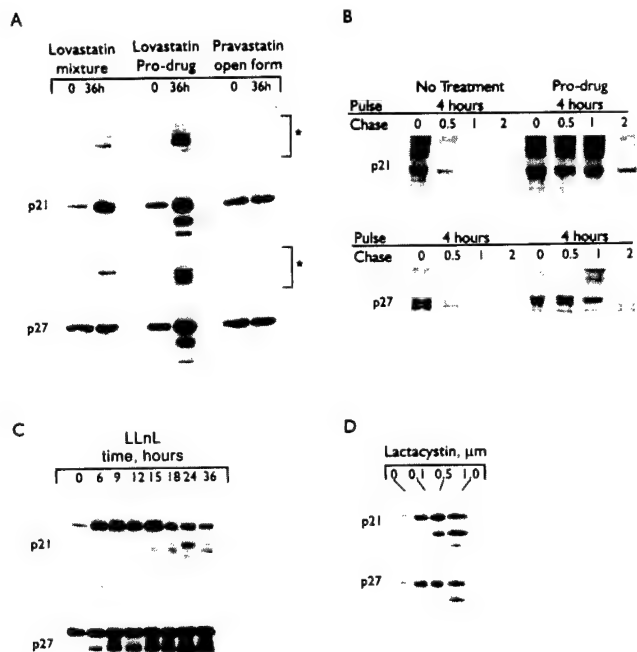
FIG. 3. Induction of p21 and p27 by proteasome inhibitors. MDA-MB-157 tumor cells were treated with (*A*) 40 μM of either lovastatin mixture (open and closed rings), lovastatin closed β-lactone ring (pro-drug), or pravastatin for 36 hr, (*C*) 10 μM LLnL for 0–36 hr, or (*D*) indicated concentrations of lactacystin for 24 hr and subjected (50 μg/lane) to Western blot analysis with the indicated antibodies. Brackets in *A* indicate the high molecular weight laddering of p21 and p27, diagnostic for poly-ubiquitination. (*B*) For turnover studies, cells were treated with 40 μM pro-drug (or no drug) for 36 hr at which point the cells were incubated for 4 hr with [^{35}S]methionine and [^{35}S]cysteine (pulse) and subsequently incubated in the presence of an excess of nonradioactive methionine and cysteine for the additional times indicated (chase). p21 and p27 were precipitated from nondenatured protein extracts with polyclonal antibodies (p27-C19 and p21-C19-G, Santa Cruz Biotechnology), separated by SDS/PAGE, and detected by autofluorography.

To directly determine the abilities of the lovastatin mixture, lovastatin pro-drug, and pravastatin to inhibit HMG-CoA reductase we prepared cell extracts from MDA-MB-157 cells and assayed for HMG-CoA reductase as described (27). The results of this assay revealed that while both pravastatin and the lovastatin mixture inhibited the HMG-CoA reductase in a dose-dependent manner the pro-drug form of lovastatin was incapable of inhibiting the activity of HMG-CoA reductase over the concentration range examined (Fig. 2). The data strongly suggest that the pro-drug form of lovastatin induces the CKIs through a pathway independent of HMG-CoA reductase and that inhibition of this enzyme may not be essential for CKI induction.

Inhibition of the Proteasome by Lovastatin. Previous reports have shown that both p21 and p27 are substrates for ubiquitination and proteasome-dependent degradation (5, 6, 28). Western blot analysis of cell extracts treated with lovastatin mixture and the pro-drug shows that antibodies to both p21 and p27 recognize specific proteins of higher molecular masses (i.e., 70–90 kDa) that are likely to correspond to ubiquitinated forms of these CKIs (Fig. 3*A*). Pravastatin does not cause similar results. The pro-drug affects the stability of p21 and p27 by altering the turnover rates of these CKIs. Compared with untreated cells, the pro-drug-treated cells degraded both p21 and p27 much more slowly (Fig. 3*B*). The increased half-life (0.13 versus 1.5 hr for both p21 and p27) accounts for the net increase of protein observed from drug treatment (Fig. 3*B*). Furthermore, treatment of cells with two

different proteasome inhibitors (LLnL and lactacystin) resulted in a dramatic induction of p21 and p27 in a dose- and time-dependent fashion (Fig. 3 *C* and *D*). This finding suggests that the proteasome pathway has a role in the lovastatin-mediated stabilization of the CKIs.

We next evaluated the kinetics of proteasome inhibition by the pro-drug form of lovastatin (Fig. 4). The ability of lactacystin, the pro-drug, lovastatin mixture, and pravastatin to inhibit the proteasome complex (a mixture of 26S and 20S proteasomes) in MDA-MB-157 cell extracts was measured directly by using a fluorescence assay containing a fluorogenic peptide substrate for the chymotrypsin-like activity of this complex (29, 30). Lactacystin was capable of inhibiting the peptidase activity of the proteasome completely at 1 μM (Fig. 4*A*). The pro-drug also inhibits the proteasome activity in a dose-dependent fashion with half-maximal inhibition occurring at 40 μM. The lovastatin mixture, which contains only 20% of the pro-drug form, also inhibited the proteasome activity but at much higher concentrations, reflecting the low percentage of the pro-drug form and that in the mixture, lovastatin may block the peptidase mediated inhibition by the pro-drug. Pravastatin, on the other hand, was incapable of inhibiting the proteasome over the concentration ranges examined (i.e., up to 6.4 mM) (Fig. 4*A*). This analysis clearly revealed that the pro-drug form of lovastatin inhibits the proteasome activity *in vitro*. Because the concentration required to inhibit the proteasome *in vitro* is higher than that used to arrest cells, we also performed the proteasome experiments *in vivo* by first treating cells with the inhibitors, followed by measurement of the peptidase activity of the proteasome (Fig. 4*B*). These analyses revealed that lovastatin mixture, its pro-drug form, and lactacystin inhibited the activity of the proteasome at concentrations similar to those required to achieve G_1 arrest *in vivo*. Differences in drug potency *in vivo* and *in vitro* are likely caused by different rates of uptake and metabolism. Furthermore, mevalonate was able to abrogate the inhibitory activity of these agents on the proteasome (Fig. 4*B* and see below). These studies (Figs. 1–4) suggest that a specific proteasome-mediated pathway contributes to increased expression, via stabilization, of p21 and p27 in cells treated with the lovastatin mixture or the pro-drug.

Mevalonate Abrogates the Lovastatin- and Lactacystin-Mediated Inhibition of the Proteasome. In this study we are proposing that mevalonate also has a dual function. Mevalonate reverses the lovastatin inhibition of HMG-CoA reductase and restores cholesterol biosynthesis. Unexpectedly, mevalonate also abrogates the lactacystin/pro-drug inhibition of the proteasome. Fig. 5*A* shows that the G_1 arrest mediated by both lovastatin and its pro-drug form can be abrogated by mevalonate. Because the pro-drug form of lovastatin does not inhibit HMG-CoA reductase (Fig. 2), it follows that mevalonate must have another role in reversing the pro-drug mediated G_1 arrest. If our hypothesis is correct and the lovastatin-mediated inhibition of the proteasome leads to G_1 arrest, then mevalonate should modulate proteasome activity. We directly addressed the ability of mevalonate to abrogate the effects of lactacystin on cells (Fig. 5*B*). Treatment of cells with 10 μM lactacystin resulted in significant (i.e., 70%) apoptosis of cells (Fig. 5*B*). [Lactacystin (10 μM) also completely inhibited the proteasome activity as shown in Fig. 4.] Intriguingly, when cells were treated with lactacystin in the presence of increasing concentrations of mevalonate, the lactacystin-mediated apoptosis was completely abrogated. However, addition of mevalonate after lactacystin does not reverse the apoptotic effects of lactacystin (data not shown). These results show that mevalonate abrogates the effects of lactacystin inhibition of the proteasome *in vivo*.

The reversal of lovastatin-mediated inhibition of HMG-CoA reductase by mevalonate is biochemically sound and documented extensively. However, the abrogation of proteasome inhibition by mevalonate represents an exciting enigma, because it suggests a unique function for mevalonate. One way mevalonate might abrogate proteasome inhibition is through activation of the proteasome itself. To examine whether mevalonate could modulate the proteasome activity we pretreated cells with increasing concentrations of mevalonate for 36 hr and measured the proteasome activity (29, 30). These studies in two breast cancer cell lines (MDA-MB-157 and MDA-MB-436) revealed that when cells were treated with increasing concentrations of mevalonate, the peptidase activity of the proteasome increased 300–500% over the concentration range examined (Fig. 5*C*). The mevalonate-mediated increase in the peptidase activity occurred if cells were pretreated with mevalonate for the indicated times, not when mevalonate was added to cell extracts (data not shown). We believe that mevalonate abrogates the action of both lactacystin and the pro-drug form of lovastatin on the proteasome by either increasing the activity of the proteasome complex, increasing the assembly of the active complexes, or unmasking inactive complexes. Alternatively, mevalonate also may either prevent the cellular uptake of the pro-drug or inactivate the β-lactone. Although the mechanism of mevalonate abrogation of proteasome inhibition currently is not known, our studies suggest that in addition to being an intermediate of cholesterol bio-
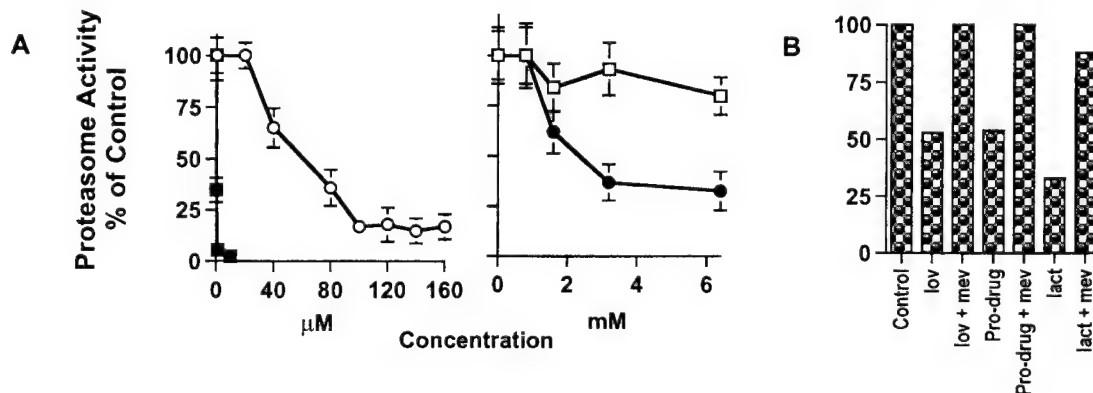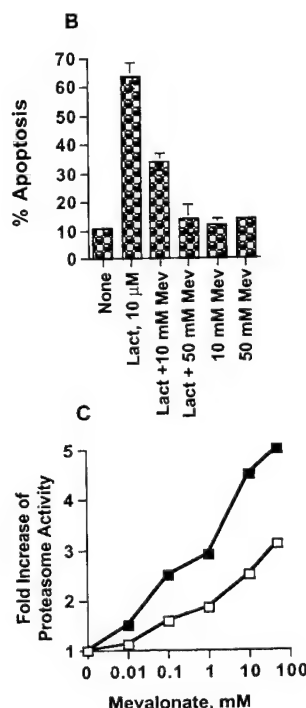

FIG. 4. Inhibition of the proteasome activity by the pro-drug form of lovastatin and lactacystin. Cell extracts were prepared from either MDA-MB-157 cells (*A*) without drug treatment or (*B*) treated with either lovastatin (lov) (40 μM), pro-drug (40 μM), or lactacystin (lact) (1 μM) in the presence or absence of mevalonate (mev) (5 mM) for 36 hr and assayed for proteasome enzyme activity. The extracts in *A* were incubated in the presence of the indicated concentrations of the drugs for 20 min at 37°C at which point the fluorogenic peptide substrate (100 μM final concentration) for the chymotrypsin-like activity of the proteasome (i.e., Suc-LLVY-AMC) was added to extracts. The fluorescence assays (excitation/emission 380/440 nm) were conducted at 37°C for 750 sec, and $n = 3$. The pretreated extracts in *B* were not further incubated in the presence of the inhibitors and were directly assayed for the proteasome activity. ■, lactacystin; ○, pro-drug; ●, lovastatin; □, pravastatin.

A

Treatment	% G1	% S	% G2
None	56	12	31
Mev, 4 mM	56	12	32
Lov, 40 μM	61	4	35
Lov + Mev	51	13	34
Pro-drug, 40 μM	62	3	34
Pro-drug + Mev	53	12	34

B

C

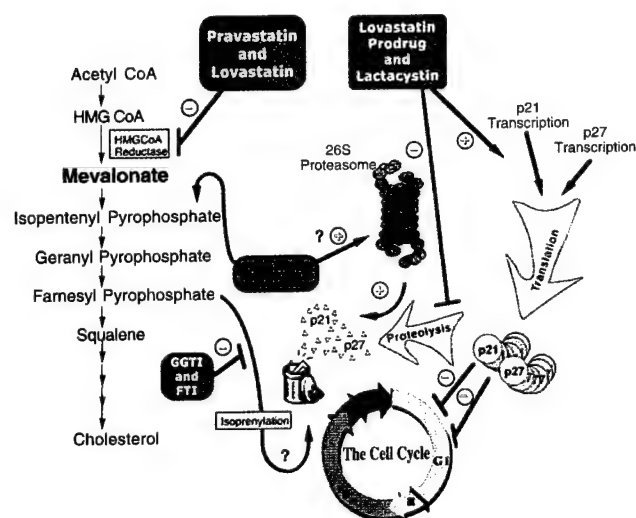

FIG. 6. Cell cycle regulation by inhibitors of HMG-CoA reductase and proteasome.

FIG. 5. Mevalonate reversal of lovastatin, lovastatin pro-drug, and lactacystin. (*A*) MDA-MB-157 cells were treated with the indicated concentration of lovastatin (lov) or the pro-drug in the presence or absence of 4 mM mevalonate (Mev) for 36 hr and subjected to flow cytometric measurements of DNA content. (*B*) MDA-MB-157 cells were treated with 10 μM lactacystin (lact) in the presence or absence of 10 mM or 50 mM mevalonate for 36 hr. At the end of treatment cells were subjected to flow cytometric measurement of DNA content. Percent apoptosis reflects the accumulation of cells with sub-G_1 DNA content. (Apoptosis also was measured by chromosome condensation/ 4',6-diamidino-2-phenylindole staining; data not shown.) (*C*) Induction of the proteasome activity by mevalonate. MDA-MB-436 (closed symbols) and MDA-MB-157 (open symbols) were treated with the indicated concentrations of mevalonate for 36 hr. After treatment, crude cell extracts were prepared and assayed for proteasome enzyme activity by measuring the chymotrypsin-like activity of the proteasome (described for Fig. 4*B*). Values are expressed as fold increase over no treatment controls. $n = 3$, and the averages of the values are indicated.

synthesis, mevalonate has a role in facilitating proteolytic degradation.

DISCUSSION

The hypothesis we present here is that lovastatin induces CKIs p21 and p27 in breast cancer cells by modulation of the ubiquitin-proteasome pathway, independent of inhibition of the HMG-CoA reductase enzyme. The model for this hypothesis is presented in Fig. 6. The left portion of this diagram illustrates the traditional role of HMG-CoA reductase inhibitors that block mevalonate synthesis, preventing the isoprenylation of key proteins implicated in cell division. The right side of the diagram illustrates our hypothesis that the proteasome is inhibited by both the pro-drug form of lovastatin and lactacystin, leading to accumulation of p21 and p27 and subsequent G_1 arrest or apoptosis. Central to our hypothesis is

the unusual discovery that mevalonate, in addition to its known ability to rescue HMG-CoA reductase inhibition, unexpectedly abrogates inhibition of the proteasome by lactacystin and the pro-drug form of lovastatin. This process leads to the degradation of the CKIs and resumption of cell division.

Although our results and hypothesis do not dispute the role of lovastatin (open-ring form) in the cholesterol biosynthesis pathway, they do describe alternative roles for the pro-drug form of lovastatin and mevalonate. On examination of the lovastatin literature we found that our previously unrecognized "side effects" of lovastatin and mevalonate might provide insights for numerous studies, which seemed unrelated to the cholesterol biosynthesis pathway. For example, a number of studies indicate that lovastatin and lactacystin share common ground in their biological effects (Fig. 6). Inhibitors of both HMG-CoA reductase and the proteasome have similar stimulatory effects on the differentiation of PC12 neuronal cells. Simvastatin, a lovastatin analogue, causes neurite-like outgrowth and inhibition of cell proliferation in PC12 cells, which was completely reversible by mevalonate. Lactacystin also causes neurite outgrowth of PC12 cells and results in neurogenesis and neurite outgrowth in a murine cell line (29, 31, 32). In contrast, pravastatin, which resembles only the active form of lovastatin, had no effect on these cells (33).

The above studies provide evidence that the common biological effects of lovastatin and lactacystin may be through modulation of the proteasome pathway. Other studies highlight properties of lovastatin that seem unrelated to cholesterol biosynthesis. For example, treatment of cells with the lovastatin analogue, simvastatin (more potent than lovastatin) resulted in regeneration of cultured rat skeletal muscle cells with a toxic effect on growth and differentiation, without influencing the cholesterol and phospholipid content of the cells (34). Inhibition of the HMG-CoA reductase also induces differentiation of human monocytic cells associated with growth retardation and expression of differentiation markers (35). Lovastatin also inhibited experimental lung metastasis of the highly metastatic B16F10 mouse melanoma in nude mice (36). Lastly, data from a large clinical trial of lovastatin produced the unexpected finding that lovastatin also may have chemoprevention abilities. When patients with severe hypercholesterolemia were treated with lovastatin, a decreased incidence (14 patients) of cancer of all types was observed in these patients compared with the expected rates (21 patients) during the 5-year period of the study (37). This clinical study emphasizes the significance of our finding in terms of the observed biological effects of lovastatin. We suggest that the

mechanism by which lovastatin functions as a chemopreventative agent may be through the inhibition of the proteasome, resulting in increased stabilization of p21 and p27, which have tumor suppressive abilities.

The ability of mevalonate to reverse the effects of lovastatin fits well with the idea that activity of HMG-CoA reductase is needed to provide precursors vital to cell division. However, our data suggests another role for mevalonate is to abrogate the effects of both lactacystin and the pro-drug form of lovastatin. On one hand, mevalonate acts as cornerstone of cholesterol biosynthesis, and on the other, it is an allosteric effector of the proteasome (Fig. 6). We show that mevalonate abrogates the inhibitory action of both the pro-drug and lactacystin by the up-regulation of proteasome activity. There is precedent for this hypothesis. It has been reported that whereas HMG-CoA reductase is normally a stable enzyme with an extended half-life, downstream products such as mevalonate, sterols, and their derivatives like 25-hydroxycholesterol will promote the rapid and specific degradation of this enzyme (38, 39). Because HMG-CoA reductase is degraded through the proteasome pathway (40) and mevalonate increases the activity of the proteasome (this study), it follows that addition of mevalonate could promote the degradation of this enzyme (38).

In summary, we have provided evidence that lovastatin suppresses cell proliferation through inhibition of proteasome-mediated degradation of p21 and p27, and mevalonate can abrogate this effect by activation of the proteasome. These additional effects of lovastatin and mevalonate, not only provide insights into the biochemical pathways disturbed by these agents, but also provide explanation for numerous studies documenting their unrecognized effects. One such unrecognized effect of lovastatin is its chemopreventative abilities that may be mediated through inhibition of the proteasome.

1. Hershko, A. & Ciechanover, A. (1992) *Annu. Rev. Biochem.* **61,** 761–807.
2. Hochstrasser, M. (1996) *Annu. Rev. Genet.* **30,** 405–439.
3. Ciechanover, A. (1994) *Cell* **79,** 13–21.
4. Pagano, M. (1997) *FASEB J.* **11,** 1067–1075.
5. Pagano, M., Tam, S. W., Theodoras, A. M., Beer-Romero, P., Del Sal, G., Chau, V., Yew, R. P., Draetta, G. F. & Rolfe, M. (1995) *Science* **269,** 682–685.
6. Blagosklonny, M. V., Wu, G. S., Mura, S. & Eldeiry, W. S. (1996) *Biochem. Biophys. Res. Commun.* **227,** 564–569.
7. Di Cunto, F., Topley, G., Calautti, E., Hsiao, J., Ong, L., Seth, P. K. & Dotto, G. P. (1998) *Science* **280,** 1069–1072.
8. Lee, D. H. & Goldberg, A. L. (1998) *Trends Cell Biol.* **8,** 397–403.
9. Dick, L. R., Cruikshank, A., Destree, T., Grenier, L., McCormack, T. A., Melandri, F. D., Nunes, S. L., Palombella, V. J., Parent, L. A., Plamondon, L. & Stein, R. L. (1997) *J. Biol. Chem.* **272,** 182–188.
10. Fenteany, G., Standaert, R. F., Lane, W. S., Choi, S., Corey, E. J. & Schreiber, S. L. (1995) *Science* **268,** 726–731.
11. Rettersol, K., Stuggard, M., Gorbitz, C. & Ose, L. (1996) *Am. J. Cardiol.* **78,** 1369–1374.
12. Corsini, A., Maggi, F. M. & Catapano, A. L. (1995) *Pharmacol. Res.* **31,** 9–27.
13. Endo, A., Kuroda, M. & Tansawa, K. (1976) *FEBS Lett.* **72,** 323–326.
14. Maltese, W. A. (1990) *FASEB J.* **4,** 3319–3328.
15. Keyomarsi, K., Sandoval, L., Band, V. & Pardee, A. B. (1991) *Cancer Res.* **51,** 3602–3609.
16. Rao, S., Lowe, M., Herliczek, T. & Keyomarsi, K. (1998) *Oncogene* **17,** 2393–2402.
17. Gray-Bablin, J., Rao, S. & Keyomarsi, K. (1997) *Cancer Res.* **57,** 604–609.
18. Hengst, L. & Reed, S. I. (1996) *Science* **271,** 1861–1864.
19. Terada, Y., Inoshita, S., Nakashima, O., Yamada, T., Kuwahara, M., Sasaki, S. & Marumo, F. (1998) *J. Am. Soc. Nephrol.* **9,** 2235–2243.
20. Lee, S. J., Ha, M. J., Lee, J., Nguyen, P. M., Choi, Y. H., Pirnia, F., Kang, W.-K., Wang, X.-F., Kim, S.-J. & Trepel, J. B. (1998) *J. Biol. Chem.* **273,** 10618–10623.
21. Vogt, A., Sun, J., Qian, Y., Hamilton, A. D. & Sebti, S. M. (1997) *J. Biol. Chem.* **272,** 27224–27229.
22. Muller, C., Bockhorn, A. G., Klusmeier, S., Kiehl, M., Roeder, C., Kalthoff, H. & Koch, O. M. (1998) *Int. J. Oncol.* **12,** 717–723.
23. DeClue, J. E., Vass, W. C., Papageorge, A. G., Lowy, D. R. & Willumsen, B. M. (1991) *Cancer Res.* **51,** 712–717.
24. Bradfute, D. L., Silva, C. J. & Simoni, R. D. (1992) *J. Biol. Chem.* **267,** 18308–18314.
25. Stubbs, R. J., Schwartz, M. & Bayne, W. F. (1986) *J. Chromat.* **383,** 438–443.
26. Hall, M., Bates, S. & Peters, G. (1995) *Oncogene* **11,** 1581–1588.
27. Larsson, O., Barrios, C., Latham, C., Ruiz, J., Zetterberg, A., Zickert, P. & Wejde, J. (1989) *Cancer Res.* **49,** 5605–5610.
28. Maki, C. G. & Howley, P. M. (1997) *Mol. Cell. Biol.* **17,** 355–363.
29. Fenteany, G., Standaert, R. F., Reichard, G. A., Corey, E. J. & Schreiber, S. L. (1994) *Proc. Natl. Acad. Sci. USA* **91,** 3358–3362.
30. Maupin-Furlow, J. A. & Ferry, J. G. (1995) *J. Biol. Chem.* **270,** 28617–28622.
31. Saito, Y., Tsubuki, S., Ito, H. & Kawashima, S. (1990) *Neurosci. Lett.* **120,** 1–4.
32. Tsubuki, S., Saito, Y., Tomioka, M., Ito, H. & Kawashima, S. (1996) *J. Biochem.* **119,** 572–576.
33. Sato-Suzuki, I. & Murota, S.-I. (1996) *Neurosci. Lett.* **220,** 21–24.
34. Veerkamp, J. H., Smit, J. W. A., Benders, A. A. G. M. & Oosterhof, A. (1996) *Biochem. Biophys. Acta* **1315,** 217–222.
35. Weber, C., Erl, W. & Weber, P. C. (1995) *Cell Biochem. Funct.* **13,** 273–277.
36. Jani, J. P., Specht, S., Stemmler, N., Blanock, K., Singh, S. V., Gupta, V. & Katoh, A. (1993) *Invasion Metastasis* **13,** 314–324.
37. Stein, E. A., Lazkarzewski, P., Steiner, P. & The Lovastatin Study Groups I–IV (1993) *Arch. Intern. Med.* **153,** 1079–1087.
38. McGee, T. P., Cheng, H. H., Kumagai, H., Omura, S. & Simoni, R. D. (1996) *J. Biol. Chem.* **271,** 25630–25638.
39. Correll, C. C., Ng, L. & Edwards, P. A. (1994) *J Biol. Chem.* **269,** 17390–17393.
40. Moriyama, T., Sather, S. K., McGee, T. P. & Simoni, R. D. (1998) *J. Biol. Chem.* **273,** 22037–22043.

UCN-01-mediated G1 arrest in normal but not tumor breast cells is pRb-dependent and p53-independent

Xiaomei Chen[1], Michael Lowe[1] and Khandan Keyomarsi*,[1],[2]

[1]Division of Molecular Medicine, Wadsworth Center, Albany, New York, NY 12201-0509, USA; [2]Department of Biomedical Sciences, State University of New York, Albany, New York, NY 12222, USA

In this study we investigated the growth inhibitory effects of UCN-01 in several normal and tumor-derived human breast epithelial cells. We found that while normal mammary epithelial cells were very sensitive to UCN-01 with an IC_{50} of 10 nM, tumor cells displayed little to no inhibition of growth with any measurable IC_{50} at low UCN-01 concentrations (i.e. 0–80 nM). The UCN-01 treated normal cells arrested in G1 phase and displayed decreased expression of most key cell cycle regulators examined, resulting in inhibition of CDK2 activity due to increased binding of p27 to CDK2. Tumor cells on the other hand displayed no change in any cell cycle distribution or expression of cell cycle regulators. Examination of E6- and E7-derived strains of normal cells revealed that pRb and not p53 function is essential for UCN-01-mediated G1 arrest. Lastly, treatment of normal and tumor cells with high doses of UCN-01 (i.e. 300 nM) revealed a necessary role for a functional G1 checkpoint in mediating growth arrest. Normal cells, which have a functional G1 checkpoint, always arrest in G1 even at very high concentrations of UCN-01. Tumor cells on the other hand have a defective G1 checkpoint and only arrest in S phase with high concentrations of UCN-01. The effect of UCN-01 on the cell cycle is thus quite different from staurosporine, a structural analogue of UCN-01, which arrests normal cells in both G1 and G2, while tumor cells arrest only in the G2 phase of the cell cycle. Our results show the different sensitivity to UCN-01 of normal compared to tumor cells is dependent on a functional pRb and a regulated G1 checkpoint.

Keywords: UCN-01; cell cycle; p53; pRb; E6; E7

Introduction

Protein kinases are essential for cellular signal transduction leading to differentiation, gene expression, and tumor progression. Clinical and experimental studies have already established the importance of protein kinase expression in the proliferation of human breast cancer (Boorne et al., 1998), suggesting that drugs that interrupt signaling pathways mediated by protein kinases could be useful cancer therapeutic agents. UCN-01 (7-hydroxystaurosporine), a staurosporine analogue initially developed as a selective protein kinase C (PKC) inhibitor, was isolated from the culture broth of Streptomyces sp. in 1987

(Takahashi et al., 1987). Subsequent studies have shown that in addition to PKC this compound inhibits a variety of other kinases at nanomolar concentrations, including PKA, CDK1, CDK2, CDK4, MAPK, $p60^{v-Src}$ and protein tyrosine kinase (Kawakami et al., 1996; Takahashi et al., 1989; Wang et al., 1995). Studies with cultured cells revealed that UCN-01 exhibited potent anti-tumor activity against several human cancer cell lines such as human epidermoid carcinoma A431, fibrosarcoma HT1080, acute myeloid leukemia HL-60, human lung carcinoma A549, and breast carcinoma MDA-MB-468 cell lines (Kawakami et al., 1996; Shao et al., 1997; Wang et al., 1995). UCN-01 also exhibited significant anti-tumor activities in several experimental animal models in vivo (Kawakami et al., 1996; Seynaeve et al., 1993; Takahashi et al., 1987). In addition, UCN-01 has been shown to enhance anti-tumor activities of chemotherapeutic agents such as cisplatin, 5-fluorouracil, mitomycin C, etc. in vitro and in vivo (Bunch and Eastman, 1997; Pollack et al., 1996; Wang et al., 1996).

Studies identifying the cellular pathways affected by UCN-01 resulting in G1 arrest suggest that although UCN-01 possesses potent PKC-inhibitory activity, inhibition of PKC activity is not essential for its growth inhibitory activity (Courage et al., 1995). Recent studies on the role of cell cycle regulators in UCN-01-mediated G1 arrest indicate that in human epidermoid carcinoma A431 cells, UCN-01-induced G1 arrest was accompanied by decreased cyclin-dependent kinase 2 (CDK2) activity and induction of CDK inhibitors p21 and p27 (Akiyama et al., 1997). p21 and p27 are two members of the CIP/KIP family of cyclin-dependent kinase inhibitors which negatively regulate the CDKs (Harper and Elledge, 1996; Sherr and Roberts, 1995). Although the CDK inhibitor p21 is a p53-regulated gene (El-Deiry et al., 1993; Harper et al., 1993), both p21 and p27 are also regulated through p53-independent pathways (Kato et al., 1994; Michieli et al., 1994; Polyak et al., 1994; Rao et al., 1998; Sheikh et al., 1994).

The mechanism of action of UNC-01 in either normal or tumor cells and whether or not such a mechanism involves p53 or pRb remain unresolved. p53 and the retinoblastoma protein (pRb) are two major tumor suppressors that are frequently inactivated in human cancer (Berns, 1994; Friend, 1994; Harbour et al., 1988; Horowitz et al., 1990). Alterations in p53 are linked to poor prognosis, tumor progression, and decreased sensitivity to chemotherapeutic agents. As an important G1 checkpoint regulator, p53 is involved in controlling the G1 to S phase transition in response to DNA damage. Similar to p53, pRb also functions as a

*Correspondence: K Keyomarsi, Wadsworth Center, Empire State Plaza. PO Box 509, Albany, NY 12201-0509, USA
Received 19 January 1999; revised 22 April 1999; accepted 4 May 1999

negative regulator of cell cycle. Phosphorylation of pRb is necessary for the progression through G1 and is regulated primarily by cyclin D/CDK4/CDK6 complexes. The hypo-phosphorylated pRb serves as a tumor suppressor by interacting with and inhibiting cellular proteins such as E2F-DP heterodimeric transcription factors which activate many genes required for DNA replication pivotal for G1/S transition (Weinberg, 1995).

Even though UCN-01 is currently in phase 1 clinical trials in both the United States and Japan, there are several questions on the growth inhibitory effect of this agent in normal and tumor cells. In this study we examined the growth inhibitory activity and other cell cycle perturbations mediated by UCN-01 in several normal and tumor-derived breast epithelial cells. Our results reveal three novel findings on the sensitivity and mechanism of action of UCN-01 in normal and tumor cells. First, we document a significant difference in sensitivity to UCN-01 between normal and tumor cells. UCN-01 is capable of inducing a G1 arrest in normal cells at very low concentrations (i.e. 10 nM), while in tumor cells concentrations up to 80 nM did not result in a significant growth inhibition. Furthermore, we show that the UCN-01-mediated G1 arrest only occurs in normal cells and is concomitant with inhibition of CDK2 activity, decreased phosphorylation of pRb, and increased binding of p27 to CDK2. Secondly, we show that UCN-01-mediated G1 arrest is p53-independent and pRb-dependent using the E6 and E7 immortalized strains of the normal cells. Lastly, we show that at very high concentrations, there is a major difference in the mechanism by which UCN-01 mediates growth inhibition in normal *versus* tumor cells. Treatment of normal cells with UCN-01, at all concentrations examined (i.e. up to 300 nM), results only in G1 arrest, unlike staurosporine which arrests normal cells in both G1 and G2. Treatment of tumor cells, on the other hand, with high concentrations of UCN-01 results only in an S phase arrest, unlike staurosporine which arrest tumor cells only in G2. Collectively our studies suggest that the mechanism of differential sensitivity of UCN-01 in normal *versus* tumor cells is dependent on a regulated G1 checkpoint involving a functional pRb pathway.

Results

UCN-01 selectively arrests normal, but not tumor, cells in G1

We initially investigated whether UCN-01 has a different growth inhibitory effect in normal *versus* tumor cells. For this purpose we examined the effects of UCN-01 in several normal and tumor-derived breast epithelial cells (Figure 1). The two normal cell strains (81N and 76N) were established from reduction mammoplasties obtained from two different individuals (Band and Sager, 1989). The proliferation of these normal cell strains are dependent on growth factors and strictly regulated by checkpoint controls. Furthermore, at the end of their lifespan, these normal mammary epithelial cells stop proliferating and become senescent (Band and Sager, 1989; Gray-Bablin et al., 1997). We also examined MCF-10A, a

near diploid immortalized cell line which is a subline of a breast epithelial cell strain, MCF-10. This cell line was derived from human fibrocystic mammary tissue and was immortalized after extended cultivation in medium containing low concentrations of calcium (Soule et al., 1990). The MCF-10A cell line also contains a wild-type Rb gene with homozygous deletion of the p15^{INK4B} and p16^{INK4A} genes as described (Iavarone and Massague, 1997). Therefore, MCF-10A has lost its strict growth factor requirement, checkpoint regulation (specifically, G1 to S transition) and the ability to senesce. In addition to these two normal and immortalized cell types we examined four breast cancer cell lines with different p53 and pRb status (Rao et al., 1998). Following treatment of cells with 0–80 nM UCN-01 for 48 h, growth inhibition was analysed by the MTT assay (Figure 1a), and the effect of UCN-01 on cell cycle distribution was examined by flow cytometry (Figure 1b). The data clearly shows that normal breast epithelial cell strains 76N and 81N were highly sensitive to UCN-01, revealing a 60–70% growth inhibition following treatment with only 20 nM UCN-01 and an IC$_{50}$ of 10–12 nM. Breast cancer cell lines T47D and MDA-MB-157 cells showed little to no response to UCN-01 over the concentration range examined. MCF-10A, MCF-7 and MDA-MB-436, showed an intermediate response to UCN-01 with a 20–25% growth inhibition at 40 nM, and less than 50% growth inhibition at 80 nM of UCN-01. These results demonstrate that at low concentrations (i.e. 0–80 nM) normal cell strains are much more sensitive to UCN-01 than tumor cells. However at 'iso-effective' doses of UCN-01 (i.e. >300 nM) tumor cells respond by significant inhibition of cell proliferation (data not shown). Flow cytometry analysis revealed that treatment of normal cells (76N and 81N) with UCN-01 resulted in a significant accumulation of cells in the G1 phase of the cell cycle (i.e. an increase of 15% in G1 phase) in a dose-dependent fashion (Figure 1b). The G1 accumulation in normal cells was concurrent with an S phase decrement (Figure 1b), while G2+M phase had no significant change (data not shown). The partial growth inhibition of UCN-01 in MCF-10A and MCF-7 cell lines was due to a slight (less than 5%) accumulation in G1 (data not shown). Lastly, UCN-01 was ineffective in inducing any accumulation in the G1 phase of the cell cycle in MDA-MB-157 or MDA-MB-436 cell lines. In fact treatment of MDA-MB-436 cells with 80 nM UCN-01 resulted in a slight increase in S phase (Figure 1b). Additionally treatment of tumor cells with >300 nM UCN-01 resulted in a significant accumulation of cells in S phase (data not shown). The data from Figure 1 suggests that UCN-01 selectively mediates growth inhibition in normal but not tumor cells by arresting the cells in the G1 phase of the cell cycle.

UCN-01-mediated G1 arrest in normal cells results in inactive cyclin/CDK2 complexes due to increased p27 binding to CDK2

To determine which key cell cycle regulators were required for UCN-01-mediated G1 arrest in normal cell strains, we examined the expression of several positive and negative cell cycle proteins in both 76N and 81N
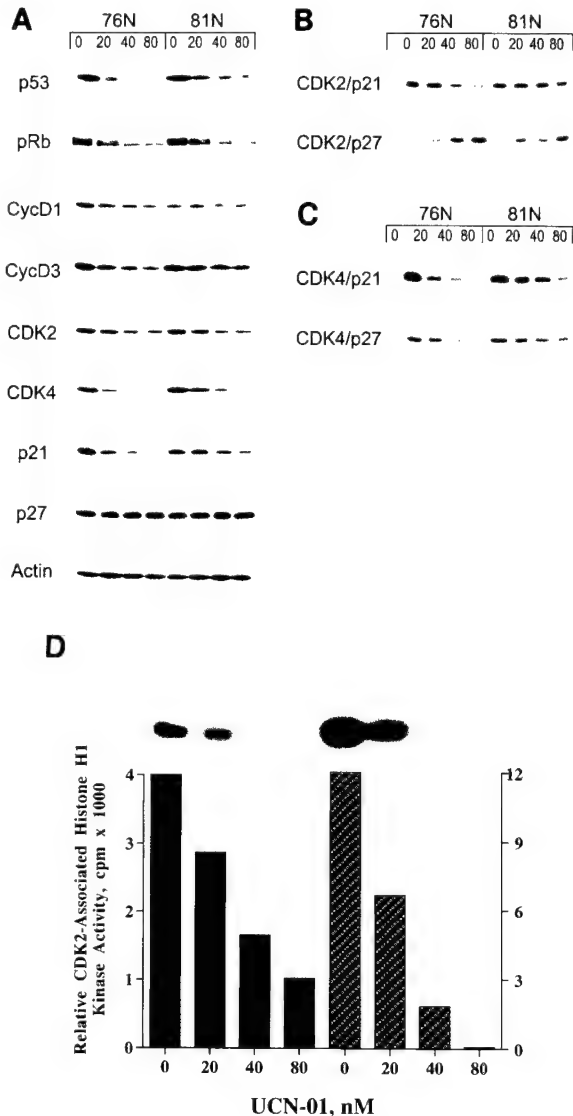
mortal cell strains. Both normal cell strains were treated with the indicated concentrations of UCN-01 for 48 h at which point cells were harvested and subjected to Western blot analysis with antibodies to p27, p21, pRb, p53, CDK2, CDK4, cyclin D1, and cyclin D3 (Figure 2a). These analyses revealed that the total levels p53 and pRb tumor suppressor proteins decreased significantly in the normal cell strains following UCN-01 treatment. In untreated cells pRb is present in both its phosphorylated (upper band) and unphosphorylated (lower band) forms. However the only form of pRb remaining at 40–80 nM UCN-01 is its hypo-phosphorylated form. The generation of hypo-phosphorylated pRb occurred concomitantly with growth inhibition, G1 arrest, decreased expression of cyclin D1, cyclin D3, CDK2 and CDK4 in a dose-dependent manner following UCN-01 treatment (Figure 2a). Additionally the expression of cyclin A and cyclin E were also down regulated by UCN-01 (data not shown).

The simultaneous decrease in p53 and p21 (Figure 2a) in normal cells suggest that in these cells p21 expression may be strongly influenced by p53 and that the UCN-01-induced G1 arrest in these cells is independent of p21. The levels of p27 were unchanged

following UCN-01 treatment. This analysis raised the question whether p21 and p27 play a role in UCN-01-mediated G1 arrest. Does the decrease in the CDK4 and CDK2 levels in response to UCN-01 contribute to this arrest? The Western blot analysis in Figure 2a suggests that a likely explanation for the UCN-01-mediated G1 arrest could be due to a sequence of events initiating with down regulation of CDK4 and cyclin D3 leading to the inhibition of CDK2 activity necessary for cells to overcome the G1 restriction point. We addressed this hypothesis by initially examining the association of p21/p27 with CDK2 or CDK4 in a two step experiment consisting of an immunoprecipitation with anti-CDK2 or anti-CDK4 antibodies followed by Western blot analysis with p21 or p27 (Figure 2b and c). Additionally, we examined the CDK2-associated kinase activity by measuring the phosphorylation of histone H1 in immunoprecipitates prepared from UCN-01-treated cells using an antibody to CDK2 (Figure 2d). Treatment of normal cells with UCN-01 caused a rapid decrease of CDK2 activity. At 40 nM UCN-01 (the concentration causing G1 arrest and pRb hypo-phosphorylation) the level of CDK2 activity reaches its nadir. The decreased CDK2 activity observed (Figure 2d) was coupled with increased
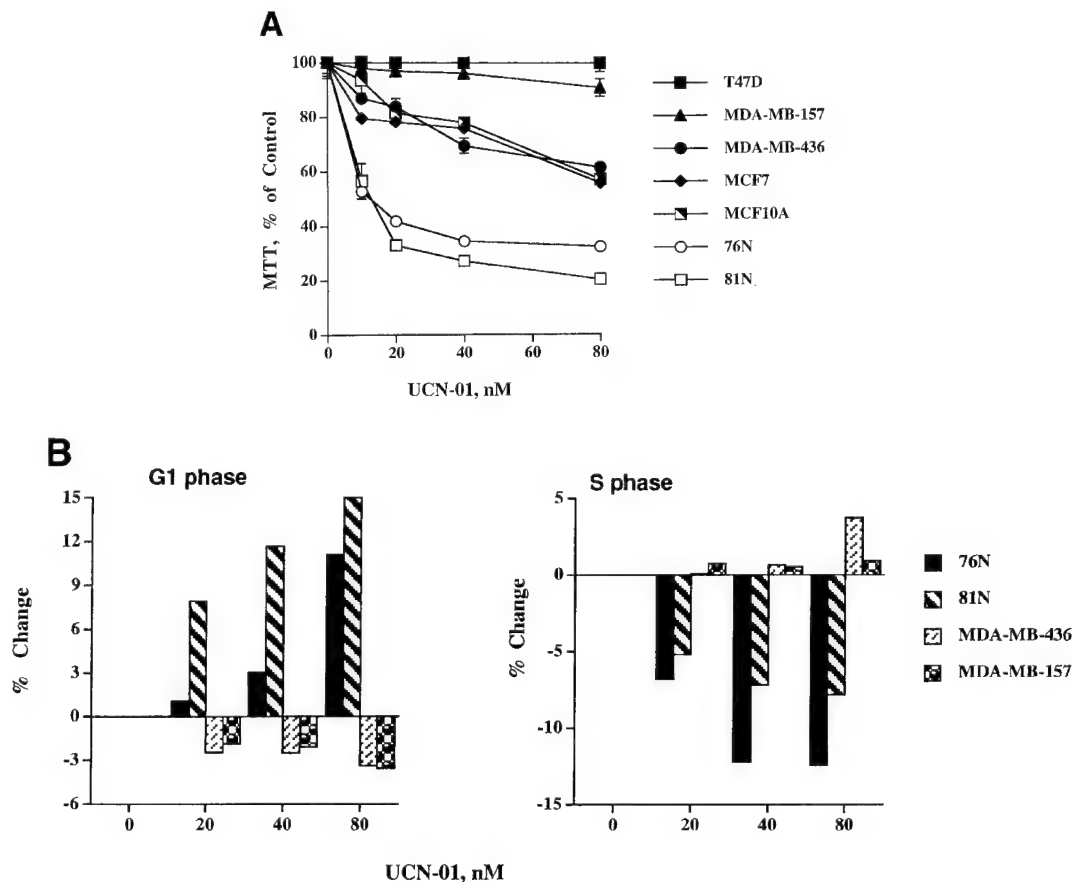
Figure 1 Normal cells are significantly more sensitive to UCN-01 than tumor cells. (**a**) Seven different human breast epithelial cell lines comprised of normal cell strains (76N, 81N), immortalized cell line (MCF10A) and breast tumor cell lines (MCF-7, MDA-MB-157, MDA-MB-436 and T47D) were treated with UCN-01 at 0, 10, 20, 40, and 80 nM for 48 h. Growth inhibition by UCN-01 was measured by the MTT assay. The experiment was repeated three times and error bars are indicated for each condition and each cell line. In most cases the error bars were smaller than the symbol size and cannot be seen. (**b**) Per cent change in cell cycle distribution of cells in G1 and S phase following UCN-01 treatment of normal (76N and 81N) and tumor (MDA-MB-157 and MDA-MB-436) cells. The bar graph reflects the per cent change of G1 and S phases of UCN-01-treated cells relative to the untreated controls, for each cell line

A

	76N	81N
	0 20 40 80	0 20 40 80

p53

pRb

CycD1

CycD3

CDK2

CDK4

p21

p27

Actin

B

	76N	81N
	0 20 40 80	0 20 40 80

CDK2/p21

CDK2/p27

C

	76N	81N
	0 20 40 80	0 20 40 80

CDK4/p21

CDK4/p27

D

UCN-01, nM

Figure 2 Cell cycle perturbation induced by UCN-01 in normal cell strains. Normal cell strains (76N and 81N) were treated with the indicated concentrations (nM) of UCN-01 for 48 h. Following treatment cells were harvested, cell lysates prepared and subjected to (**a**) Western blot analysis, (**b**) CDK2 immune-complex formation, (**c**) CDK4 immune-complex formation, and (**d**) Histone H1 kinase analysis. For Western blot analysis 50 μg of protein extract from each condition was analysed by Western blot analysis with the indicated antibodies or actin used for equal loading. The blots were developed by chemiluminescence reagents. The same blots were sequentially hybridized with different antibodies (see Materials and methods). The blots were stripped between the antibodies in 100 mM 2-mercaptoethanol, 62.5 mM Tris-HCl (pH 6.8) and 2% SDS for 10 min at 55°C. For immunoprecipitation followed by Western blot analysis, equal amounts of protein (300 μg) from cell lysate prepared from each cell line were immunoprecipitated with anti-CDK2 (polyclonal) (**b**) or anti-CDK4 (polyclonal) (**c**) coupled to protein A beads and the immunoprecipitates were subjected to Western blot analysis with the indicated antibodies. For kinase activity, equal amounts of protein (300 μg) from cell lysates were prepared from each cell line immunoprecipitated with anti-CDK2 antibody (polyclonal) coupled to protein A beads using histone H1 as substrate. For each cell line we show the resulting autoradiogram of the histone H1 SDS–PAGE and the quantitation of the histone H1 associated kinase activities by Cerenkov counting. The numbers on the left ordinate refer to c.p.m. obtained from H1 kinase assay for 76N cells (solid bars), and the numbers on the right ordinate refer to the c.p.m. obtained from H1 kinase assay for 81N cells (shaded bars)

binding of p27 to CDK2 in the normal cells. The binding of p21 to CDK2 however, decreased in these cells (Figure 2b). These observations raise the question, why is there increased binding of p27 to CDK2 in normal cells (Figure 2b) when the levels of p27 don't change?

Recently several laboratories have proposed that p21 and p27 can function as adaptor molecules, which promote the association of CDK4 with D-type cyclins and increase CDK4 kinase activity (LaBaer et al., 1997; Planas-Silva and Weinberg, 1997; Rao et al., 1998). Since UCN-01 causes the arrest of cells, apparently by increasing binding of p27 to CDK2 complexes (Figure 2b), it can be hypothesized that this increased binding may be due to the switching of p27 from CDK4 to CDK2, mediated by UCN-01. To test this hypothesis we examined the association of p21 and p27 to CDK4 following UCN-01 treatment (Figure 2c). Our results clearly demonstrate that in untreated normal cells p21 and p27 bind to CDK4, and upon treatment with UCN-01, both p21 and p27 are released from CDK4 in a dose-dependent fashion (Figure 2c) which corresponds to the binding (i.e. switching partners) of p27 to CDK2 (Figure 2b). The decrease in CDK4-associated p21 and p27 (Figure 2c) could further be explained by the decrease in mass of CDK4 (Figure 2a). The total amount of CDK2 and CDK4 immunoprecipitated in Figure 2b and c were also analysed by Western blotting with antibodies to CDK2 and CDK4, and reveal that the fold decrease in the levels of these kinases following UCN-01 treatment were identical to those observed in Figure 2a (data not shown). The residual association of p27 to CDK4 at 40 and 80 nM UCN-01 is a reflection of the sensitivity of the immunoprecipitation assay (Figure 2c) as compared to Western blot analysis (Figure 2a). Our results suggest that UCN-01-mediated G1 arrest in normal epithelial cells is through decreased expression of CDK4 and CDK2. As CDK4 decreases, p27 is released from CDK4 and binds to CDK2, resulting in a decreased CDK2 kinase activity and decreased phosphorylation of pRb.

UCN-01 has no effect on cell cycle regulators in tumor cells

While UCN-01 had a profound affect in inducing G1 arrest and lowering the expression of key cell cycle regulators in normal cells, tumor cells showed no significant change in any of the cell cycle regulators examined (Figure 3). Furthermore, although the expression of some of these regulators was different between the three different tumor cell lines examined, within each tumor cell line the levels remained unchanged. For example, the levels of cyclin D1, CDK2 and CDK4 were the same within and between each cell line, following UCN-01 treatment. Cyclin D3 is overexpressed in MCF-7 cell line, moderately expressed in MDA-MB-157 and not expressed in MDA-MB-436 cells. MCF-7 cells was the only cell line examined which was wild-type for p53 and pRb and no significant change in the levels of these tumor suppressors was observed following UCN-01 treatment. Although pRb is expressed in MDA-MB-157 cells, it is functionally inactive as previously reported (Gray-Bablin et al., 1996). Lastly, the levels of p21 and

p27 are elevated in MCF-7 compared to the other two cell lines, while p16 was absent in MCF-7 and overexpressed in MDA-MB-157 and MDA-MB-436 (Figure 3). We also examined the CDK2 kinase activity in these tumor cell lines and as expected the activity of CDK2 was unchanged following UCN-01 treatment in all tumor cell lines examined (data not shown). These results suggest that tumor cells have lost the checkpoint control affected by UCN-01 resulting in no growth inhibition or cell cycle perturbation following treatment.

UCN-01-mediated G1 arrest is through a p53-independent and pRb-dependent pathway

To directly determine if alterations in p53 or pRb mediate G1 arrest in normal but not tumor cells, we examined the effects of UCN-01 in E6 and E7 strains of 76N cells. 76NE6 and 76NE7 are immortalized cell strains derived from normal mammary epithelial cell strain 76N by infection with human papilloma virus (HPV) 16E6 or 16E7 (Band et al., 1990, 1991). The E6/p53 and E7/pRb interaction promote degradation/inactivation of p53 and pRb respectively, resulting in

the loss of normal phenotype (Band et al., 1993; Dyson et al., 1992; Werness et al., 1990). We initially examined the pattern of growth inhibition of UCN-01 in 76NE6 and 76N-E7 as compared to the parental 76N cells (Figure 4a). This analysis revealed that 76NE6 were as sensitive to the growth inhibitory activity of UCN-01 as 76N parental cell strain with a super-imposable dose-response curve and an IC_{50} of 10 nM. 76NE7 cells were much more resistant to UCN-01; however, their growth was also retarded with an IC_{50} of 75 nM (Figure 4a). Flow cytometry analysis revealed that the UCN-01-mediated growth inhibition in 76NE6 and 76NE7 cells were quite different. Treatment of 76NE6 cells resulted in accumulation of cells in the G1 phase of the cell cycle with a concomitant decrease in S phase cells (Figure 4a) identical to the pattern observed in 76N cells following drug treatment (Figure 1b). However, treatment of 76NE7, pRb deficient, cells resulted in accumulation of cells in S phase at 80 nM UCN-01 with a concomitant decrease in the G1 phase, opposite to the pattern observed with 76NE6, p53-deficient cells (Figure 4b). This data suggests that UCN-01-induced G1 arrest is dependent on a functional Rb, but not a functional p53.

Next we examined the expression of key cell cycle regulatory proteins in 76NE6 and 76NE7 cells following UCN-01 treatment (Figure 5a). 76NE6 cells are devoid of p53, but express pRb at very high levels (Band et al., 1990, 1991). Treatment of these cells with UCN-01 resulted in accumulation of the hypo-phosphorylated form of Rb, a decrease in CDK4 levels, and an increase in p21 and p27 levels. The levels of CDK2 and cyclin D1 remained unchanged during the course of treatment and p16 levels were undetectable. 76NE7 cells, on the other hand over express p16, apparently due to pRb inactivation (Khleif et al., 1996; Reznikoff et al., 1996). Treatment of 76NE7 cells with UCN-01 resulted in no detectable changes in any of the cell cycle regulators examined (Figure 5a). Next we measured the binding of p21 and p27 to CDK2 and CDK4 in 76NE6 and 76NE7 cells (Figure 5b and c). This analysis revealed that in 76NE6 cells the binding of p21 and p27 to CDK2 increased, while in 76NE7 cells the binding of these CKIs to CDK2 or CDK4 remained unchanged. Furthermore the increased binding of both CKIs to 76NE6 cells was concomitant with decreased binding of p21 and p27 to CDK4 suggesting a switching of partners of these CKIs from CDK4 to CDK2 mediated by UCN-01 (Figure 5b and c). Lastly, measurement of CDK2 activity in 76NE6 and 76NE7 cells revealed that treatment of 76NE6 cells with UCN-01 resulted in a dose-dependent decline in the kinase activity with maximum inhibition achieved at 40 nM (Figure 5d). The increased expression and binding of p21 and p27 to CDK2 observed (Figure 5b) contributes to the inhibition of CDK2 kinase activity in 76NE6 cells. The CDK2 activity in 76NE7 cells (Figure 5d) on the other hand, was completely unabated by UCN-01 treatment. The fact that we observe 76NE7 cells arrest in S phase without loss of CDK2 activity could suggest that this arrest occurred in later S phase and not early S phase, a point where CDK2 activity would be required. Furthermore, these results strongly suggest that the UCN-01-mediated G1
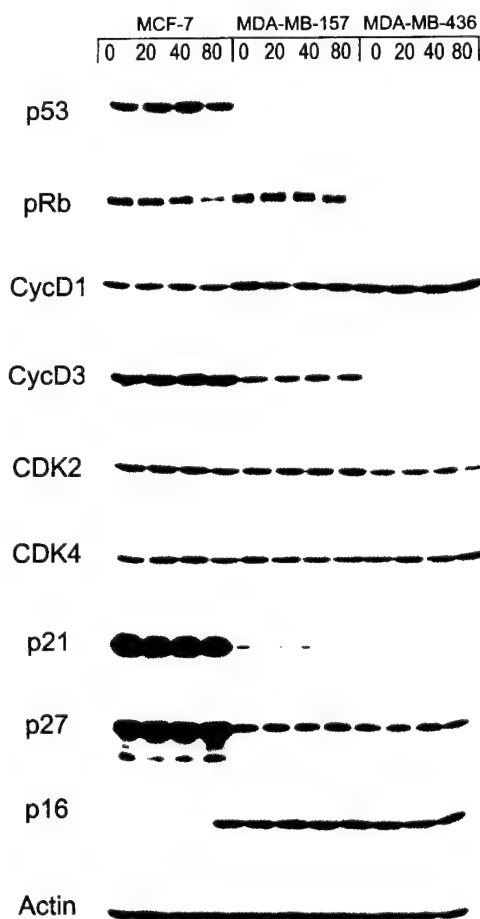
Figure 3 No change in the expression of cell cycle regulators by UCN-01 in tumor cells. MCF-7, MDA-MB-157 and MDA-MB-436 tumor cell lines were treated with the indicated concentrations (nM) of UCN-01 for 48 h. Following treatment cells were harvested. cell lysates prepared and subjected to Western blot analysis as described for Figure 2

arrest, and decreased CDK2 activity are p53-independent, but pRb-dependent.

High concentrations of UCN-01 induces S phase arrest in tumor and 76NE7 but not normal and 76NE6 cells

While examining the cell cycle effects of UCN-01 in tumor (Figure 1) and 76NE7 (Figure 4B) cells we noticed that treatment with 80 nM UCN-01 resulted in a slight increase in S phase and no G1 accumulation. These results raised the question if UCN-01 treatment of cells without a regulated G1 checkpoint and/or functional pRb could lead to only an S phase arrest. To explore this possibility we examined cell cycle phase distribution of 76NE6 and 76NE7 cells at low (i.e. 80 nM) and high (i.e. 300 nM) concentration of UCN-01. At 300 nM the growth of both cell types is completely inhibited (data not shown). We observed a clear difference between the ability of 76NE6 cells and 76NE7 cells to arrest in G1 or S phase (Figure 4b, and data not shown). Treatment of 76NE6 cells, which have an intact pRb, with any concentration of UCN-01

resulted only in a G1 arrest. However, treatment of 76NE7 cells, which have no detectable pRb, results in only an S phase arrest at higher concentrations of UCN-01 (i.e. $\geqslant 80$ nM) (Figure 4b, and data not shown). These results suggest that the disruption of the pRb pathway abrogates the ability of cells to arrest in G1 in response to UCN-01 treatment, instead they arrest in the S phase of the cell cycle.

To determine if synchronization of normal cells would sensitize their ability to arrest in S *versus* G1 phase, we synchronized 81N normal cells in the G1/S boundary by double-thymidine block prior to UCN-01 treatment (Figure 6). Under these conditions up to 30% of the cells (i.e. threefold higher than the asynchronous controls) accumulate in S phase following release from this block, and the cells undergo synchronous traverse through the cell cycle for the duration of the experiment (Figure 6). Following the double thymidine block, cells were treated with 300 nM UCN-01 for 3–12 h. We used a high (i.e. 300 nM) concentration of UCN-01, since this concentration was sufficient to arrest 76NE7 cells in the S phase of the cell
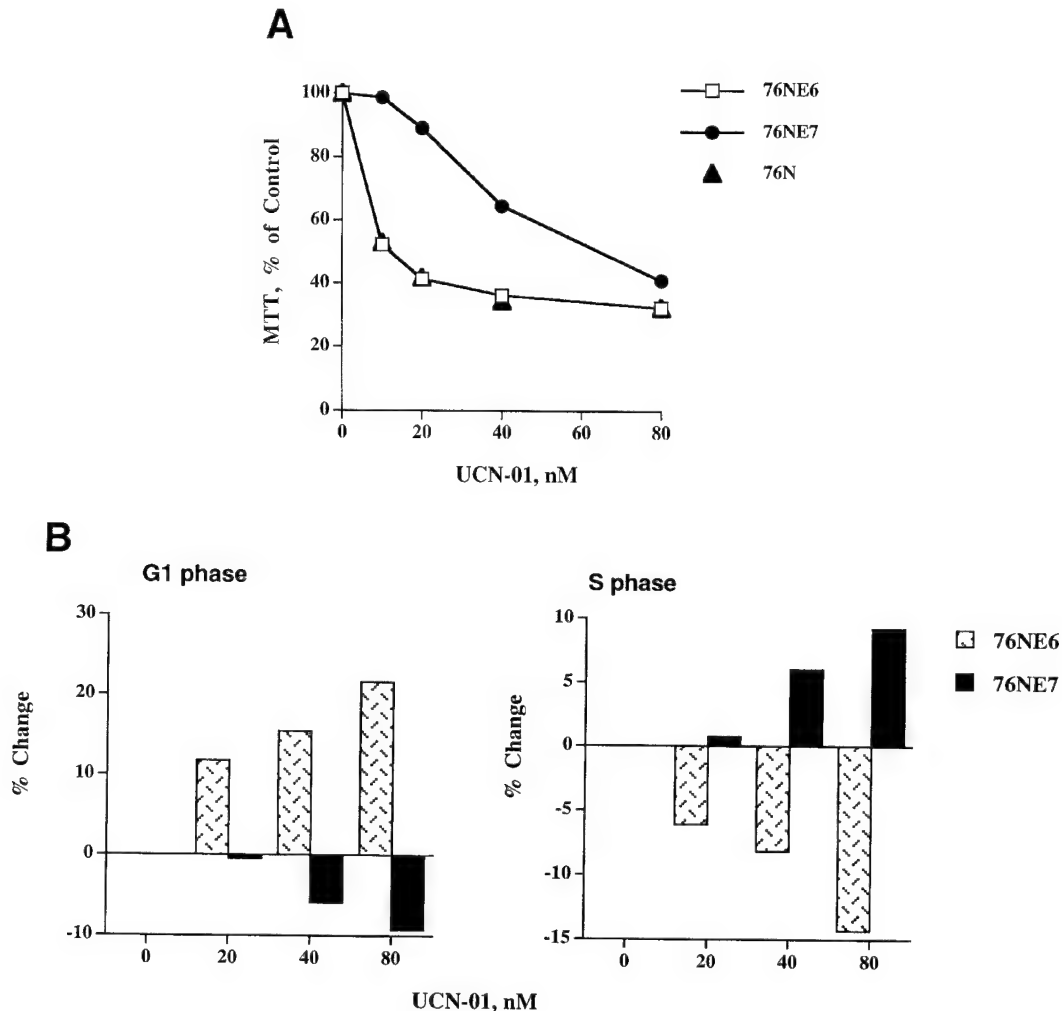
Figure 4 UCN-01-mediated G1 arrest is pRb-dependent and p53-independent. (a) 76N, 76NE6, and 76NE7 cells were treated with the indicated concentrations of UCN-01 for 48 h and subjected to growth inhibition analysis as measured by MTT assay and repeated three times. Error bars are indicated for each condition and each cell line. In all cases the error bars were smaller than the symbol size and cannot be seen. (b) Per cent change in cell cycle distribution of cells in G1 and S phase following UCN-01-treatment. The bar graph reflects the per cent change of G1 and S phases of UCN-01-treated cells relative to the untreated controls, for each cell line

cycle (Figure 6). At every time interval examined, treatment of 81N with UCN-01 resulted in the accumulation of cells in the G1 but not S phase of the cell cycle (Figure 6). Hence, the UCN-01-mediated G1 accumulation occurred in both asynchronous and synchronized cells. Our results suggest that normal cells, with a functional pRb and G1 checkpoint, are incapable of arresting in any other phase but G1 upon treatment with UCN-01, no matter what their cell cycle distribution is prior to treatment.
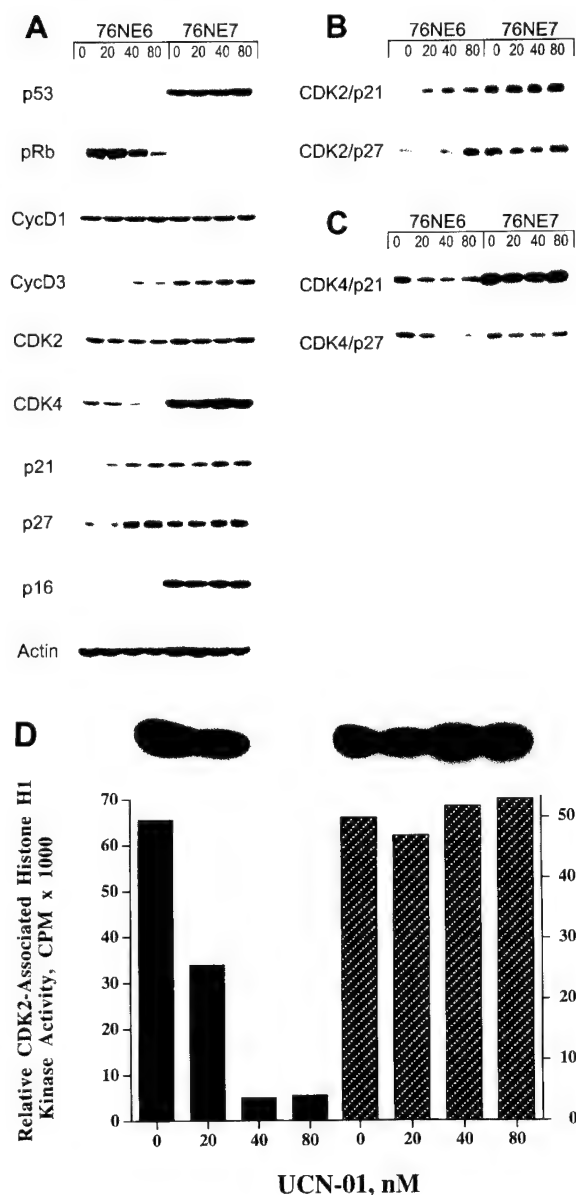
Figure 5 Cell cycle perturbation induced by UCN-01 in 76NE6 and 76NE7 cells. 76NE6 and 76NE7 cells were treated with the indicated concentrations (nM) of UCN-01 for 48 h. Following treatment cells were harvested, cell lysates prepared and subjected to (**a**) Western blot analysis, (**b**) CDK2 immune-complex formation, (**c**) CDK4 immune-complex formation and (**d**) Histone H1 kinase analysis as described for Figure 2. In (**d**) the numbers on the left ordinate refer to c.p.m. obtained from H1 kinase assay for 76NE6 cells (solid bars) and the numbers on the right ordinate refer to the c.p.m. obtained from H1 kinase assay for 76NE7 cells (shaded bars)

The results obtained with UCN-01-treated normal cells are quite different than those with staurosporine-treated cells. It has been well documented that staurosporine, a close structural analogue of UCN-01, can arrest normal cells in both G1 and G2 phases of the cell cycle, and tumor cells in only the G2 phase of the cell cycle. Our results show that UCN-01, also known as 7-hydroxy staurosporine, arrests normal cells in G1 and tumor cells in S phase when used in high concentrations. To compare the effects of staurosporine and UCN-01 in normal *versus* tumor cells we treated two normal cell strains and two tumor cell lines with equally cytotoxic concentrations of UCN-01 and staurosporine (Figure 7). UCN-01 and staurosporine produced quite different effects. These results show that as predicted normal cells respond to high concentrations of staurosporine by arresting in both G1 and G2. However, treatment of these cells with high concentrations of UCN-01 resulted in only a G1 arrest. Furthermore, tumor cells, which have a defect in the pRb pathway, respond to high concentrations of staurosporine (as high as 300 nM, data not shown) by arresting predominately in the G2 phase of the cell cycle. On the other hand, the same tumor cells respond to UCN-01-mediated growth inhibition by arresting in the S phase of the cell cycle (Figure 7). These results clearly indicate that normal and tumor cells respond to these very close structural analogues quite differently. Furthermore, the ability of cells to arrest in either G1 or S phase by UCN-01 is dictated by a functional pRb, while the ability of cells to arrest in G2 by staurosporine is independent of pRb.

Discussion

In this manuscript we investigated the growth inhibitory effects and cell cycle pathways affected by UCN-01 in several normal and tumor-derived breast epithelial cells. This data revealed three novel findings: First, we found that normal cells are significantly more sensitive to UCN-01 than tumor cells. Treatment of normal cells with concentration as low as 10 nM resulted in 50% growth inhibition. Tumor cells were much more resistant to growth inhibitory effects of UCN-01 and concentrations as high as 80 nM resulted in minor to no growth inhibition. The normal cells used in this study were established from reduction mammoplasty samples which undergo senescence after several passages (Band and Sager, 1989). They are normal, diploid, mortal cells with regulated checkpoint control. As shown in Figures 1 and 2 these cells are very sensitive to UCN-01. On the other hand MCF-10A cell line, a near diploid immortalized cell line, was much more resistant to the growth inhibitory activity of UCN-01. In fact the growth inhibitory activity of UCN-01 in MCF-10A was similar to that of MCF-7 and MDA-MB-436, two cancer cell lines used in this study (Figure 1a). These observations suggest that the pathways altered by the immortalization process (i.e. deletions in p15 and p16 genes for example) may compromise the function of the pRb pathway, rendering the MCF-10A cells relatively resistant to low concentrations of UCN-01. Furthermore, the serum concentration in the culture medium of
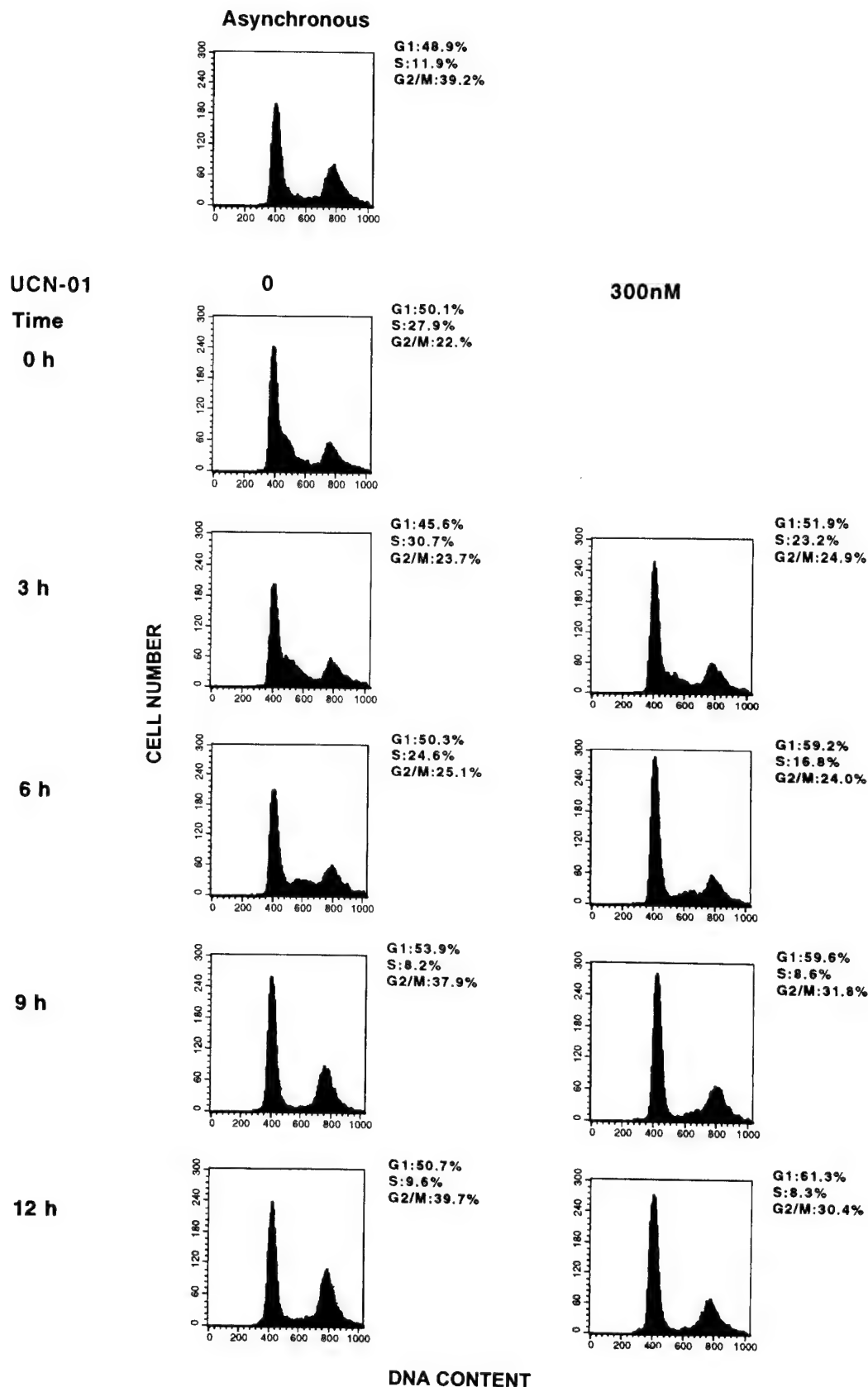
Figure 6 Synchronization of normal cells in the G1/S phase does not abrogate their ability to arrest in G1 by UCN-01. Asynchronously growing 81N cells (top panel) were synchronized at the G1/S boundary by double-thymidine block (see Materials and methods). Synchronized cells were treated with either 0 or 300 nM UCN-01. At the indicated times following UCN-01 treatment cells were harvested for analysis by flow cytometry

normal and tumor cells did not account for the differences in UCN-01-mediated growth inhibition.

The growth inhibitory effects of UCN-01 in normal cells are due to a G1 arrest. We show that such an arrest was concomitant with decreased CDK4 expression, pRb phosphorylation and CDK2 activity, coincident with increased binding of p27 to CDK2 and switching of p27 from CDK4 to CDK2. In addition, UCN-01 treatment also results in down regulation of cyclins D1 and D3 which are usually active in early G1 suggesting that UCN-01 targets an early event in the G1 phase of normal cells. There were no significant cell cycle perturbations observed in tumor cells by UCN-01. Several studies have reported that UCN-01 inhibits cell cycle progression from G1 to S phase in various mammalian transformed cell lines (Akiyama *et al.*, 1997; Kawakami *et al.*, 1996; Seynaeve *et al.*, 1993). However, it is not clear from these studies why some cells respond to UCN-01 by arresting in the G1 phase of the cell cycle while others accumulated in S phase. In this study we clearly show that normal cells with a regulated G1 checkpoint respond to UCN-01 by arresting in G1 while tumor cells, depending on their pRb status arrest either in G1 or S. For example, both MCF-7 cells and MCF-10A which have an intact pRb respond to the growth inhibitory activity of UCN-01 by arresting in the G1

phase of the cell cycle (data not shown). However MDA-MB-436, T47D, and MDA-MB-157 cell lines which are pRb negative (mutations/functional inactivity), arrest in the S phase of the cycle (Figure 7 and data not shown).

Secondly, our studies suggest that the pRb pathway is involved in UCN-01-mediated G1 arrest in normal but not tumor cells. Using the 76NE6 and 76NE7 model system where the HPV E6 binds to and degrades p53, and HPV E7 interacts with pRb and pRb-like proteins and inactivate the pRb pathway. We found that UCN-01 inhibited the growth in G1, and perturbed key cell cycle regulatory proteins in 76NE6 similarly to that of the parental 76N normal cell strain (Figures 2 and 5). However, UCN-01 was incapable of mediating G1 arrest or perturbing the cell cycle regulators not only in tumor cells with a defective pRb pathway such as MDA-MB-157 and MDA-MB-436 (Figure 3) but also in E7 immortalized 76NE7 cells (Figures 4 and 5). These results clearly suggest that the UCN-01-mediated G1 arrest is dependent on a functional pRb and when cells contain a mutant or non-functional pRb, they arrest in the S phase of cell cycle instead.

The mechanism by which UCN-01 mediates G1 arrest through pRb may involve CDK4. We base this hypothesis on the striking decline in CDK4 levels
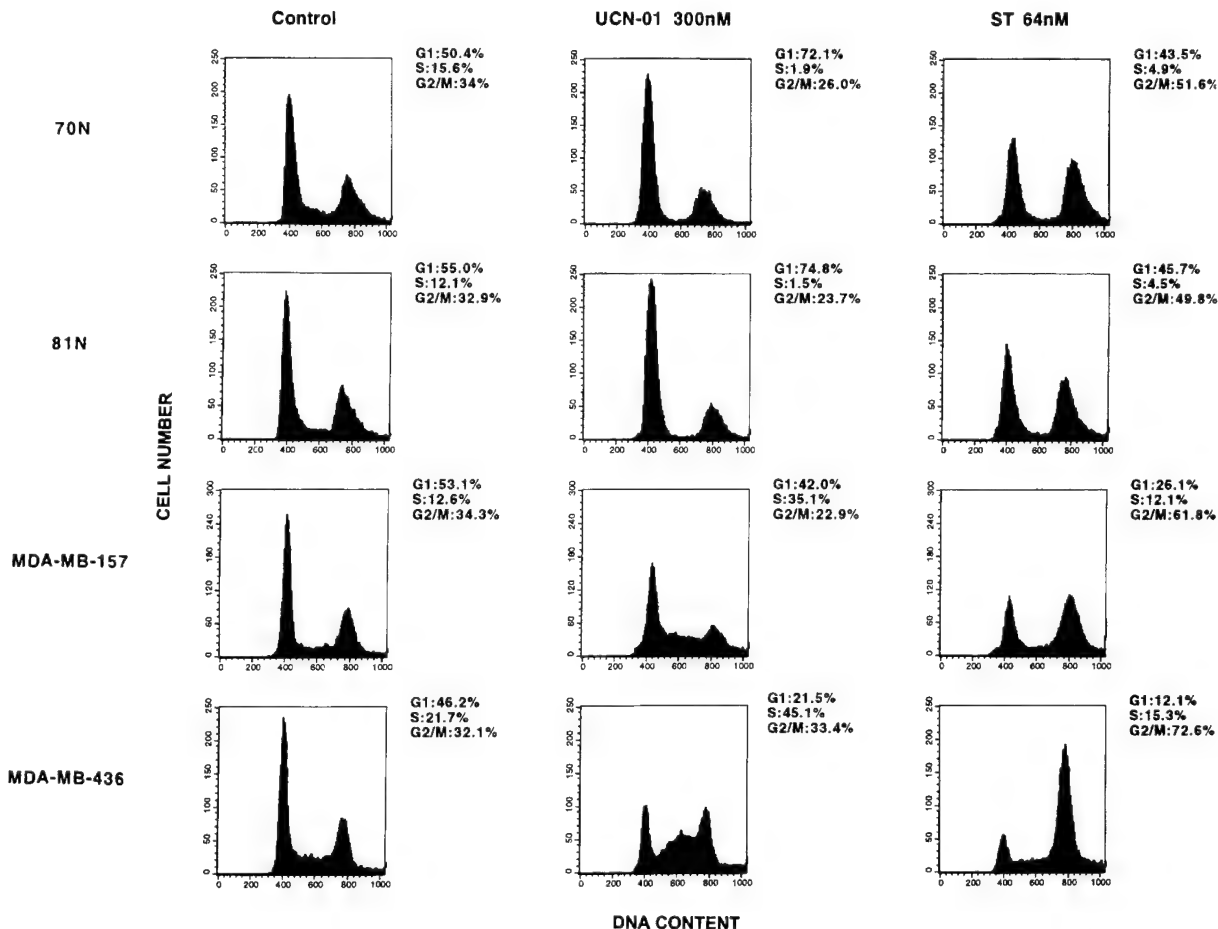
Figure 7 UCN-01 and staurosporine act at different cell cycle checkpoints. Normal breast epithelial (70N and 81N) cell strains and tumor (MDA-MB-157 and MDA-MB-436) cell lines were treated with no drug or equally cytotoxic concentrations of UCN-01 (i.e. 300 nM) or staurosporine (i.e. 64 nM) for 48 h. Following treatment cells were harvested for analysis by flow cytometry

shortly after UCN-01 treatment in the normal cells (Figure 2). The decrease in CDK4 levels occurs only in cells with a functional pRb. Although the immediate downstream effects of UCN-01 responsible for a decline in CDK4 are currently unknown, a likely possibility could involve a feedback regulation between pRb and CDK4. Specifically we suggest that upon the initial hypo-phosphorylation of pRb, a signal is generated to down regulate CDK4 synthesis, resulting in further hypo-phosphorylation of pRb and subsequent G1 arrest.

Lastly, we show that normal and tumor cells respond differently to high concentrations of UCN-01 as compared to staurosporine. Treatment of asynchronous or G1/S-arrested normal cells with either high (300 nM) or low concentrations of UCN-01 results in only a G1 arrest (Figures 6 and 7). On the other hand, treatment of tumor cells with high concentrations of UCN-01 completely inhibits their growth by arresting them in the S phase of the cell cycle (Figure 7). The effect of UCN-01 on normal and tumor cells is very different than its structural analogue, staurosporine, which arrests normal cells in G1 and G2 and tumor cells only in G2 (Figure 7). The G2 (staurosporine) versus S (UCN-01) phase arrest seen in the same tumor cells treated with equally toxic concentrations of these two drugs (Figure 7) is very surprising, since these two agents differ only in the presence of a 7-OH group on UCN-01. Although this structural difference is subtle the two agents have different specificity toward CDKs. In a series of experiments (reviewed in Meijer, 1996) aimed at examining the specificity of UCN-01 and staurosporine toward different proteins kinases, it was discovered that even though the IC_{50}s of these two analogues against purified PKC were similar (i.e. 7 nM for UCN-01, and 5 nM for staurosporine), their IC_{50}s toward CDKs were quite different. UCN-01 displayed IC_{50}s of 30–32 nM against purified CDK1, CDK2 and CDK4. On the other hand, staurosporine displayed IC_{50}s of 3–9 nM against CDK1 and CDK2 and $>10\,000\ \mu$M against CDK4. These studies suggest that the mechanism by which UCN-01 and staurosporine mediate their growth inhibitory effects may be different, and that CDKs and not PKC could dictate such difference. It is also important to consider the role of ATP in this process since at high concentrations of ATP in CDK assays (as would occur in living cells), UCN-01 is actually a relatively poor CDK antagonist (Wang et al., 1995). Nonetheless, the results presented in this study are consistent with CDK inhibition as the mechanism by which UCN-01 and staurosporine mediate their growth inhibitory potential.

The common link between UCN-01 and staurosporine is that at low concentrations, both agents arrest normal cells in G1 and such an arrest is lost in tumor cells. The mechanistic basis of staurosporine-induced G1 arrest in normal cells and its loss in tumor cells was recently reported to be through pRb since mouse embryonic fibroblasts from pRb knockout mice treated with staurosporine were incapable of arresting in G1 (Orr et al., 1998). These and other studies performed on bladder carcinoma cell line 5673 (Schnier et al., 1996) provided strong support for the importance of pRb in inducing G1 arrest in cells by staurosporine. The studies we have presented here also provide strong evidence for the role of pRb in UCN-01-mediated G1

arrest in normal cells and loss of G1 arrest in tumor cells lacking pRb. Thus the ability of both UCN-01 and staurosporine to induce G1 arrest seems to be through pRb, independent of p53. The difference between these two agents is twofold: First, these two agents are different in their ability to induce either G2 arrest, with staurosporine, or S phase arrest, with UCN-01. Secondly, staurosporine induces G2 arrest in both normal and tumor cells, while UCN-01 mediates S phase arrest only in tumor cells. The mechanism by which UCN-01 induces S phase arrest in tumor but not normal cells, although unclear at this point, does not involve either p53 or pRb since treatment of tumor cells lacking both p53 and pRb resulted in S phase arrest.

In summary, our results show that UCN-01 can induce G1 arrest in normal cells at very low concentrations while tumor cells are completely resistant to UCN-01-mediated G1 arrest. This G1 arrest is independent of p53, and dependent on pRb. We also show that tumor cells respond to UCN-01-induced growth inhibition by arresting in S phase independent of either p53 or pRb. Understanding the mechanism by which tumor cells arrest in S phase in response to UCN-01 could provide insight into the regulation of the S phase checkpoint in normal and tumor cells.

Materials and methods

Materials, cell lines and culture conditions

UCN-01 was provided by the National Cancer Institute. Serum was purchased from Hyclone Laboratories (Logan, Utah, USA) and cell culture medium from Life Technologies, Inc. (Grand Island, NY, USA). All other chemicals used were reagent grade. The culture conditions for 76N, 81N and 70N normal cell strains, MCF-10A immortalized cell line, and MCF-7, ZR75T, MDA-MB-157, Hs578T, T47D and MDA-MB-231 breast cancer cell lines were described previously (Keyomarsi et al., 1995; Keyomarsi and Pardee, 1993). 76N-E6 and 76N-E7 cell lines (gifts from Dr V Band, Tufts Medical Institute Boston, MA, USA) were immortalized and cultured as described previously (Band et al., 1990, 1991). All cells were cultured and treated at 37°C in a humidified incubator containing 6.5% CO_2 and maintained free of mycoplasma as determined by Hoechst staining (Hessling et al., 1980).

MTT assay

The MTT (3-[4,5-dimethylthiazol-2yl]-2,5-diphenyltetrazolium bromide) assay was performed as described (Carmichael et al., 1988). Exponentially growing cells were counted by a Coulter Counter (Halieah, FL, USA) and plated at a density of 25 000 cells/ml in the wells of 96-well tissue culture plates (200 μl culture fluid per well) and allowed to recover for 24 h prior to drug treatment. Cells were incubated with the indicated concentration of UCN-01 or staurosporine for 48 h and subjected to the MTT survival assay. Each data point represents the average of six determinations, and the MTT assay for each experimental condition was performed at least three times.

Cell synchronization and flow cytometry

Normal mammary epithelial (81N) cells were synchronized at the G1/S boundary by the double thymidine block procedure as previously described (Keyomarsi et al., 1995). UCN-01

(300 nM) was added following the release of cells from thymidine block. Cells were harvested at the indicated times, cell density was measured using a Coulter Counter and flow cytometry analysis was performed as described previously (Rao et al., 1998).

Blotting, immunoprecipitation and H1 kinase analysis

Cell lysates from UCN-01-treated cells were prepared and subjected to Western blot analysis as previously described (Rao et al., 1998). Primary antibodies used were pRb monoclonal antibody (PharMingen, San Diego, CA, USA), at a dilution of 1:100, monoclonal antibody to p16 (a gift from Jim DeCaprio, Dana Farber Cancer Institute) at a dilution of 1:20, CDK2, CDK4, and p27, monoclonal antibodies (Transduction Laboratories, Lexington, KY, USA) each at a dilution of 1:100, p21 and p53 monoclonal antibodies (Oncogene Research Products/Calbiochem, San Diego, CA, USA) at a dilution of 1:100 cyclin D1 monoclonal antibody (Santa Cruz Biochemicals, Santa Cruz, CA, USA) at a dilution of 1:100, and actin monoclonal antibody (Boehringer-Mannheim, Indianapolis, IN, USA) at 0.63 μg/ml in Blotto. Following primary antibody incubation, the blots were washed and incubated with goat anti-mouse horseradish peroxidase conjugate at a dilution of 1:5000 in Blotto for 1 h and finally washed and developed with the Renaissance chemiluminescence system as directed by the manufacturers (NEN Life Sciences Products, Boston, MA, USA).

For immunoprecipitations followed by Western blot analysis, 300 μg of cell extracts were used per immunoprecipitation with polyclonal antibody to CDK2 (Rao et al.,

1998) or CDK4 (Santa Cruz Biochemicals, Santa Cruz, CA, USA) as previously described (Rao et al., 1998). The immunoprecipitates were then electrophoresed on 13% gels, transferred to Immobilin P, blocked and incubated with the indicated antibodies at dilutions described above. For Histone H1 kinase assay the immunoprecipitates were incubated with kinase assay buffer containing 60 μM cold ATP and 5 μCi of [^{32}P]ATP in a final volume of 50 μl at 37°C for 30 min. The products of the reaction were then analysed on a 13% SDS–PAGE gel. The gel was then stained, destained, dried and exposed to X-ray film. For quantitation, the protein bands corresponding to histone H1 were excised and the radioactivity of each band was measured by Cerenkov counting.

References

Akiyhama T, Yoshida T, Tsujita T, Shimizu M, Mizukami T, Okabe M and Akinaga S. (1997). Cancer Res., 57, 1495–1501.

Band V, Dala S, Delmolino L and Andropphy EJ. (1993). EMBO J., 12, 1847–1852.

Band V, DeCaprio JA, Delmolino L, Kulesa V and Sager R. (1991). J. Virol., 65, 6671–6676.

Band V and Sager R. (1989). Proc. Natl. Acad. Sci. USA, 86, 1249–1253.

Band V, Zajchowski D, Kulesa V and Sager R. (1990). Proc. Natl. Acad. Sci. USA, 87, 463–467.

Berns A. (1994). Curr. Biol., 4, 137–139.

Boorne A, Donnelly N and Schrey M. (1998). Breast Cancer Res. Treat., 48, 117–124.

Bunch R and Eastman A. (1997). Cell Grow. Diff., 8, 779–788.

Carmichael J, Mitchell JB, DeGraff WG, Gamson J, Gazder AF, Johnson BE, Glatstein E and Minna JD. (1988). Br. J. Cancer, 57, 540–547.

Courage C, Budworth J and Gescher A. (1995). Br. J. Cancer, 71, 697–704.

Dyson N, Guida P, Munger K and Harlow E. (1992). J. Virol., 66, 6893–6902.

El-Deiry WS, Tokino T, Velculescu VE, Levy DB, Parsons R, Trent JM, Lin D, Mercer WE, Kinzler KW and Vogelstein B. (1993). Cell, 75, 817–825.

Friend S. (1994). Science, 265, 334–335.

Gray-Bablin J, Rao S and Keyomarsi K. (1997). Cancer Res., 57, 604–609.

Gray-Bablin J, Zalvide J, Fox MP, Knickerbocker CJ, DeCaprio JA and Keyomarsi K. (1996). Proc. Natl. Acad. Sci. USA, 93, 15215–15220.

Harbour JW, Lai SL, Whang-Peng J, Gasdar AF, Minna JD and Kaye FJ. (1988). Science, 241, 353–357.

Harper JW, Adami GR, Wei N, Keyomarsi K and Elledge SJ. (1993). Cell, 75, 805–816.

Harper JW and Elledge SJ. (1996). Curr. Opin. Gene. Dev., 6, 56–64.

Hessling JJ, Miller SE and Levy NL. (1980). J. Immunol. Meth., 38, 315–324.

Horowitz JM, Park S, Bogenmann E, Cheng J, Yandell DW, Kaye FJ, Minna JD, Dryja TP and Weinberg RA. (1990). Proc. Natl. Acad. Sci., 87, 2775–2779.

Iavarone A and Massague J. (1997). Nature, 387, 417–422.

Kato J, Matsuoka M, Polyak K, Massague J and Sherr CJ. (1994). Cell, 79, 487–496.

Kawakami K, Futami H, Takahara J and Yamaguchi K. (1996). Biochem. Biophys. Res. Comm., 219, 778–783.

Keyomarsi K, Conte D, Toyofuku W and Fox MP. (1995). Oncogene, 11, 941–950.

Keyomarsi K and Pardee AB. (1993). Proc. Natl. Acad. Sci. USA, 90, 1112–1116.

Khleif SN, Degregori J, Yee CL, Otterson GA, Kaye FJ, Nevins JR and Howley PM. (1996). Proc. Natl. Acad. Sci. USA, 93, 4350–4354.

LaBaer J, Garrett MD, Stevenson LF, Slingerland J, Sandhu C, Chou HS, Fattaey A and Harlow E. (1997). Genes Dev., 11, 847–862.

Meijer L. (1996). Trends Cell Biol., 6, 393–397.

Michieli P, Chedid M, Lin D, Pierce JH, Mercer WE and Givol D. (1994). Cancer Res., 54, 3391–3395.

Orr MS, Reinhold W, Yu L, Schreiber-Agus N and O'Connor PM. (1998). J. Biol. Chem., 273, 3803–3807.

Planas-Silva MD and Weinberg RA. (1997). Mol. Cell. Biol., 17, 4059–4069.

Pollack IF, Kawecki S and Lazo JS. (1996). J. Neuro., 84, 1024–1032.

Polyak K, Kato J.-Y, Soloman MI, Sherr CJ, Masasgue J, Roberts JM and Koff A. (1994). Genes Dev., 8, 9–22.

Rao S, Lowe M, Herliczek T and Keyomarsi K. (1998). Oncogene, 17, 2393–2402.

5702

Reznikoff CA, Yeager TR, Belair CD, Savelieva E, Puthenveettil JA and Stadler WM. (1996). *Cancer Res.*, **56,** 2886 – 2890.

Schnier JB, Nishi K, Goodrich DW and Bradbury EM. (1996). *Proc. Natl. Acad. Sci. USA*, **93,** 5941 – 5946.

Seynaeve C, Stetler-Stevenson M, Sebers S, Kaur G, Sausville E and Worland P. (1993). *Cancer Res.*, **53,** 2081 – 2086.

Shao R, Shimizu T and Pommier Y. (1997). *Exp. Cell Res.*, **234,** 388 – 397.

Sheikh MS, Li XS, Chen JC, Shao ZM, Ordonez JV and Fontana JA. (1994). *Oncogene*, **9,** 3407 – 3415.

Sherr CJ and Roberts JM. (1995). *Genes Dev.*, **9,** 1149 – 1163.

Soule HD, Maloney TM, Wolman SR, Peterson Jr WD, Brenz R, McGrath CM, Russo J, Pauley RJ, Jones RF and Brooks SC. (1990). *Cancer Res.*, **50,** 6075 – 6086.

Takahashi I, Asano K, Kawamoto I, Tamaoki T and Nakano H. (1989). *J. Antibiot.*, **42,** 564 – 570.

Takahashi I, Kobayashi E, Asano K, Yoshida M and Nakano H. (1987). *J. Antibiot.*, **40,** 1782 – 1784.

Wang Q, Fan S, Eastman A, Worland P, Sausville E and O'Connor P. (1996). *J. Nat. Cancer Ins.*, **88,** 956 – 965.

Wang Q, Worland P, Clark J, Carlson B and Sausville E. (1995). *Cell Grow. Diff.*, **6,** 927 – 936.

Weinberg RA. (1995). *Cell*, **81,** 323 – 330.

Werness BA, Levine AJ and Howley PM. (1990). *Science*, **248,** 76 – 79.

Activation of the Estrogen Signaling Pathway by p21[WAF1/CIP1] in ER Negative Breast Cancer Cells

Xiaomei Chen[1], Christopher Danes[1], Michael Lowe[1], Thaddeus W. Herliczek[1], and Khandan Keyomarsi[1,2,*].

[1] Division of Molecular Medicine, Wadsworth Center, Albany, NY 12201-0509.

[2] Department of Biomedical Sciences, State University of New York, Albany, NY 12222.

* To whom correspondence should be addressed:

Wadsworth Center
Empire State Plaza
P.O. Box 509
Albany, NY 12201-0509

Phone: (518) 486-5799
Fax: (518) 486-5798
E-mail: keyomars@wadsworth.org

Running title: P21[WAF1/CIP1] sensitizes ER negative tumor cells to anti-estrogens.

Key Words: P21WAF1/CIP1, ER negative breast tumor, anti-estrogen.

Abstract

Background: The steroid hormone, estrogen, regulates the proliferation of normal mammary gland as well as most estrogen receptor (ER)-positive mammary carcinomas. Several cell cycle regulatory proteins have been implicated for the growth stimulatory action of estradiol as well as the growth inhibitory activity of anti-estrogens. We propose the novel hypothesis that p21, a cyclin dependent kinase inhibitor which acts as the brake of the cell cycle, plays a significant role in regulating the estrogen receptor (ER) signaling pathway. *Methods*: The effects of p21 on the ER pathway was investigated by overexpression of p21 using a tetracycline inducible system in a breast cancer cell line negative for ER and p21. Activity of the estrogen-signaling pathway was monitored by examining the activity of the ER-promoter-Luciferase and Estrogen-Response-Element (ERE)-Luciferase in transient transfection assays. Additionally the growth modulating affects of estradiol and anti-estrogens were assessed on the p21-overexpressing clones. *Results*: A strong positive correlation was found ($p < 0.001$) between the expression of p21 and estrogen receptor in breast cancer cell lines and tumor tissues from 60 breast cancer patients. Overexpression of p21 in a p21 and ER negative cell line leads to induction of ER- and ERE-Luciferase activities in an estrogen responsive manner. The transcriptional activation of both ER- and ERE- was induced significantly by the addition ß-estradiol to the culture medium of the p21 clones. Lastly, the expression of p21 leads to the sensitization of these p21 stable clones to the growth inhibitory effects of a potent anti-estrogen (i.e. ICI 182780) and the growth stimulatory effects of ß-estradiol. *Conclusion:* Taken together, these results suggest that p21 has a novel role in activation of the estrogen-signaling pathway.

Introduction:

Breast cancer is the most common malignancy and the second leading cause of cancer related deaths among women in the United States. One in eight American women may be afflicted with some form of breast cancer in their lifetime; approximately 30% will die from this disease(1). Considerable evidence indicates that estrogens are important regulators of growth and differentiation in normal breast tissue and also play an important role in the development and progression of estrogen receptor positive breast carcinoma(2). In fact, the various recognized risk factors of breast cancer such as, age at menarche, age at first pregnancy, and age at menopause all suggest that endogenous ovarian steroids may profoundly affect initiation, promotion, and progression of carcinogenesis through a cascade reaction initiated by the activation of estrogen receptor (ER)(2,3).

The estrogen receptor is a 67-kDa estrogen-modulated transcription factor that belongs to the super-family of ligand-activated and nuclear transcription factors which includes receptors for steroids, thyroids and retinoic acid(4-6). In the presence of estrogen (the ligand) the estrogen receptor dimerizes and binds to specific sequences (estrogen response elements or ERE) located in the 5' flanking region of ER responsive genes (such as progesterone receptor) activating their transcription and manifesting their growth stimulating affects(7,8). At the onset, the majority, 46-77%, of breast cancers(9) are ER positive and up to 70% of them respond to hormone manipulation(10) while about 10% of receptor-negative breast cancers exhibit hormonal responsiveness(11). The ER status of a breast tumor also effects its intrinsic biological character. For example, ER-positive tumors are more likely to be histologically well differentiated, diploid, and have lower S phase fraction(12). Consequently, the presence of a functional ER serves as a marker of differentiation and a predictor of disease-free survival in both node-negative and node-positive breast cancer patients(13,14).

3

As breast tumors progress, a molecular diversity in ER expression leads to resistance to anti-estrogen therapy and to broader problems of tumor progression and cellular heterogeneity that also is characterized by advanced breast cancer(15). The hallmark of some hormone-resistant tumors are reduction or lack of ER expression resulting in abnormal proliferation in epithelial cells, leading to a more aggressive metastatic phenotype(12,14,16).

One pathway whereby ER mediates mitogenesis is through the cell cycle. Under conditions where ER is expressed and functional, estrogenic stimulation of cell growth mediates G1 to S transition and inhibition of the ER signaling pathway by anti-estrogens effects cell cycle progression resulting in G1 arrest(17,18). Several studies have already shown that cyclin D1, a G1 cyclin, can interact directly with the ligand-binding domain of ER and can stimulate ER transactivation in a ligand- and cyclin-dependent-kinase(CDK)-independent fashion(19-22). However, the role of CDK inhibitors in mediating a negative growth signal through ER and the estrogen signaling pathway has remained elusive. p21$^{cip1/WAF1}$ is major negative regulator of the G1 checkpoint, by binding to and inhibiting the activities of most cyclin/CDK complexes (reviewed in(23-25)). Additionally, p21 and p27 can function as adaptor molecules, which promote the association of CDK4 with D-type cyclins and increase CDK4 kinase activity (26-29). p21 may also be involved in G1 arrest mediated by anti-estrogenic inhibition of ER. In fact, transfection of ER or p21 in breast cancer cells results in growth inhibition or apoptosis of the transfected cells(30,31). Since ER and p21 both have growth regulatory effects in normal and tumor cells, we hypothesized that p21 may be a mediator of the estrogenic actions in breast cancer cells. Additionally, modulation of the estrogen signaling pathway by p21 may be therapeutically (i.e anti-estrogens) beneficial in breast cancer cells not expressing ER.

4

We found a strong correlation (i.e $p<0.001$) between ER and p21 expression in both breast cancer cell lines and tumor tissue samples obtained from breast cancer patients. We examined the effect of ER on p21 expression and vis-á-vis, the effect of p21 on ER expression and function. Ectopic expression of ER in a cell line endogenously devoid of both p21 and ER did not result in transactivation or expression of p21. However, we observed a significant effect of p21 on activation of the estrogen signaling pathway and expression of ER-related molecules when we introduced p21 stably into ER/p21 negative breast cancer cells. We also found that while prior to p21 expression, these breast cancer cells were completely refractory to estrogens or anti-estrogens, expression of p21 sensitized these cells to the growth stimulatory effects of estrogens and growth inhibitory effects of anti-estrogens. Our results suggest that forced expression of the cell cycle regulator, p21, in breast cancer cells appears to increase the expression of ER-related molecules whose regulation may in turn be relatable to estrogen and anti-estrogen action.

Materials and Methods:

Materials, cell lines, and culture conditions: 17ß-estrodial, and the 3-(4,5-dimethylthiazol-2-yl)-2,5-diphenyltetrazolium bromide (MTT) were purchased from Sigma Chemical Co. (St. Louis, MO), ICI 182,780 from Tocris Cookson Inc (Ballwin, MO), serum from Hyclone Laboratories (Logan, Utah), and cell culture medium from Life Technologies, Inc. (Grand Island, NY). All other chemicals used were reagent grade. The culture conditions for normal 76N and 81N cell strains, and breast cancer cell lines MCF-7, ZR75T, T47D, BT20, MDA-MB-157, Hs578T, MDA-MB-436, MDA-MB-231, and HBL100 were described previously(*32*). All cells were cultured and treated at 37°C in a humidified incubator containing 6.5% CO_2 and maintained free of mycoplasma as determined by Hoechst staining(*33*). Snap frozen surgical specimens from patients diagnosed with breast cancer were obtained from the Quantitative Diagnostic Laboratories (Almhurst, Illinois). All tumor tissue samples were treatment-naïve as they were resected prior to any type of therapy given. Additionally most of the ER/21 positive tumro tissue samples had a well differentiated phenotype.

Plasmid constructs: The ER promoter-reporter construct used, ER3500-230LUC, kindly provided by Dr. Ronald J. Weigel, contains the full-length ER promoter(*34*). The ERE2-tk-luciferase/SV-neo plasmid was provided by Drs. Nancy E Davidson(*35*) and Benita Katzenellenbogen(*36*) and contains two EREs and the viral thymidine kinase promoter, driving the expression of the Luciferase reporter gene (ERE-tk-Luc) (*35*) and can monitor ER-ß-estradiol-induced transcription. The ER cDNA (HEO) was provided by Dr. Myles Brown. The p21-promoter luciferase reporter plasmid was provided by Dr. Wafik El-Deiry(*37*). The pBSTR1 self-contained, one plasmid, tetracycline inducible vector was provided by Dr. Steven Reeves (*38*). The pBSTRp21 vector was constructed by ligating a Not1-linked 559 bp fragment containing the coding region for p21 from the CIP-1 cDNA provided by Dr. Stephen Elledge (*39*).

6

Transfection, flow cytometry, and luciferase assays. For stable transfection MDA-MB-436 were cultured to 70% confluency as described(*40*) and transfected by electroporation at 0.25 kV and 960µF capacitance. For each transfection 1x10^7 cells were suspended in 0.5 ml of serum free α-MEM media, with 40µg of plasmid (pBSTR1 or pBSTR1-p21 vector) in a 0.4cm gap cuvette. Following transfection, cells were plated with complete medium, allowed to attach/recover for 48 hours and cultured in selection medium containing tetracycline (1 µg/ml) and puromycin (0.5ug/ml). Fresh medium was added every other day until colonies were isolated (2-3 weeks). For each transfection, 25 stable clones and one pooled population were isolated. Inducible expression of p21 was monitored by Western blot analysis (see below).

For transient transfections, all cells were cultured to 70% confluency and then transfected by electroporation at voltages ranging from 0.25-0.32V and 960 µF capacitance. For each transient transfection to determine transfection efficiency cells were co-transfected with a GFP containing vector [i.e pEGFPC-1 (Clonetech, Palo Alto)]. For each transfection condition 1x10^7 cells were suspended in 0.5 ml of serum free media, with 40µg of plasmid (promoter-luciferase + pEGFPC-1) in a 0.4cm gap cuvette at a ratio of 1:4 GFP vector to the promoter-luciferase vector. Following electroporation, cells were plated with complete medium and harvested 48 hours post transfection for analysis.

Percent transfection efficiency by GFP expression was assayed 2 different ways. In the first assay we performed immunohistochemistry with GFP to visualize

7

number of cells transfected and the intensity of transfection. Cells expressing GFP by fluorescent microscopy were then enumerated and several fields were used for accuracy. In the second assay we collected live cells and subjected them to flow cytometry to analyze transfection efficiency as measured by examining cell fluorescence as a result of GFP expression. Live cells were analyzed for transfection efficiency by centrifugation at 1000 x g for 10 minutes, and resuspension in phosphate buffered saline (PBS). GFP expression was measured on a Becton Dickinson FACScan flow cytometer (Becton Dickinson San Jose, CA) using an excitation wavelength of 350nm and absorbency at 485nm. Data was analyzed using the CellQuest program (Becton Dickinson San Jose, CA) and efficiency was measured as a percentage of cells expressing GFP over background fluorescence. These two measurements by the flow cytometry FACScan allowed us to calculate percent efficiency, which we then compared to the immunohistochemistry. In all cases the measurements from both assays matched.

For some experiments (see legends) cells were transiently transfected using the GenePORTER transfection reagent (GPR), as this method of transfection yields high (>60%) transfection efficiency in MDA-MB-436 cells. For these experiments, 1X 10^6 cells were plated in 100mm dishes and 40µg of plasmid (promoter-luciferase + pEGFPC-1) were mixed with 30 µl of GPR and 5 ml of culture media, and added to cells. Cells were harvested 24 hours post transfection for analysis.

For luciferase assays cells were washed in phosphate buffer saline and lysed in extraction buffer (100 mM potassium phosphate, 1 mM dithiothreitol), sonicated, and subjected to 100,000 X g centrifugation, all at 4°C. 50µg high-speed-supernatant

from each condition were mixed with luciferase buffer containing 1 mM dithiothreitol, 15 mM potassium phosphate, 25 mM Gly-Gly pH 7.8, 4mM EGTA, 15 mM $MgSO_4$ in a total volume of 500 µl and assayed for luciferase activity in the LUMAT luminometer as described (41). D-Luciferin (Sigma) was added at a saturating substrate concentration (0.2 mM in luciferase buffer).

MTT assay: The MTT (3-[4,5-dimethylthiazol-2yl]-2,5-diphenyltetrazolium bromide) assay was performed as described (42). For each cell line used in this study, including MCF-7, MDA-MB-231, Hs578T, MDA-MB-436 parental, 436/p21 clones, and 436/vector alone controls we initially performed growth assays using direct counting of live cells. Once we established the number of cells to be plated and the concentration of drug to be used for each experiment, we then performed the growth assays as measured by the MTT assay. In all cases examined the fold increase (or decrease) of cell number to treatment was directly proportional (1:1) to the increase (or decrease) in MTT dye reduction assays. For examining the growth modulating effects of 17ß-estrodial, or ICI 182,780 on the indicated cell lines, exponentially growing cells were counted by a Coulter Counter (Halieah, Florida) and plated at a density of 1500 cells/well in the wells of 96 well tissue culture plates (200 µl culture fluid per well) in estrodial free medium (DMEM media without phenol red and supplemented with 5% Dextran Charcoal Stripped-Fetal Bovine Serum). After 24 hours, cells were treated with 17ß-estrodial, or ICI 182,780 at indicated concentration, and redosed every other day for the duration of the experiment. At the end of each experiment the plates were subjected to the MTT assay. Each data point represents the average of six determinations, and the MTT assay for each experimental condition was performed at least 3 times. The data is presented either as percent increase over or percent decrease from untreated cells.

9

Cell and tissue extraction and Western blot analysis: Cell lysates from the indicated cell lines and transfected cells and tissue homogenates prepared form snap frozen surgical specimens were prepared and subjected to Western blot analysis as previously described(*28,43*). All cell lines were routinely harvested at 70% confluency and 24 hours prior to harvesting the cells received fresh media. Briefly, 50 μg of protein from each condition was electrophoresed in each lane of either a 7% sodium dodecyl sulfate-polyacrylamide gel (SDS-PAGE) (pRb, ER), 10% SDS-PAGE (p53, cyclin D1, cyclin D3) or 13% SDS-PAGE (p21, p27, CDK2) and transferred to Immobilon P overnight at 4° C at 35mV constant volts. The blots were blocked overnight at 4 ° C in Blotto (5% nonfat dry milk in 20mM Tris, 137 mM NaCl, 0.25% Tween, pH 7.6). After six, 10 minute washes in TBST (20mM Tris, 137mM NaCl, 0.05% Tween, pH 7.6), the blots were incubated in primary antibodies for 3 hours. Primary antibodies used were pRb monoclonal antibody (PharMingen, San Diego, CA), monoclonal antibodies to ER-α (Novartis and Santa Cruz, see below for antibody characterization) monoclonal antibodies to p27, cyclin D1, cyclin D3, and CDK2 (Transduction Laboratories, Lexington, KY) monoclonal antibodies to p21 and p53 (Oncogene Research Products/Calbiochem, San Diego, CA) all at 0.1μg/ml in Blotto and actin monoclonal antibody (Boehringer-Mannheim, Indianapolis, IN) at 0.63 μg/ml in Blotto. Following primary antibody incubation, the blots were washed and incubated with goat anti-mouse horseradish peroxidase conjugate (PIERCE, Rockford, IL) at a dilution of 1:5,000 in Blotto for 1 hour and finally washed and developed with the Renaissance chemiluminesence system as directed by the manufacturers (NEN Life Sciences Products, Boston, MA).

ER antibodies and antigen competition assays: The antigen used to generate the Novartis ER mouse monoclonal IgG1 antibody (clone 6F11) is the recombinant protein corresponding to the full-length estrogen receptor molecule. Although detailed epitope mapping have not yet been performed with this antibody, it has been shown that the 6F11 clone not only recognizes full length ER-alpha, but also a truncated form of ER-alpha consisting of the first 184 amino acids (Novartis, personal communications). Hence the Novartis ER antibody recognizes the amino terminus of the ER-alpha receptor. The antigen used to generate the Santa Cruz ER mouse monoclonal IgG$_{2a}$ antibody is a recombinant protein corresponding to amino acids 495-595 mapping at the carboxy terminus of ER-alpha.

Although neither antibodies was made against a peptide, but rather to either the full length or C-terminus 100 amino acids, we performed competition assays using the full length recombinant ER protein. For these analysis we first performed Western blot analysis similar to those presented in Fig 3B with limiting amounts of either the Novartis (N) or Santa Cruz (SC) ER antibody. Once the lowest concentrations of antibody capable of detection of the "ER-related" bands were determined, we performed antibody competition assays. For these assays new Western blots were prepared (again similar to those presented in Fig 3B) and hybridized with limiting antibody concentrations in the presence of increasing amounts of the full length recombinant ER protein.

11

Results:

Correlation between expression of p21 and estrogen receptor: In our initial analysis of cyclin-dependent kinase inhibitor (CKI) expression in normal versus tumor cells, we found a curious correlation between p21/p27 and ER status in breast tumor cell lines. In every ER positive breast tumor cell line examined, both p21 and p27 were overexpressed relative to ER negative tumor cell lines (Fig 1A). Western blot analysis of 9 breast cancer cell lines, 4 of which are positive for ER expression reveal that p21 and p27 are expressed at much higher levels in ER positive than ER negative breast cancer cell lines. To further investigate the correlation between the CKIs and ER, we examined the expression of p21 and p27 in 60 breast tumor tissue samples with known ER status (Fig 1B). These 60 breast tumor specimen include 30 which are ER positive and 30 which are ER negative. Tissue extracts from these 60 tumor samples were subjected to Western blot analysis with antibodies against p21, p27, ER and actin. This analysis revealed that there is a striking correlation between the expression of p21 and ER (25/30 ER+ samples are also positive for p21, while 27/30 ER- samples are also negative for p21; i.e. $p<0.001$) (Fig 1B). The correlation between p27 and ER however is not as strong as p21 and ER in tumor tissue samples. In fact in most of the ER negative tumor tissues, a significant level of p27 is expressed, while most of these tumors were devoid of p21 (Fig 1B, ER negative panels). This lack of strong correlation between p27 and ER suggests that expression of p27 may not have a direct effect on the ER pathway.

ER does not induce p21 expression or transcriptional activation. The strong correlation between ER and p21, observed in figure 1, suggested that there could be a cross talk between these two proteins. Since ER itself is a transcription factor it was logical to hypothesize that ER could activate the expression of p21 through direct or indirect pathways. To this end we transiently transfected MDA-MB-436 cell line with a

12

cDNA to ER (Fig 2) and assessed the transcriptional activity of ER and whether it could induce the expression of p21. MDA-MB-436 is a breast cancer cell line which is ER negative and devoid of any detectable p21 at the level of RNA or protein (Fig 1 and(*44*)). For the transactivation analysis, the ER cDNA was co-transfected with a ERE-Luciferase reporter gene construct (ERE-tk-Luc)(*35*). The results reveal that although transient transfection of ER cDNA in the MDA-MB-436 cell line lead to the expression of ER protein (Fig 2A) and its activity as a transcription factor- measured by the ability of ER transfected cells to activate ERE-tk-Luc (Fig 2B), p21 expression was not detected (Fig 2A). Furthermore, the expression of ER in MDA-MB-436 cells does not alter the expression of other cell cycle regulatory proteins such as p27, CDK2, CDK4, cyclin D1, cyclin D3, pRb, or p53 (Fig 2A).

We also examined whether ER could activate the transcription of p21 in MDA-MB-436 cells. For this experiment we co-transfected MDA-MB-436 cells with a cDNA to ER and a cDNA harboring p21 promoter-Luciferase system(*45*) (Fig 2A & 2C). The results revealed that the transfected ER did not induce the activity of p21 promoter since no change in p21 promoter-Luciferase activity was observed in MDA-MB-436 cells transfected with p21 promoter-Luciferase cDNA alone as compared to cells co-transfected with both the cDNAs to p21-promoter-lucifease and ER (Fig 2C). MCF-7 have a very high p21 promoter-Luciferase activity (Fig 2C), which correlate with the high level of endogenous p21 expression (Fig 1 & Fig 2A). Collectively the results from figure 2 suggest that under conditions where ER is introduced into cells transiently, it has no detectable effects on the expression of p21 or transactivation of its promoter.

Induced expression of p21 in tumor cells leads to the expression of ER antibody-reactive proteins. Next, we performed the reverse experiment to that of Figure 2, by examining the direct effect of p21 on the induction of ER signaling pathway. Because ectopic expression of p21 typically would arrest cells, we used an inducible system

13

under the expression of tetracycline-responsive promoters(*46*). Following transfection of MDA-MB-436 with a vector containing the tetracycline-inducible (Tet) system in one plasmid(*38*), twenty-five stable clones were selected with puromycin and isolated, propagated and analyzed by Western blot for the expression of p21 at 0 and 72 hours after tetracycline removal (Fig 3A). The Western blot analysis of 5 representative p21 positive (out of 15 positives) and 2 p21 negative clones shows that p21 can be induced to be expressed at very high levels in these clones (Fig 3A).

The expression of ER-α was also examined in the MDA-MB-436 parental and 436/p21 stable clones in the presence or absence of ß-estradiol at the level of RNA (data not shown) and protein using two antibodies to ER with different epitope specificity (Fig 3B). Neither Northern blot analysis or RT-PCR assays detected any appreciable expression of the ER-α message, or any alternatively spliced ER-α message in the 436/21 clones (data not shown). Similarly, Western blot analysis revealed that overexpression of p21 in the MDA-MB-436 cells did not result in the expression of the wild-type 67 kDa ER-α which was detected in the MCF-7 cells by both antibodies (Fig 3B, thick arrow). However, the 2 different ER antibodies detected a 87-kDa [with ER α (N)-mapped to the amino terminus of ER] and a 62-kDa [with ER α (SC)-mapped to the carboxy terminus of ER] protein that are over expressed in the 436/p21 clones (compared to MCF-7 cells) and are induced following ß-estradiol stimulation in both MCF-7 and the 436/p21 clones (Fig 3B-thin arrows). Levels of p21 and p27 remain unaffected by the addition of ß-estradiol. Normal breast epithelial cells 81N, breast tumor MDA-MB-436 and 436/mock cells were included as negative controls, which express neither wild-type ER-α, nor the 87 or the 62 kDa ER-α reactive proteins (Figure 3B). Antigen competition show that the presence of the full length ER-α recombinant protein could specifically compete off not only the band corresponding to the wild-type ER-α in MCF-7 cells, but also the two "ER-related" bands detected with the aforementioned antibodies in 436/21 clones in a dose

14

dependent fashion (data not shown). These results suggest that the bands reacting with the antibodies used are in fact ER-related and specific.

Estrogen inducible transactivation of the ER promoter by p21. Since p21 expression did not result in any detectable 67 kDa ER-α, we next set out to examine if the ER transactivation has been activated in the p21 clones. The ER promoter reporter plasmid(*34,38*) (i.e. ER-Luc) was transfected into p21 stable clones, parental cells, and vector alone (i.e. mock) transfected clones (Fig 4A) and the ability of ß-estradiol to modulate the transactivation of ER was assessed (Fig 4B). The rationale for using ß-estradiol is that ER can auto-regulate its own expression in an estrogen dependent pathway(*47*). These analyses reveal that p21 induces the ER-Luc reporter system, and the addition of estradiol to the cells further increases the luciferase activity (Fig 4). In the p21 clones 7 & 12 ER-Luc is up-regulated by up to 40 fold over the mock clone 16 or the parental cells in the absence of any estradiol (Fig 4A). The degree of this up-regulation depends on the amount of p21 expressed in each clone. For example p21 clone 12 has a much higher p21 expression than clone 7 (data not shown) and harbors a much higher basal ER transcriptional activity than clone 7 as revealed by the higher ER-Luc activity in the absence of any ß-estradiol activity (Fig 4A). Furthermore, we found that the transactivation of ER-Luc in the p21 clones was further induced by ß-estradiol. Addition of ß-estradiol to all cells increased the ER-Luc activity only in the p21 clones by 3.2-7.5 fold with no detectable increases in the mock transfected or parental cells (Fig 4B). This was the first indication that overexpression of p21 may have activated an estrogenic response in otherwise ER-α negative breast cancer cells.

Induced expression of p21 leads to the activation of the estrogen signaling pathway in ER negative breast cancer cells. Due to the estrogen inducible

15

transactivation of the ER promoter in the p21 clones (Fig 4), we next asked whether the ER responsive elements (i.e. ERE sequences) can also be induced in these clones in an estrogen responsive manner by ERE-tk-Luc(35). Transient transfection with the ERE-tk-Luc plasmid in the presence or absence of ß-estradiol revealed that the ERE-tk-Luc activity was induced in both the MCF-7 and the p21 stable clones by ß-estradiol (fig 5A). However, in the mock clone 16 and the parental MDA-MB-436 not expressing p21, no induction of luciferase was observed by estradiol and the luciferase activity remained at basal/undetectable levels. We found that compared to the mock or parental cells, the ERE-tk-Luc activity was induced >100 fold in the p21 stable clones (Fig 5A). Furthermore treatment of cells with ß-estradiol further induced the luciferase activity by 3 to 6 fold in p21 clones 12 and 25, respectively (Fig 5B). To further examine the fold difference in sensitivity to ß-estradiol between MCF-7 cells and 436/p21 clones, both cell lines were transfected with ERE-tk-Luc plasmid followed by treatment with increasing concentrations of ß-estradiol (0.1 to 500 nM). Measurement of the luciferase activity in these cells revealed a similar dose response pattern of ß-estradiol dependent induction of ERE- activity in the MCF-7 cells as compared to the 436/p21 clone 25 (Fig 5C). Lastly, cells were treated with the potent anti-estrogen ICI 182, 780 to determine whether the estrogenic response of the ERE-tk-Luc activity would be abrogated. We found that in cells treated with both ß-estradiol and the ICI 182,780 the stimulatory effects of estradiol on the ERE-tk-Luc activity were abrogated in the p21 clones by ICI182,780 down to basal levels, and in ER positive MCF-7 cells to slightly below the basal levels (Fig 5 A, B). Collectively these data suggest that the estrogen signaling pathway is functional in the p21 clones. The expression of p21 activates ERE transactivation in MDA-MB-436 cells through both ß-estradiol independent (i.e. high basal activity of ERE-tk-Luc) and dependent (i.e. ERE-tk-Luc activity induced by ß-estradiol) pathways. Furthermore, the ß-estradiol

dependent response in both MCF-7 and 436/p21 clones is abrogated by anti-estrogen ICI 182, 780.

p21 sensitizes breast cancer cells to the growth stimulatory effects of ß-estradiol and growth inhibitory effects of endocrine therapy: Having shown a strong correlation between ER and p21 in breast tumor tissue samples (Fig 1) and also that p21 overexpression leads to the ER- and ERE-transactivation inducible by estrogen in otherwise ER negative breast cancer cells (Figs 4 & 5), we now have the tools to examine if ER negative cells overexpressing p21 are more sensitive to growth altering effects of ß-estradiol and anti-estrogens than their parental counterparts. To determine whether overexpression of p21 has rendered the ER negative MDA-MB-436 cells sensitive to the growth stimulatory effects of ß-estradiol, cells were treated with indicated concentrations of ß-estradiol (Fig 6A) MCF7 cells which are ER positive are very responsive to the growth stimulatory effects of ß-estradiol and show a 75% increase in cell proliferation (as analyzed by the MTT assay(29)) at only 5 nM ß-estradiol as compared to no ß-estradiol culture conditions. The growth rate of MCF-7 did not further increase with increasing concentration of the ligand. P21 stable clones of MDA-MB-436 cells, although not as sensitive as MCF-7 to ß-estradiol, responded quite dramatically to the ligand as their rate of proliferation increased by 25-40% by ß-estradiol. ß-estradiol had no growth stimulatory effects on MDA-MB-436 parental or mock-transfected cells.

To compare how overexpression of ER in ER negative cells affects their proliferation in response to ß-estradiol, we transfected the cDNA to ER into three different ER negative breast cancer cell lines. Culturing of these cell lines in medium containing ß-estradiol resulted in decreased rate of proliferation as compared to transfected cells not treated with ß-estradiol (Fig 6B). The results from figure 6 suggest that although the overexpression of both p21 and ER results in the

17

modulation of the estrogen signaling pathway, these effects are completely opposite to each other.

Next, to examine if the overexpression of p21 has rendered the ER negative MDA-MB-436 cells sensitive to the growth inhibitory effects of ICI 182,780, cells were treated with the indicated concentrations of ICI182,780. MCF-7 cells which are naturally ER positive respond to anti-estrogens effectively with 34% growth inhibition observed at 20nM ICI 182,780 (Fig 7). MDA-MB-436 parental cell line or a mock transfected clone which are ER negative and unresponsive to the transactivation effects of estrogen, show little to no responsiveness to ICI 182,780 at concentrations up to 80 nM. However when we examined the ability of 2 different p21 clones (9 & 12) to respond to ICI 182,780, we found that the p21 clones are responsive to the growth inhibitory activity of this anti-estrogen exhibiting 15-28% growth inhibition at 80nM drug (Fig 7). The response of the 436/p21 clones to ICI 182,781 were not as inhibitory as MCF-7, but when higher concentrations of drug were used the growth of the p21 clones were inhibited with similar efficacy as that of MCF-7 (data not shown). These data also corroborate our ERE-transactivation studies suggesting that overexpression of p21 in ER negative breast cancer cells can activate the estrogen-signaling pathway in these cells.

Discussion:

In this article we provide evidence for a novel role of p21 in the activation of the estrogen signaling pathway in breast cancer cells in the absence of a detectable wild-type 67 kDa ER-α. Our findings presented show: (a) a strong correlation between p21 and ER expression in breast cancer cell lines and tumor tissue samples from breast cancer patients, (b) that overexpression of p21 in ER/p21 negative breast cancer cells results in the ability of cells to transactivate ER and estrogen response elements (i.e. ERE sequences) activities in an estrogen responsive fashion, (c) that the 436/p21 clones have become sensitized to the mitogenic effects of ß-estradiol and lastly, (d) that overexpression of p21 sensitizes these ER negative breast cancer cells to the growth inhibitory effects of anti-estrogens.

The p21 mediated activation of the estrogen signaling pathway occurs in the absence of any detectable wild-type ER-α by Western blot analysis. However, 2 ER-antibody reactive proteins (87 and 62 kDa) are expressed in the p21 clones whose expression are induced by the addition of ß-estradiol in both MDA-MB-436/p21 clones and MCF-7 cell line. Even though the wild-type ER-α is not detectable in the p21 stable clones, these cells resemble MCF-7 in their ability to activate the estrogenic response pathway. Both MCF-7 and the p21 clones of MDA-MB-436 cells exhibit transactivation of ERE activities in a ligand inducible fashion abrogated by the addition of ICl182,780 (Fig 5). Furthermore the proliferation of both cell types is stimulated by the mitogenic action of ß-estradiol (Fig 6), and inhibited by the anti-estrogen ICl 182,780 (Fig 7). Additionally the ER-promoter activity itself is transactivated in the p21 stable clones, responsive to ß-estradiol (Fig 4). Collectively these observations suggest that the 87 and 62 kDa ER reactive proteins may be different variants of ER-α, capable of activating the estrogenic pathway, however with lower potency than wild-type ER-α. This is a plausible hypothesis because if the expression of the wild-type ER-α was induced by p21 to similar levels/activity as in MCF-7 cells, it could result in

19

cessation of cell proliferation by ß-estradiol (see Fig 6B). In fact, one of the distinct characteristics of cells transfected with the ER cDNA is that they exhibit estrogen mediated growth inhibitory properties(30). Although the precise mechanisms of this paradoxical response to estradiol is unknown, it is conjectured that overexpression of ER beyond a certain level, alters the gene expression machinery of the cell by either turning on ER-dependent activation of unknown lethal genes or switching off of important "house-keeping" genes(30). We also observe this phenomena when we transiently transfect ER cDNA into 3 different ER negative breast cancer cell lines. Treatment of these ER overexpressing cells with ß-estradiol results in inhibition of cell proliferation (Fig 6B).

Our emerging hypothesis from these studies is that overexpression of p21 leads to the expression of ER like proteins which can activate the estrogen-signaling pathway. However, since the activity of these ER like proteins are lower than the wild-type ER-α , the cells do not exhibit the same response as cells in which ER-α is overexpressed. Rather overexpression of p21 mediates an "MCF-7 like" estrogenic phenotype where their proliferation is stimulated by the ligand and inhibited by anti-estrogens.

The novel role of p21 in mediating an ER like response in otherwise ER negative breast cancer cells is another example of the pleiotropic functions of p21 in cell growth and differentiation. p21 has multiple roles not only in regulating cell growth through activation or inhibition of CDKs (reviewed in(23-25)), but also in mediating differentiation (48-50) and inhibiting apoptosis (51,52). A prerequisite for terminal differentiation is exit from cell cycle, and p21 expression is induced during terminal differentiation both in vitro(48-50) and in vivo(53,54). For example, ectopic expression of p21 has been shown to promote differentiation of the megakaryoblastic leukemia cell line CMK(55) and the myelomonocytic cell line U937(56). Furthermore, disruption of p21 in normal diploid fibroblasts resulted in an extension of in vitro life span and a

bypass of senescence(*57*). Here we show another role for p21, that of modulation of the estrogenic pathway, without detectable expression of the wild-type 67-kDa ER-α. These results suggest that p21 can uncouple the detectable expression of ER from its downstream effects on the activation of the estrogen pathway. The precise mechanisms by which p21 has achieved the estrogenic activation is currently unknown, however it is apparent that overexpression of p21 in an otherwise ER negative cell line can render these cells equipped with an "MCF-7 like", well-differentiated phenotype, responsive to anti-estrogens. Although the effect of p21 on the estrogen signaling pathway may represent a novel function for function p21, it is also possible that the putative general CDK inhibitory properties of p21 (also shared by p27 and p57) may have a role in modulation of the estrogen signaling pathway.

The p21 mediated activation of the estrogen signaling pathway in the absence of a detectable ER, has profound clinical implications. A number of agents currently used in the clinic for the treatment of breast cancer, result in the induction of p21. For example Taxol, a potent and highly effective anti-neoplastic agent for the treatment of advanced, drug-refractory, metastatic breast cancers, results in the up-regulation of p21 in the ER negative MDA-MB-435 cell line (*58*). Similarly, treatment of MCF-7 cells with paclitaxel(*59*), doxorubicin in the presence or absence of neu differentiation factor (NDF)(*60*), or the vinca alkaloid analogue, vinorelbine, in combination with a progesterone analogue(*61*), all result in induction of p21. Lastly treatment of a number of breast cancer cell lines and primary cultures from 20 different invasive ductal carcinoma of the breast with adriamycin resulted in a significant accumulation of p21(*62*). Similar to chemotherapeutic agents, several differentiation inducing agents also result in the induction of p21 in the treated cells. For example, p21 is induced in HL60 leukemia cells by differentiative agents such as vitamin D3 (*63*); 12-0 tetradecanoyl phorbol-13 acetate; retinoic acid; dimethlysulfoxide (*50,64*); butyrate (*50*); in melanoma cells p21 is induced when cells are terminally differentiated with

21

interferon and mezerein (*65*); and in leukemia cells p21 is induced by okadaic acid (*66*). Since treatment of breast cancer with several chemotherapeutic drugs as well as differentiative agents results in the induction of p21(*58*)-(*62*), and since the increased expression of p21 can lead to the induction of the estrogen signaling pathway (this study), it follows that subsequent to chemotherapy of ER negative breast cancer, the estrogen signaling pathway may become activated. The clinical translation of this hypothesis lies in the potential of p21 positive, ER negative breast cancers to respond to anti-estrogens. Hence a treatment strategy which would arise from this study would be to combine chemotherapy with anti-hormonal therapy in ER negative cancers which score positive for p21. Since chemotherapeutic agents can induce p21 and p21 can activate the estrogen pathway, such a combination therapy could benefit ER negative breast cancer patients which were rendered unresponsive to anti-estrogens. The induction of the ER signaling pathway in otherwise ER negative tumors by increased levels of p21 could ultimately promote tumor cell differentiation and result in tumor regression and improved survival rates. This treatment strategy could also benefit the 10% of patients with negative ER/PR breast cancers, but high basal levels of p21.

Acknowledgments

REFERENCES

(1)   Jiang S-Y, Jordan VC: Growth regulation of estrogen receptor negative breast cancer cells transfected with complementary DNAs for estrogen receptor. J. Nat'l. Cancer Inst. 84:580-591, 1992

(2)   Bernstein L, Ross RK: Endogenous hormones and breast cancer risk. Epidemiol. Rev. 15:48-65, 1993

(3)   Pike MC, Spicer DV, Dahmoush L, Press MF: Estrogens, progestogens, normal breast cell proliferation and breast cancer risk. Epidemiolo. Rev. 15:17-35, 1993

(4)   Mangelsdorf DJ, Thummel C, Beato M, Herrlich P, Schutz G, Umesono K, et al: The nuclear receptor superfamily: the second decade. Cell 83:835-839, 1995

(5)   Beato M, Herrlich P, Schutz G: Steroid hormone receptors: many actors in search of a plot. Cell 83:851-857, 1995

(6)   Evans RM: The steroid and thyroid hormone receptor superfamily. Science 240:889-895, 1988

(7)   Katzenellenbogen JA, O'Malley BW, Katzenellenbogen BS: Tripartite steroid hormone pharmacology: Interaction with multiple effector sites as a basis for the cell- and promoter-specific action of these hormones. Mol. Endocrinol. 10:119-131, 1996

(8)   Tsai M-J, O'Malley BW: Molecular mechanisms of action of steroid/thyroid receptor superfamily members. Annu Rev. Biochem. 63:451-486, 1994

(9)   Robertson JFR: Oestrogen receptor: a stable phenotype in breast cancer. Brit. J. Cancer 73:5-12, 1996

(10)   Saeed-Sheikh M, Garcia M, Pujol P, Fontana JA, Rochefort H: Why are estrogen-receptor-negative breast cancers more aggressive than the estrogen-receptor-positive breast cancers. Inv. Met. 14:329-336, 1994

(11) Williams MR, Todd JH, Ellis IO, Dowle CS, Haybittle JL, Elston CW, et al: Oestrogen receptors in primary and advanced breast cancer: An eight year review of 704 cases. Br. J. Cancer 55:67-73, 1987

(12) McGuire WL, Chamness GC, Fuqua SAW: Estrogen receptor variants in clinical breast cancer. Molec. Endocrin. :1571-1577, 1991

(13) Clark GC, Osborne CK, McGuire WL: Correlations between estrogen receptor and patients characteristics in human breast cancer. J. Clin. Oncol. 2:1102-1109, 1984

(14) Osborne CK, Yochmowitz MG, Knight WAl, McGuire WL: The value of estrogen and progesterone receptors in the treatment of breast cancer. Cancer 12:2884-2888, 1980

(15) Clarke R, Brunner N: Acquired estrogen independence and antiestrogen resistance in breast cancer. Trends Endocrinol. Metab. 7:291-301, 1996

(16) Lemieux P, Fuque S: The role of the estrogen receptor in tumor progression. J. Steroid Biochem. Molec. Biol. 56:87-91, 1996

(17) Wakeling AE, Dukes M, Bowler J: A potent specific pure antiestrogen with clinical potential. Cancer Res. 51:3867-3873, 1991

(18) Watts CK, Brady A, Sarcevic B, deFazio A, Musgrove EA, Sutherland RL: Antiestrogen inhibition of cell cycle progression in breast cancer cells is associated with inhibition of cyclin-dependent kinase activity and decreased retinoblastoma protein phosphorylation. Molec. Endoc. 9:1804-1813, 1995

(19) McMahon C, Suthiphongchai T, DiRenzo J, Ewen ME: P/CAF associates with cyclin D1 and potentiates its activation of the estrogen receptor. Proc. Natl. Acad. Sci. USA 96:5382-5387, 1999

(20) Zwijsen RML, Buckle RS, Hijmans EM, Loomans CJM, Bernards R: Ligand-independent recruitment of steroid receptor coactivators to estrogen receptor by cyclin D1. Genes & Dev. 12:3488-3498, 1999

(21) Zwijsen RML, Wientjens E, Klompmaker R, Van Der Sman E, Bernards R, Michalides RJAM: Cdk-independent activation of estrogen receptor by cyclin D1. Cell 88:405-415, 1997

(22) Neuman E, Ladha MH, Lin N, Upton tM, Miller SJ, DiRenzo J, et al: Cyclin D1 stimulation of estrogen receptor transcriptional activity independent of cdk4. Mol. Cell. Bio, 17:5338-5347, 1997

(23) Sherr CJ, Roberts JM: Inhibitors of mammalian G1 cyclin-dependent kinases. Genes & Dev. 9:1149-1163, 1995

(24) Harper JW: Cyclin Dependent Kinase Inhibitors. Cancer Surv. 29:91-108, 1997

(25) Sherr C, Roberts J: CDK inhibitors: positive and negative regulators of G1-phase progression. Genes Dev. 13:1501-1514, 1999

(26) LaBaer J, Garrett MD, Stevenson LF, Slingerland J, Sandhu C, Chou HS, et al: New functional activites for the p21 family of cdk inhibitors. Genes & Dev. 11:847-862, 1997

(27) Planas-Silva MD, Weinberg RA: The restriction point and control of cell proliferation. Curr. Opin. Cell Biol. 9:768-772, 1997

(28) Rao S, Lowe M, Herliczek T, Keyomarsi K: Lovastatin mediated G1 arrest in normal and tumor breast cells in through inhibition of CDK2 activity and redistribution of p21 and p27, independent of p53. Oncogene 17:2393-2402, 1998

(29) Chen X, Lowe M, Keyomarsi K: UCN-01 mediated G1 arrest in normal but not tumor cells is pRb dependent and p53 independent. Oncogene 18:5691-5702, 1999

(30) Levenson AS, Jordan VC: Transfection of human estrogen receptor (ER) cDNA into ER-negative mammalian cells. J. Steroid Biochem. Mol. Biol. 51:229-239, 1994

(*31*) Duttaroy A, Qian JF, Smith JS, Wang E: Up-regulated p21(CIP1) expression is part of the regulation quantitatively controlling serum deprivation-induced apoptosis. J. Cell Biochem. 64:434-446, 1997

(*32*) Gray-Bablin J, Zalvide J, Fox MP, Knickerbocker CJ, DeCaprio JA, Keyomarsi K: Cyclin E, a redundant cyclin in breast cancer. Proc. Natl. Acad. Sci. 93:15215-15220, 1996

(*33*) Hessling JJ, Miller SE, Levy NL: A direct comparison of procedures for the detection of mycoplasma in tissue culture. J. Immunol. Meth. 38:315-324, 1980

(*34*) DeConinck EC, McPherson LA, Weigel RJ: Transcriptional regulation of estrogen receptor in breast carciomas. Mol. Cell. Biol. 15:2191-2196, 1995

(*35*) Ferguson AT, Lapidus RG, Baylin SB, Davidson NE: Demethylation of the estrogen receptor gene in estrogen receptor-negative breast cancer cells can reactivate estrogen receptor gene expression. Cancer Res. 55:2279-2283, 1995

(*36*) Ince BA, Montano MM, Katzenellenbogen BS: Activation of transcriptionally inactive human estrogen receptors by cyclic adenosine 3', 5'-mmonophosphate and ligands including antiestrogens. Molec. Endrocrin. 8:1397-1406, 1994

(*37*) Zeng Y-X, Somasundaram K, El-Deiry WS: AP2 inhibits cancer cell growth and activates p21WAF1/CIP1 expression. Nature Gen. 15:78-82, 1997

(*38*) Paulus W, Baur I, Boyce FM, Breakefield XO, Reeves S: Self-Contained, tetracycline-regulated retroviral vector system for gene delivery to mammalian cells. J. Virology 70:62-67, 1996

(*39*) Harper JW, Adami GR, Wei N, Keyomarsi K, Elledge SJ: The p21 Cdk-interacting protein Cip1 is a potent inhibitor of G1 cyclin-dependent kinases. Cell 75:805-816, 1993

(40)   Keyomarsi K, Conte D, Toyofuku W, Fox MP: Deregulation of cyclin E in breast cancer. Oncogene 11:941-950, 1995

(41)   Brasier AR, Tate JE, Habener JF: Optimized use of the firefly luciferase assay as a reporter gene in mammalian cell lines. BioTechniques 7:1116-1122, 1989

(42)   Carmichael J, Mitchell JB, DeGraff WG, Gamson J, Gazder AF, Johnson BE, et al: Chemosensitivity testing of human lung cancer cell lines using the MTT assay. Br. J. Cancer 57:540-547, 1988

(43)   Keyomarsi K, O'Leary N, Molnar G, Lees E, Fingert HJ, Pardee AB: Cyclin E, a Potential Prognostic Marker for Breast Cancer. Cancer Res. 54:380-385, 1994

(44)   Gray-Bablin J, Rao S, Keyomarsi K: Lovastatin Induction of cyclin-dependent kinase inhibitors in human breast cells occurs in a cell cycle independent fashion. Cancer Res. 57:604-609, 1997

(45)   Somasundaram K, Zhang H, Zeng YX, Houvras Y, Peng Y, Zhang H, et al: Arrest of the cell cycle by the tumor-suppressor BRCA1 requires the CDK-inhibitor p21WF1/CIP1. Nature 389:187-190, 1997

(46)   Gossen M, Bujard H: Tight control of gene expression in mammalian cells by tetracycline-responsive promoters. Proc. Natl. Acad. Sci. 89:5547-5551, 1992

(47)   Castles CG, Oesterreich S, Hansen R, Fuqua SAW: Auto-regulation of the estrogen receptor promoter. J. Steroid Biochem. Molec. Biol. 62:155-163, 1997

(48)   MIssero C, Calautti E, Eckner R, Chin J, Tsai L, Livingston D, et al: Involvement of the cell-cycle inhibitor CIP1/WAF1 and the E1A-associated p300 protein in terminal differentiation. Proc. Natl. Acad. Sci. USA 92:5451-5455, 1995

(49)   Halevy O, Novitch BG, Spicer DB, Skapek SX, Rhee J, Hannon GJ, et al: Correlation of terminal cell cycle arrest of skeletal muscle with induction of p21 by MyoD. Science 267:1018-1021, 1995

(50) Steinman RA, Hoffman B, Iro A, Guillouf C, Liebermann DA, El-Houseini ME: Induction of p21 (WAF1/CIP1) during differentiation. Oncogene 9:3389-3396, 1994

(51) Haapajarvi T, Kivinen L, Heiskanen A, des Bordes C, Datto MB, Wang XF, et al: UV radiation is a transcriptional inducer of p21(Cip1/Waf1) cyclin-kinase inhibitor in a p53-independent manner. Exp. Cell Res. 248:272-279, 1999

(52) Smolewski P, Niewiadomska H, Krykowski E, Robak T: Expression of p21 and MDM-2 proteins on tumor cells in responding and non-responding patients with Hodgkin's disease. Neoplasma 46:212-218, 1999

(53) Gartel AL, Serfas MS, Gartel M, Goufman E, Wu GS, El-Deiry WS, et al: p21 expression is induced in newly nondividing cells in diverse epithelial and during differentiation of the Caco-2 intestinal cell line. Exp. Cell Res. 227:171-181, 1996

(54) Macleod KF, Sherry N, Hannon G, Beach D, Tokino T, Kinzler K, et al: p53-dependent and independent expression of p21 during cell growth, differentiation, and DNA damage. Genes & Develop. 9:935-944, 1995

(55) Matsumura I, Ishikawa J, Nakajima K, Oritani K, Tomiyama Y, Miyagawa J, et al: Thrombopoietin-induced differentiation of a human megakaryoblastic leukemia cell line, CMK, involves transcriptional activation of p21 (WAF1/CIP1) by STAT5. Mol. Cell. Biol. 17:2933-2943, 1997

(56) Liu M, Lee M-H, Cohen M, Bommakanit M, Freedman LP: Transcriptional activation of the cdk inhibitor p21 by vitamin D3 leads to the induced differentiation of the myelomonocytic cell line U937. Genes & Dev. 10:142-153, 1996

(57) Brown JP, Wei W, Sedivy JM: Bypass of senescence after disruption of p21Cip1/WAF1 gene in normal diploid human fibroblasts. Science 277:831-834, 1997

(*58*) Yu D, Jing T, Liu B, Yao J, Tan M, McDonnell TJ, et al: Overexpression of ErbB2 blocks Taxol-induced apoptosis by upregulation of p21CIP1, which inhibits p34Cdc2 kinase. Molecular Cell 2:581-591, 1998

(*59*) Barboule N, Chadebech P, Baldin V, Vidal S, Valette A: Involvement of p21 in mitotic exit after paclitaxel treatment in MCF-7 breast adenocarcinoma cell line. Oncogene 15:2867-2875, 1997

(*60*) Bacus SS, Yarden Y, Oren M, Chin DM, Lyass L, Zelnick CR, et al: Neu differentiation factor (Heregulin) activates a p53-dependent pathway in cancer cells. Oncogene 12:2535-2547, 1996

(*61*) Sugiyama K, Shimizu M, Akiyama T, Ishida H, Okabe M, Tamaoki T, et al: Combined effect of navelbine with medroxyprogesterone acetate against human breast carcinoma cells in vitro. Br. J. Can. 77:1737-1743, 1998

(*62*) Guillot C, Falette N, Paperin M-P, Courtois S, Gentil-Perret A, Treilleux I, et al: p21 WAF1/CIP1 response to genotoxic agents in wild-type TP53 expressing breast primary tumours. Oncogene 14:45-52, 1997

(*63*) Jiang H, Lin J, Su Z, Collart FR, Huberman E, Fisher PB: Induction of differentiation in human promyelocytic HL-60 leukemia cells activates p21, WAF1/CIP1, expression in the absence of p53. Oncogene 9:3397-3406, 1994

(*64*) Jiang H, Lin J, Su A-z, Collart FR, Huberman E, Fisher PB: Induction of differentiation in human promyelocytic HL-60 leukemia cells activates p21, WAF1/CIP1, expression in the absence of p53. Oncogene 9:3397-3406, 1994

(*65*) Jiang H, Fisher PB: Use of a sensitive and efficient subtraction hybridization protocol for the identification of genes differentially regulated during the induction of differentiation in human melanoma cells. Molec. and Cell. Differen. 3:285-299, 1993

(*66*) Zhang W, Grasso L, McClain CD, Gambel AM, Cha Y, Travali S, et al: p53-independent induction of WAF1/CIP1 in human leukemiaa cells is correlated

with growth arrest accompanying monocyte/macrophage differentiation. Cancer Res. 55:668-674, 1995

(67) Bacus SS, Chin D, Ortiz R, Potocki D, Zelnick C: Application of image analysis in the evaluation of cellular prognostic factors in breast cancer. Tut. Cytology :143-156, 1994

(68) Bacus SS, Ruby SG: Application of image analysis to the evaluation of cellular prognostic factors in breast carcinoma. Path. Annual 28:179-204, 1993

(69) De Wet JR, Wood KV, DeLuca M, Helinski DR, Subramani S: Firefly luciferase structure and expression in mammalian cells. Mol. Cell. Biol. 7:725-737, 1987

Figures Legends

Figure 1. High correlation between the expression of p21 and ER in breast cancer cell lines and tumor tissue specimens. **(A)** Cell extracts from breast cancer cell lines and **(B)** 60 breast tumor patient samples were subjected to Western blot analysis with the indicated antibodies. In panel **(A)** lanes 1-4 are extracts prepared form ER positive breast cancer cell lines (MCF-7, T47D, ZR75T, and BT20T, respectively) and lanes 5-9 are extracts prepared from ER negative breast cancer cell lines (MDA-MB-157, MDA-MB-231, MDA-MB-436, HS578T, and HBL100). In panel **(B)** Breast cell lines used as controls for each gel are in lanes 1-3 (76N normal mortal, MCF-10A immortalized, and MDA-MB-157 tumor cell lines). These cell lines were used as controls for the expression of p21 in the tumor tissue samples as they compared to normal and tumor cell lines with different levels of p21 expression. All the ER positive tumor tissues were also positive for progesterone receptor (data not shown). The percent ER (and PgR) was measured according to Bacus et. al (*67,68*) in each of the tumor tissue samples and corroborated by Western blot analysis with ER. Sub-panels **I-III** within panel **(B)** each represent 20 tumor tissues each, 10 ER positive, 10 ER negative. *Note that in the evaluation of the ER/PR by immunohistochemistry, only the staining of the cell nuclei considered positive (67,68). It is possible that the Western blot for lane 7 of sub-panel B is detecting a cytoplasmic (i.e. inactive) form of ER in that specific tumor tissue. Consistent with a potentially inactive ER, the tumor also lacks p21 as shown on the Western blot analysis.*

Figure 2: Ectopic expression of ER does not induce p21 expression. MDA-MB-436 and MCF-7 were transiently transfected with the indicated cDNAs (40 µg total DNA) in complete medium. All cells were transfected by GenePORTER transfection reagent system. Forty-eight hours post transfection, cells were harvested and subjected to

either **(A)** Western blot analysis with the indicated antibodies and **(B, C)** assayed for Luciferase activity according to established procedures (*41,69*). For all transient transfections a plasmid harboring Green Fluorescent Protein (GFP) was co-transfected in each cell line. Percent efficiency and level of expression of GFP were monitored on a FACS scan. Values presented are Luciferase units and adjusted for transfection efficiency via GFP expression. The transfections were performed 5 times and error bars are indicated for each condition. In most all cases the error bars were smaller than the visible increments and cannot be seen.

Figure 3. Ectopic expression of p21 in MDA-MB-436 tumor cell line induced expression of ER-antibody reactive proteins. **(A)** Western blot analysis of p21 and actin using cell extracts from stable, puromycin resistant MDA-MB-436 clones, transfected with the tetracycline inducible plasmid containing p21 cDNA and cultured in medium containing 1 µg/ml tetracycline (plus tet) or no tetracycline for 72 hours (minus Tet). MCF-7 and MDA-MB-436 parental cell lines were used as positive and negative controls, respectively, for p21 expression. **(B)** Cells were cultured in medium without tetracycline in the presence or absence of 500 nM ß-estradiol for 48 hours. Cells were then harvested, protein extract prepared and subjected to Western blot analysis with the indicated antibodies. The thick arrow corresponds to the wild-type ER-α protein migrating at 67 kDa. The thin arrows correspond to the 87 and 62kDa kDa, ER-α antibody-reactive protein. SC refers to ER-α antibody clone C-311 from Santa Cruz Biochemicals. N refers to ER-α antibody clone 6F11 from Novacastra. Normal mammary epithelial cells, 81N were used as negative control and MCF-7 was used as positive control for ER expression.

Figure 4: Activation of ER-Luc system in p21 transfectant clones. (A) ER-Luciferase plasmid DNAs were transfected into the indicated mock or p21 clones, and to MDA-

MB-436 parental cell lines in the presence or absence of ß-estradiol, and assayed for luciferase activity. All cells were transfected by electroporation at 0.32V. In these experiments 40 µg of plasmid DNA was added in transfection using 10^7 cells. Cells were transfected in estrogen stripped medium supplemented with Dextran Charcoal Stripped-Fetal Bovine Serum (5%) without tetracycline in the presence or absence of 500 nM ß-estradiol. Forty-eight hours later, cells were harvested and assayed for luciferase activity. Values presented are luciferase units as measured on a luminometer. Panel **(B)** shows fold induction of ER-Luc activity by ß-estradiol calculated from the values in panel A. For all transient transfections a plasmid harboring Green Fluorescent Protein (GFP) was co-transfected in each cell line. Percent efficiency and level of expression of GFP were monitored on a FACS scan. Values presented are Luciferase units and adjusted for transfection efficiency via GFP expression. The transfections were performed 8 times and error bars are indicated for each condition. In most all cases the error bars were smaller than the visible increments and cannot be seen.

Figure 5: Activation of ERE-tk-Luc system in p21 clones. **(A)** ERE-tk-Luciferase plasmid DNAs were transfected into the indicated mock or p21 clones, and to MDA-MB-436 parental and MCF-7 cell lines in the presence or absence of 500 nM ß-estradiol and 50 µM ICI 182,780 and assayed for Luciferase activity. All cells were transfected by electroporation at 0.32V. In these experiments 40 µg of plasmid DNA was added in transfection using 10^7 cells. Cells were transfected in estrogen stripped medium supplemented with Dextran Charcoal Stripped-Fetal Bovine Serum (5%) without tetracycline in the presence or absence of ß-estradiol and ICI 182,780. Forty-eight hours later, cells were harvested and assayed for Luciferase activity. Values presented are Luciferase units as measured on a luminometer. In panel A the values on the left ordinate refer to those obtained with MCF-7 cells, while the

values on the right ordinate refer to the values obtained with the MDA-MB-436 cells (parental and clones). Panel **(B)** shows fold induction of ERE-tk-Luc activity by ß-estradiol calculated from the values in panel A. Panel **(C)** shows dose response of ß-estradiol mediated ERE-tk-Luc activation. MCF7 (black bars) and MDA-MB-436/p21 clone 25 (shaded bars) were transfected with ERE-tk-Luc, followed by treatment with the indicated concentrations of ß-estradiol, and measurement of the luciferase activity. For all transient transfections a plasmid harboring Green Fluorescent Protein (GFP) was co-transfected in each cell line. Percent efficiency and level of expression of GFP were monitored on a FACS scan. Values presented are Luciferase units and adjusted for transfection efficiency via GFP expression. The transfections were performed 7 times and error bars are indicated for each condition. In most all cases the error bars were smaller than the visible increments and cannot be seen.

Figure 6. ß-estradiol increases the growth in p21 expressing breast tumor cells, while inhibits the growth in ER expressing breast tumor cells. (A) ß-estradiol mediated growth increase in MDA-MB-436/p21 clones. Two p21 clones, MCF7 cells, MDA-MB-436 parental cells and mock clone were treated with increasing concentrations of ß-estradiol for seven days, growth increase was measured by MTT assay. **(B)** Expression of ER causes growth inhibition in ER negative breast tumor cells. Three ER negative breast cell lines were transfected with ER cDNA plasmid. ER is transfected in these cells with similar transfection efficiencies (i.e. 53-68%) as determined by co-transfection with a vector harboring a cDNA to green fluorescent protein (GFP) and Western blot analysis with ER antibody (data not shown). After transfection, cells were grown in presence or absence of ß-estradiol 10nM for 48h. The growth inhibition by ß-estradiol was measured by MTT assay. The transfections and the following MTT assay were performed 5 times and error bars are indicated for

each condition. In most all cases (panel B) the error bars were smaller than the visible increments and cannot be seen.

Figure 7: Overexpression of p21 sensitizes cells to anti-estrogens. Cells were cultured in estradiol free medium supplemented with dextran-coated charcoal-stripped fetal bovine serum for 48 hours days prior to seeding. On day 0, cells were seeded into 96 well plates (2,500 cells/well).   The following day (day 1) media containing the indicated concentrations of ICI 182,780 were added and media were changed and drug redosed very other day. On day 5 cells were harvested and growth inhibition was measured by the MTT assay as described. The growth inhibition were performed 5 times and error bars are indicated for each condition.

FIGURE 1

FIGURE 2

FIGURE 3

FIGURE 4

A

B
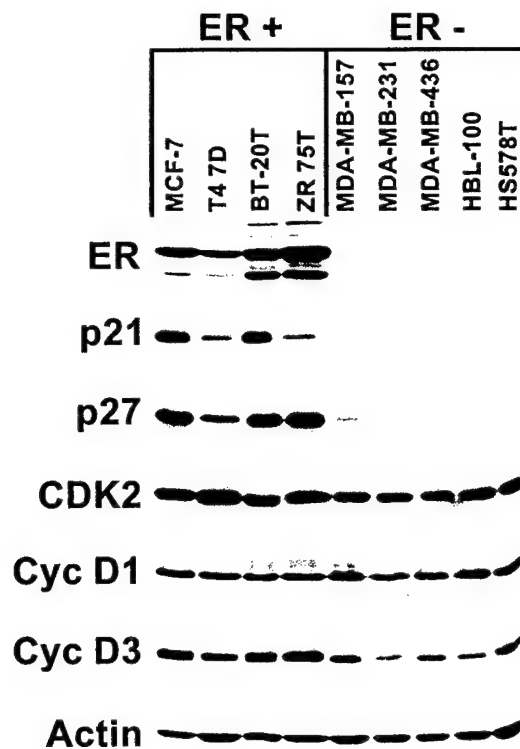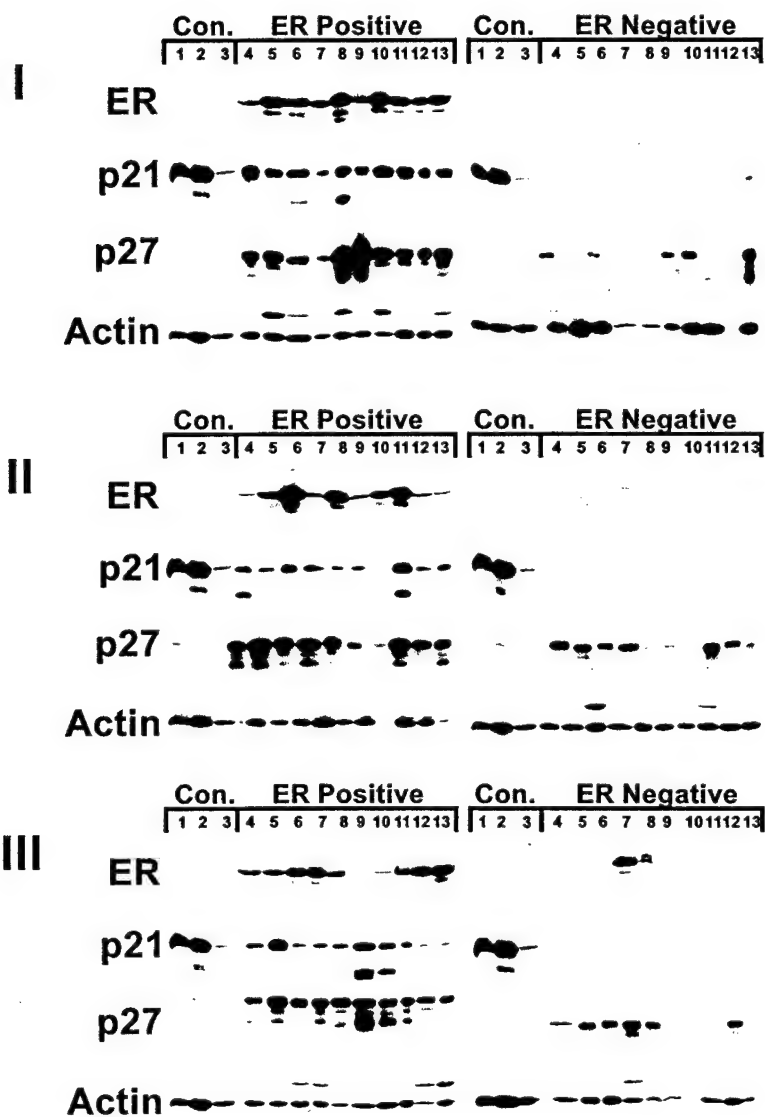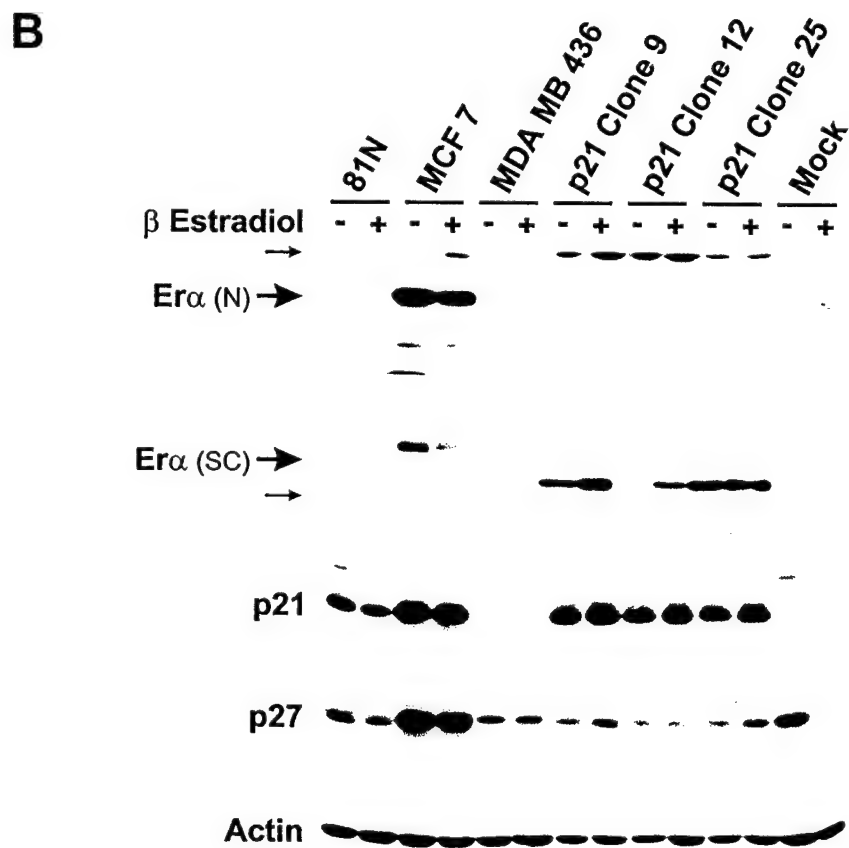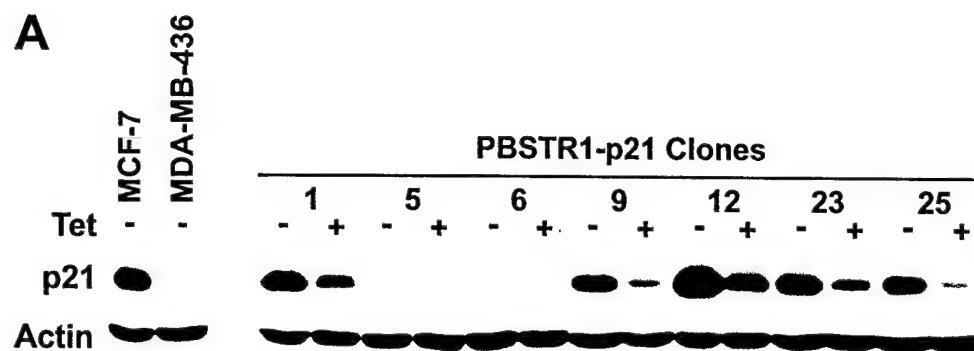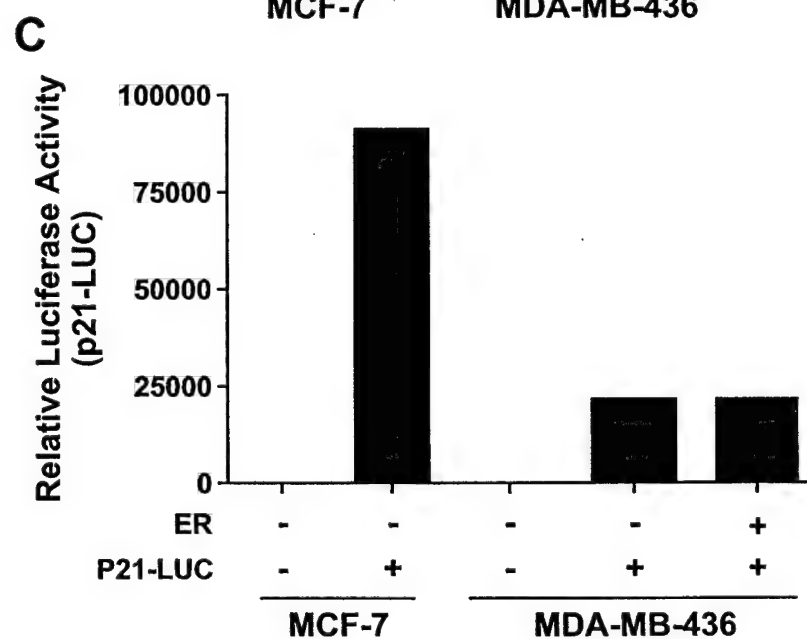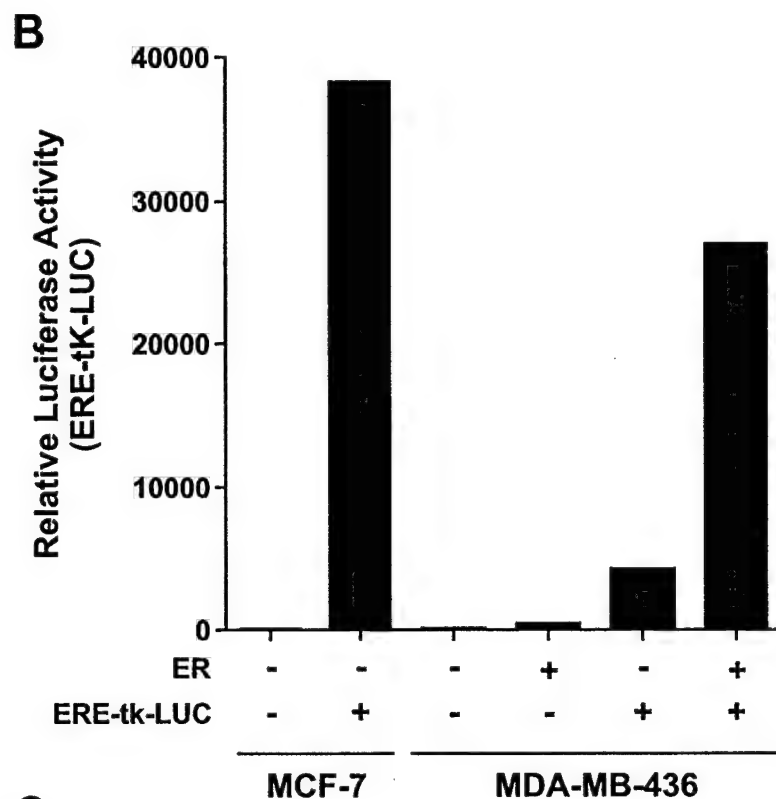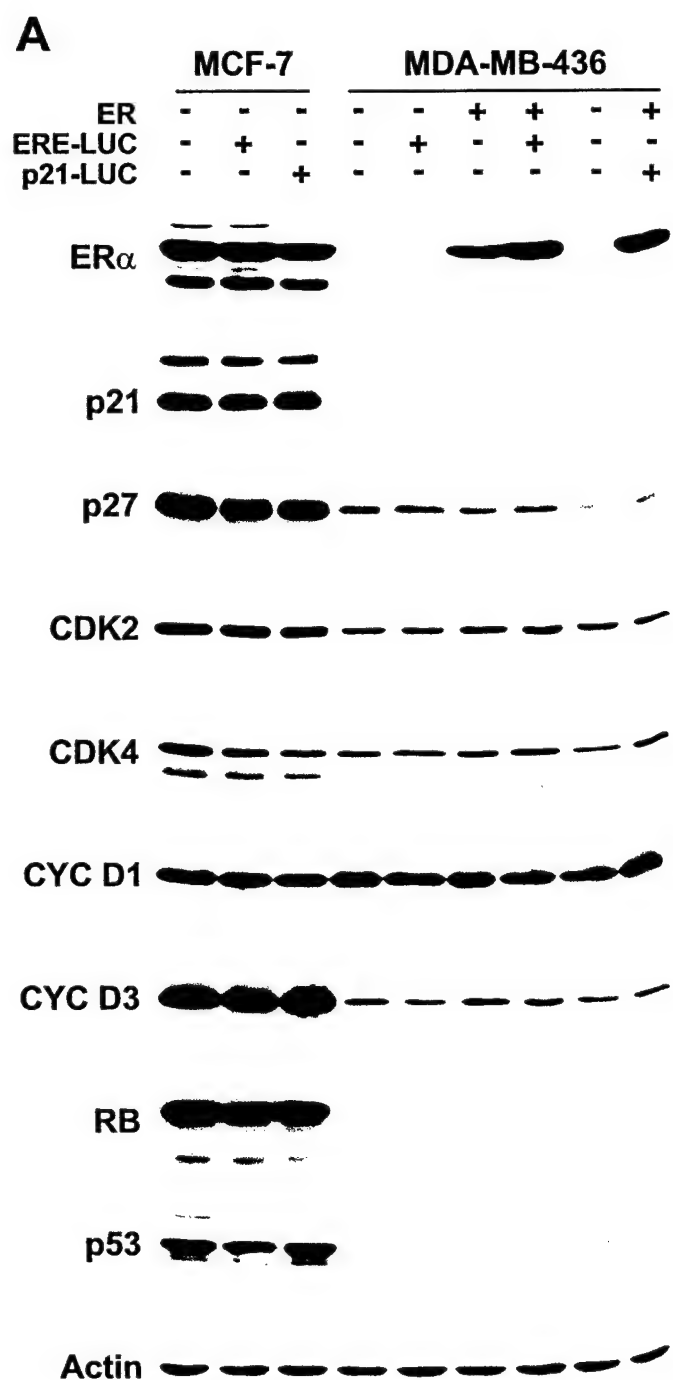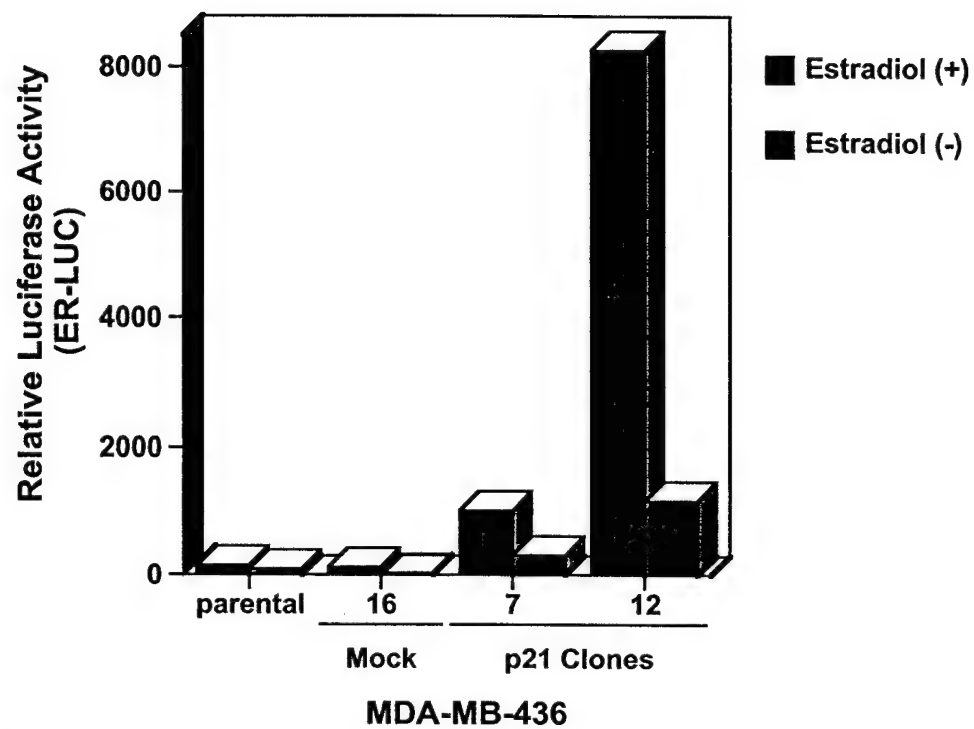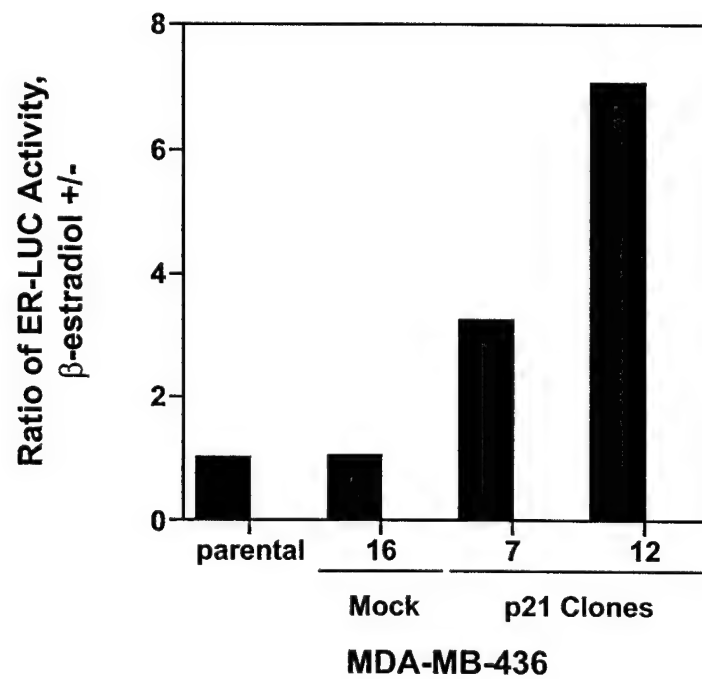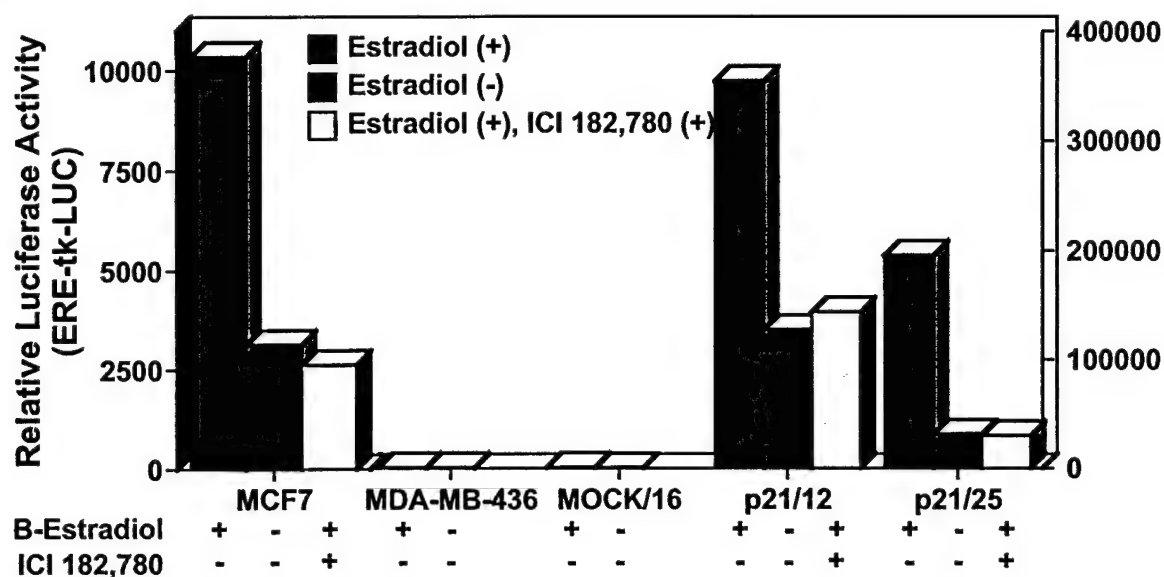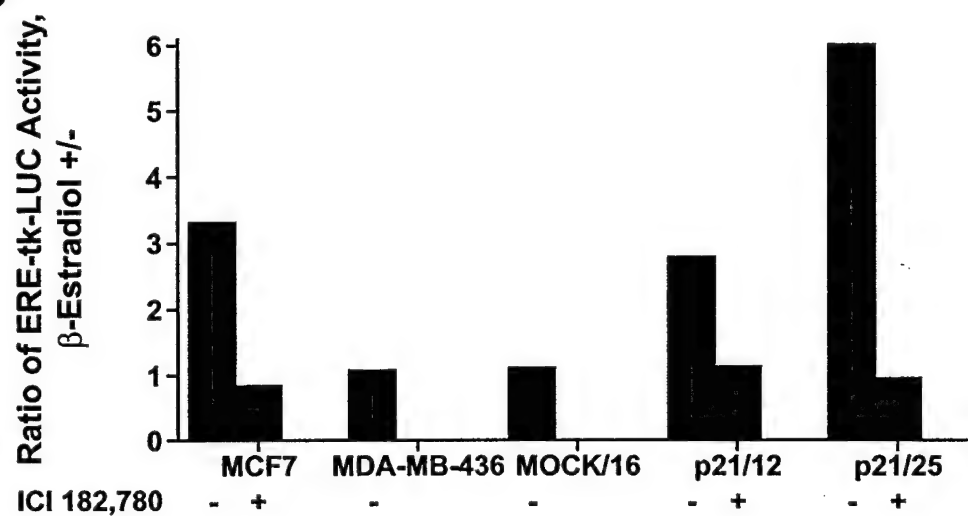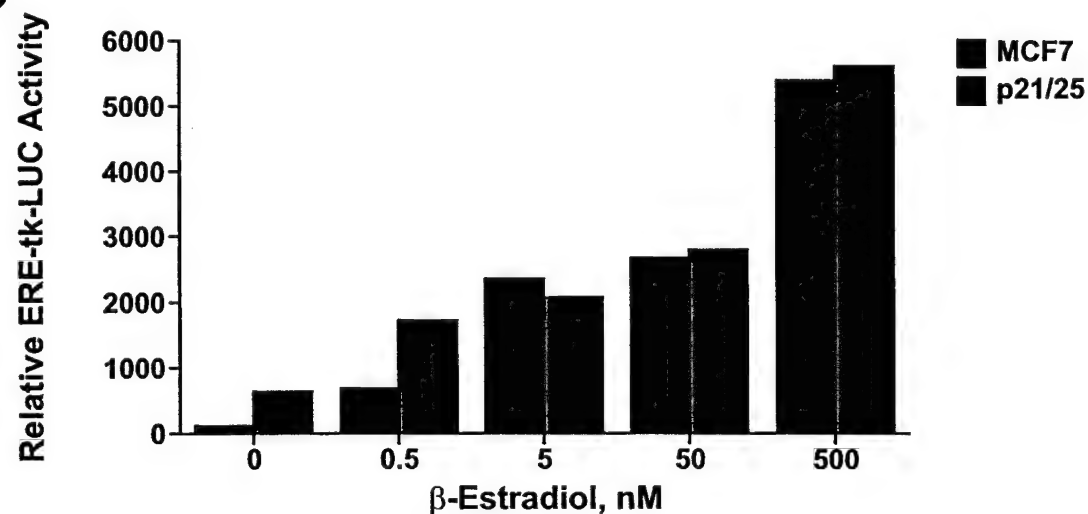
FIGURE 5

FIGURE 6

A
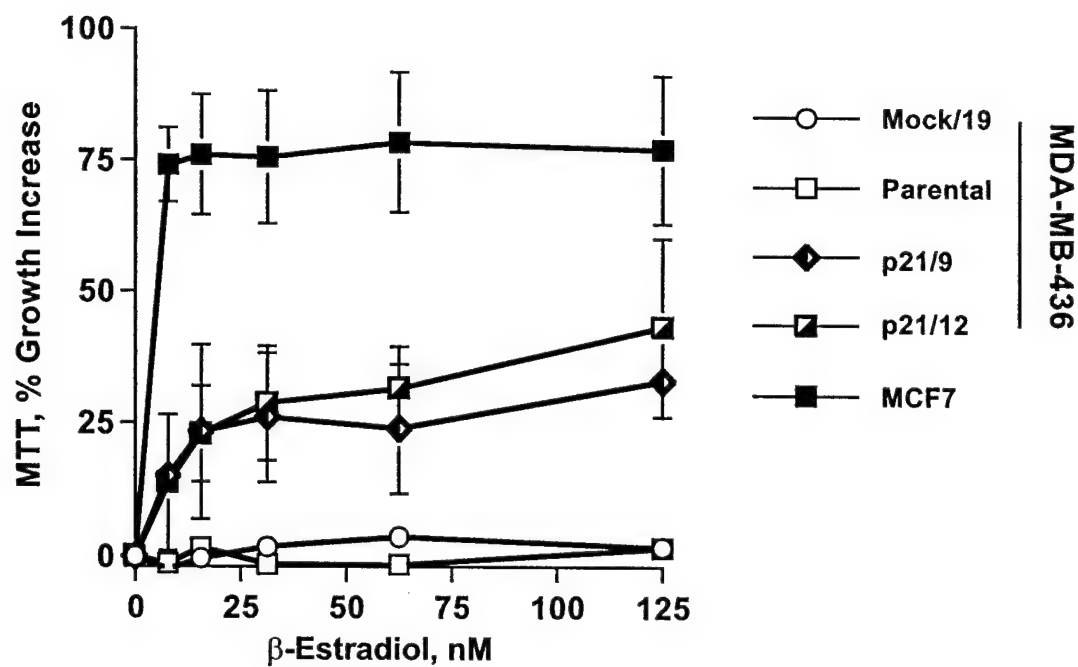
B
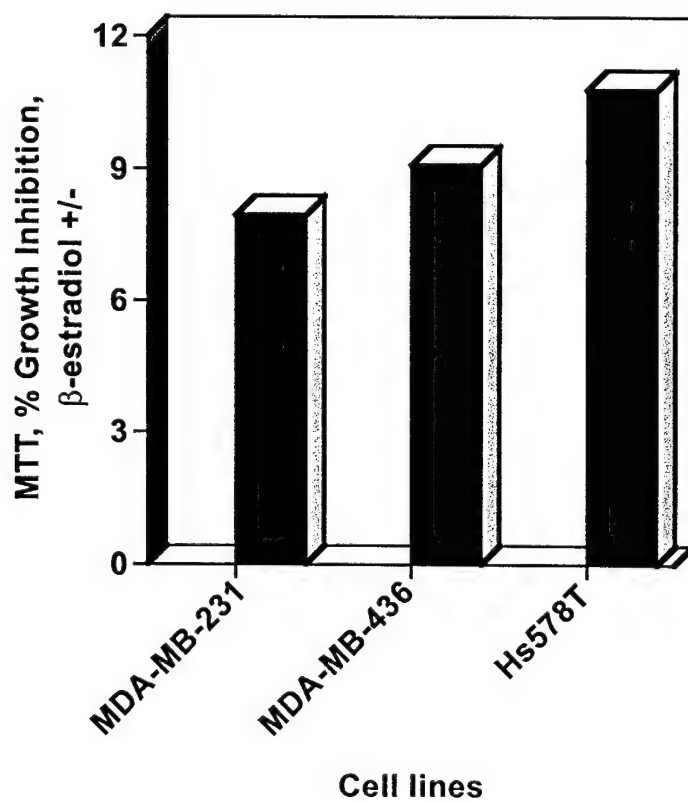
FIGURE 7
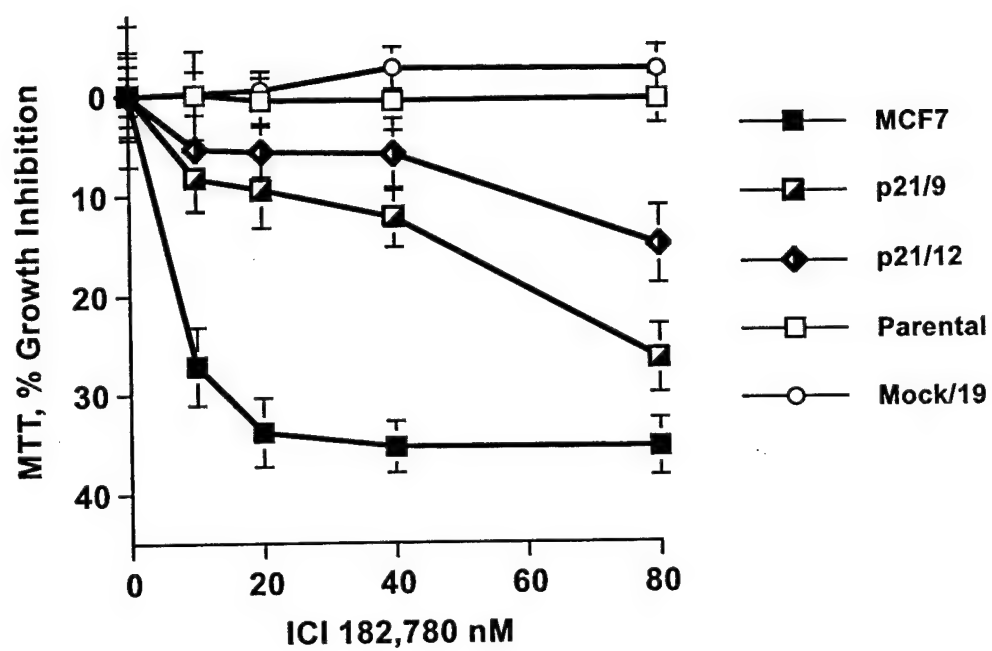
Selective killing of breast cancer cells by reversible, G1 arrest of normal cells

Xiaomei Chen[1], Michael Lowe[1], Thaddeus Herliczek[1], Michael J. Hall[2], Christopher Danes[1], David A. Lawrence[2,3], and Khandan Keyomarsi[1,3*]

[1,2] Division of Molecular Medicine, [1]Laboratory of Diagnostic Oncology, [2]Laboratory of Clinical and Experimental Endocrinology and Immunology, Wadsworth Center, Albany, New York 12201-0509.

[3] Department of Biomedical Sciences, State University of New York, Albany, NY 12222.

* To whom correspondence should be addressed:

Wadsworth Center
Empire State Plaza
P.O. Box 509
Albany, NY 12201-0509

Phone: (518) 486-5799
FAX: (518) 486-5798
E-mail: keyomars@wadsworth.org

Running title: Staurosporine protects normal cells

Key Words: Staurosporine, cell cycle, Doxorubicin, Camptothecin, pRb, p21, p27

Abstract

Background: Two major limiting factors in human cancer chemotherapy are toxicity to the normal tissues and drug resistance in the tumor tissues. We show that taking advantage of cell cycle checkpoint differences between normal and cancer cells can circumvent these limitations and protect the normal proliferating cells from the toxic effects of chemotherapeutic agents. *Methods:* Normal mammary epithelial cells were initially treated with Staurosporine (ST) at cytostatic (i.e. non-lethal) concentrations, which preferentially arrest normal cells in G0/G1 phase of the cell cycle without affecting the proliferation of tumor cells. Following the selective arrest of normal cells in G0/G1, both normal and tumor cells were treated with Doxorubicin or Camptothecin, two cytotoxic (i.e. lethal) chemotherapeutic agents. *Results:* Only tumor cells were selectively killed by chemotherapeutic agents while normal cells were unaffected and resumed proliferation following removal of drug. Additionally, normal circulating lymphocytes induced to proliferate *in vitro* were also protected against the toxic affects of chemotherapeutic agents by ST-mediated G0/G1 arrest. The reversible arrest of normal cells in G0/G1 by ST increased the maximum tolerated doses of Doxorubicin in excess of 100-fold over the concentrations that completely eradicated all tumor cells in culture. ST-mediated G0/G1 arrest is pRb-dependent and p53-independent. It is also accompanied by a rapid and significant decrease in CDK4 protein levels, followed by accumulation of hypo-phosphorylated pRb, increased binding of CKIs (p21, p27) to CDK2, and inhibition of CDK2 activity in normal cells. *Conclusions:* By targeting cancer cells that have defective checkpoints governed by the pRb pathway, while inducing G0/G1 arrest in normal cells, we have designed a strategy to selectively kill breast cancer cells while protecting normal cells.

2

Introduction

Treatment of cancer with chemotherapy and radiation therapy has severe side effects that damage healthy proliferating cells such as hematopoietic precursors, hair follicle, cells and the epithelial lining of the intestine. These side effects often limit the doses of chemotherapy administered, allowing tumor cells to gain growth advantage by escaping treatment and developing drug resistance. Since cancer therapy targets proliferating cells and tissues, all cells that proliferate, whether normal or tumor are affected by the treatment. If however the normal dividing cells in the body were to stop proliferating reversibly, the toxic effects of chemotherapy would potentially be diminished (1-5). Here, we introduce a novel therapeutic strategy to selectively target cancer cells, while leaving normal proliferating cells intact. This strategy of protection from chemotherapy is based on the genotypic differences between normal and tumor cells that govern cell cycle regulation. Unlike normal cells, which are controlled by tight cell cycle checkpoint regulation, tumor cells have a deregulated cell cycle, which is responsible for their continued and unabated proliferation (6). Our treatment strategy takes advantage of this difference in cell cycle regulation between normal and tumor cells, maintaining the normal cells in a state of reversible G0/G1 arrest while selectively killing the tumor cells with cytotoxic chemotherapeutic agents.

To explore the feasibility of cellular protection through reversible cell cycle arrest, we targeted the pRb (retinoblastoma) pathway, which governs the transition from G0/G1 to S, or the restriction point (7). pRb is a major tumor suppressor that is frequently inactivated in human cancer. Furthermore, alterations in pRb are linked to poor prognosis, tumor progression, and decreased sensitivity to chemotherapeutic agents (8-

3

12). As an important tumor suppressor, pRb is involved in controlling the progression through G0/G1. The hypo-phosphorylated pRb serves as a tumor suppressor by binding to and inhibiting cellular proteins such as E2F-DP heterodimeric transcription factors. The activity of E2F is required for the transactivation of many genes essential for DNA replication, and is necessary for the cells to traverse from G0/G1 to S phase (7,13-15). Sequential phosphorylation of pRb throughout the cell cycle by different cyclin/cyclin dependent kinase (CDK) complexes dissociates the pRb-E2F complexes and allows free E2F to transactivate genes that promote entry into S phase. Several studies have provided genetic and biochemical evidence that mutations in either the RB gene itself or in genes whose products influence its phosphorylation state (i.e cyclin D1, CDK4, CDK6, E2F), render the functional inactivation of pRb and contribute to tumor progression (4,9,16). The protection strategy described in this report takes advantage of the deregulated pRb pathway in tumor cells to protect normal cells against the toxic effects of chemotherapeutic agents.

The approach taken for this "protection" strategy involved two steps: First, the normal proliferating cells are blocked in the G0/G1 phase of the cell cycle by pre-treatment with cytostatic, non-lethal agents. Tumor cells will not respond to these agents, because they have lost the G0/G1 checkpoint; they will continue to proliferate. Next, both normal and tumor cells are treated with conventional chemotherapeutic agents which will specifically kill proliferating tumor cells. Normal cells are protected because of the G0/G1 mediated arrest achieved in the first step. For this "protection" strategy to succeed, two major criteria must be met: (i) There must be differential sensitivity of normal versus tumor cells to cytostatic agents. The cytostatic agents used

4

must specifically arrest the proliferation of normal cells and be minimally or not inhibitory to tumor cells; and (ii) the arrested normal cells must remain viable and completely recover from the inhibitory effects of the cytostatic agents.

The cytostatic drug used in these experiments is the protein kinase inhibitor Staurosporine (ST). We show that treatment of normal cells with sub-nanomolar concentrations of ST is sufficient to reversibly arrest normal proliferating mammary epithelial cells in the G0/G1 phase of the cell cycle. Tumor cells are refractory to low concentrations of ST and their proliferation continues unabated. Following the treatment with ST, both normal and tumor cells are then treated with toxic concentrations of either Doxorubicin or Camptothecin. This 2-step treatment strategy is toxic to all tumor cells examined, while normal cells recovered fully following drug removal. We show that the pRb pathway is critical for the effectiveness of this protection strategy. Our results suggest that the G0/G1 checkpoint pathway can be targeted effectively in normal cells to protect these healthy cells against the toxic effects of chemotherapeutic agents.

Materials and Methods:

Materials, Cell lines, and Culture Conditions: Olomoucine and Roscovitine were kindly provided by Dr. Laurent Meijer (Cell Cycle Laboratory CNRS, Station Biologique, BP 74 29682 Roscoff Cedex, Bretagne, France). Flavopiridol was provided by the Pharmaceuticals Resources Branch of the National Cancer Institute (Bethesda, MD). ST was purchased from Boehringer Mannheim GmbH (Mannheim, Germany). MTT [3-(4,5-dimethylthiazol-2-yl)-2,5-diphenyltetrazolium bromide], Camptothecin, and Doxorubicin were purchased from Sigma Chemical Co., (St. Louis, Mo). Serum was purchased from Hyclone Laboratories (Logan, Utah) and cell culture medium from Life Technologies, Inc. (Grand Island, NY). All other chemicals used were reagent grade. The culture conditions for 76N, 81N, and 70N normal cell strains, MCF-10A immortalized cell line, and MCF-7, ZR75T, MDA-MB-157, Hs578T, T47D, and MDA-MB-231 breast cancer cell lines were described previously (*17,18*). 76N-E6 and 76N-E7 cell lines (gifts from Dr. V Band, Tufts Medical Institute, Boston, MA) were immortalized and cultured as described previously (*19,20*). All cells were cultured and treated at 37°C in a humidified incubator containing 6.5% CO_2 and maintained free of mycoplasma as determined by Hoechst staining (*21*).

MTT Assay: The MTT assay was performed as described. Briefly, cells were plated at a density of 2500/well in each well of a 96 well tissue culture plate and allowed to recover for 24 hours prior to drug treatment. Cells were treated with the indicated concentrations of Olomoucine, Roscovitine, Flavopiridol, or ST for 48 hours and subjected to the MTT

6

survival assay as described (22). Each data point represents the average of six determinations, and the MTT assay for each experimental condition was performed at least 3 times.

All protection and "MTD" (Maximum Tolerated Dose) experiments were performed on 96 well cultures as described above. For protection experiments, both normal and tumor cells were initially treated with 0.5 nM ST for 48 hours. Next the media was removed and fresh media containing 0.5 µM Camptothecin or 0.125 µM Doxorubicin was added to the cells for 24 hours, after which the media was replaced with drug free media and the cells allowed to recover for 12 days. Media was replaced every other day during the recovery period. For "MTD" experiments, cells were initially treated with 0.5 nM ST for 48 hours, followed by treatment with increasing concentrations of Camptothecin for an additional 24 hours. The cells were then washed and incubated in drug free media for the 12 day recovery period. At the end of the recovery period, cytotoxicity of each treatment for each cell line was monitored by the MTT assay as described above.

DNA Content Analysis: Flow cytometry was performed on normal and tumor cells following treatment with ST to determine cell cycle distribution. Briefly, medium was removed 24-36 hrs after the initial plating of cells on 10 cm plates (10^6 cells/plate), and replaced with fresh medium in the presence or absence of increasing concentrations of ST for 48 hrs. Cells were then harvested and flow cytometry analysis was performed. For Fluorescence-Activated Cell Sorter (FACS) analysis, 10^6 cells were centrifuged at 1,000 X g for 5 min, fixed by the gradual addition of ice cold 70% ethanol (30 min at 4°C), and washed with phosphate buffered saline. Cells were then treated with RNAse (10 µg/ml) for 30 minutes at 37° C, washed once with phosphate buffered saline, and

7

resuspended and stained in 1 ml of 69 µM propidium iodide in 38 mM sodium citrate for 30 minutes at room temperature. The cell cycle phase distribution was determined by analytical DNA flow cytometry as described previously (17).

Western blot, immunoprecipitation, and H1 kinase analysis. Cell lysates were prepared and subjected to Western blot analysis as previously described (23). Briefly, in each lane, 50 µg of protein from each condition was electrophoresed using either 7% sodium dodecyl sulfate-polyacrylamide gel electrophoresis (SDS-PAGE) (pRb), 10% SDS-PAGE (p53) or 13% SDS-PAGE (p21, p27, CDK2, CDK4) and transferred to Immobilon P overnight at 4° C at 35mV constant volts. The blots were blocked overnight at 4 ° C in Blotto (5% nonfat dry milk in 20mM Tris, 137 mM NaCl, 0.25% Tween 20, pH 7.6). After six, 10 minute washes in TBST (20mM Tris, 137mM NaCl, 0.05% Tween 20, pH 7.6), the blots were incubated in primary antibodies for 3 hours. Primary antibodies used were pRb monoclonal antibody (PharMingen, San Diego, CA), monoclonal antibodies to p27, CDK2, and CDK4 (Transduction Laboratories, Lexington, KY) monoclonal antibodies to p21 and p53 (Oncogene Research Products/Calbiochem, San Diego, CA), all at 0.1µg/ml in Blotto, and actin monoclonal antibody (Boehringer-Mannheim, Indianapolis, IN) at 0.63 µg/ml in Blotto. Following primary antibody incubation, the blots were washed and incubated with goat anti-mouse horseradish peroxidase conjugate at a dilution of 1:5,000 in Blotto for 1 hour and finally washed and developed with the Renaissance chemiluminesence system as directed by the manufacturers (NEN Life Sciences Products, Boston, MA).

For immunoprecipitations followed by Western blot analysis, 300 µg of cell extracts were used per immunoprecipitation with polyclonal antibody to CDK2 (23) or CDK4 (Santa Cruz Biochemicals, Santa Cruz, CA), as previously described (24). The immunoprecipitates were then electrophoresed inn 13% gels, transferred to Immobolin P, blocked, and incubated with the indicated antibodies at dilutions described above.

8

For the Histone H1 kinase assay, the immunoprecipitates were incubated with kinase assay buffer containing 60 μM cold ATP and 5 μCi of [^{32}P] ATP in a final volume of 50 μl at 37°C for 30 minutes. The products of the reaction were then analyzed on a 13% SDS-PAGE gel. The gel was then stained, destained, dried, and exposed to X-ray film.

Lymphocyte Isolation: Heparinized blood from normal donors was diluted 1:1 with phosphate buffered saline without Mg^{++} and Ca^{++} (PBS). Peripheral blood mononuclear cells (PBMC) were isolated by overlaying the blood/PBS mixture on 15 mls of Ficoll-Paque (Pharmacia Biotech, Uppsala, Sweden) in a 50 mL conical tube and centrifuging at 1000g for 12 min at RT. The PBMC layer was removed and washed 1X in PBS at room temperature and 2 X with PBS at 4° C. Cells were suspended at 2 x10^6/mL in RPMI-1640 with L-glutamine, 0.9% NaHCO$_3$, 1 mM sodium pyruvate, 1X nonessential amino acids (Biowhittaker, Walkersville, Maryland). Cells were plated at various densities and stimulated with Phytohemagglutinin (PHA) (Sigma Chemical, St Louis, MO) at a final concentration of 10μg/mL. For drug treatment followed by MTT assays, PHA stimulated or unstimulated, or PHA+ ST treated cells were plated in each well of 96 well plates at a density of 10,000 cells/well, and analyzed described above for mammary epithelial cells.

9

Results:

Staurosporine, but not CDK inhibitors, distinguish between normal and tumor cells and arrest only normal cells in G1. To examine the effectiveness of the protection strategy described above, we used a model system comprised of normal proliferating, immortal, and tumor-derived mammary epithelial cell lines. The three normal proliferating cell strains (81N, 70N, and 76N) were established from reduction mammoplasties obtained from three different individuals (25). The proliferation of these normal cell strains is strictly regulated by checkpoint controls; at the end of their lifespan, these normal cells stop proliferating and become senescent (25,26). We also examined MCF-10A, a near diploid immortalized cell line that has lost its strict growth factor requirement, its checkpoint regulation (specifically, G1 to S transition) and the ability to senesce (27). Lastly, we have a panel of 10 breast cancer cells that have different p53, pRb, and tumorigenicity statuses as determined previously (26,28). Using a subset of these cells we examined the two criteria required for our hypothesis to be validated: that the cytostatic agent used must differentially inhibit the proliferation of normal versus tumor cells, and that the arrest of normal cells by the cytostatic agent must be reversible. Initially, we examined several agents with known and specific cell cycle targets. These included Olomucine and Roscovitine, two purine analogues (29,30), and Flavopiridol, a flavone analogue (31). All three specifically target the CDKs. We also examined ST a potent protein kinase C inhibitor (32,33). When we measured the growth inhibitory activity of these 4 agents against a panel of 7 different normal and tumor cell lines (Figs 1 & 2) by the MTT assay, we found that the three specific CDK inhibitors, (i.e. Olomucine, Roscovitine and Flavopiridol) could not differentiate between

10

normal and tumor cells. All three agents inhibited the growth of normal and tumor cells (Fig 1). For these analyses we treated two normal breast epithelial cell strains, 76N and 81N, one immortal cell line, MCF 10A, and four breast tumor cell lines, MCF7, T47D, MDA-MB-157, and MDA-MB-436 with the indicated concentrations of the agents for 48 hours. At the end of treatment, cell growth inhibition was analyzed by MTT assay. The data show that Olomoucine, Roscovitine, Flavopiridol inhibit cell growth of both normal and tumor cells with similar potency, although 81N and 76N normal cells were slightly more sensitive to the agents than all other cells examined (Fig 1A-C). However, upon removal of drug, normal cells did not recover from growth inhibition/cytotoxicity mediated by these CDK inhibitors (data not shown). These results suggest that these three CDK inhibitors do not meet the first criterion required for the protection hypothesis, namely significant differential sensitivity between normal and tumor cells.

Unlike the CDK inhibitors ST (at very low concentrations[1]), could dramatically differentiate between normal and tumor cells (Fig 2A). The results show that treatment of normal breast epithelial cell strains 76N and 81N with concentrations as low as 0.5 nM ST resulted in 40-55% growth inhibition. Higher concentrations of ST (i.e 2nM) inhibited the growth of these normal cell strains by up to 75%. Tumor cells, on the other hand, were refractory to these low concentrations of ST. Treatment of breast cancer cell lines such as T47D, MDA-MB-436, MDA-MB-157, and MCF 7 with concentrations as high as 8 nM resulted in minimal or no growth inhibition (Fig 2A). These results indicate that ST inhibited the proliferation of normal cells, with a significantly greater differential

---

[1] At higher concentrations (i.e ≥32nm) Staurosporine is equally (and irreversibly) toxic to normal and tumor cells (24).

11

from tumor cells than Olomoucine or Roscovitine or Flavopiridol. These results also provide evidence that ST meets the first criteria of the protection strategy, i.e. to inhibit proliferation of normal cells at a significantly lower cytostatic dose than is required for inhibition of cancer cells' proliferation. To examine the ability of ST to meet the second criteria of the protection strategy, namely reversibility of growth inhibition, we measured the rate of recovery of growth inhibition of the normal cell strain 81N treated with increasing concentrations of ST (Fig 2B). Following 48 hours of treatment, ST was removed and the cells were allowed to recover for 12 days. The data reveal that treatment of normal cells with concentrations of ST up to 0.5 nM resulted in a complete recovery from growth inhibition, while concentrations higher than 1 nM resulted in no recovery (Fig 2B). The data from figure 2 suggested that ST is a potential candidate for a cytostatic agent and that it meets both the criteria of the protection hypothesis by reversibly inhibiting the growth of normal cells without perturbing the proliferation of tumor cells.

Flow cytometry analysis revealed that treatment of normal cells with ST resulted in accumulation of these cells in the G1 phase of the cell cycle with a concurrent S phase decrease. Normal cells (70N and 81N) accumulated in the G1 phase following treatment of these cells with only 0.5 nM ST for 48 hours. The ST-mediated G1 accumulation in normal cells was concomitant with a decrease in S phase, with no significant change in the G2/M content (Figure 3). Treatment of tumor cells (i.e MDA-MB-157 and MDA-MB-436) with ST, on the other hand, resulted in no perturbation of the cell cycle in all tumor cell lines examined at concentrations up to 10 nM (Fig 3).

These results suggest that the growth inhibitory activity of low concentrations of ST (i.e. 0.5 – 10 nM) in normal cells is mainly due to G1 arrest mediated by ST.

The loss of ST-mediated G1 arrest in tumor cells is due to a defect in the pRb function. To analyze the specific involvement of p53 or pRb function in ST-mediated G1 arrest, we examined the effects of ST in E6 and E7 immortalized variants of 76N cells. The 76NE6 and 76NE7 cell lines were derived by infection with human papilloma virus (HPV) 16E6 or 16E7 (*19,20*). The E6/p53 and E7/pRb interaction promote degradation/inactivation of p53 and pRb respectively, resulting in the loss of the normal phenotype (*34-36*). ST treatment of 76NE6 cells resulted in dose dependent growth inhibition (data not shown) with an identical dose response curve as the parental 76N strain (see Fig 1). The growth inhibition in 76NE6 resulted in a significant accumulation of cells in the G1 phase with only 0.5 nM ST (Fig 3) even though these cells have a defective p53 pathway. However, 76NE7 cells were completely refractory to the growth inhibitory activity of ST up to 10 nM with little cell cycle perturbation (Fig 3). Similarly, ST had no effect on the cell cycle of tumor cells examined due to a defect in the pRb pathway in these cell lines. The inactivation of the pRb in tumor cells is due to either mutation/deletion of the Rb gene (i.e MDA-MB-436 (*37*)), or overexpression of p16 (i.e. MDA-MB-157, MDA-MB-436 (*28*)), cyclin D (i.e. MDA-MB-436, T47D (*24*)) or E (i.e. MDA-MB-157 (*28*)). Our results suggest that ST-mediated G1 arrest in normal cells is dependent on a functional pRb, but not p53.

Decreased CDK4 levels and increased binding of p27 to CDK2 in a pRb dependent fashion are associated with ST mediated G1 arrest in normal cells. To examine how ST affects the cell cycle in normal and immortalized cells, we examined the expression and activity of key regulatory molecules associated with G1/S progression in these cell lines (Fig 4). Western blot examination revealed that the levels

13

of cell cycle regulators such as CDK4, p53, pRb, p21, and CDK2 decline in 76N and 81N normal cell strains treated with ST while p27 levels are unaffected (Fig 4, left panels). The protein levels of cyclin D3, cyclin E, and cyclin A were also reduced following ST treatment (data not show). Most significant is the rapid and complete disappearance of CDK4 in response to ST, which occurred prior to complete hypo-phosphorylation of pRb[2] and concomitantly with a decrease in CDK2 activity as measured by the phosphorylation of Histone H1 (Fig 4, left panels). Analysis of immune-complex formation between CDK2 and cyclin-dependent-kinase inhibitors, p21 and p27, revealed that increased binding of p27 to CDK2 is sufficient to account for the rapid decrease in CDK2 activity. However, since there were no changes in p27 levels in response to ST treatment, we also examined the association of p21 and p27 with CDK4 to determine if p27 had switched partners from CDK4 to CDK2. These analyses revealed that the increase in binding of p27 to CDK2 and the concomitant inactivation of CDK2 is most probably due to the transfer of p27 from disappearing levels of CDK4 in response to ST treatment (Fig 4, left panels). A similar analysis performed with 76NE6 and 76NE7 immortalized cell lines showed that the E6 (p53 inactive) cell line behaved similarly to the normal breast cells in response to ST (Fig 4, right panels). Following treatment of 76NE6 cells with ST, CDK4 levels decreased dramatically before hypo-phosphorylation of pRb and concomitant with inactivation of CDK2. The only difference between 76NE6 and the parental cell strain was that the p21 levels increased significantly in 76NE6 cells following ST treatment, due to p53 independent

---

[2] In untreated cells pRb is present in both its phosphorylated (upper band) and unphosphorylated (lower band) forms. However the only form of pRb remaining at 4-10 nM ST is its hypo-phosphorylated form.

14

mechanisms. Furthermore, both p21 and p27 were found associated with CDK2 prior to CDK2 inactivation and concurrent with switching from CDK4 (Fig 4, right panels). 76NE7 (pRb inactive) cells, however, were completely refractory to ST treatment and no changes in any of the cell cycle regulator levels or activities were observed (Fig 4, right panels). Similar to 76NE7 cells, analysis of breast cancer cell lines indicated that ST had no effect on the levels or activities of any of the cell cycle regulators examined (data not shown). Collectively, these results suggest that treatment of normal proliferating mammary epithelial cells with ST results in a dramatic decline of CDK4 in a pRb dependent fashion. Decreased CDK4 levels, followed by the inactivation of CDK2 due to switching of p27 from CDK4 to CDK2, is associated with the G1 arrest in 76N, 81N normal and 76NE6 immortalized cells.

Pre-treatment with ST protects normal cells against the toxic effects of DNA damaging agents. To examine the "protection strategy", both normal and tumor cells were initially pre-treated with ST to arrest normal cells in G1, followed by treatment of both cell types with cytotoxic concentrations of Doxorubicin or Camptothecin (Fig 5). For these analyses we used the normal cell strain 81N and 2 breast cancer cell lines: MDA-MB-436 and MDA-MB-157. All cells were initially treated with 0.5 nM ST for 48h, followed by treatment with either 0.125 µM Doxorubicin or 0.5 µM Camptothecin for 24h. At the end of this 2-step treatment, the cells were allowed to recover for 12 days. The MTT assay was performed at the indicated time intervals during the experiment to measure the response of cells to the described treatments (Fig 5). The results show that pretreatment of normal cells with ST inhibited the proliferation of these cells by 30-

15

50% while breast cancer cells continued to proliferate without any perturbation in their growth kinetics. Following removal of ST, normal cells recovered from ST-mediated growth inhibition and their rate of proliferation and total cell number by the end of the experiment approached that of control untreated cells. The ST-mediated arrest of normal cells made these cells refractory to the toxic effects of either Doxorubicin (Fig 5A) or Camptothecin (Fig 5B), i.e. the normal cells were not significantly affected by the subsequent chemotherapeutic treatment. In fact, ST-pretreatment of the chemotherapeutic-treated normal cells produced results similar to untreated cells, where as normal cells not pre-treated with ST had significantly more growth inhbition after the chemotherapeutic treatments as they did not recover at the end of the experiment (Fig 5). ST did not significantly affect the proliferation of cancer cells, and the ST-pre-treatment did not alter substantially the cytotoxicity of Doxorubicin or Camptothecin. These results show that pretreatment of normal cells with ST protected them against the toxic effects of Doxorubicin and Camptothecin, while tumor cells, which are insensitive to ST, were killed by the chemotherapeutic agents.

ST Increases the Maximal Tolerable Dose of Camptothecin by 2 Logs. One of the limitations in cancer therapy is the maximal tolerable dose (MTD) of a drug administered to patients that can effectively treat the cancer without causing intolerable toxicity to the host. If the MTD of a chemotherapeutic agent could be increased, larger drug doses could be given in order to destroy more tumor cells without killing normal healthy cells. It is our hypothesis that pre-treatment with a drug such as ST can increase the MTD of chemotherapy. We tested this possibility using five different cell lines, including two

16

normal breast epithelial cell strains 81N and 70N, breast cancer cell line MDA-MB-436, and the immortalized 76NE6 and 76NE7 cell lines (Fig 6). All cells were pretreated with 0.5 nM ST for 48 h followed by treatment with the indicated concentrations of Camptothecin for 24 h. After drug removal, cells were incubated in drug free media and allowed to recover for 14 days. Growth inhibition was monitored by the MTT assay at the end of the 2-week period (Fig 6). The results reveal that tumor cells, unaffected by pretreatment with ST, were very sensitive to Camptothecin with an IC50 of 20 nM. Normal cell strains (81N and 70N), which arrest in G1 in response to ST, were protected against the toxic effects of Camptothecin and had an IC50 of 1 μM. 76NE6 immortalized cells behaved similarly to normal cell strains and were even more refractory to Camptothecin (i.e IC50: 3 nM) following pre-treatment with ST. Lastly, 76NE7 cells behaved identically to tumor cells in their response to Camptothecin with a superimposable dose response curve to that of the tumor cells. Pretreatment of ST increased the IC50 of Camptothecin in normal cells by 50-fold compared to tumor cells and by 150 fold in 76NE6 as compared to 76NE7 cells. These results suggest that ST-mediated G1 arrest can significantly protect normal cells against the toxicity of chemotherapeutic agents by targeting the G1 checkpoint regulated by the pRb pathway. Tumor or immortalized cells that are defective in the pRb pathway are not affected by ST, cannot be protected and thus are sensitive to very low concentrations of Camptothecin.

ST protects peripheral blood lymphocytes against the toxic affects of Camptothecin. Immunosuppression, as measured in part by a reduced circulating

lymphocyte count, is one of the major side effects of cancer therapy, resulting in impaired patient performance status. To determine whether pretreatment with ST can protect lymphocytes against the toxic effects of chemotherapy, we tested our protection strategy by assessing its effects on PHA-induced human peripheral blood mononuclear cell (PBMC) proliferation. Without PHA, 80% of the lymphocyte population from healthy donors were in G0/G1 phase with less than 2% in S phase (Fig 7 A). To drive cells into S phase, PBMC were stimulated with PHA resulting in approximately 20% lymphocytes in S phase 48 h post-induction (Fig 7A). These actively dividing lymphocytes were highly sensitive to Camptothecin (IC50 of 10 nM) with a very steep dose response curve (Fig 7B, half-filled squares). Pre-treatment with ST completely reversed the Camptothecin-mediated toxicity (Fig 7B, closed squares). For these analyses, the lymphocytes were initially induced with PHA to proliferate for 48 h in the presence or absence of increasing concentrations of ST (i.e 2, 4, and 10nM). Cells were then treated with the indicated concentrations of Camptothecin for 24 h and growth inhibition was monitored by the MTT assay (Fig 7B). Treatment of cells with 0.125µM Camptothecin, without pre-treatment with ST, killed more than 90% of the dividing lymphocytes, while cell death could be reduced to 72%, 43%, or less than 5% by pre-treating with 2nM, 4nM, or 10nM ST, respectively. Hence, pre-treating the PBMC preparations with ST made treatment with Camptothecin (≤ 2 µM) ineffective.

The ST-mediated protection from Camptothecin toxicity is most probably due to ST-mediated G1 arrest of the lymphocytes (Fig 8), i.e. 10 nM ST blocked (11%, S + G2/M; Fig 8C) activation of lymphocytes by PHA (26%, S + G2/M; Fig 8B). The blockage by ST was reversible; i.e. after removal of ST at 48 h the preparations not

pretreated with ST had 19% of the cells in S + G2/M at 96 h (Fig 8E) and the ST-protected (0-48h) cells had 30% of the cell in the S + G2/M (Fig 8F). Thus, the cells initially blocked from entering the cell cycle in the presence of ST entered upon its removal. Additionally, when cells were incubated in PHA continuously for 96 h in the absence of ST, cells start to apoptose (i.e 23% in sub G1; Fig 8E) while ST lowered PHA-induced apoptosis at 96 h (i.e. 2% in sub G1; Fig 8F). Collectively the results show that treatment of circulating lymphocytes with ST not only protects the cells from Camptothecin-mediated toxicity but also from PHA mediated apoptosis, by reversibly arresting the cells in G1 and prolonging the life span of PHA stimulated cells.

Discussion:

In this paper, we show that a 2-step treatment strategy protects normal proliferating cells against the toxic effects of chemotherapeutic agents by protecting normal cells with a cytostatic agent, prior to administration of conventional chemotherapy. Since treatment of normal cells by the cytostatic agent reversibly arrests them in G0/G1, they are not susceptible to cell death mediated by the chemotherapeutic agents. Tumor cells having a defective G1 checkpoint, on the other hand, are unresponsive to the G1 arrest mediated by the cytostatic agent and continue to proliferate, which makes them susceptible to the chemotherapeutic agents.

Conventional cancer therapy targets all proliferating cells and in the process of killing cancer cells, many normal healthy cells in the body are compromised, causing significant side effects to the patients such as increased infections. One of the advantages of the treatment strategy described herein is the selective protection of its normal cells. Normal cells, whether they are proliferating mammary epithelial cells, precursors of the hematopoietic system, or cancer-specific lymphocytes have functional checkpoint controls that are tightly regulated. Tumor cells on the other hand are very heterogeneous with different checkpoint deregulations (6). Our treatment strategy targets the G1/S transition checkpoint governed by the pRb pathway, an important pathway altered in the majority of cancers (38). Defects in the pRb pathway, which result in its inactivation as a tumor suppressor, are caused by a variety of mechanisms, including overexpression of cyclin D or E, overexpression of CDK4 and/or CDK6, or inactivation of p16 (7,28,39-43). Loss of p16, or overexpression of CDK4 or cyclin D1, would increase the amount of CDK4 available for assembly with cyclin D1, which

20

initiates phosphorylation of pRb. pRb phosphorylation leads to inactivation of the S-phase inhibitory action of pRb by releasing free E2F to transactivate the genes necessary for the G1 to S transition. We show that in normal cells, low concentrations of ST target this pathway under conditions where the pathway is tightly regulated and the levels of its components are neither overexpressed nor inactivated. Specifically, we show that upon treatment of normal cells with very low concentrations of ST (i.e. 0.5 –2 nM), the levels of CDK4 decrease substantially. We propose that the ST-mediated cell cycle perturbation of CDK4 results in a cascade of downstream events, leading to G0/G1 arrest of normal cells. In untreated proliferating normal cells, CDK4 is found in complexes with p27 in which the kinase is active (Fig 4 and (24,44,45)). CDK4/p27 complexes serve two purposes; to increase binding efficiency of CDK4 to cyclin D1 and to sequester p27, controlling the amount of p27 available for inhibition of CDK2 activity (23,24,44,46). Upon disruption of CDK4 levels by ST, p27 can no longer remain bound to CDK4 and is released, which allows binding to CDK2 and inhibition of CDK2 activity (Fig 4). Hypo-phosphorylation of pRb and subsequent G1 arrest follow inhibition of its activity. The exact mechanism by which ST disrupts CDK4 levels is currently unknown, however it is clear that ST mediated a decrease in CDK4 levels, a pRb-dependent primary event leading to G1 arrest of normal cells (Fig 4). We show that in cells that have been transformed by the E7 gene, which targets pRb, ST can no longer disrupt CDK4 levels or lead to G0/G1 arrest (Figs 3 & 4). Similar to E7 immortalized cells, the tumor cells examined also were refractory to ST-mediated CDK4 disruption, as they have a deregulated pRb pathway. Our results suggest that that CDK4 may be the rate-

21

limiting step of ST-mediated G1 arrest specifically in normal cells that have a functional and pRb-dependent G1 checkpoint.

Another strength of the protection strategy is its potential ubiquitous nature as it pertains to different chemotherapeutic agents used for the second step of treatment. Pretreatment of normal cells with ST protected them against the cytotoxic effects of two chemotherapeutic agents with different modes of action. Camptothecin is a toposiomerase I inhibitor and triggers DNA degradation in S phase while Doxorubicin inhibits topoisomerase II, which causes double-stranded DNA breakage, and induces cells to arrest in S and G2 (47). Since pretreatment of normal cells arrested the cells in the G0/G1 making the cells quiescent, they are refractory to the toxic affects of these chemotherapeutic agents. We show that treatment of quiescent circulating lymphocytes exposed to increasing concentrations of Camptothecin had minimal cytoxicity, while treatment of proliferating lymphocytes with the drug resulted in pronounced loss of cell survival (Fig 7). The effectiveness of this strategy against other commonly used chemotherapeutic agents needs to be further investigated, however it is reasonable to assume that as long as the normal proliferating cells are arrested in G0/G1 by ST they should be protected from the toxic effects of different chemotherapeutic agents that target proliferating cells.

Another advantage of the protection strategy is its potential for generating an increased therapeutic index. In figure 6 we show that pretreatment of normal cells with ST protected these cells from Camptothecin at concentrations 50 to 150-fold higher than those causing toxicity to tumor cells. In other words the MTD of Camptothecin was increased by 2 logs, when normal cells were pretreated with ST. The clinical

22

implications of increasing the therapeutic index of any given drug is that by increasing the dose of drug administered it may be possible to shorten the time course of chemotherapy, reduce the frequency by which drug resistance is achieved, potentially decrease the rate of relapse of tumors, and/or achieve a higher frequency of complete response to conventional chemotherapy.

In summary, we show that normal proliferating mammary epithelial cells or dividing lymphocytes can withstand otherwise lethal doses of chemotherapy if they are pretreated with ST, which arrests them in G0/G1 prior to administration of chemotherapy. Tumor cells are refractory to low concentrations of ST and do not arrest in G1 due to defective G1 checkpoints. The G1 checkpoint targeted by low concentrations of ST in normal cells is regulated by the pRb pathway. Since pRb is tightly regulated in normal cells and defective in most tumors, this treatment strategy is highly specific and effective for protecting normal cells against toxicity of chemotherapeutic agents with different modes of action.

Acknowledgments

Figure Legends

Figure 1: **Lack of differential growth inhibition by specific cyclin dependent kinase inhibitors in normal versus tumor cells**. Seven different human breast epithelial cell lines: normal cell strains (76N, 81N), an immortalized cell line (MCF10A), and breast tumor cell lines (MCF-7, MDA-MB-157, MDA-MB-436, and T47D) were treated with the indicated concentrations of **(A)** Olomoucine, **(B)** Roscovitine, and **(C)** Flavopiridol for 48h. Growth inhibition was measured by the MTT assay as described in Methods. Percent of control was indicated for each cell line, and each data point represents the average of six determinations. The assays were performed at least three times and error bars are indicated for each condition and each cell line.

Figure 2. Normal cells are significantly more sensitive to ST than tumor cells. A. Seven different normal and tumor breast cell lines (as described in Figure 1) were treated with increasing concentrations (0-8nM) of ST for 48 h. Growth inhibition by ST was measured by the MTT assay. The experiment was repeated 3 times and error bars are indicated for each condition and each cell line. In almost all cases the error bars were smaller than the symbol size and cannot be seen. **B.** Recovery from growth inhibition mediated by the indicated concentrations of ST were examined in 81N normal cells. Recovery was measured by MTT assay every day during the 48 h of treatment and every 3rd day following drug removal (arrow). The experiment was repeated 3 times and error bars are indicated for each condition.

Figure 3. ST arrests normal and E6 immortalized cells in G1. Two normal breast epithelial cell strains (70N and 81N), two immortal cell lines (76NE6 and 76NE7), and two breast tumor cell lines (MDA-MB-157 and MDA-MB-436) were treated with ST at 0, 0.5, and 10nM for 48h. The cell cycle distribution changes were monitored by flow

25

cytometry. The relative percentages of cells in each cell phase of each cell line are indicated in the figure.

Figure 4. Cell cycle perturbation induced by ST in normal cells is pRb dependent. Normal cell strains (76N and 81N), 76NE6 (p53 inactive), and 76NE7 (pRb inactive) were treated with the indicated concentrations of ST for 48 h. Following treatment cells were harvested and cell lysates were prepared and subjected to Western blot analysis, CDK2 kinase analysis, CDK2 immune-complex formation, and CDK4 immune-complex formation. For Western blot analysis, 50 µg of protein extract from each condition was analyzed by Western blot analysis with the indicated 7 antibodies. Actin was used to demonstrate equal loading. The blots were developed with chemiluminescence reagents. The same blots were sequentially hybridized with different antibodies (see Materials and Methods). The blots were stripped between antibodies with solution containing 100 mM 2-mercaptoethanol, 62.5 mM Tris-HCl (pH 6.8), and 2% SDS for 10 min at 55°C. For CDK2 kinase activity, equal amounts of protein (300 µg) from cell lysates were prepared from each cell line and immunoprecipitated with anti-CDK2 antibody (polyclonal) coupled to protein A beads, using Histone H1 as substrate. For each cell line the resulting autoradiogram of the Histone H1 SDS-PAGE is shown. For immunoprecipitation followed by Western blot analysis, equal amounts of protein (300 µg) from cell lysate prepared from each cell line were immunoprecipitated with anti-CDK2 (polyclonal) or anti-CDK4 (polyclonal) coupled to protein A beads and the immunoprecipitates were subjected to Western blot analysis with the indicated antibodies.

Figure 5. Pretreatment with ST protects normal, but not tumor cells from the toxic effects of Doxorubicin and Camptothecin. Normal cell strain 81N and tumor cell lines MDA-MB-436 and MDA-MB-157 were each treated with the following

conditions as described in the "Material and Methods". Control (■) (no drug treatment); **(A)** Doxorubicin (●) or **(B)** Camptothecin (●) alone (0.125 or 0.5 µM, respectively, for 24 h); ST alone, 0.5 nM (O) (48 h treatment); and **(A)** ST (0.5 nM) + Doxorubicin (0.125µM) (□) or **(B)** ST (0.5 nM) + Camptothecin (0.5 µM) (□) (pretreatment of 0.5nM ST for 48h followed by Doxorubicin or Camptothecin treatment for an additional 24 hours). All cells were allowed to recover for 12 days following drug removal, and growth inhibition was measured by the MTT assay at the indicated time intervals. Each experiment was repeated 3 times and the averages of the three experiments are shown.

Figure 6. Pretreatment with ST increases the maximal tolerable dose of Camptothecin by 2 logs. Normal cell strains 70N and 81N, immortal cell lines 76NE6 and 76NE7, and breast tumor cell line MDA-MB-436 were pretreated with 0.5 nM ST for 48h followed by treatment with the indicated concentrations of Camptothecin for 24h. Following the removal of Camptothecin, cells were allowed to recover in drug-free medium for 12 days. Recovery from growth inhibition was measured by the MTT assay. The experiment was repeated 3 times and error bars are indicated for each condition.

Figure 7. ST protects normal proliferating lymphocytes against the toxic effects of Camptothecin. **(A)** Normal circulating lymphocytes were isolated as described in Materials and Methods and incubated with 10 µg/ml PHA. At the indicated time intervals following PHA activation, cell cycle progression was monitored by flow cytometry. **(B)** Normal circulating lymphocytes were treated with either PHA alone, or PHA and ST for 48 h, followed by treatment with the indicated concentrations of Camptothecin for an additional 24 h. Non-stimulated cells (i.e. without PHA) were incubated in drug free medium for the first 48 h, followed by treatment with

27

Camptothecin for an additional 24 h. The experiment was repeated 3 times and error bars are indicated for each condition.

Figure 8: Reversal of ST-mediated G1 arrest in PHA stimulated lymphocytes. Normal human lymphocytes were either not stimulated for 48 **(A)** or 96 **(D)** hours, treated with PHA alone (10µg/ml) for 48 h **(B)** or 96 h **(E)**, treated with PHA and ST (10nM) for 48h **(C)**, or treated with PHA + ST for 48 h, followed by removal of ST and continued incubation in the presence of PHA for an additional 48 h **(F).** At the end of each treatment cells were subjected to flow cytometry. The experiment was repeated 3 times and the result of a representative experiment is shown.

References

(1)   Kohn KW, Jackman J, O'Connor PM: Cell cycle control and cancer chemotherapy. J. Cell Biochem. 54:440-452, 1994

(2)   Darzynkiewicz Z: Apoptosis in anticancer strategies: modulation of cell cycle or differentiation. J. Cell Biochem. 58:151-159, 1995

(3)   Hartwell LH, Kastan MB: Cell cycle control and cancer. Science 266:1821-1828, 1994

(4)   Stone S, Dayananth P, Kamb A: Reversible, p16-mediated cell cycle arrest as protection from chemotherapy. Cancer Res. 14:3199-3202, 1996

(5)   Pardee AB, James LJ: Selective killing of transformed baby hamster kidney (BHK) cells. Proc. Natl. Acad. Sci. 72:4994-4998, 1975

(6)   Pardee AB: G1 events and regulation of cell proliferatrion. Science 246:603-608, 1989

(7)   Weinberg RA: The retinoblastoma protein and cell cycle control. Cell 81:323-330, 1995

(8)   T'ang A, Varley JM, Chakraborty S, Murphree AL, Fung Y-KT: Structural rearrangement of the retinoblastoma gene in human breast carcinoma. Science 242:263-266, 1988

(9)   Adams PD, Kaelin WG: Negative control elements of the cell cycle in human tumors. Curr. Opin. Cell Biol. 10:791-797, 1998

(10)   Hooper ML: Tumour suppressor gene mutations in humans and mice: parallels and contrasts. EMBO J 17:6783-6789, 1998

(*11*)   Oesterreich S, Fuqua SA: Tumor suppressor genes in breast cancer. Endocr. Relat. Cancer 6:405-419, 1999

(*12*)   Cordon-Cardo C: Molecular alterations in bladder cancer. Cancer Surv. 32:115-131, 1998

(*13*)   Bartek J, Bartkova J, Lukas J: The retinoblastoma protein pathway and the restriction point. Curr. Opin. Cell Biol. 8:805-814, 1996

(*14*)   Bartek J, Bartkova J, Lukas J: The retinoblastoma protein pathway in cell cycle control and cancer. Exp. Cell Res. 237:1-6, 1997

(*15*)   Ikeda MA, Jakoi L, Nevins JR: A unique role for the Rb protein in controlling E2F accumulation during cell growth and differentiation. Proc. Natl. Acad. Sci. USA 93:3215-3220, 1996

(*16*)   Kamb A: Cell cycle regulators and cancer. Trends Gen. 11:136-140, 1995

(*17*)   Keyomarsi K, Conte D, Toyofuku W, Fox MP: Deregulation of cyclin E in breast cancer. Oncogene 11:941-950, 1995

(*18*)   Keyomarsi K, Pardee AB: Redundant cyclin overexpression and gene amplification in breast cancer cells. Proc. Natl. Acad. Sci. USA 90:1112-1116, 1993

(*19*)   Band V, DeCaprio JA, Delmolino L, Kulesa V, Sager R: Loss of p53 protein in human papillomavirus type 16 E6-immortalized human mammary epithelial cells. J. Virology 65:6671-6676, 1991

(*20*)   Band V, Zajchowski D, Kulesa V, Sager R: Human papilloma virus DNAs immortalize normal human mammary epithelial cells and reduce their growth factor requirements. Proc. Natl. Acad. Sci. USA 87:463-467, 1990

(21) Hessling JJ, Miller SE, Levy NL: A direct comparison of procedures for the detection of mycoplasma in tissue culture. J. Immunol. Meth. 38:315-324, 1980

(22) Carmichael J, Mitchell JB, DeGraff WG, Gamson J, Gazder AF, Johnson BE, et al: Chemosensitivity testing of human lung cancer cell lines using the MTT assay. Br. J. Cancer 57:540-547, 1988

(23) Rao S, Lowe M, Herliczek T, Keyomarsi K: Lovastatin mediated G1 arrest in normal and tumor breast cells is through inhibition of CDK2 activity and redistribution of p21 and p27, independent of p53. Oncogene 17:2393-2402, 1998

(24) Chen X, Lowe M, Keyomarsi K: UCN-01 mediated G1 arrest in normal but not tumor cells is pRb dependent and p53 independent. Oncogene 18: 5691-5702, 1999

(25) Band V, Sager R: Distinctive traits of normal and tumor-derived human mammary epithelial cells expressed in a medium that supports long-term growth of both cell types. Proc. Natl. Acad. Sci. USA 86:1249-1253, 1989

(26) Gray-Bablin J, Rao S, Keyomarsi K: Lovastatin Induction of cyclin-dependent kinase inhibitors in human breast cells occurs in a cell cycle independent fashion. Cancer Res. 57:604-609, 1997

(27) Soule HD, Maloney TM, Wolman SR, Peterson WD, Jr., Brenz R, McGrath CM, et al: Isolation and characterization of a spontaneously immortalized human breast epithelial cell line, MCF-10. Cancer Res. 50:6075-6086, 1990

(28) Gray-Bablin J, Zalvide J, Fox MP, Knickerbocker CJ, DeCaprio JA, Keyomarsi K: Cyclin E, a redundant cyclin in breast cancer. Proc. Natl. Acad. Sci. 93:15215-15220, 1996

(*29*)   Deazevedo WF, Leclerc S, Meijer L, Havlicek L, Strand M, Kim SH: Inhibition of cyclin-dependent kinases by purine analogues-crystal structure of human cdk2 complexed with roscovitine. Eur. J. Bioch. 243:518-526, 1997

(*30*)   Meijer L, Borgne A, Mulner O, Chong JPJ, Blow JJ, Inagaki N, et al: Biochemical and celllular effects of roscovitine, a potent and selective inhibitor of the cyclin-dependent kinases, cdc2, cdk2, and cdk5. Euor. J. Biochem. 243:527-536, 1997

(*31*)   Kaur G, Stetler-Stevenson M, Sebers S, Worland P, Sedlacek H, Myers C, et al: Growth inhibition with reversible cell cycle arrest of carcinoma cells by falvone L86-8275. J. Natl. Can. Ins. 84:1736-1740, 1992

(*32*)   Senderowicz AM, Sausville EA: Preclinical and Clinical Development of Cyclin-Dependent Kinase Modulators. J. Natl. Cancer Inst. 92:376-387, 2000

(*33*)   Tamaoki T: Use and specificity of staurosporine, UCN-01, and calphostin C as protein kinase inhibitors. Methods Enzymol. 201:340-347, 1991

(*34*)   Band V, Dala S, Delmolino L, Andropphy EJ: Enhanced degradation of p53 protein in HPV-6 and BPV-1 E6-immortalized human mammary epithelial cells. EMBO J. 12:1847-1852, 1993

(*35*)   Dyson N, Guida P, Munger K, Harlow E: Homologous sequences in adenovirus E1A and human papillomavirus E7 proteins mediate interaction with the same set of cellular proteins. J. Virol. 66:6893-902, 1992

(*36*)   Werness BA, Levine AJ, Howley PM: Association of human papillomavirus types 16 and 18 E6 proteins with p53. Science 248:76-9, 1990

(*37*)   Lee EY-HP, To H, Shew J-Y, Bookstein R, Scully P, Lee W-H: Inactivation of the Retinoblastoma susceptibility gene in human breast cancers. Science 241:218-221, 1988

(*38*)   Rao RN: Targets for cancer therapy in the cell cycle pathway. Curr. Opin. Oncol. 8:516-524, 1996

(*39*)   Kaelin WG: Recent insights into the functions of the retinoblastoma susceptibility gene product. Cancer Invest. 15:243-254, 1997

(*40*)   Strauss M, Lukas J, Bartek J: Unrestricted cell cycling and cancer. Nat. Med. 1:1245-1246, 1995

(*41*)   Sherr CJ: Cancer Cell Cycles. Science 274:1672-1677, 1996

(*42*)   Ueki K, Ono Y, Henson JW, Efird JT, Deimling Av, Louis DN: CDKN2/p16 or RB alterations occur in the majority of glioblastomas and are inversely correlated. Cancer Res. 56:15-153, 1996

(*43*)   He J, Allen JR, Collins VP, Allalunis-Turner MJ, Godbout R, Day RS, et al: CDK4 amplification is an alternative mechanism to p16 gene homozygous deletion in glioma cell lines. Cancer Res. 54:5804-5807, 1994

(*44*)   LaBaer J, Garrett MD, Stevenson LF, Slingerland J, Sandhu C, Chou HS, et al: New functional activites for the p21 family of cdk inhibitors. Genes & Dev. 11:847-862, 1997

(*45*)   Blain SW, Montalvo E, Massague J: Differential interaction of the cyclin-dependent kinase (CDK) inhibitor p27Kip1 with cyclin A-CDK2 and cyclin D2-CDK4. J. Biol. Chem. 272:25863-25872, 1997

(*46*)   Planas-Silva MD, Weinberg RA: Estrogen-dependent cyclin E-cdk2 activation through p21 redistribution. Mol. Cell. Biol. 17:4059-4069, 1997

(*47*)   Del Bino G, Darznkiewicz Z: Camptothecin, teniposide, or 4'-(9-acridinylamino)-3-methanesulfon-m-anisidide, but not mitoxantrone or doxorubicin, induces degradation of nuclear DNA in the S phase of HL-60 cells. Cancer Res. 51:1165-1169, 1991
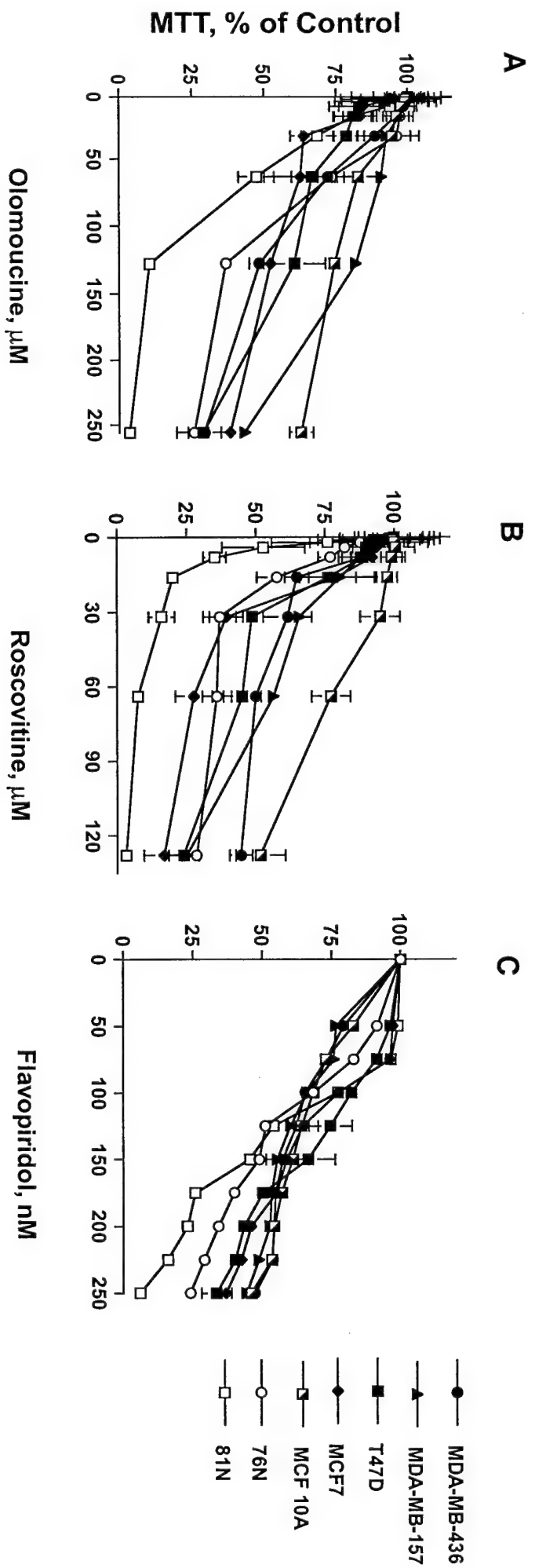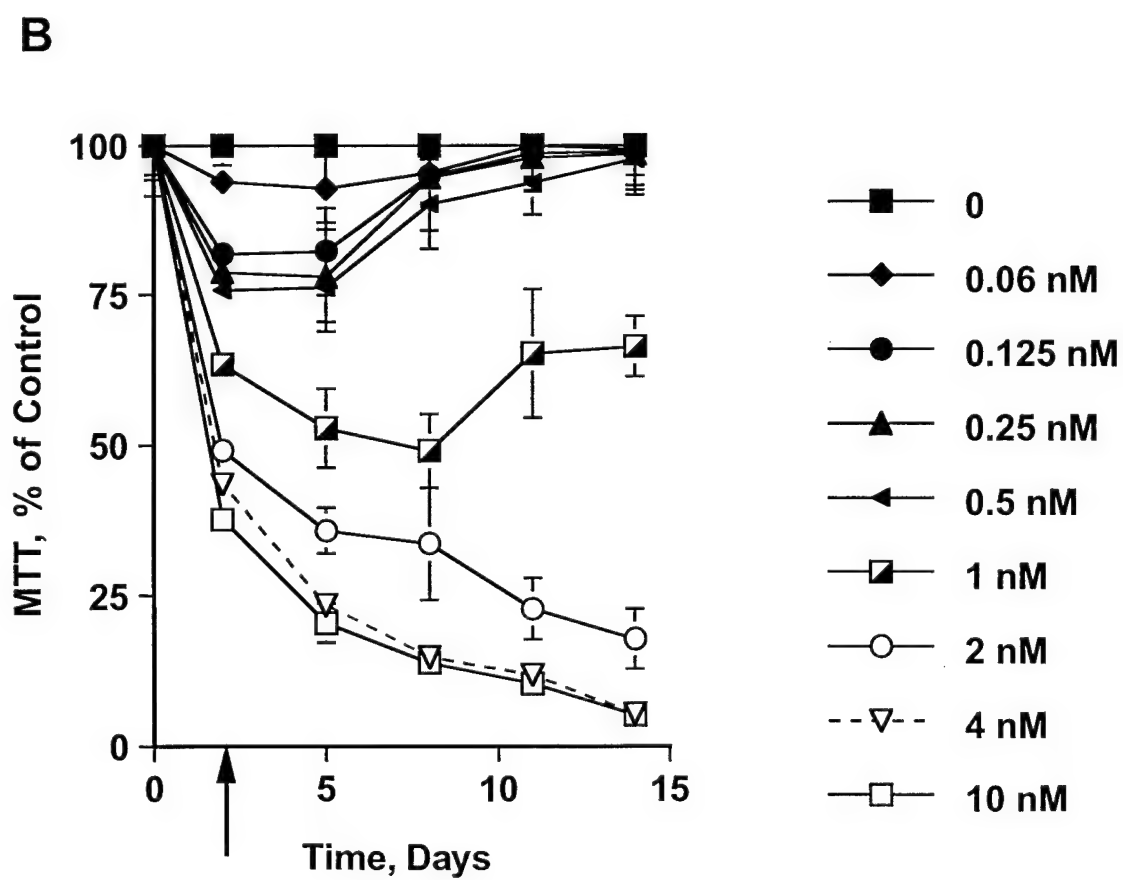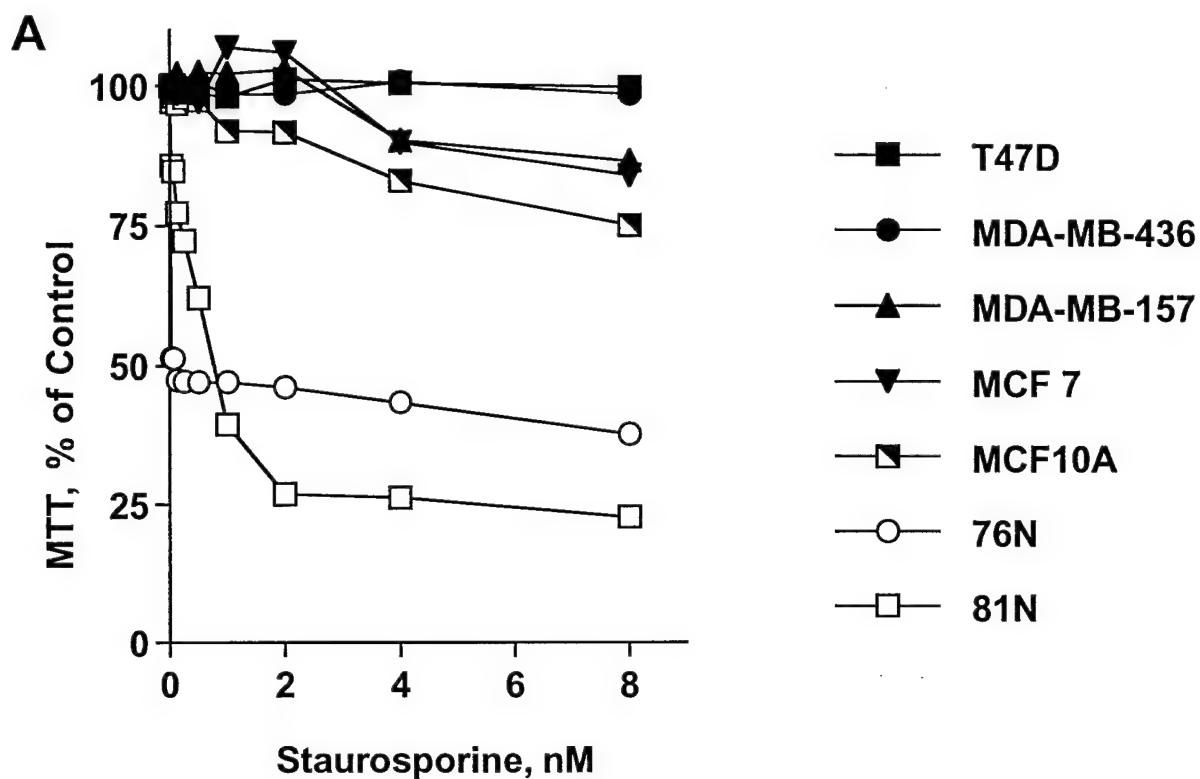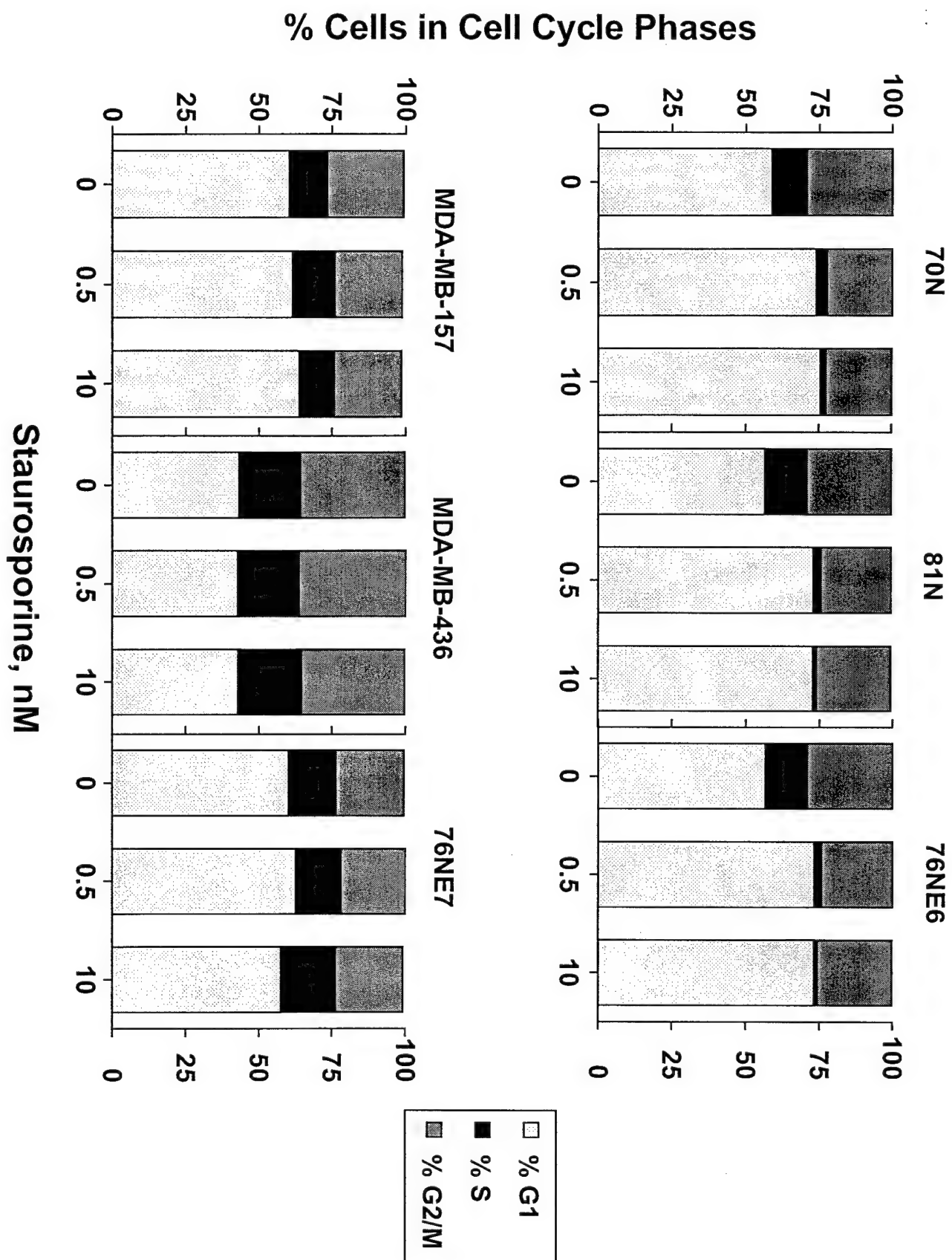
FIGURE 1

MTT, % of Control

A — Olomoucine, μM

B — Roscovitine, μM

C — Flavopiridol, nM

MDA-MB-436
MDA-MB-157
T47D
MCF7
MCF 10A
76N
81N

FIGURE 2

A

B

FIGURE 3

% Cells in Cell Cycle Phases

Staurosporine, nM

Legend: □ % G1 ■ % S ▨ % G2/M

FIGURE 4

FIGURE 5

MTT, % of Control

A: <u>Doxorubicin</u>

81N, Normal

MDA-MB-436, Tumor

MDA-MB-157, Tumor
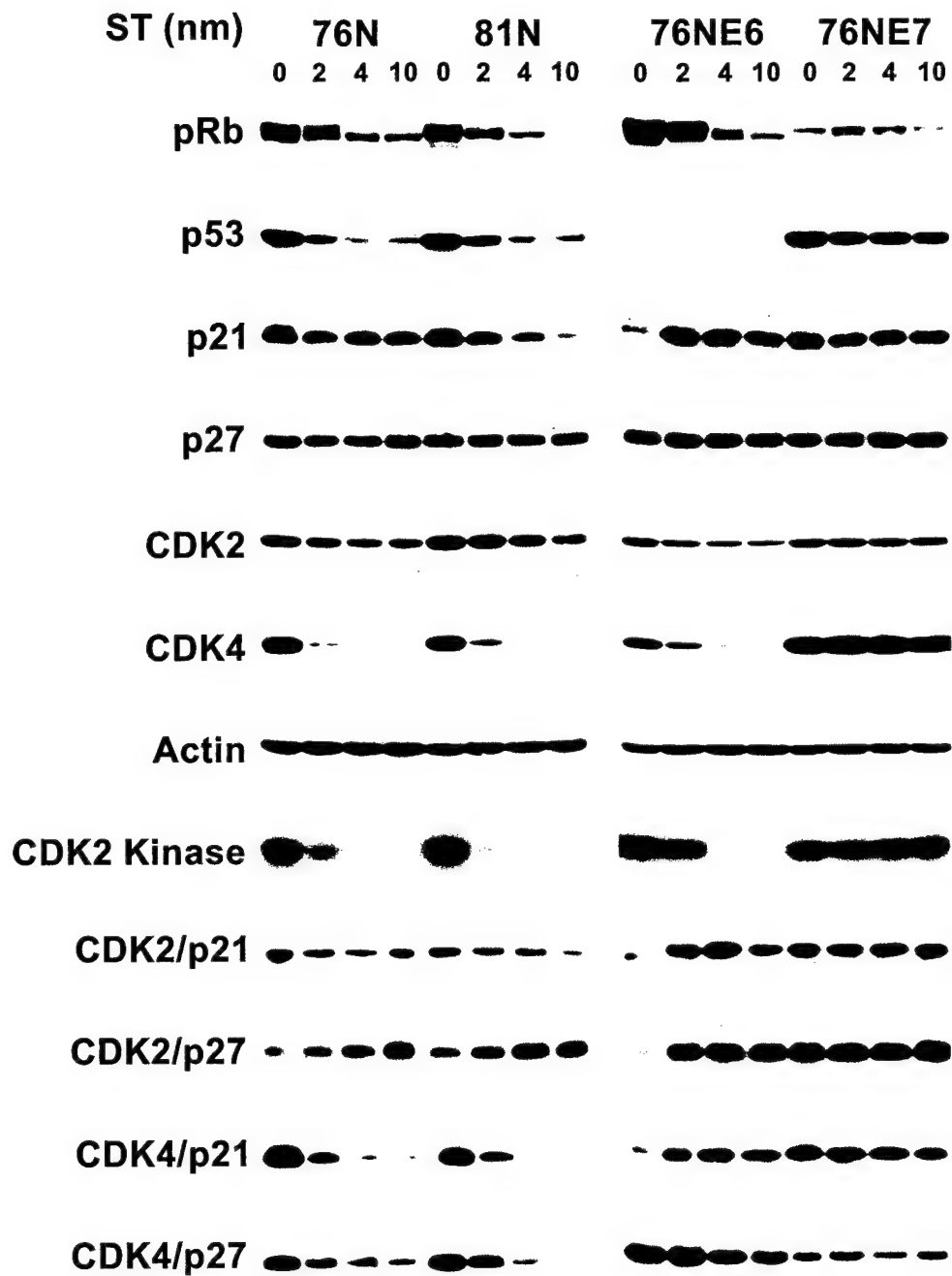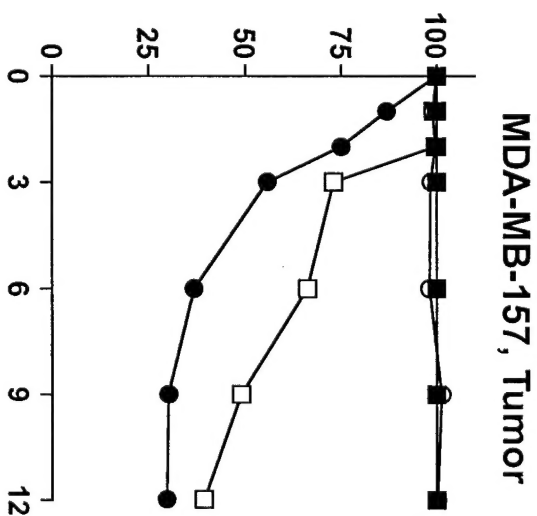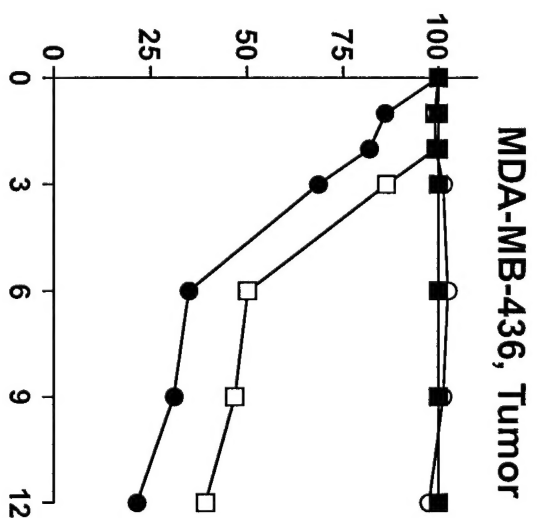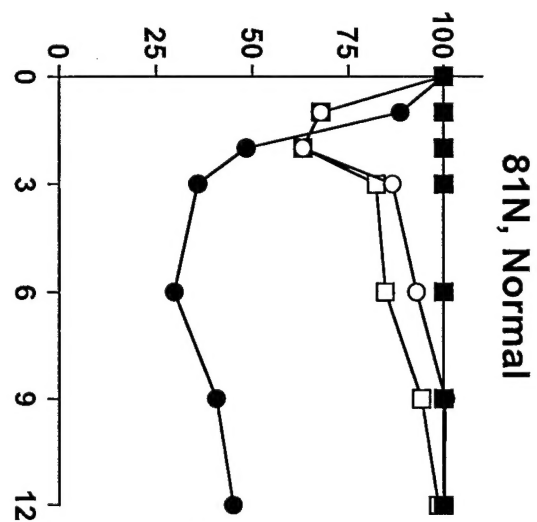
B: <u>Camptothecin</u>
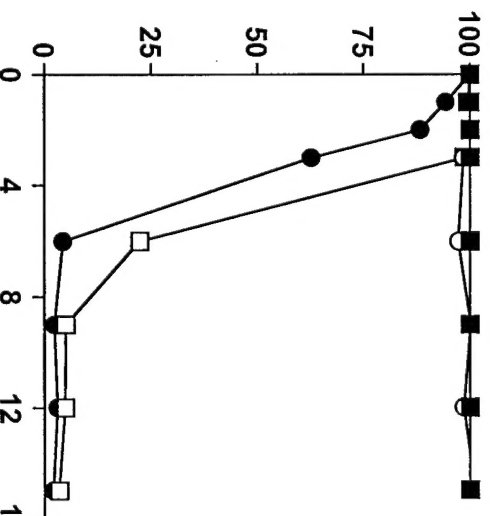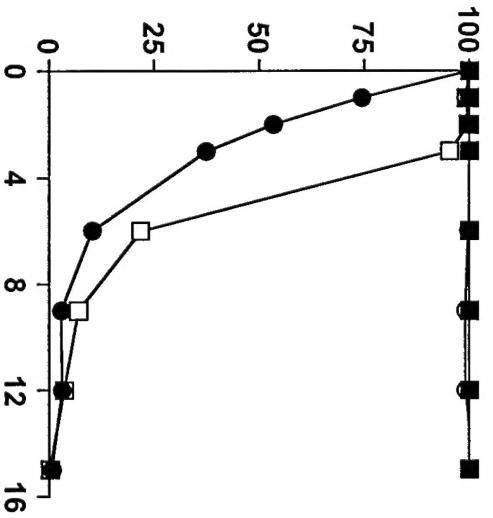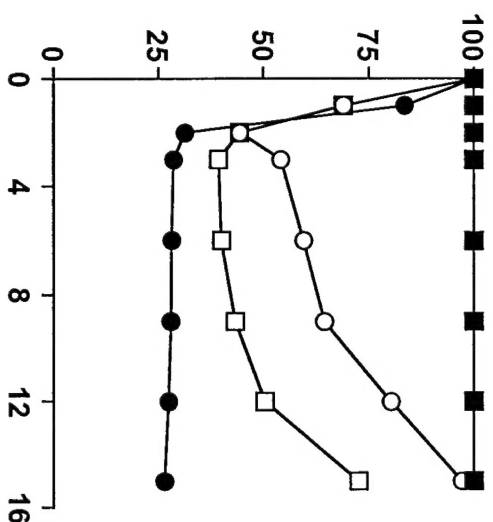
Time, Days

FIGURE 6

FIGURE 7

FIGURE 8